Characterization of the Virulence-Related Roles of the *Legionella pneumophila* Chaperonin, HtpB, in Mammalian Cells

by

Audrey Chong

Submitted in partial fulfillment of the requirements
for the degree of Doctor of Philosophy

at

Dalhousie University
Halifax, Nova Scotia
March 2007

Your file Votre référence
ISBN: 978-0-494-27158-2
Our file Notre référence
ISBN: 978-0-494-27158-2

DALHOUSIE UNIVERSITY

To comply with the Canadian Privacy Act the National Library of Canada has requested that the following pages be removed from this copy of the thesis:

Preliminary Pages

Examiners Signature Page (pii)

Dalhousie Library Copyright Agreement (piii)

Appendices

Copyright Releases (if applicable)

Table of Contents

List of Figures

List of Tables

Abstract

Legionella pneumophila is the facultative intracellular bacterium that causes an acute pneumonia known as Legionnaires' disease. During the infection of host cells, one of the most abundant proteins expressed by *L. pneumophila* is HtpB, a member of the 60-kDa chaperonin family of molecular chaperones. *L. pneumophila* uses HtpB to attach to and invade HeLa cells, but the continued synthesis and release of HtpB by internalized bacteria suggests that HtpB may also play a role in the intracellular events directed by *L. pneumophila*. Intracellular events leading to the generation of the *L. pneumophila* replicative vacuole include recruitment of mitochondria and endoplasmic reticulum (ER)-derived vesicles, evasion of fusion with lysosomes, and association with the ER. To investigate whether HtpB contributes to these events, the intracellular trafficking of HtpB-coated beads in Chinese hamster ovary (CHO) and U937 cells was examined by fluorescence and electron microscopy. Internalized HtpB-coated beads mimicked the ability of virulent *L. pneumophila* to recruit mitochondria and transiently induce actin rearrangements, but did not mimic the ability of *L. pneumophila* to avoid fusion with lysosomes. cAMP translocation assay and immunogold electron microscopy were performed to investigate whether HtpB has access to the host cytoplasm after being released into the *L. pneumophila*-containing vacuole (LCV). By these methods, HtpB was found to be delivered into the host cytoplasm where it associates with the cytoplasmic face of the LCV. CHO cells expressing HtpB displayed altered actin organization, demonstrating a role for HtpB in this compartment. HtpB and GroEL co-sedimented with and induced depolymerization of F-actin in vitro, suggesting a direct interaction between bacterial chaperonins and actin. This interaction was excluded as the underlying mechanism for the HtpB-mediated cytoskeletal rearrangements since ectopically expressed GroEL was unable to alter actin organization in CHO cells. In summary, this study reports the translocation of HtpB into the host cytoplasm, and the ability of HtpB to attract mitochondria and remodel the actin cytoskeleton in mammalian cells. These novel abilities described for HtpB may contribute to the intracellular establishment of *L. pneumophila*, and provide support for the concept of molecular chaperones as virulence factors.

List of Abbreviations and Symbols Used

%	percent
~	approximately
≤	equal to or less than
<	less than
°	degree
2ME	2-mercaptoethanol or β-mercaptoethanol
A	adenine
Å	angstrom
aa	amino acid
Ab	antibody
ACES	(2-[2-amino-2-oxoethyl]-amino)ethanesulfonic acid
ADP	adenosine diphosphate
Ala	alanine
Amp^R	ampicillin resistant
ARF	ADP ribosylation factor
ATP	adenosine triphosphate
BCIP	5-bromo-4-chloro-3-indolylphosphate
BCYE	buffered charcoal yeast extract
BiP	binding protein
bp	basepair
BSA	bovine serum albumin
BYE	buffered yeast extract

C	Celsius or cytosine
cAMP	cyclic adenosine monophosphate
CCT	chaperonin-containing TCP-1
CDTA	1,2-cyclodiaminohexanetetraacetic acid
CFU	colony forming unit
CHO	Chinese hamster ovary
CIRCE	controlling inverted repeat of chaperone expression
cm	centimeter
CMFDA	5-chloromethylfluorescein diacetate
Cm^R	chloramphenicol resistant
CO_2	carbon dioxide
Cpn	chaperonin
CR	complement receptor
ddH_2O	double-distilled water
DE or DEAE	diethylaminoethyl cellulose
D-mMDH	denatured mMDH
DMSO	dimethylsulfoxide
DNA	deoxyribonucleic acid
dNTP	deoxyriboncleoside triphosphate
Dot	defective in organelle trafficking
Dox	doxycycline
DTT	dithiothreitol
EDTA	ethylenediaminetetraacetic acid

EGTA	ethyleneglycol-bis(β-aminoethyl)-N,N,N′,N′-tetraacetic acid
EP	exponential phase
ER	endoplasmic reticulum
ERAD	ER-associated degradation
ERGIC	ER-Golgi intermediate compartment
ERK	extracellular signal-regulated kinase
F-actin	filamentous actin
FBS	fetal bovine serum
fg	femtogram
g	gram or gauge
g	gravity
G	guanine
G418	geneticin
Gal	galactose
GalNAc	N-acetyl-D-galactosamine
GAP	GTPase activating protein
GEF	guanine nucleotide exchange factor
GFP	green fluorescent protein
Glu	glutamate
Gly	glycine
GST	glutathione-S-transferase
GTP	guanosine triphosphate
GTPase	guanosine triphosphatases

h	hour
HA	hemaglutinin
HEPES	4-2-hydroxyethyl-1-piperazineethanesulfone acid
His	histidine
Hsp60	60 kDa heat shock protein
HtpB	heat shock protein B
HUVEC	human vascular endothelial cell
Icm	intracellular multiplication
IFN	interferon
IgG	immunoglobulin G
IL	interleukin
Ile	isoleucine
IOD	integrated optical density
IPTG	isopropyl- β-D-galactoside
kb	kilobase
K_d	dissociation constant
kDa	kiloDalton
Km^R	kanamycin resistant
kV	kilovolt
L	liter
LAMP	lysosome-associated membrane protein
LB	Luria-Bertani
LCV	*Legionella*-containing vacuole

LPS	lipopolysaccharide
M	molar
mA	milliAmpere
MAb	monoclonal antibody
MAP	Merlin-associated protein
MAPK	mitogen-activated protein kinase
MDH	malate dehydrogenase
MEM	minimal essential media
Met	methionine
MHC	major histocompatibilty complex
MIF	mature intracellular form
min	minute
mL	milliliter
mM	millimolar
mMDH	mitochondrial MDH
MOI	multiplicity of infection
MOMP	major outer membrane protein
MOPS	3-[N-morpholino]propane-sulfonic acid
mRNA	messenger RNA
MW	molecular weight
N	normal or nucleotide
NBT	nitrobluetetrazolium
NF-κB	nuclear factor κB

ng	nanogram
nm	nanometer
N-mMDH	native mMDH
No.	number
ns	no significance
O.D.	optical density
p10	*Bordetella pertussis* 10 kDa co-chaperonin
PAb	polyclonal antibody
PAMP	pattern-associated molecular patterns
PBS	phosphate buffered saline
PBSG	PBS containing 2 % goat serum
PCR	polymerase chain reaction
PE	post-exponential
PEP	phosphoenolpyruvate
pI	isoelectric point
PI4P	phosphatidylinositol-4-phosphate
PMSF	phenylmethylsulphonyl fluoride
ppGpp	guanosine 3',5'-bipyrophosphate
PPIase	peptidyl-prolyl-cis/trans isomerase
PrP^c	cellular prion protein
PRR	pathogen recognition receptor
psi	pound force per square inch
RER	rough ER

RNA	ribonucleic acid
RNAi	RNA interference
rpm	revolution per minute
rRNA	ribosomal RNA
RT	room temperature
RTX	repeats in toxin
s	second
SD	standard deviation
SDS	sodium dodecyl sulfate
SDS-PAGE	SDS-polyacrylamide gel electrophoresis
Sm^R	streptomycin resistant
SNARE	soluble N-ethylmaleimide-sensitive fusion protein attachment receptor
T	thymine
TAE	tris acetate EDTA
TBS	tris buffered saline
TCP-1	T-complex polypeptide 1
TEM	transmission electron microscopy
Tet	tetracycline
Thr	threonine
TLR	toll-like receptor
TNF	tumor necrosis factor
TRAPP	transport of protein particles
TrDx	Texas red dextran

TriC	TCP-1 ring complex
tRNA	transfer RNA
TrOv	Texas red ovalbumin
tTA	tetracycline-controlled transactivator
TTBS	Tween 20-tris buffered saline
U	unit
V	Volt
v/v	volume per volume
Val	valine
w/v	weight per volume
β-NADH	reduced β-nicotinamide adenine dinucleotide
μg	microgram
μL	microliter
μm	micrometer
μM	micromolar
σ	sigma factor

Acknowledgements

I want to thank my supervisor, Dr. Rafael Garduno, for his patience and his mentorship. I would also like to thank my supervisory committee members, Dr. Ross Davidson, Dr. Roy Duncan, Dr. David Mahony, and Dr. Catherine Too for their valuable guidance over the past few years. I would like to extend my gratitude to Dr. Howard Shuman for agreeing to be my external examiner. I want to thank Dr. Michele Swanson and the Swanson lab for generously hosting me in their lab at the University of Michigan. Thank you to Elizabeth Garduno for her technical support, and to Dr. Gary Faulkner and Mary Anne Trevors for their help and expertise on the electron microscope. My thanks also to Craig Campbell, Dave Allan, Dr. Jason LeBlanc, Dr. Michael Morash, Dr. Karen Brassinga, Dr. Fanny Ewann, and Matthew Croxen for their help and friendship throughout this process. I am deeply grateful to Gary Sisson for imparting his wicked sense of humor and for his technical expertise. Special thanks to my family and friends for their support and confidence in me. Lastly but not least, my sincerest gratitude to Jen Chase for her unwavering support, understanding, and encouragement.

Chapter 1: Introduction

Among the bacterial pathogens that have evolved to live inside host cells, some are facultative intracellular pathogens that can grow either within host cells or in the extracellular milieu (e.g., *Listeria* spp., *Brucella* spp.), and some have become so highly adapted that they are unable to survive outside this intracellular niche (e.g., *Chlamydia* spp.). The ability of intracellular pathogens to cause disease depends on their ability to survive and replicate within host cells. To this end, intracellular bacterial pathogens employ a variety of strategies to control their intracellular fate and promote their survival in host cells. Once inside, some pathogens such as *Listeria moncytogenes* (Cossart and Lecuit, 1998), *Shigella flexneri* (Fernandez-Prada et al., 2000; Ogawa and Sasakawa, 2006), and *Francisella* spp. (Checroun et al., 2006) escape from their vacuoles and proliferate as free entities in the host cytosol. Other pathogens such as *Mycobacterium tuberculosis* (Clemens and Horwitz, 1995; Clemens, 1996), *Chlamydia trachomatis* (Fields and Hackstadt, 2002), *Coxiella burnetti* (Heinzen et al., 1999), *Brucella abortus* (Celli, 2006), and *L. pneumophila* (Horwitz, 1983b) remain and replicate within a membrane-limited vacuole, initially formed when they are internalized by host cells. Different tactics are used among these 'vacuolar' pathogens to transform their vacuoles into an environment suitable for bacterial replication. Such tactics include: 1) stalling vacuole maturation at various stages to delay fusion with degradative lysosomes (e.g., *M. tuberculosis*), 2) surviving within a degradative phagolysosomal environment (e.g., *C. burnetii*), and 3) escaping from the normal endocytic pathway by completely re-routing the vacuole via interaction with organelles of the secretory pathway (e.g., *C. trachomatis, B. abortus, L. pneumophila*). Elucidation of the microbial factors and host pathways

involved in these processes are critical for understanding the pathogenesis of intracellular bacteria.

Over 180 elderly people were stricken by an atypical pneumonia of unknown origin during a Legionnaires' conference in Philadelphia in 1976; 34 of them died (Fraser et al., 1977). *L. pneumophila* was identified as the etiologic agent after nearly 6 months of research (McDade et al., 1977). In the 30 years following the original outbreak, research has contributed a vast amount of knowledge to the ecology and pathogenesis of *L. pneumophila*. The ability of *L. pneumophila* to survive and replicate in human alveolar macrophages is thought to result from its adaptation to an intracellular lifestyle within free-living amoebae, the natural environmental reservoir of *L. pneumophila* (Swanson and Hammer, 2000). Human infection occurs by accidental inhalation of contaminated aerosols (Fields et al., 2002). The intracellular events leading to the replication of *L. pneumophila* are strikingly similar whether infecting amoebae or human cells, and involve avoidance of the endocytic pathway, recruitment of mitochondria, interception of host secretory vesicles, and association with the ER (Horwitz, 1983c; Robinson and Roy, 2006; Sauer et al., 2005b; Sturgill-Koszycki and Swanson, 2000; Swanson and Isberg, 1995). Thus, *L. pneumophila* appears to employ a mechanism that exploits a fundamentally basic process common to these evolutionarily distant hosts.

The chaperonin family consists of two groups of functionally related proteins. Group I chaperonins are found in bacteria, mitochondria and chloroplasts (Gupta, 1995); Group II chaperonins are found in the eukaryotic cytosol and in *Archaebacteria* (Valpuesta, 2002). Chaperonins are conserved proteins with an essential role in protein folding and protein complex assembly (Gupta, 1995; Lin and Rye, 2006). The universal

nature and the essentiality of chaperonins suggest that these are ancient proteins with a long evolutionary history. Multiple functions have been described for chaperonins in addition to assisting in protein folding: they appear to function as signaling molecules, adhesins, invasins, insect toxins, and lipochaperonins (Maguire et al., 2002, Yoshida et al., 2001, Török et al., 1997). Because chaperonins are able to tolerate amino acid sequence variation in certain domains (e.g., residues not involved in protein folding function) (Brocchieri and Karlin, 2000), these versatile proteins may provide a vehicle for the adaptation of organisms to their specific environments.

The current literature regarding the ecology and molecular pathogenesis of *L. pneumophila*, as well as the current literature concerning the biology and function of Group I chaperonins will be reviewed in the next chapter. The objectives and hypothesis of the work presented in this thesis will also be stated in the next chapter.

Chapter 2: Literature Review

2.1. *L. pneumophila* Biology

2.1.1. Legionellosis

Legionnaires' disease and Pontiac fever are the two classical presentations of disease caused by the legionellae (Fraser et al., 1977; Glick et al., 1978; Kaufmann et al., 1981; McDade et al., 1977). Legionellae are gram-negative bacteria that inhabit freshwater environments or soil where they parasitize and replicate intracellularly in various protozoa (Fields, 1996). There are currently 48 species with 70 serogroups in the genus *Legionella* (Fields et al., 2002). In the United States, approximately 90% of human infections are caused by *L. pneumophila*, and most of these are serogroup 1 (Yu et al., 2002). The rest are caused by other *L. pneumophila* serogroups and other *Legionella* species (Yu et al., 2002). Although rarely, *Legionella*-like amoebal pathogens, which are obligate intracellular bacteria closely related to *Legionella* spp., also account for some incidences of respiratory disease (Marrie et al., 2001).

Pontiac fever is a mild, self-limiting, flu-like disease (Glick et al., 1978). Infected individuals usually recover within a few days and do not require hospitalization (Glick et al., 1978). In contrast, Legionnaires' disease is a severe pneumonic disease with additional symptoms that can include high fever, headache, non-productive cough, muscle ache, diarrhea, and delirium (Fields et al., 2002; Fraser et al., 1977). The mortality rate for Legionnaires' disease is 5-30 % in general, but this rate is closer to 50 % during nosocomial outbreaks reflecting the higher numbers of susceptible individuals among the population in these outbreaks (Marston et al., 1994). High-risk individuals include the immunocompromised and the elderly (Marston et al., 1994). Erythromycin

was the most effective treatment in the first documented Legionnaires' disease outbreak of 1976 and remained the drug of choice until its recent replacement with azithromycin and fluoroquinolones (Fields et al., 2002; Fraser et al., 1977).

2.1.1.1. Immune Response to *L. pneumophila* Infection

Host response to *L. pneumophila* infection involves both innate and adaptive immunity. Toll-like receptor (TLR) stimulation by *L. pneumophila* is thought to play a principal role in eliciting an innate immune response. TLR2 recognizes a broad range of bacterial products including peptidoglycan, lipoproteins, and mycobacterial cell-wall lipoarabinomannan, whereas TLR5 and TLR9 have a more specific range of ligands (Medzhitov, 2001). TLR5 recognizes bacterial flagellin, and TLR9 recognizes unmethylated CpG motifs found in bacterial DNA (Medzhitov, 2001). Studies with *L. pneumophila* and its lipopolysaccharide (LPS) demonstrated the stimulation of TLR2-dependent signaling in murine macrophages resulting in the secretion of interleukin-12 (IL-12) and tumor necorsis factor-α (TNF-α), respectively (Arata et al., 1993; Archer and Roy, 2006; Girard et al., 2003; Neild and Roy, 2003). TLR9 stimulation by *L. pneumophila* also led to IL-12 production in murine dendritic cells and macrophages (Newton et al., 2007). *L. pneumophila* flagellin activates signaling via TLR5 resulting in IL-8 production in lung epithelial cells (Hawn et al., 2003). A deficiency in TLR5 function was linked to increased susceptibility to Legionnaires' disease (Hawn et al., 2003). Although a receptor has not yet been identified, the *L. pneumophila* 60-kDa heat shock protein, HtpB, was shown to increase mRNA levels of various cytokines, and induce secretion of IL-1 by macrophages (Retzlaff et al., 1994). The production of pro-

inflammatory cytokines in turn stimulates the production of additional cytokines, as well as macrophage activation and lymphocyte recruitment required for clearance of *L. pneumophila* (Neild and Roy, 2004).

Humoral and cell-mediated branches of the adaptive immune response are induced during *L. pneumophila* infection. Immunization of guinea pigs with the major secretory protease and HtpB induced both humoral and cell-mediated immune responses, and provided protection against a subsequent challenge with *L. pneumophila* (Blander and Horwitz, 1991; Blander and Horwitz, 1993). Similarly, immunization of guinea pigs with HtpB and the outer membrane protein, OmpS, also induced both responses (Weeratna et al., 1994). The latter study showed that while HtpB induced a greater humoral response, OmpS stimulated a better cell-mediated response, and a higher survival rate was observed in OmpS immunized guinea pigs in comparison to HtpB immunized mice (Weeratna et al., 1994). In addition, antibodies to *Legionella* promote uptake and replication in human monocytes (Horwitz and Silverstein, 1981b). Thus, despite a robust humoral response, protection afforded by antibodies to *L. pneumophila* infection is not well defined.

The cell mediated response appears to play a major role in protection against *Legionella* infection. As mentioned above, protection from OmpS immunization in mice was linked to better stimulation of a cell mediated response (Weeratna et al., 1994). In response to *L. pneumophila* antigens, mononuclear cells from recovered patients were shown to proliferate and generate cytokines that activate monocytes (Horwitz, 1983a). These activated monocytes were resistant to the intracellular growth of *L. pneumophila*. Macrophages activated by interferon-γ (IFN-γ) are resistant to intracellular growth of *L.*

pneumophila (Horwitz and Silverstein, 1981a; Nash et al., 1988); this restriction on intracellular growth was found to be due to downregulation of transferrin resulting in low levels of intracellular iron (Byrd and Horwitz, 1989). In addition, the ability of dendritic cells to present *Legionella* antigens on their major histocompatibility (MHC) class II molecules combined with their ability to restrict *L. pneumophila* growth may facilitate priming of a T-cell mediated response (Neild and Roy, 2003). T cells play a role in protection from *L. pneumophila* infection since mice depleted of T cells showed a delay in clearance of bacteria from the lungs, and demonstrated enhanced susceptibility to *L. pneumophila* infection (Susa et al., 1998).

2.1.2. Microbial Ecology

Legionellae are normally found in a variety of aquatic environments where they survive in biofilms and replicate intracellularly in protozoa (Fields et al., 2002; Fliermans et al., 1981; Orrison et al., 1981). Whether *L. pneumophila* can multiply extracellularly in aquatic environments is unclear. The inability of *L. pneumophila* to utilize cystine, the oxidized form of cysteine, suggests that growth would be restricted to an intracellular environment where cysteine would be available (Ewann and Hoffman, 2006). *L. pneumophila* persisted for 15 days in a biofilm, and replication was observed only with the addition of *Hartmanella vermiformis* (Murga et al., 2001). Additionally, protozoa have been detected in water associated with Legionnaires' disease outbreaks (Barbaree et al., 1986; Fields et al., 1989). Collectively, these studies indicate that *L. pneumophila* requires association with protozoa for multiplication in the environment. However, *L. pneumophila* microcolonies have been detected in biofilms without protozoa (Rogers and

Keevil, 1992), and a recent study reported that *L. pneumophila* could grow, albeit much less robustly, in the absence of protozoa using heat-killed microbial cells as a source of nutrients in a biofilm (Temmerman et al., 2006).

In contrast, there is ample evidence that protozoa serve as a protective and replicative niche, as well as an arena to select for enhanced virulence traits in *L. pneumophila*. *L. pneumophila* was described as an amoebal pathogen of the genera *Acanthamoeba* and *Naegleria* in an early study (Rowbotham, 1980). Since then, *L. pneumophila* has been reported to multiply in other amoebae and in *Tetrahymena pyriformis* (Fields, 1996). In addition to amplifying bacterial numbers, the amoebae also provide protection to intracellular *L. pneumophila* from high temperatures and high concentrations of chlorine (Kilvington and Price, 1990; Rohr et al., 1998). Vesicles expelled from *Acanthamoeba* containing numerous *L. pneumophila* were similarly resilient (Berk et al., 1998). These vesicles would potentially deliver a respirable infectious dose of *L. pneumophila*. These observations provide evidence that protozoa play a significant role in transmission of *L. pneumophila*. The *L. pneumophila*-amoeba interaction also explains why eradication of legionellae from water systems is such a challenge.

L. pneumophila does not appear to be adapted to its human host since no person-to-person transmission has been documented. Thus, human infection is disadvantageous for *L. pneumophila* because genetic variants selected from the human host are not propagated (Swanson and Hammer, 2000). The intracellular infection of *L. pneumophila* in the human macrophage model is remarkably similar to the protozoan model (Fields et al., 2002; Gao et al., 1997). In fact, most of the genes required for intracellular replication

in the human host are required in the protozoan host (Gao et al., 1997; Segal and Shuman, 1999). The current perspective is that the ability of *L. pneumophila* to infect and replicate in mammalian cells is a consequence of its evolutionary capacity to infect and replicate in protozoan hosts (Abu Kwaik et al., 1998; Harb et al., 2000; Swanson and Hammer, 2000).

2.1.3. The Developmental Cycle of *L. pneumophila*

Differentiation of *L. pneumophila* in protozoa was observed in early studies. Ultrastructural studies revealed less morphological variation in media-grown bacteria whereas a range of short rods to long filamentous forms were observed in intracellularly-grown *L. pneumophila* (Katz and Nash, 1978; Rodgers, 1979). In documenting the life cycle of *L. pneumophila* in amoeba, Rowbotham (1986) noted two morphological forms of the bacterium. Transmissive (non-replicative) forms were shorter and displayed motility, numerous poly-β-hydroxybutyrate inclusions, and smooth cell walls, whereas replicative forms lacked these phenotypes (Rowbotham, 1986). Similar morphological and structural differences between amoeba-grown bacteria and media-grown bacteria have since been described (Cirillo et al., 1994; Greub and Raoult, 2003). Following replication within amoeba, *L. pneumophila* exhibits changes in LPS, fatty acid, and outer membrane protein profiles (Barker et al., 1993), and enhanced resistance to antibiotics and biocides than in vitro grown bacteria (Barker et al., 1992; Barker et al., 1995). Most significantly, in relation to human infection, amoeba-grown *L. pneumophila* showed enhanced ability to infect mammalian cells in vitro compared to agar-grown bacteria (Cirillo et al., 1994; Cirillo et al., 1999). In a murine lung infection model, co-infection

with *L. pneumophila* and *H. vermiformis* potentiated the replication of *L. pneumophila* resulting in more severe pneumonia and higher mortality compared to infection with *L. pneumophila* alone (Brieland et al., 1996). *L. pneumophila* grown in *H. vermiformis* was also demonstrated to be more virulent than their free living counterparts in a mouse model (Brieland et al., 1997).

Virulence of *L. pneumophila* correlates with its sequential growth phases in broth and in eukaryotic cells. Broth-grown post-exponential (PE) phase *L. pneumophila* were found to be motile, cytotoxic, salt-sensitive (a characteristic of virulent strains), osmotically resistant, infectious, and able to avoid intracellular degradation (Byrne and Swanson, 1998). These traits promote the dissemination of *L. pneumophila* from one host to another and are referred to as 'transmissive' traits (Byrne and Swanson, 1998; Molofsky and Swanson, 2004). In contrast, exponential phase (EP) bacteria did not exhibit these traits unless they were exposed to spent medium (Byrne and Swanson, 1998). At least two of these phenotypic switches were observed in experiments with macrophages: *L. pneumophila* released from spent macrophages were motile and sodium sensitive (Byrne and Swanson, 1998). Based on these observations, Byrne and Swanson (1998) proposed a model in which *L. pneumophila* virulence regulation is dictated by nutrient supply. When nutrients become limiting within the host, *L. pneumophila* expresses factors to lyse the spent host, to survive and disperse into the environment, and to re-establish infection by avoiding lysosome degradation. Phenotypic conversion to a replicative form occurs upon arrival within a nutrient rich environment. Sauer et al. (2005a) linked nutrient acquisition to *L. pneumophila* differentiation by demonstrating that acquisition of an essential amino acid (threonine) by phagosomal transporter A

(PhtA) is required for transmissive forms of *L. pneumophila* to differentiate to replicative forms in broth and in murine macrophages. Thus, *L. pneumophila* utilizes its Pht transporter family to gauge amino acid availability before entering the replicative phase.

These morphological changes were finally connected with a developmental cycle in a HeLa cell model (Faulkner and Garduno, 2002; Garduno et al., 1998b; Garduno et al., 2002). Differentiation between a replicative form and a 'cyst-like' mature intracellular form (MIF) was characterized by ultrastructural studies (Garduno et al., 1998b; Garduno et al., 2002). MIFs appear late in HeLa cell infection and are described as stubby rods with poly-β-hydroxybutyrate inclusions, intracytoplasmic membrane laminations, and an electron dense outer membrane (Garduno et al., 1998b), phenotypes similar to the form first observed by Rowbotham (1986) in protozoa. Despite some resemblance between MIFs and in vitro grown post exponential (PE) phase bacteria (both are Giménez stain positive, motile, osmotically resistant, and infectious), MIFs are distinct from PE phase bacteria (Garduno et al., 2002). MIFs exhibit a lower respiration rate, are more environmentally resilient, and more infectious than PE phase *L. pneumophila* (Garduno et al., 2002). Full differentiation into MIFs has only been observed in vivo. Thus, the PE phase bacteria appear to represent intermediates in the differentiation cycle to produce MIFs. The protein expression profile of MIFs is different from that of PE phase bacteria, which is consistent with previous reports comparing protein expression profiles between media-grown and intracellularly-grown *L. pneumophila* (Abu Kwaik et al., 1993; Cirillo et al., 1994). Recently, microarray analysis of the global gene expression profiles of *L. pneumophila* strains in both *A. castellanii* and

in broth culture revealed a shift in gene expression correlating with the conversion of *L. pneumophila* from a replicative form to a transmissive form (Bruggemann et al., 2006).

2.1.3.1. The Stringent Response Model of Virulence Regulation

In the stringent response, *E. coli* reacts to various nutritional stresses by inhibiting rRNA, ribosome and protein synthesis leading to growth arrest (Chatterji and Ojha, 2001). The effector molecule of this pathway is guanosine 3',5'-bispyrophosphate (ppGpp), which is synthesized by the ppGpp synthase, RelA, in response to uncharged transfer RNAs (tRNAs). Accumulation of ppGpp increases the amount of the stationary-phase sigma factor (RpoS) resulting in the expression of stationary phase genes.

Analogous to the adaptive response in *E. coli*, the proposed model for the expression of virulence traits in *L. pneumophila* involves the synthesis of ppGpp by RelA in response to limiting amino acid levels leading to the induction of signaling pathways regulated by the stationary-phase sigma factor (RpoS), the flagellar sigma factor (FliA), and a two-component regulatory system (LetA/S) (Molofsky and Swanson, 2004). These pathways, in turn, coordinate the induction of multiple virulence traits (Molofsky and Swanson, 2004). When *L. pneumophila* detects an adequate supply of intracellular nutrients, the bacterium down-regulates its transmissive traits and differentiates into its replicative form (Molofsky and Swanson, 2004).

In support of this model, Hammer and Swanson (1999) found that *L. pneumophila* accumulated ppGpp and expressed virulence traits in response to amino acid starvation. RpoS expression was found to increase during stationary phase of *L. pneumophila* (Hales and Shuman, 1999). Since RpoS induced only some virulence traits (sodium sensitivity and flagellin expression), other factors (not yet identified) were proposed to co-operate

with RpoS to fully induce virulence in *L. pneumophila* during post-exponential phase (Bachman and Swanson, 2001). The '*Legionella* transmission activator and sensor' (LetA/S) two component regulatory system was discovered to induce transmission traits in stationary phase in response to ppGpp production (Hammer et al., 2002). A *letA* mutation led to dramatically decreased transcriptional levels of *dotA* (encoding for a component of the type IVB secretion system) and *ralF* (encoding for a type IVB secretion system substrate) (Shi et al., 2006). In addition, the *letA* mutation dramatically decreased the secretion of macrophage infectivity protein (Mip) (Shi et al., 2006). LetA/S regulates expression of transmission traits indirectly by relieving carbon storage regulator (CsrA) repression of virulence genes (Molofsky and Swanson, 2003). CsrA is expressed during exponential phase; overexpression of CsrA in *L. pneumophila* post-transcriptionally inhibits expression of transmission traits (Fettes et al., 2001; Molofsky and Swanson, 2003). The LetA/S-dependent developmental switch is enhanced by LetE (Bachman and Swanson, 2004). The flagellar sigma factor FliA of *L. pneumophila* may activate promoters of virulence genes in addition to the promoters of the flagellar regulon because FliA was demonstrated to be required not only for the synthesis of the flagellum and for motility (Fettes et al., 2001; Heuner et al., 2002), but it is also required for lysosome evasion and cytotoxicity (Hammer et al., 2002; Molofsky et al., 2005).

Contradictory to evidence supporting the involvement of the stringent response in regulating virulence in *L. pneumophila*, a *relA* mutant unable to synthesize ppGpp could still grow intracellularly in amoebae and human macrophages (Abu Zant et al., 2006; Zusman et al., 2002). Furthermore, RpoS but not RelA was required for the induction of the pore-forming activity induced in PE phase bacteria (Abu Zant et al., 2006). To further

confuse the issue, neither RpoS nor LetA/S contribute to intracellular growth of *L. pneumophila* in macrophages (Hales and Shuman, 1999; Hammer et al., 2002), but is required for intracellular growth in *A. castellanii* (Gal-Mor and Segal, 2003; Hales and Shuman, 1999). These observations suggest that there is not a link between the stringent response and the RpoS-dependent developmental switch in *L. pneumophila*, therefore, differentiation into the infectious form may be induced by additional signals and involve additional regulators of gene expression.

2.1.4. Attachment and Invasion

The ability of *L. pneumophila* to enter into host cells is critical for its survival since an intracellular environment is required for efficient replication. Uptake of *L. pneumophila* into human monocytes and macrophages occurs via conventional phagocytosis (Gibson et al., 1994; Payne and Horwitz, 1987; Steinert et al., 1994), coiling phagocytosis (Bozue and Johnson, 1996; Horwitz, 1984), and macropinocytosis (Watarai et al., 2001). Engulfment of *L. pneumophila* within plasma membrane coils has been observed to occur with macrophages (Horwitz, 1984) and amoebae (Bozue and Johnson, 1996; Cirillo et al., 1999). Heat-killed, chemically fixed, and avirulent *L. pneumophila* can also be phagocytosed in this manner, thus the intracellular fate of the internalized bacteria must be determined by a factor on the bacterial surface rather than by mode of entry (Bozue and Johnson, 1996; Horwitz, 1984; Joshi et al., 2001). Complement and antibody opsonized bacteria are also efficiently taken up by monocytes following binding to complement receptors CR1 and CR3, or to Fc receptors (Husmann and Johnson, 1992; Payne and Horwitz, 1987), but complement-independent

phagocytosis has also been observed (Gibson et al., 1994; Steinert et al., 1994; Weissgerber et al., 2003). Virulent bacteria taken up by complement-dependent or – independent phagocytosis are able to replicate intracellularly. The relevance of opsonization in human infection is questionable since complement levels in the human lung are usually low and antibodies specific for *L. pneumophila* would not yet be produced during the initial stages of infection (Reynolds and Newball, 1974). Macropinocytotic uptake of *L. pneumophila* has only been demonstrated in bone marrow-derived macrophages from permissive A/J mice (Watarai et al., 2001). The mouse *Lgn1* locus and the bacterial Dot/Icm secretion system are both required to induce this mode of entry (Watarai et al., 2001). Macropinosomes were formed during closure of the plasma membrane and were found to be transient (they shrunk within 15 min of formation) (Watarai et al., 2001).

Since there are no complement components or antibodies in the aquatic environment, phagocytosis by amoebae must occur via complement-independent phagocytosis. As already mentioned, *L. pneumophila* can be ingested by amoebae via coiling phagocytosis and also by conventional phagocytosis (Bozue and Johnson, 1996; Cirillo et al., 1999). Venkataraman et al. (1997) identified a 170-kDa galactose/N-acetyl-D-galactosamine (Gal/GalNAc) lectin on *H. vermiformis* that mediated *L. pneumophila* attachment and invasion of the protozoa (Venkataraman et al., 1997). While bacterial uptake into *H. vermiformis* was blocked by the presence of Gal or GalNAc monomers, uptake by *A. polyphaga* was less dramatically affected (Harb et al., 1998). A 170-kDa protein in *A. polyphaga* was implicated in the attachment and entry of *L. pneumophila*, although whether this protein is similar to the lectin identified in *H. vermiformis* remains

to be determined (Harb et al., 1998). *L. pneumophila* mutants severely defective in attachment to *A. polyphaga* were not affected in attachment to *H. vermiformis* (Harb et al., 1998). These observations indicate that *L. pneumophila* uses different receptors to bind to different protozoan hosts (Harb et al., 1998).

2.1.4.1. Bacterial Factors Promoting Uptake

In addition to phagocytes, *L. pneumophila* can invade and replicate within various non-phagocytic cells, e.g., alveolar epithelial cells (Gao et al., 1998; Mody et al., 1993), human embryonic lung fibroblasts (Oldham and Rodgers, 1985); HeLa cells (Garduno et al., 1998a; Weissgerber et al., 2003) suggesting that entry into host cells involves bacterial-driven processes (Hoffman, 1997). Considering the multiple ways in which *L. pneumophila* is internalized and the diversity of its host range, it is not surprising that several bacterial factors have been linked to attachment and entry. These factors include MOMP, LaiA, the type IV pilus, LvhB2, HtpB, Mip, EnhC, RtxA, and LpnE, as described below.

The *L. pneumophila* major outer membrane protein (MOMP), encoded by *ompS*, promotes binding since antibodies specific for MOMP blocked the attachment of *L. pneumophila* to HeLa cells (Garduno et al., 1998a). An earlier study had shown that opsonization of purified MOMP with complement component C3 induced phagocytosis by monocytes implicating a role for MOMP in uptake (Bellinger-Kawahara and Horwitz, 1990). A *L. pneumophila* protein (LaiA) with homology to an integrin analogue of *Saccharomyces cerevisiae* was found to play a role in adherence and entry into epithelial cells (Chang et al., 2005). Deletion of *laiA* did not affect intracellular growth of *L.*

pneumophila in human macrophages, but showed reduced virulence in a mouse infection model. The type IV pilus of *L. pneumophila* is involved in attachment to mammalian and protozoan cells (Stone and Abu Kwaik, 1998). The *L. pneumophila* pilin mutant containing an insertion mutation in the pilin gene, $pilE_L$, showed a 50% decrease in adherence to human and amoebal cells, but demonstrated intracellular replication similar to that of wild-type (Stone and Abu Kwaik, 1998). A putative *L. pneumophila* protein, encoded by *lvhB2*, with similarity to type IV pilin subunit was found to play a role in infection of epithelial cells and monocytes at lower temperatures (Ridenour et al., 2003). Mutagenesis of *lvhB2* resulted in a 100-fold decrease in entry and intracellular replication of *L. pneumophila* at 30°C, but not at 37°C.

HtpB (heat shock protein B) is the *L. pneumophila* chaperonin that is localized to the bacterial cell surface and mediates invasion in a HeLa cell model (Garduno et al., 1998a; Garduno et al., 1998). Purified HtpB promoted the uptake of coated latex beads and competed with virulent *L. pneumophila* for internalization into HeLa cells (Garduno et al., 1998a). Avirulent *L. pneumophila* strains display less surface localized HtpB (Allan, 2002; Hoffman et al., 1990), while hyperinfectous MIFs display enriched levels of HtpB on the bacterial cell surface (Garduno et al., 2002). These observations support the idea that HtpB plays a role in the virulence of *L. pneumophila*.

The macrophage infectivity potentiator (Mip) of *L. pneumophila* is a surface protein that has peptidyl-prolyl-cis/trans isomerase (PPIase) activity (Cianciotto et al., 1989; Fischer et al., 1992). *L. pneumophila* Mip mutants were 50-100 fold less invasive for amoeba and macrophages than their parental strains demonstrating a role in the invasion of host cells, but no differences in intracellular survival were detected between

Mip mutants and parental strains (Wintermeyer et al., 1995). Mip is required for the early stages of infection in mammalian cells and protozoa (Cianciotto and Fields, 1992; Cianciotto et al., 1989), as well as for virulence in animal models (Cianciotto et al., 1990). Guinea pigs infected with Mip mutants showed fewer disease symptoms and slower disease progression (Cianciotto et al., 1990). PPIase activity of Mip appears to be involved in virulence since *L. pneumophila* strains with very low to no PPIase activity displayed significant reduction in invasion and initiation of intracellular replication in macrophages and protozoa (Helbig et al., 2003; Köhler et al., 2003). In addition, Köhler et al. (2003) found that the dimerization ability located at the N-terminus of Mip also contributes to the virulence function of the protein. N-terminally truncated Mip mutants lacking the dimerization domain, but with PPIase activity, were significantly attenuated in a guinea pig infection model (Köhler et al., 2003).

Two gene clusters, enhanced entry 1 (*enh1*) and *enh2*, have been reported to enhance the entry of *L. pneumophila* into host cells (Cirillo et al., 2000). Over-expression of either of these two loci enhanced the entry of virulent *L. pneumophila* into epithelial cells and monoctyes, whereas deletion of representative genes within each loci (*rtxA* from *enh1*; *enhC* from *enh2*) greatly diminished the ability of *L. pneumophila* to invade host cells (Cirillo et al., 2000). Analysis of the *rtxA* sequence (repeats in structural toxin A) revealed the presence of eight RTX repeat regions similar to those found in the hemolysin from pathogenic *E. coli* and cytotoxin from *Bordetella pertussis* (Cirillo et al., 2000). RtxA was also shown to play a role in virulence in mice, and in the adhesion and uptake by *A. castellanii* (Cirillo et al., 2001; Cirillo et al., 2002). Analysis of the *enhC* sequence revealed a tetratricopeptide repeat region thought to promote protein-protein interactions

that has similarity to those repeats found in eukaryotic cells (Cirillo et al., 2000). A similar tetratricopeptide repeat region was found in LpnE (*L. pneumophila* entry). LpnE is required for efficient entry into macrophages and epithelial cells (Newton et al., 2006).

2.1.4.2. Involvement of the Host Actin in *L. pneumophila* Uptake

Phagocytosis involves host cell surface receptor engagement to initiate the signaling cascades that result in actin polymerization (Kwiatkowska and Sobota, 1999). These actin rearrangements then drive the formation of membrane protrusions that eventually surround the bacterium into a vacuole within the host cell (Finlay and Cossart, 1997; Kwiatkowska and Sobota, 1999). Studies using cytochalasin D, an inhibitor of actin polymerization, have demonstrated the requirement for a functional actin cytoskeleton in the engulfment of *L. pneumophila* into human macrophages (King et al., 1991) (King et al., 1991), guinea pig and rat alveolar macrophages (Elliott and Winn, 1986), and HeLa cells (Garduno et al., 1998b). Microtubule inhibitors did not block entry of *L. pneumophila* into HeLa cells as severely, thus microtubules appeared to play a less prominent role than microfilaments in this process (Garduno et al., 1998b). Evaluation of microfilament morphology by fluorescence microscopy confirmed the involvement of actin during the uptake of *L. pneumophila* into human monocytes (Coxon et al., 1998; Khelef et al., 2001). Heat-killed and avirulent strains of *L. pneumophila* were also capable of inducing actin polymerization during entry, suggesting that the factor(s) required for these effects is (are) heat-resistant and preformed on the bacterial surface (Khelef et al., 2001).

In contrast, entry of *L. pneumophila* into *H. vermiformis* and *A. castellanii* is an actin-independent process (Harb et al., 1998; King et al., 1991; Moffat and Tompkins, 1992), and may even involve bacteria-directed depolymerization of the actin cytoskeleton (Venkataraman and Abu Kwaik, 2000). Contrary to these reports, Lu and Clarke (2005) found that uptake of *L. pneumophila* into the social amoeba *Dictyostelium discoideum* was an actin-mediated process.

2.1.5. *L. pneumophila*-Directed Intracellular Trafficking

L. pneumophila resides within a membrane bound compartment referred to as the *Legionella*-containing vacuole (LCV) after internalization into the host cell (Horwitz, 1983b). The LCV progresses through a series of intracellular trafficking events that eventually establishes an intracellular microenvironment amenable for legionellae replication (See Figure 2.1). First, mitochondria and ER-derived smooth vesicles are recruited to the LCV (Garduno et al., 1998b; Horwitz, 1983b; Oldham and Rodgers, 1985). The internalized *L. pneumophila* avoids the default endocytic pathway by inhibiting LCV acidification and fusion with lysosomes (Horwitz and Maxfield, 1984; Horwitz, 1983c; Sauer et al., 2005b; Sturgill-Koszycki and Swanson, 2000). Eventually, the LCV associates with ribosomes and rough ER (RER), and bacterial replication begins in this conditioned vacuole (Horwitz, 1983b). *L. pneumophila* exits the spent host cell by inducing apoptosis or necrosis (Alli et al., 2000; Gao and Abu Kwaik, 1999b; Gao and Abu Kwaik, 2000; Muller et al., 1996). Sequential trafficking events leading to the biogenesis of the replicative vacuole and exit from the host cell will be reviewed next.

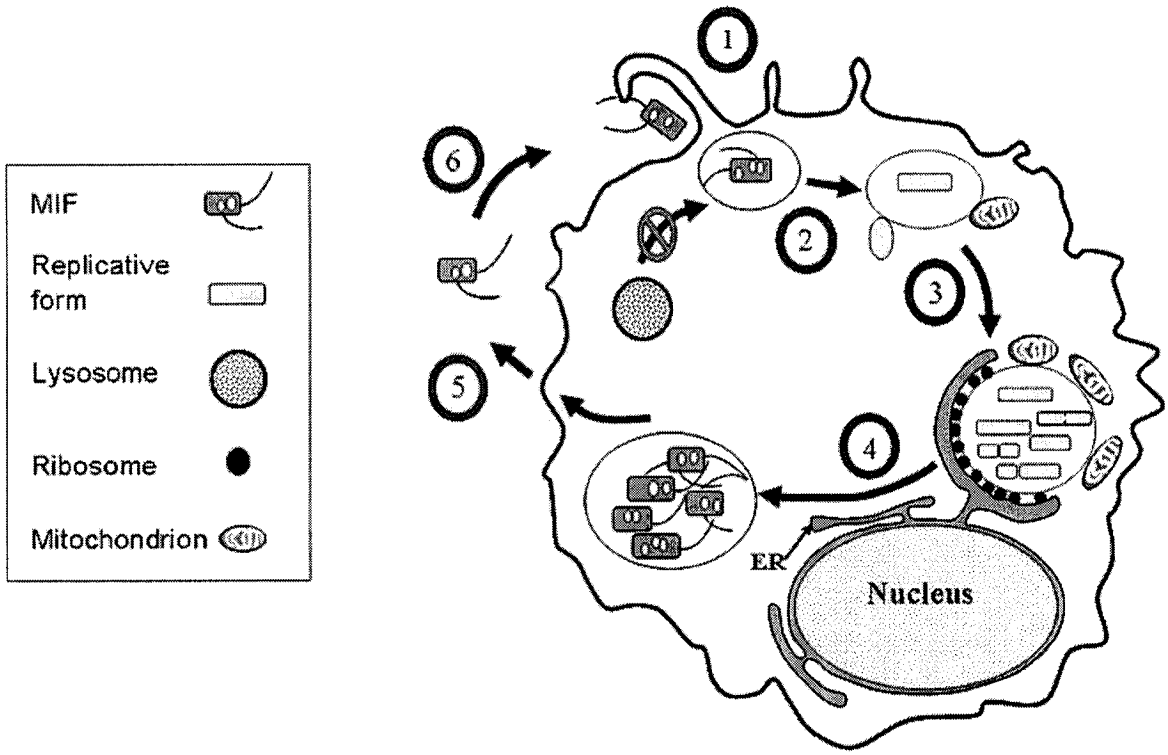

Figure 2.1. Intracellular Trafficking of the *L. pneumophila* Containing Vacuole. 1) The infectious form of *L. pneumophila* enters a host cell and is housed within a membrane bound compartment. 2) The *L. pneumophila* containing vacuole (LCV) avoids fusion with lysosomes. Instead, it associates with mitochondria and smooth vesicles. The bacterium differentiates into a replicative form. 3) The LCV becomes associated with the endoplasmic reticulum, and the LCV membrane is lined with ribosomes. Bacterial replication begins. 4) Bacteria differentiate into the mature intracellular form (MIF) once replication ceases. 5) Egress from the host cell. 6) The released bacteria begin another round of infection. Adapted from Faulkner and Garduno, 2005.

2.1.5.1. Mitochondria Recruitment

The LCV has been observed with closely associated mitochondria and smooth vesicles as early as 15 min after bacterial entry into human monocytes (Horwitz, 1983b). The mitochondria-LCV interaction is retained late into the intracellular cycle as mitochondria have been observed in association with LCVs as late at 45 h post infection in HeLa cells (Garduno et al., 1998b). Vacuoles containing a spontaneous avirulent mutant, later determined to be a *dot/icm* mutant, do not recruit mitochondria or smooth vesicles (Horwitz, 1987; Marra et al., 1992). Mitochondria and smooth vesicles remain attached to LCVs after isolation by cell fractionation indicating a very strong interaction (Tilney et al., 2001). The significance of mitochondria recruitment and association with the LCV in the pathogenesis of *L. pneumophila* has not been determined.

2.1.5.2. Inhibition of Phagosome-Lysosome Fusion

The newly formed LCV does not acidify or fuse with lysosomes in human monocytes, thus avoiding the default endocytic pathway (Clemens and Horwitz, 1995; Horwitz and Maxfield, 1984; Horwitz, 1983c; Sauer et al., 2005b; Wieland et al., 2004). It should be noted that LCVs mature into acidic phagolysosomes by 18 h post-infection in A/J mouse bone marrow-derived macrophages (Sturgill-Koszyki and Swanson, 2000), whereas LCVs remain nonacidic and LAMP-1 (lysosome-associated membrane protein 1) negative in human macrophages (Sauer et al., 2005b; Wieland et al., 2004). LCVs lack Rab5 and Rab7 confirming their seclusion from the endocytic network (Clemens et al., 2000). Rab5 and Rab7 are small GTPases that regulate endocytic membrane-trafficking

interactions (Duclos et al., 2003; Feng et al., 1995). Contrary to vacuoles containing wild-type *L. pneumophila*, vacuoles containing *dot/icm* mutants acquired Rab5 and Rab7 in a temporal pattern typical of phagosomes that progress into mature phagolysosomes (Clemens et al., 2000; Roy et al., 1998). Characterization of the intracellular fate of *dot/icm* mutants demonstrated that such mutants are unable to avoid fusion with lysosomes, thus, confirming the involvement of the Dot/Icm system in this LCV trafficking event (Berger et al., 1994; Horwitz, 1987; Marra et al., 1992; Roy et al., 1998; Swanson and Isberg, 1996; Wiater et al., 1998). In fact, Roy et al. (1998) found that vacuoles containing *dotA* mutant bacteria were positive for a transmembrane protein found in late endosomes and lysosomes, LAMP-1, as early as 5 min after internalization demonstrating that avoidance of the endocytic pathway occurs within minutes of uptake.

Dot/Icm-independent factors also appear to be involved in preventing phagosome-lysosome fusion. Phagosomes containing live PE phase *dot/icm* mutants accumulated LAMP-1, but did not acquire lysosomal and endosomal markers until 18 h post infection (Joshi et al., 2001). Exponential phase bacteria were immediately delivered to lysosomes (Joshi et al., 2001). This shows that although a functional Dot/Icm system is required to avoid LAMP-1 positive compartments, the ability to evade lysosomes may also be Dot/Icm independent. Avoidance of fusion with lysosomes is likely mediated by a pre-formed surface component since this inhibition is not overcome by inhibition of bacterial protein synthesis with erythromycin (Horwitz and Silverstein, 1983) and is resistant to formalin treatment (Joshi et al., 2001). Recently, latex beads coated with LPS-rich membrane vesicles shed by PE phase *L. pneumophila* or *dotA* mutants (but not exponential phase bacteria) were found to inhibit phagosome-lysosome fusion

(Fernandez-Moreira et al., 2006). A link to the developmental cycle was made since the composition of membrane vesicles and the LPS profile of *L. pneumophila* change as the bacteria differentiate (Fernandez-Moreira et al., 2006). To summarize, inhibition of phagosome-lysosome fusion by *L. pneumophila* is a developmentally regulated process involving both Dot/Icm-dependent and independent factors.

2.1.5.3. Interactions with the ER

Most proteins that are secreted or transported to other cellular organelles are synthesized by ribosomes attached to the ER (Matlack et al., 1998). These proteins are translocated co-translationally into the ER lumen where they are sorted and trafficked to various cellular destinations. Carbohydrates and lipids are also transported along this route. Vesicles containing cargo proteins bud off at ER exit sites, traffic through the ER-Golgi intermediate compartment (ERGIC), and eventually to the Golgi apparatus for additional post-translational modifications and sorting. Anterograde trafficking (from the ER to Golgi) is a complex process regulated by numerous molecular components including vesicle coat proteins (Barlowe, 2002; Spang, 2002), small regulatory GTPases (Zerial and McBride, 2001), and cognate soluble N-ethylmaleimide-sensitive fusion protein attachment receptor (SNAREs) (Chen and Scheller, 2001). Secretory vesicles are an ideal source of lipids for an intracellular pathogen looking to expand or remodel its phagosome membrane, and their cargo provides a source of amino acids as nutrients to support bacterial growth.

The nascent LCV becomes surrounded by smooth vesicles within 15 min after *L. pneumophila* internalization (Horwitz, 1983b; Tilney et al., 2001). These vesicles make

contact with and flatten along the surface of the LCV (Tilney et al., 2001). *L. pneumophila* converts the LCV membrane (initially derived from the plasma membrane during phagocytosis) into a membrane with the same thickness as the membrane of the recruited vesicles, indicating an exchange of membrane contents between the two compartments (Tilney et al., 2001). The ER was implicated as the source of these smooth vesicles due to the presence of ER markers on the associated vesicles and the similarity in membrane thickness between the vesicles and the ER (Abu Kwaik, 1996; Swanson and Isberg, 1995; Tilney et al., 2001). A more recent study confirmed that host vesicles attached to the LCV are derived from the ER (Robinson and Roy, 2006). Furthermore, lumenal ER markers within the attached vesicles were delivered into the lumen of the LCV (Robinson and Roy, 2006). By 2-4 h after entry, LCVs are covered with ribosomes and are surrounded by the ER (Horwitz, 1983b; Swanson and Isberg, 1995).

Several host factors involved in remodeling the LCV into an ER-like organelle have been identified. Arf1, Rab1 and Sec22b are recruited to the LCV in a Dot/Icm-dependent process (Derre and Isberg, 2004; Kagan and Roy, 2002; Kagan et al., 2004). All three factors are known to regulate membrane transport and fusion of early secretory vesicles (Chen and Scheller, 2001; Spang, 2002; Zerial and McBride, 2001). Dorer et al. (2006) confirmed that the host secretory pathway was required for the formation of a replicative vacuole. Multiple steps in the secretory pathway had to be targeted by RNA interference (RNAi), e.g., knockdown of Sec22b in combination with components of transport of protein particles (TRAPP) complex, to suppress intracellular replication of *L. pneumophila* (Dorer et al., 2006). Interestingly, the same study also found that knockdown of ER-associated degradation (ERAD) components, in particular Cdc48/97,

inhibited intracellular growth. Cdc48/97, a cytosolic component of the ERAD that removes ubiquinated proteins targeted for degradation on the ER surface, promoted the removal of bacterial effectors from the replicative vacuole (Dorer et al., 2006). In order to generate a replicative vacuole, *L. pneumophila* exploits a host degradation pathway and multiple aspects of the early secretory pathway to sustain LCV interactions with the ER.

2.1.5.4. Autophagy

Cellular autophagy is a membrane trafficking mechanism in eukaryotic cells for the turnover of proteins and organelles during starvation conditions (Kim and Klionsky, 2000). Bulk protein degradation begins with the sequestration of cytoplasmic components within double membrane structures known as autophagosomes. Autophagosomes fuse with the endocytic pathway and eventually mature into autolysosomes. The origin of autophagosomal membranes is unclear, although the ER has been suggested as a source due to some ultrastructural similarities between the two compartments and the presence of some rough ER (RER) marker proteins localized to autophagosomes (Dunn, 1990). Autophagosome biogenesis is regulated by two protein conjugation steps (Kim and Klionsky, 2000). Cytosolic Atg7 enzyme redistributes to the sequestration membrane where it sequentially catalyzes the conjugation of Atg12 to Atg5, followed by conjugation of Atg8 to phosphatidylethanolamine. The Atg5/Atg12 complex is lost upon the closure of the sequestration crescent into a double-membrane-bound autophagosome, whereas the Atg8 remains associated with the autophagosome until it fully matures into an autolysosome.

The autophagic pathway has been implicated in the formation of the *L. pneumophila* replicative vacuole in mammalian cells: 1) LCVs were shown to be surrounded by double membranes resembling nascent autophagosomes by transmission electron microscopy (Swanson and Isberg, 1995), 2) the stimulation of host autophagy increased the association of intracellular bacteria with the ER and enhanced bacterial growth (Swanson and Isberg, 1995), and 3) LCVs sequentially recruited autophagic markers, Atg7 and Atg8, and correlated with the immediate evasion of the endocytic pathway (Amer and Swanson, 2005). However, the involvement of autophagy in biogenesis of the LCV has been disputed. Electron microscopy ultrastructural analysis by Tilney et al. (2001) found the structures surrounding the bacteria to be RER. Autophagosomes, unlike the LCV, have not been observed with attached ribosomes (Kim and Klionsky, 2000). Lastly, mutation of *atg1, atg5, atg6, atg7* and *atg8* genes produced the expected defects in autophagy in *D. discoideum*, but there was no effect on either the intracellular growth of *L. pneumophila* or on the morphology of the LCV (Otto et al., 2004). The requirement for the autophagic pathway may be different for the formation of a replicative vacuole despite the similarities in other aspects of *L. pneumophila* infection in these evolutionarily distant hosts. *L. pneumophila* may only target certain aspects of the autophagic machinery in mammalian cells, whereas autophagy is not required at all for bacterial replication in protozoa. Analogous mutations in mammalian cells are required to fully assess whether these autophagy genes affect the formation, morphology, and function of the replicative vacuole.

2.1.5.5. Exit from Host Cells

After intracellular replication, release of bacteria from the spent host is required for the infection of new susceptible hosts and the establishment of a new niche for replication. *L. pneumophila* exits mammalian hosts in two stages: 1) induction of apoptosis which is independent of growth phase (Gao and Abu Kwaik, 1999b; Hagele et al., 1998), followed by 2) induction of necrosis mediated by growth phase-dependent expression of pore-forming activity (Alli et al., 2000; Byrne and Swanson, 1998). A necrotic cell will swell and burst due to physical injury, eventually leading to the development of an inflammatory response (Fiers et al., 1999). In contrast, apoptosis is a controlled cell suicide program characterized by a pronounced decrease in cell volume, membrane blebbing, chromatin condensation, nuclear fragmentation, and organelle clustering (Fiers et al., 1999). This process is mediated by a family of cysteine proteases known as caspases. *L. pneumophila* induces the activation of caspase-3 in a *dot/icm* dependent manner during the initial stages of infection (Fischer et al., 2006; Gao and Abu Kwaik, 1999a; Muller et al., 1996; Zink et al., 2002). Caspase-3 activation was shown to be required for the evasion of phagosome-lysosome fusion and intracellular replication (Molmeret et al., 2004). Despite early activation of caspase-3, Abu-Zant et al. (2005) found that apoptosis was not triggered until intracellular replication had ceased. Indeed, *L. pneumophila*-infected macrophages were found to be resistant to apoptosis-inducing agents, staurosporine and TNF-α (tumor necrosis factor α) in a Dot/Icm-dependent manner (Abu Zant et al., 2007). The delay in apoptosis was determined to be due to the induction of a strong anti-apoptotic signaling cascade involving the activation of NF-κB (nuclear factor-κB) (Abu Zant et al., 2007). Thus, in order to have time to replicate

within mammalian hosts, *L. pneumophila* stalls the induction of apoptosis by triggering anti-apoptotic signaling pathways to counteract the effect of caspase-3 induction (Abu Zant et al., 2007).

After intracellular replication ceases, necrotic killing of the host cell is mediated by a pore-forming toxin (Alli et al., 2000; Gao and Abu Kwaik, 2000; Kirby et al., 1998). Pore formation is dependent on IcmT (Molmeret et al., 2002). The *icmT* locus was able to complement five *rib* (release of intracellular bacteria) mutants that were able to grow intracellularly, but remained trapped within host protozoa and macrophages (Alli et al., 2000; Gao and Abu Kwaik, 2000; Molmeret et al., 2002). A working model of growth phase-dependent cytolysis by *L. pneumophila* proposes that expression of pore-forming activity occurs upon transition into PE phase. Insertion of pores into the phagosome membrane results in disruption of the phagosome, followed by insertion of pores into the plasma membrane leading to host cell lysis and release of intracellular bacteria (Alli et al., 2000). In protozoan hosts, *L. pneumophila* induces necrosis, but not apoptosis, to exit its host cell (Gao and Abu Kwaik, 2000; Hagele et al., 1998). In addition, two Dot/Icm secretion system effector proteins, LepA and LepB, were found to promote the nonlytic release of *L. pneumophila* from protozoan but not mammalian cells (Chen et al., 2004). Despite using a common mechanism to kill and exit evolutionarily distant host cells, *L. pneumophila* is also able to exploit an exit strategy that is unique to its protozoan hosts.

2.1.6. The Dot/Icm System

Type IV secretion systems (T4SS) are homologous to conjugation systems that deliver proteins or nucleoprotein complexes across membranes into the cytosol of the

target eukaryotic host cell (Christie and Vogel, 2000). *L. pneumophila* has at least two T4SS. A third putative T4SS has been identified with homology to the Tra proteins associated with plasmid F in *E. coli* (Brassinga et al., 2003). The Lvh (*Legionella virB* homologs) system is a Type IVA secretion system homologous to the *Agrobacterium tumefaciens* T-DNA transfer apparatus (Segal et al., 1999). The Dot/Icm (defective in organelle trafficking/intracellular multiplication) system is a Type IVB secretion system with extensive similarities to the Tra/Trb conjugal plasmid transfer apparatus (See Figure 2.2) (Berger and Isberg, 1993; Marra et al., 1992; Segal et al., 1999; Sexton and Vogel, 2002; Vogel et al., 1998). Both systems are capable of mediating the conjugation of the plasmid RSF1010 (Segal and Shuman, 1998b; Vogel et al., 1998). Components of the Lvh system can compensate for mutations in *dotB* and *dotG* in plasmid conjugation, but not for virulence (Segal et al., 1999). The Lvh system is dispensable for intracellular replication of *L. pneumophila* in human macrophages and *A. castellanii* (Segal et al., 1999), whereas the Dot/Icm system is required for virulence and initiation of intracellular growth (Berger and Isberg, 1993; Marra et al., 1992; Segal et al., 1999).

The Dot/Icm system is encoded by 26 genes found on two loci in the *L. pneumophila* genome (See Figure 2.2) (Sexton and Vogel, 2002). Few of the Dot/Icm components have been fully characterized. DotA, DotL, DotU, and IcmF are inner membrane proteins. DotA is an inner membrane protein with eight transmembrane domains that may act as a scaffolding protein (Roy and Isberg, 1997). More recently, DotA was shown to be secreted by the Dot/Icm system into culture supernatants but the function of the secreted protein is unknown (Nagai and Roy, 2001). DotL has been proposed to serve gatekeeper functions to prevent unregulated transport of effectors

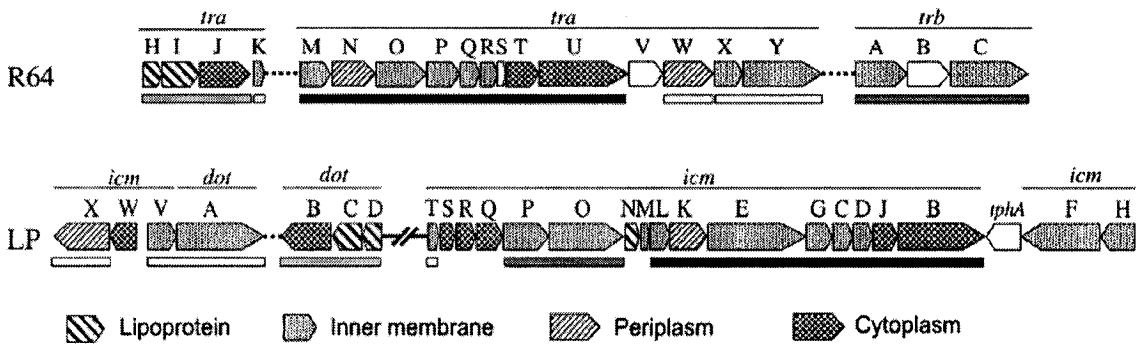

Figure 2.2. Organization of the Type IVB Secretion System Genes from the IncI Plasmid R64 and from *L. pneumophila*.
Arrows indicate genes and their orientation. Bars below the genes indicate gene homology, dotted line indicates a region of unrelated genes, and diagonal lines indicate a large gap. From Segal et al., 2005.

through the translocon (Buscher et al., 2005). DotU and IcmF are accessory components that protect the apparatus from degradation (Sexton et al., 2004a; VanRheenen et al., 2004). IcmX is a periplasmic protein essential for host cell pathogenesis although its function remains to be determined (Matthews and Roy, 2000). DotB, IcmQ, IcmR, IcmS, and IcmW are cytoplasmic proteins. DotB is a hexameric protein capable of hydrolyzing ATP (Sexton et al., 2004b). DotB may prove to be the driving force to export substrates through the Dot/Icm apparatus because mutations in the DotB ATP-binding domain resulted in a mutant protein that failed to hydrolyze ATP and could not complement a *dotB* deletion mutant for growth in macrophages (Sexton et al., 2004b). IcmR was demonstrated to be a chaperone for IcmQ (Dumenil and Isberg, 2001). Purified IcmQ was shown to form pores in lipid membranes, and pore formation was inhibited by IcmR (Dumenil et al., 2004). IcmS and IcmW interact with each other as well as a number Dot/Icm secreted proteins suggesting that they function as adaptors to target substrates to the T4SS (Bardill et al., 2005; Coers et al., 2000; Ninio et al., 2005). IcmS also interacts with LvgA (*Legionella* virulence gene A); this interaction may provide additional adaptor complex function (Vincent and Vogel, 2006). DotC, DotD, DotF, DotG, and DotH form the core subcomplex that spans the inner and outer membranes (Vincent et al., 2006). DotF and DotG are inner membrane proteins that associate with DotH, DotC and DotD in the outer membrane. IcmT is required for pore formation in macrophages and protozoa (Gao and Abu Kwaik, 2000; Molmeret et al., 2002). The subcellular location of most of the remaining proteins encoded within the *dot/icm* loci have been predicted based on sequence data: IcmB, IcmC, IcmD, IcmJ, IcmL, IcmM, and IcmP are localized to the inner membrane, and DotK is localized to the outer membrane (Segal et al., 1998).

The *dot/icm* genes were identified by genetic screens aimed at identifying genes required for intracellular growth and host cell killing (Berger and Isberg, 1993; Marra et al., 1992). Analysis of the intracellular fate of *dot/icm* mutants revealed that these mutants are unable to evade the endocytic pathway or recruit host organelles (Berger et al., 1994; Horwitz, 1987; Marra et al., 1992; Swanson and Isberg, 1996). Unlike other *dot/icm* mutants that are completely defective for intracellular growth, *icmS, icmW,* and *icmR* mutants demonstrate a limited capacity to replicate within macrophages (Coers et al., 2000). Interestingly, internalized *icmS* or *icmW* mutants are unable to avoid fusion with lysosomes, but they are still able to recruit smooth vesicles to the LCV (Coers et al., 2000; Tilney et al., 2001). Phagosomes containing *icmR* mutants manage to avoid the endocytic compartment initially, and yet these phagosomes do not support efficient replication (Coers et al., 2000). These observations suggest that evasion of phagosome-lysosome fusion and LCV remodeling are independent events requiring the function of different Dot/Icm-dependent factors (Coers et al., 2000).

In addition to these characteristics, other phenotypes relevant to pathogenesis have been attributed to the *dot/icm* genes. The Dot/Icm system appears to play a role in the uptake of *L. pneumophila* into host cells. Wild-type *L. pneumophila* was more efficiently phagocytosed by macrophages and protozoa than *dot/icm* mutants (Hilbi et al., 2001). Macropinocytotic uptake of *L. pneumphila* into mouse macrophages was enhanced by the presence of a functional Dot/Icm system (Watarai et al., 2001). Cytolysis resulting from pore formation was found to be dependent on the Dot/Icm system (See Section 2.1.5.5) (Gao and Abu Kwaik, 2000; Kirby et al., 1998; Molmeret et al., 2002). The

Dot/Icm system is required for the induction and delay of apoptosis in macrophages (See Section 2.1.5.5) (Abu Zant et al., 2007; Zink et al., 2002).

2.1.6.1. Dot/Icm Effector Proteins

Numerous proteins have been identified as putative effectors for the *L. pneumophila* Dot/Icm system (See Table 2.1). RalF (recruitment of Arf to the *Legionella* phagosome factor) was the first effector demonstrated to translocate via this secretion system (Nagai et al., 2002). RalF was found to activate and recruit ARF1 (ADP ribosylation factor), a small GTPase that regulates vesicle traffic between the ER and Golgi, to the LCV by acting as an ARF-GEF (ARF-guanine nucleotide exchange factor) (Nagai et al., 2002). LidA (lowered viability in the presence of *dot*) was identified in a genetic screen for substrates that showed high viability in the absence of a functional Dot/Icm system and low viability in the presence of an intact translocation system (Conover et al., 2003). LidA was found to localize to the cytoplasmic face of the LCV and its ectopic expression in eukaryotic cells resulted in the disruption of the ERGIC compartment (Derre and Isberg, 2005). Recently, LidA was shown to collaborate with SidM in recruiting early secretory vesicles to the LCV by targeting a small regulatory GTPase Rab1 (Machner and Isberg, 2006). SidM functions as a guanine nucleotide exchange factor for Rab1 (Machner and Isberg, 2006; Murata et al., 2006). The Sid (substrate of Icm/Dot) family of proteins was identified by a global approach using a bacterial two-hybrid screen (IcmG/DotF was used as bait) in combination with a bacterial protein translocation assay (Luo and Isberg, 2004). Many of the Sid proteins have one or more paralogs present in the *L. pneumophila* genome. SidC was shown to be translocated

Table 2.1. Effectors Delivered by the *Legionella pneumophila* Dot/Icm Secretion System.

Effectors	Size (aa)	Localization after translocation	Function	Reference
RalF	374	Cytoplasmic face of LCV	Guanine nucleotide exchange factor for ARF proteins	Nagai et al., 2002
LidA	729	Cytoplasmic face of LCV	Recruitment of Rab1 and early secretory vesicles to LCV	Conover et al., 2003; Derre and Isberg, 2005
LepA	1151	Unknown	Release of *L. pneumophila* from protozoa	Chen et al., 2004
LepB	1294	Unknown	Release of *L. pneumophila* from protozoa	Chen et al., 2004
YlfA	425	Host cytoplasm, early secretory vesicles	* Recruitment of early secretory vesicles to LCV	Campodonico et al., 2005
YlfB	405	Unknown	Unknown	Campodonico et al., 2005
VipA	339	Unknown	Inhibit lysosomal protein trafficking in yeast	Shohdy et al., 2005
VipD	615	Unknown	Inhibit lysosomal protein trafficking in yeast	Shohdy et al., 2005
VipF	286	Unknown	Inhibit lysosomal protein trafficking in yeast	Shohdy et al., 2005
Sid Family				
SidA	474	Translocation into host cells not confirmed	Unknown	Luo and Isberg, 2004
SidB	417	Translocation into host cells not confirmed	Unknown	Luo and Isberg, 2004

SidC (paralog: SdcA)	917 (908)	Anchors to PI4P on the cytoplasmic face of LCV	* LCV biogenesis or bacterial egress from host cell	Luo and Isberg, 2004; Weber et al., 2006
SidD	507	Translocation into host cells not confirmed	Unknown	Luo and Isberg, 2004
SidE family (SidE, SdeA, SdeB, SdeC)	(1495, 1504, 1926, 1538)	Cytoplasmic face of LCV (shown for SdeA only)	* Early events in LCV biogenesis	Luo and Isberg, 2004; Bardill et al., 2005
SidF	912	Translocation into host cells not confirmed	Unknown	Luo and Isberg, 2004
SidG	965	Translocation into host cells not confirmed	Unknown	Luo and Isberg, 2004
SdhA (paralogs: SidH, SdhB)	1429 (2225, 1875)	Cytoplasmic face of LCV	Prevent host cell death	Laguna et al., 2006
SidM (DrrA)	647	Cytoplasmic face of LCV	Guanine nucleotide exchange factor for Rab1	Machner and Isberg, 2006; Murata et al., 2006

* Putative function

into the host by the Dot/Icm system (Luo and Isberg, 2004), and was later shown to specifically bind to phosphatidylinositol-4-phosphate (PI4P) found on the LCV (Weber et al., 2006). LepA (*Legionella* effector protein A) and LepB were identified based on the presence of α-helical coiled-coils commonly found in SNAREs; these two proteins were found to be translocated by the Dot/Icm system and were involved in the release of *L. pneumophila* from protozoa (Chen et al., 2004). The Vip (vacuole protein sorting [VPS] inhibitor protein) effectors were identified using a screening system in yeast that interfered with membrane trafficking (Shohdy et al., 2005). Three of four Vip genes identified were shown to be translocated from *L. pneumophila* into macrophages via the Dot/Icm system. All three are structurally distinct and inhibited trafficking in yeast by different mechanisms (Shohdy et al., 2005). YlfA (yeast lethal factor A) was identified independently using a yeast genetic system to screen for *L. pneumophila* proteins that interfered with yeast growth (Campodonico et al., 2005). A paralog of YlfA, YlfB, was identified on an unlinked region of the chromosome. Both proteins were translocated by the Dot/Icm system into host cells. YlfA was found in the host cytoplasm after translocation but a hydrophobic domain at the N-terminus of YlfA also targets the protein to vesicles of the early secretory pathway several hours after infection indicating a role in the recruitment of such vesicles to the LCV.

None of the *L. pneumophila* strains lacking single or multiple effectors described above demonstrate any acute defect in the ability to grow intracellularly which has been attributed to the apparent functional redundancy of effectors and the multiple points of the secretory pathway that are targeted in host cells. Recently, *L. pneumphila* mutants lacking the Dot/Icm substrate SdhA were found to be severely impaired for intracellular

growth in mouse bone marrow derived macrophages (Laguna et al., 2006). The defect in intracellular growth was attributed to the increased host cell death caused by infection with the *L. pneumophila sdhA* mutant since phagosomes containing the *L. pneumophila sdhA* mutant were able to avoid the endocytic pathway (Laguna et al., 2006). SdhA was proposed to play a role in preventing host cell death, thus preventing premature termination of intracellular replication (Laguna et al., 2006). The intracellular growth defect was amplified with a triple mutant of SdhA, and its two paralogs SidH and SdhB (Laguna et al., 2006). Single mutations affecting SidH and SdhB had little effect on *L. pneumophila* intracellular growth supporting the theory of functional overlap amongst the Dot/Icm effectors (Laguna et al., 2006).

2.2. Chaperonin Biology

2.2.1. Classification

Molecular chaperones are composed of several families of unrelated proteins that transiently assist in the assembly and disassembly of macromolecules in vivo, but are not components of the final assembled structures (Ellis, 1993). Chaperonins are a class of molecular chaperones with highly related sequences found in nearly all organisms (Gupta, 1995). They oligomerize into radially symmetric double ring structures to perform their function as protein folders (Lin and Rye, 2006). Folding of the non-native polypeptide bound within the central cavity of the ringed structure is ATP-dependent. Based on phylogenetic analysis, the chaperonins are classified into two groups (Gupta, 1995). This section will provide a general comparison between the two chaperonin groups.

Group I chaperonins (GroEL, Hsp60, Cpn60) are found in eubacteria, chloroplasts, and mitochondria (Bukau and Horwich, 1998). They assemble into two homomultimeric rings of seven subunits each stacked on top of each other (Braig et al., 1994; Braig et al., 1995). These chaperonins work in conjunction with a co-chaperonin (GroES, Hsp10, Cpn10) that also forms a homoheptameric ring (Xu et al., 1997). Association of the co-chaperonin ring with the chaperonin complex is dependent on ATP binding to the latter complex. The co-chaperonins function as a lid over the folding cavity of the chaperonin complex that can enclose non-native polypeptides of up to ~60-kDa during a protein folding cycle (Brinker et al., 2001). Proteins too large to be enclosed can still use the complex for folding through multiple rounds of binding and release with the chaperonin ring *in trans* to the bound co-chaperonin (Chaudhuri et al., 2001). The *E. coli* chaperonin, GroEL, has been found to interact with approximately 300 polypeptides in vivo (Houry et al., 1999); however, only 85 of these are absolutely dependent on GroEL for folding (Kerner et al., 2005). Thirteen of the 85 are essential proteins which explains why GroEL is required under all growth conditions (Fayet et al., 1989; Kerner et al., 2005). To date, multiple *groEL* gene sequences have been detected among α-proteobacterial genomes such as *Sinorhizobium meliloti* (5 copies), *Bradyrhizobium japonicum* (5 copies), *Rhodobacter sphaeroides* (2 copies) (Gupta, 1995; Karlin and Brocchieri, 2000). Duplications have also been found in *Chlamydiae, Cyanobacteria* and several Gram positive species (Gupta, 1995; Karlin and Brocchieri, 2000; Karunakaran et al., 2003). The presence of multiple *groEL* genes have been attributed to independent gene duplication events (Gupta, 1995), although the reason for these duplications is unclear.

Group II chaperonins are found in the cytosol of archaea and eukaryotic cells (Valpuesta et al., 2002). These chaperonins are also known as T-complex polypeptide 1 (TCP-1), TCP-1 ring complex (TriC) or chaperonin-containing Tcp-1 (CCT). The oligomeric ring assemblies of Group II chaperonins are much more complex in comparison to the Group I assemblies. The CCT complex consists of eight distinct subunits in each ring (Frydman et al., 1992; Gutsche et al., 1999; Lewis et al., 1992). Each subunit is encoded by different but homologous genes thought to have evolved by gene duplication from a common ancestor (Archibald et al., 2000; Kubota et al., 1994). Group II chaperonins do not require association with co-chaperonins in order to function. Instead, the central ring cavity is capped by an extra region at the tip of the apical domain of Group II chaperonins (Gutsche et al., 1999; Llorca et al., 2001). Sealing of the group II chaperonin complex cavity, similarly to that of the Group I chaperonin cavity, is an ATP dependent event (Llorca et al., 1994; Llorca et al., 2001). Actin and tubulin were the first in vitro and in vivo substrates described for the Group II chaperonins (Frydman et al., 1992; Gao et al., 1992; Sternlicht et al., 1993). Although GroEL has been shown to bind to actin and tubulin, it cannot fold these cytoskeletal proteins (Tian et al., 1995). A still expanding list of substrates that interact with Group II chaperonins has since been identified and include proteins such as cofilin, actin-depolymerization factor 1, cyclin E, myosin heavy chain, Von Hippel-Lindau tumor suppressor protein (reviewed by Spiess et al., 2004). The overall structural similarity between the two chaperonin groups indicates a conservation of design either due to a common origin or to convergent evolution; the differences between them is likely a reflection of the independent evolution needed to adapt to their respective environments.

2.2.2. GroEL Chaperonin Structure and Protein Folding Cycle

Most of the information regarding structure and function of the Group I chaperonins comes from studies of GroEL. Each GroEL monomer is a 57-kDa protein with 547 amino acids folded into three functional domains (See Figure 2.3a) (Hemmingsen et al., 1988; Lin and Rye, 2006). The equatorial domain houses the residues involved in intersubunit interactions and ATP binding (Braig et al., 1994). Inter-ring contacts are also mediated by the equatorial region. The equatorial region is connected to the apical domain via a slender hinge-like intermediate domain. The apical domain makes up the mouth of the central cavity and contains the binding sites for substrates and GroES (Braig et al., 1993; Fenton et al., 1994). The cavity is lined with hydrophobic amino acid residues from two α-helices of the apical domain that bind the exposed hydrophobic residues of the non-native protein substrate (Braig et al., 1995; Xu et al., 1997). Domain analysis of GroEL substrates revealed that GroEL preferentially binds to substrates with multiple αβ domains which typically have α-helices and β-sheets containing extensive hydrophobic surfaces (Houry, 2001).

The folding cycle begins with substrate binding to the open *trans* ring of the GroEL-GroES complex, followed by the binding of seven ATP molecules (one to each GroEL subunit) and a seven membered GroES ring to the newly occupied GroEL ring (See Figure 2.3b) (Xu et al., 1997). Mobile β-hairpin loop segments in GroES mediate contact with the GroEL apical domain (Xu et al., 1997). A global conformational change occurs upon GroES binding (See Figure 2.3a). The lower hinge of the intermediate

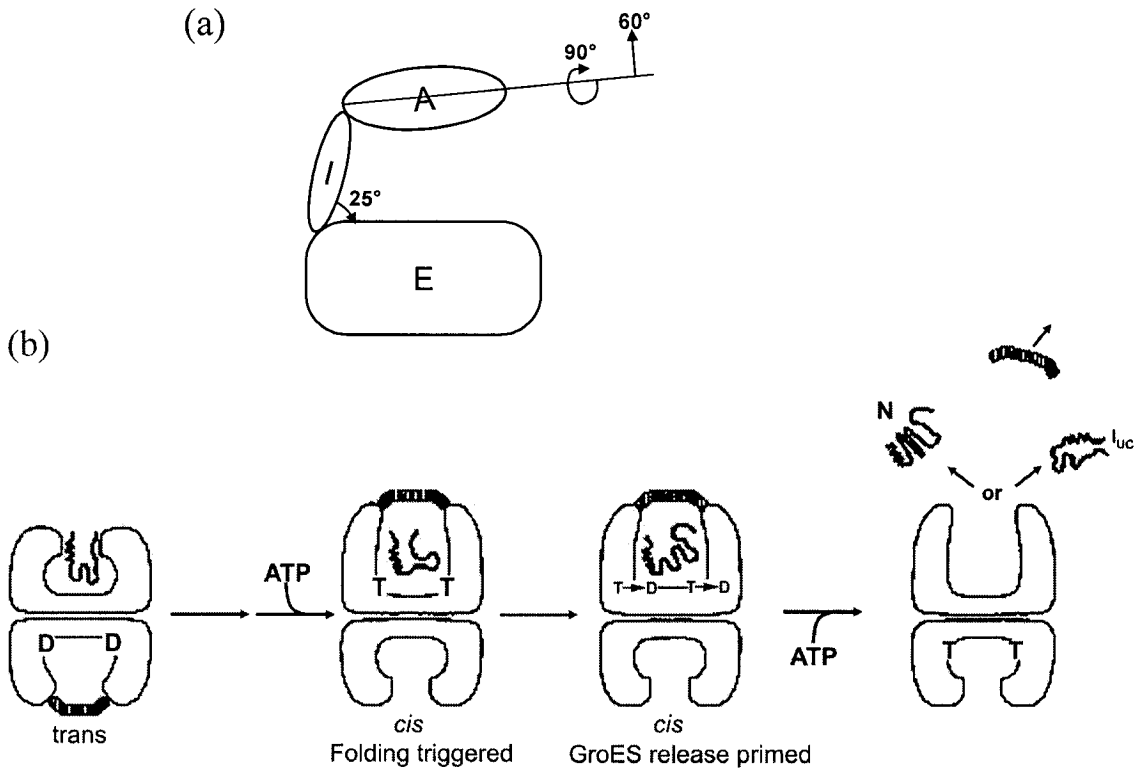

Figure 2.3. Monomeric Structure of GroEL and the Protein Folding Cycle.
(a) The GroEL monomer has an apical (A), an intermediate (I), and an equatorial (E) domain. Adapted from Bukau and Horwich, 1998. (b) The non-native protein substrate binds to the open *cis* ring. Upon ATP and GroES binding to the GroEL ring complex, the intermediate domain rotates downwards 25° to lock in the ATP molecule. The apical domain swings upwards 60° and rotates around its axis 90° to release the bound substrate into the enlarged central cavity. Hydrolysis of ATP primes the release for GroES from the complex. Binding of ATP to the *trans* ring ejects GroES and the protein from the cavity. The released protein is either fully folded into its native (N) form, or non-native form that must be rebound by chaperonin or by a different chaperone to reach native form (I_{UC}). From Rye et al., 1997.

domain rotates 25° downward onto the equatorial domain locking in the bound ATP; the upper hinge of the intermediate domain rotates 60° upwards elevating the apical domain which is accompanied by a 90° clockwise rotation about its axis (Xu et al., 1997). Elevation of the apical domains results in an enlarged central cavity from 85 000 $Å^3$ to 175 000 $Å^3$ (Xu et al., 1997). The hydrophobic lining of the cavity is twisted away from the non-native substrate which is released into the now hydrophilic cavity. Substrate release into the cavity occurs within one second of ATP and GroES binding (Rye et al., 1997). The GroEL-GroES *cis* complex will not dissociate until ATP in the *cis* complex is hydrolyzed, thus folding is timed by the hydrolysis of ATP giving the substrate ~20 s in the folding conducive cavity (Rye et al., 1997). The GroEL-GroES interaction weakens once ATP hydrolysis on the *cis* ring takes place, and the GroES ring is released from the complex with the binding of 7 ATP molecules to the *trans* ring. Substrate binding to the open *trans* ring facilitates GroES release, but this has been found to occur only after ATP hydrolysis (Rye et al., 1999). This ensures that folding occurs only on one ring at any given time. Following disassembly of the GroES lid, the protein is ejected from the cavity regardless of whether it is folded (Todd et al., 1994; Weissman et al., 1994; Weissman et al., 1995). A released protein with remaining hydrophobic surfaces can be recaptured for multiple folding cycles until the proper conformation is achieved (Weissman et al., 1994).

2.2.3. Organization and Regulation of the Chaperonin Genes in Bacteria

The *groES* and *groEL* genes form a bicistronic operon (with *groES* upstream of *groEL*) known as the *groE* operon in *E. coli* (Hemmingsen et al., 1988). Analysis of *groE*

operons from numerous bacteria indicates that the organization of the operon is highly conserved as they are all arranged in the same order of promoter-*groES-groEL* (Segal and Ron, 1996). The exception to this organization is in *Mycobacterium bovis* where the two genes are not in an operon (Segal and Ron, 1996). In bacteria with multiple copies of *groEL*, the *groEL* genes are organized as monocistronic operons in addition to the *groE* operon or as multiple *groE* operons (Segal and Ron, 1996). For example, *M. tuberculosis* has a *groE* operon and a second separate *groEL* gene (Kong et al., 1993; Rinke de Wit et al., 1992), and *S. meliloti* has four *groE* operons and one *groEL* gene (Capela et al., 2001; Rusanganwa and Gupta, 1993).

In *E. coli*, the *groE* operon is regulated as part of the main heat shock regulon by the alternative sigma factor σ^{32} (Yura et al., 1993). σ^{32} recognizes the heat inducible promoters (TCTNCCTTGAA-N_5-CCCCATNTA) directly upstream of heat shock genes (e. g., *dnaK, lon, clpP, htpg, grpE, groE*) and acts as a transcriptional activator (Yura et al., 1993). σ^{32} levels are regulated by two mechanisms. Translation of σ^{32} increases with temperature owing to the destabilization of a secondary RNA structure that overlaps the translation start (Morita et al., 1999; Yura et al., 1993). Under normal conditions, DnaK facilitates the degradation of σ^{32} (Yura et al., 1993). Upon exposure to heat or other stresses that brings about protein denaturation, unfolded proteins sequester DnaK from σ^{32} which is then free to induce the heat shock genes (Yura et al., 1993). The *groE* operon has a second promoter immediately downstream of the heat shock promoter that is recognized by the vegetative sigma factor, σ^{70}, to ensure the constitutive expression of the *groE* operon at all temperatures (Zeilstra-Ryalls et al., 1991; Zhou et al., 1988). The *groE* operons from the proteobacteria division (e.g., *Neisseria gonorrhoeae, Coxiella*

burnetii, L. pneumophila, Salmonella typhi, Yersinia enterocolitic, Helicobacter pylori) are mainly regulated by σ^{32} (Segal and Ron, 1996).

In *Bacillus subtilis* and *Chlamydia trachomatis*, the *groE* operon is regulated by a transcriptional regulator HrcA (heat regulation at CIRCE) and an operator designated CIRCE (controlling inverted repeat of chaperone expression) (Mogk et al., 1997; Tan et al., 1996; Wilson et al., 2005; Yuan and Wong, 1995). This system has also been found to regulate the *dnaK* operon. The CIRCE element has been detected in numerous bacteria including *Mycobacteria, Cyanobacteria, Spirochaeta,* and some proteobacteria (Segal and Ron, 1996). CIRCE is an inverted repeat element (TTAGCACTC-N_9-GAGGCTAA) located between the transcription initiation site and the coding region (Segal and Ron, 1996). HrcA binds to CIRCE to repress transcription of the operon downstream (Schulz and Schumann, 1996). In *B. subtilis*, the HrcA regulatory system was found to be regulated by the level of unfolded protein in the cell similarly to the DnaK/σ32 titration model (Mogk et al., 1997; Yuan and Wong, 1995). The key chaperone here is GroEL rather than DnaK. The GroE chaperonins bind to and promote proper folding of HrcA. When GroEL levels are sequestered by unfolded proteins, large amounts of inactive HrcA repressor accumulate which leads to increased expression from the *dnaK* and *groE* operons (Mogk et al., 1997) . Conversely, overexpression of GroEL resulted in decreased expression from these operons. The *groE* operons of some bacteria such as *A. tumafaciens* (Segal and Ron, 1996) and *B. japonicum* (Babst et al., 1996) are regulated by both the HrcA/CIRCE system and σ^{32}.

In addition to transcriptional regulation, the *groE* operon can be regulated by a post-transcriptional mechanism. Deletion of the transcribed CIRCE in *B. subtilis* resulted

in increased stability of the *groE* transcript from 5 min to 17 min under non-heat-shock conditions (Yuan and Wong, 1995). Segal and Ron (1996) found that *groE* transcripts with deleted CIRCE had longer half lives in *A. tumefaciens*. Thus, CIRCE, when transcribed, is involved in regulating transcript stability. To summarize, the *groE* operon in bacteria is regulated as part of the stress response either by an alternative sigma factor or by an inverted repeat element or a combination of the two.

2.2.4. Accessory Functions of Bacterial Chaperonins

Chaperonins were initially characterized to be strictly cytoplasmic proteins because of their large molecular size, complex structural organization, and the lack of known secretion signals in chaperonin sequences examined to date. There is considerable evidence that a number of bacteria surface localize or secrete their chaperonins (Frisk et al., 1998; Garduno et al., 1998; Hennequin et al., 2001; Rao et al., 1994; Scopio et al., 1994; Yamaguchi et al., 1997). The extracytoplasmic chaperonins display a range of roles that are not necessarily related to their protein folding function, but are involved in bacterial virulence and host response to bacterial infection. This section will highlight some of the accessory functions mediated by bacterial chaperonins which include attachment to host cells, stimulation of the host immune system, and maintenance of bacterial endosymbiosis.

2.2.4.1. Chaperonins as Adhesion Factors

A diverse number of organisms have been reported to use their surface-exposed GroELs as adhesins or invasins. The surface-exposed GroEL of *Clostridium difficile* (Hennequin et al., 2001), *Helicobacter pylori* (Yamaguchi et al., 1997), and *Mycobacterium avium* (Rao et al., 1994) are involved in adherence. The *L. pneumophila* chaperonin mediates both attachment and invasion of host cells (Garduno et al., 1998a). GroEL from *Borrelia burgdoferi* and *Haemophilus ducreyi* bind to glycosphingolipids to mediate attachment to host cells (Kaneda et al., 1997; Pantzar et al., 2006). The *Salmonella enterica* serovar Typhimurium GroEL is responsible for bacterial aggregation and binding to the intestinal mucosa (Ensgraber and Loos, 1992). GroEL found on the surface of the probiotic bacterium *Lactobacillus johnsonii* La1 is involved in attachment to the intestinal mucus and epithelial cells, immunomodulation, and aggregation of *H. pylori*, indicating that GroEL plays a role in gastrointestinal homeostasis (Bergonzelli et al., 2006). Watarai et al. (2003) reported that the surface localized *Brucella abortus* GroEL binds to cellular prion protein (PrP^c) and mediates entry into host cells; however, both the surface localization of GroEL and its role in *Brucella* infection has been disputed (Fontes et al., 2005).

2.2.4.2. Chaperonins as Cell Signaling Molecules

Several studies demonstrate the ability of chaperonins to modulate host cell activities by functioning as cell signaling molecules. Chaperonins have been found to initiate signaling pathways by binding to immune receptors expressed on the surface of host cells. The innate immune system uses pathogen recognition receptors (PRRs) to bind

to conserved molecular structures (known as pattern-associated molecular patterns [PAMP]) found in pathogens (Medzhitov, 2001). PRRs can be secreted (e.g., LPS binding protein), expressed on the cell surface (e.g., toll like receptors [TLRs]) or reside in intracellular compartments (e.g., double-stranded RNA-activated protein kinase) (Medzhitov, 2001). Kol et al. (2000) found that human Cpn60 and chlamydial GroEL activate human monocytes through CD14 signaling, a pathway shared by LPS. A study by Vabulas et al. (2001) found that endocytosed human Cpn60 and chlamydial GroEL are recognized by both TLR2 and TLR4. More recent studies demonstrate that TLR4, but not TLR2, is the signaling receptor for chlamydial GroEL (Bulut et al., 2002; Sasu et al., 2001). Chlamydial and mycobacterial chaperonins have been shown to activate signaling pathways via TLR4 to induce NF-kB activation (Bulut et al., 2002; Bulut et al., 2005).

Chaperonins from other bacteria also have a stimulatory effect on mammalian cells. For example, purified GroEL from *M. bovis, M. leprae, E. coli* and *L. pneumophila* increased the steady-state levels of pro-inflammatory cytokine mRNA in macrophages (Retzlaff et al., 1994). GroEL from *E. coli* (Galdiero et al., 1997), *M. tuberculosis* (Friedland et al., 1993), and *C. trachomatis* (Kol et al., 1999) have been found to induce the production of pro-inflammatory cytokines by monocytes. Human vascular endothelial cells (HUVECs) were stimulated to produce multiple adhesion molecules by GroEL from *E. coli* (Galdiero et al., 1997) and *C. trachomatis* (Kol et al., 1999). In addition, GroEL from some bacterial pathogens can modulate the growth rate of cultured cells. GroEL from *C. pneumoniae* stimulates proliferation of human vascular smooth muscle cells via TLR4 and p44/42 mitogen-actvated protein kinase (MAPK) activation (Sasu et al., 2001). The GroEL secreted by *Actinobacillus actinomycetemcomitans* has been found to trigger

epithelial cell proliferation by activating the ERK1/2 (extracellular signal-regulated kinase 1/2) MAPKs, although prolonged exposure to GroEL is cytotoxic (Zhang et al., 2001; Zhang et al., 2004b). GroEL is also secreted by *Bartonella bacilliformis* (Minnick et al., 2003). The *B. bacilliformis* GroEL induces the proliferation of HUVECs, but the mechanism of induction is unknown (Minnick et al., 2003). A *B. bacilliformis* strain overexpressing GroEL was found to accelerate HUVEC apoptosis relative to strains producing less GroEL during infection (Smitherman and Minnick, 2005). Acceleration of apoptosis was inhibited by a pan-caspase inhibitor which led to the proposal that accumulation of GroEL produced by intracellular *B. bacilliformis* may stimulate caspase-3, analogous to caspase-3 stimulation by the human Cpn60 homolog, resulting in apoptosis (Smitherman and Minnick, 2005). In addition to altering cell growth, the GroEL from *A. actinomycetemcomitans* was found to be a potent mediator of bone resorption in an in vitro mouse bone model (Kirby et al., 1995). GroEL from *E. coli* also displayed osteolytic activity, but not GroEL from *M. tuberculosis* and *M. leprae* (Kirby et al., 1995). However, the co-chaperonin from *M. tuberculosis* did display osteolytic activity (Meghji et al., 1997). The osteolytic activities of the *E. coli* GroEL and the *M. tuberculosis* GroES were found to be due to their ability to induce osteoclast formation from myeloid precursors (Meghji et al., 1997; Reddi et al., 1998). The ability to stimulate cytokine production and alter growth offer evidence of the cell signaling/effector function of bacterial chaperonins in eukaryotic cells.

2.2.4.3. Autoimmune Diseases Associated with Chaperonins

Bacterial chaperonins are implicated in autoimmune disease due to two features: 1) high amino acid sequence conservation, and 2) high immunogenicity. Antibodies produced in response to the presence of bacterial chaperonins and T-cells activated by bacterial chaperonins can cross-react with and attack mammalian chaperonins to trigger an autoimmune response (Theofilopoulos, 1995). There are numerous autoimmune diseases that have been linked to immunity against bacterial chaperonins. Some examples of autoimmune disorders in which anti-chaperonin antibodies have been detected include psoriasis (Rambukkana et al., 1993), coronary heart disease (Ciervo et al., 2002), juvenile chronic arthritis (Danieli et al., 1992; de Graeff-Meeder et al., 1993), and Kawasaki disease (Yokota et al., 1993). *Chlamydia pneumoniae* GroEL was found to co-localize with human Cpn60 within atherosclerotic plaque macrophages (Kol et al., 1998). Autoimmunity to GroEL has also been implicated in infertility. Damage to the fallopian tubes was linked to the cross-reactivity of anti-chlamydial GroEL antibodies with human Cpn60 in women with chronic chlamydial infections (Spandorfer et al., 1999; Witkin et al., 1993). Interestingly, some bacterial chaperonins have an anti-inflammatory ability. Administration of mycobacterial GroEL provided protection from experimentally induced arthritis in a rat model (Prakken et al., 1998; van Eden et al., 1988) and suppressed experimentally induced asthma in a mouse model (Rha et al., 2002; Riffo-Vasquez et al., 2004). That chaperonins are able to induce inflammatory and anti-inflammatory responses in mammalians hosts attest to the complexity of the relationship between the protein and the immune system.

2.2.4.4. Chaperonin Function in Endosymbiotic Bacteria

Additional functions have been described for the GroEL of endosymbiotic bacteria. The chaperonin from the symbiotic bacterium *Enterobacter aerogenes* was identified as the neurotoxin found in the saliva of the antlion *Myrmeleon bore* larvae (Yoshida et al., 2001). Interestingly, a single amino acid substitution in the *E. coli* GroEL converts the benign chaperonin into the insect toxin. Endosymbiotic bacteria, in particular produce large amounts of their GroEL (also known as symbionin). In *Buchnera* sp. (the primary endosymbiont of aphids), GroEL constitute ~10 % of the total bacterial protein and show a low increase during heat shock conditions (Fares et al., 2002). Sequence analysis of GroEL from different endosymbionts revealed specific amino acid substitutions in key positions involved in substrate and GroES binding (Fares et al., 2002; Fares et al., 2005). These amino acid changes are thought to enhance GroEL interaction with the mutationally unstable *Buchnera* proteome (Fares et al., 2002). Thus, constitutive overexpression of GroEL and the action of positive selection on the evolution of GroEL suggests that GroEL is responsible for the maintenance of the endosymbiotic lifestyle by buffering against the accumulation of slightly deleterious mutations in the *Buchnera* genome (Fares et al., 2005). In addition, GroEL from *Buchnera* sp. is involved in the persistence and transmission of plant luteoviruses (Banerjee et al., 2004; Filichkin et al., 1997; Hogenhout et al., 1998).

2.2.5. Characteristics of the *L. pneumophila* Chaperonin

There is one copy of the 60-kDa chaperonin gene within the *L. pneumophila* genome (Chien et al., 2004). The *L. pneumophila* chaperonin gene, *htpB*, is encoded

within an operon downstream of its co-chaperonin gene, *htpA*, which is typical of the *groE* operon organization found in bacteria (Hoffman et al., 1990). The *htpAB* operon is transcribed as a polycistronic mRNA transcript (~2 kb) from a consensus heat shock promoter (Hoffman et al., 1990). HtpB is a 548 amino acid polypeptide with a molecular weight of ~62-kDa and exhibits 86 % amino acid sequence similarity to GroEL (Hoffman et al., 1990). Sequencing of the recombinant HtpB purified from *E. coli* indicated that the N-terminal Met-Ile-Met is posttranslationally cleaved leaving Ala as the N-terminal residue of the mature protein (Hoffman et al., 1990).

Originally characterized as the major cytoplasmic membrane protein of *L. pneumophila*, HtpB was investigated because of its immunodominant properties (Blander and Horwitz, 1993; Gabay and Horwitz, 1985; Sampson et al., 1986). HtpB was the most prominent antigen recognized by antibodies in sera from patients infected with *L. pneumophila* serogroups 1-8 and other species of *Legionella*, demonstrating that HtpB is a genus common antigen (Gabay and Horwitz, 1985; Sampson et al., 1986). Immunization of guinea pigs with purified HtpB provided a high level of protective immunity when challenged with a lethal aerosol dose of *L. pneumophila* (Blander and Horwitz, 1993), although a much lower survival rate was found in a later study (Weeratna et al., 1994). The immunoprotective potential of HtpB was attributed to abundant levels of the protein produced by *L. pneumophila* and to the release of the protein into the LCV of infected phagocytes (Blander and Horwitz, 1993). In *E. coli*, GroEL is detected in low levels under non-heat shock conditions and exhibits a more dramatic increase (~10-fold) after heat shock (Hemmingsen et al., 1988). In contrast, HtpB is one of the most abundant proteins detected in *L. pneumophila* under normal conditions with only a 2-fold increase

upon heat shock (Hoffman et al., 1989). In addition to induction by heat shock, HtpB levels are up-regulated by *L. pneumophila* during association with host cells and remain elevated throughout the intracellular infection of eukaryotic host cells (Abu Kwaik et al., 1993; Fernandez et al., 1996; Hoffman et al., 1990). Immunogold labeling studies revealed an increased level of surface-exposed HtpB correlating with the induction of HtpB by heat shock and host cell contact (Fernandez et al., 1996; Garduno et al., 1998). Moreover, large amounts of released HtpB have been detected in the lumen of the LCV by immunoelectron and fluorescence microscopy studies (Fernandez et al., 1996; Garduno et al., 1998; Hoffman et al., 1990).

The unusually high constitutive level of HtpB in *L. pneumophila* suggests that this protein may have other functions besides protein folding. *Haemophilus ducreyi* has a similar GroEL expression pattern (Parsons et al., 1997). High basal level of GroEL detected in *H. ducreyi* was found to be involved in chain formation and adherence to host cells (Frisk et al., 1998; Parsons et al., 1997). In *L. pneumophila*, a role in virulence has been demonstrated for HtpB, since surface localized HtpB functions as an invasin (Garduno et al., 1998a). Sustained upregulation of HtpB during infection and release of HtpB into the LCV lumen indicates that this chaperonin plays a role in virulence beyond that of an invasin. In addition, HtpB appears to moonlight as a signaling molecule. HtpB-coated beads have been shown to increase IL-1β mRNA by stimulating protein kinase C activity in the presence of cytochalasin D (inhibiting bead internalization), indicating that HtpB can engage host cell surface receptors to initiate signaling cascades leading to cytokine production (Retzlaff et al., 1996). When ectopically expressed in yeast, HtpB interferes with Ras2p-activated pathways (Riveroll, 2005). Together, these findings not

only highlight the differences between HtpB and GroEL, but they also reveal that HtpB has non-chaperone capabilities.

2.3. Objectives and Hypothesis

The surface-associated *L. pneumophila* 60-kDa chaperonin, HtpB, has been established as an invasion factor that mediates entry into HeLa cells (Garduno et al., 1998a). Based on the observations that HtpB is highly expressed throughout the course of intracellular infection (Fernandez et al., 1996) and is capable of interfering with eukaryotic signaling pathways (Riveroll, 2005), my working hypothesis is that HtpB plays (an) additional role(s) in the virulence of *L. pneumophila*. This thesis explores the functional relevance of HtpB in relation to the intracellular events directed by *L. pneumophila*. In Chapter 4, two forms of HtpB (a ~60-kDa form and an ~80-kDa form) were purified from *L. pneumophila*. The 80-kDa complex, previously observed by Allan (2002), was characterized to determine whether this higher molecular weight HtpB is the surface-associated form of HtpB. In Chapter 5, fluorescence and electron microscopy trafficking studies of HtpB-coated beads were done to characterize the role of HtpB in the intracellular trafficking of *L. pneumophila*. As an extension of previous HtpB localization studies, in Chapter 6, I investigated whether HtpB is translocated into the host cytoplasm during infection. Molecular and cell biology approaches were used to investigate the function of HtpB in this intracellular location. The findings from this study may advance our understanding of *L. pneumophila* intracellular parasitism, and offer some insights into chaperonin biology.

Chapter 3: Materials and Methods

3.1. Bacterial Strains and Growth Conditions

Bacterial strains used in this study are listed in Table 3.1. All *L. pneumophila* strains were grown at 37 °C on buffered charcoal yeast extract (BYCE) agar or in buffered yeast extract (BYE) broth. BCYE contained 10 g/L yeast extract, 1 g/L (2-[2-amino-2-oxoethyl]-amino)ethanesulfonic acid (ACES), 1 g/L α-ketoglutaric acid, 16g/L agar, 1.5 g/L activated charcoal with the pH adjusted to 6.6 using 6 N KOH. After autoclaving, 0.4 g/L L-cysteine (filter sterilized, pH adjusted to 6.6 with 6 N KOH) and 1 mL of 25 % (w/v) iron pyrophosphate (filter sterilized) were added to the media. BYE broth contained the same components as BCYE agar except no charcoal and agar were added, and the broth was filter sterilized instead of autoclaved. Filter sterilized L-cysteine and iron pyrophosphate were added to BYE broth prior to use. When appropriate, media was supplemented with thymidine and antibiotics at the following concentrations: 100 μg/mL thymidine, 100 μg/mL streptomycin, 30 μg/mL kanamycin, 5 μg/mL chloramphenicol.

Escherichia coli strains (Clontech) were grown on Luria-Bertani (LB) agar or in LB broth supplemented with the appropriate antibiotic selection as follows: 100 μg/mL ampicillin, 20 μg/mL chloramphenicol. LB broth contained 5 g/L yeast extract, 10 g/L tryptone, 10 g/L NaCl. The same components were used for LB agar with the addition of 15 g/L agar to the mixture. *E. coli* strains with plasmids containing the *htpAB* or *htpB* insert were grown at 30 °C on LB agar or in LB broth supplemented with the appropriate antibiotic selection as specified in Table 3.1. The rest of the *E. coli* strains were grown at 37 °C on LB agar or in LB broth with the appropriate antibiotic selection as specified in

Table 3.1. *L. pneumophila* and *E. coli* stocks were frozen in nutrient broth containing 10 % dimethysulfoxide (DMSO) for long-term storage.

3.2. Mammalian Cell Culture and Growth Conditions

Cell lines used in this study are listed in Table 3.1. CHO-AA8 Tet-Off cells (BD Biosciences Clontech) were routinely grown in α-Minimal Essential Medium (αMEM) (Gibco) supplemented with 5 % fetal bovine serum (FBS) (HyClone), 100 U/mL penicillin, 100 μg/mL streptomycin, 250 ng/mL amphotericin B, and 300 μg/mL geneticin (G418) (Gibco). CHO-*htpB* cells were maintained in the same media as CHO-AA8 Tet-Off cells, with the addition of 200 μg/mL hygromycin B (BD Biosciences Clontech), and 10 ng/mL doxycycline (BD Biosciences Clontech). The presence of hygromycin B assures the stable maintenance of the integrated plasmid, and doxycycline suppresses the expression of recombinant HtpB.

Human macrophage-like U937 cells were kept in suspension in RPMI 1640 (Gibco) supplemented with 10 % FBS (Sigma), 2 mM L-glutamine (Gibco), 100 U/mL penicillin, and 100 μg/mL streptomycin (Gibco) at 37 °C in 5 % CO_2. Cells were activated into an adherent, macrophage-like form with 60 ng/mL phorbol 12-myristate 13-acetate (Sigma) at a density of 3 X 10^6 cells/well in 6-well culture plates (Falcon). Twenty-four hours after activation, the cells were washed once with RPMI 1640 supplemented with 5 % FBS and 2 mM L-glutamine to remove any non-adherent cells. Adherent U937 cells were typically incubated for another 24-48 h in RPMI 1640 with 5 % fetal bovine serum and 2 mM L-glutamine prior to addition of beads or bacteria.

Table 3.1. Bacterial Strains and Mammalian Cell Lines Used in This Study.

Strains/cell lines	Description	Source or Reference
L. pneumophila		
Lp02	Philadelphia-1, serogroup 1, salt sensitive, restriction deficient, thymidine auxotroph (Sm^R)	Dr. Ralph Isberg (TUFTS University Medical School), Berger and Isberg, 1993
Lp02 dotA (JV309)	Lp02 *dotA* mutant, salt tolerant (Sm^R)	Dr. Ralph Isberg (TUFTS University Medical School), Berger and Isberg, 1993
Lp02 dotB (JV918)	Lp02 *dotB* mutant, salt tolerant (Sm^R)	Dr. Joseph Vogel (Washington University), Sexton et al., 2004
Lp02 RSF1010::*htpAB*	Lp02 containing plasmid RSF1010::*htpAB* (Km^R)	Allan, 2002
Lp02 pBH6119::*htpAB*	Lp02 containing plasmid pBH6119::*htpAB*, (Sm^R, Thy^+)	Dr. Karen Brassinga (University of Virginia)
Lp02 pMMB207C	Lp02 containing plasmid pMMB207C (Sm^R Cm^R)	This study
Lp02 pJC158	Lp02 containing plasmid pJC158 (Sm^R Cm^R)	This study
Lp02 pJC203	Lp02 containing plasmid pJC203 (Sm^R Cm^R)	This study
Lp02 pAC17	Lp02 containing plasmid pAC17 (Sm^R Cm^R)	This study
Lp02 pAC2	Lp02 containing plasmid pAC2 (Sm^R Cm^R)	This study
JR32	Salt sensitive isolate of AM511 (AM511: Philadelphia 1, serogroup 1, streptomycin resistant, restriction deficient, modification positive)	Dr. Howard Shuman (Columbia University), Sadowsky et al. 1993; (Marra et al. 1992)
JR32 pMMB207C	JR32 containing plasmid pMMB207C, Cm^R	This study
JR32 pJC158	JR32 containing plasmid pJC158, Cm^R	Chen et al., 2004
JR32 pJC203	JR32 containing plasmid pJC203, Cm^R	Chen et al., 2004
JR32 pAC17	JR32 containing plasmid pAC17, Cm^R	This study
JR32 pAC2	JR32 containing plasmid pAC2, Cm^R	This study

E. coli		
DH5α	F^- Φ80Δ*lacZ*ΔM15 Δ(*lacZYA-argF*)*U*169 *supE*44 *hsdR*17 *recA*1 *endA*1 *gyrA*96 *thi*-1 *relA*1	
JM109 pSH16	JM109 [F' {traD36 $proAB^+$ $lacI^q$ lacZΔM15} *endA1 recA1 hsdR17* (r_k^- m_k^+) *supE44 thi-1 gyrA96* Δ(*lac-proAB*)] containing plasmid pSH16, Amp^R	Hoffman et al., 1989
DH5α pBlueScript::*htpB*	DH5α containing plasmid pBlueScript::*htpB*, Amp^R	This study
DH5α pBlueScript::*groEL*	DH5α containing plasmid pBlueScript::*groEL*, Amp^R	This study
DH5α pTRE2hyg	DH5α containing plasmid pTRE2hyg, Amp^R	This study
DH5α pTRE2-*htpB*hyg	DH5α containing plasmid pTRE2-*htpB*hyg, Amp^R	This study
DH5α pTRE2-*groEL*hyg	DH5α containing plasmid pTRE2-*groEL*hyg, Amp^R	This study
DH5α pTRE2-*dsRed2*hyg	DH5α containing plasmid pTRE2-*dsRed2*hyg, Amp^R	This study
DH5α pMMB207C	DH5α containing plasmid pMMB207C, Cm^R	This study
DH5α pJC158	DH5α containing plasmid pJC158, Cm^R	This study
DH5α pJC203	DH5α containing plasmid pJC203, Cm^R	This study
DH5α pAC17	DH5α containing plasmid pAC17, Cm^R	This study
DH5α pAC2	DH5α containing plasmid pAC2 , Cm^R	This study
Mammalian cell lines		
CHO-AA8 Tet-Off	Chinese hamster ovary-derived cell line that expresses the tetracycline-controlled transactivator (tTA), neomycin resistant	Dr. Neal Ridgeway (Dalhousie University), BD Biosciences Clontech
CHO-*htpB*hyg	CHO-AA8 Tet-Off containing plasmid pTRE2-*htpB*hyg, neomycin and hygromycin B resistant	This study
U937	Human macrophage –like cell line	Dr. Andrew Issekutz (Dalhousie University)

Sm^R, Km^R, Cm^R, and Amp^R indicate resistance markers to streptomycin, kanamycin, chloramphenicol, and ampicillin respectively. Thy^+ indicates *L. pneumophila* strains that have the thymidylate synthase gene and is able to grow in the absence of thymidine.

3.3. Polyclonal HtpB Antibody Production

The following description for the generation and harvest of the polyclonal HtpB antibody (subsequently referred to as HtpB PAb1) was performed by Dr. Rafael Garduño. Recombinant HtpB (100 μg) purified from *E. coli* JM109(psh16) (Hoffman et al., 1989) was dispensed in a total of 300 μl of complete Freund's adjuvant, thoroughly emulsified, and subcutaneously injected into a New Zealand White rabbit (3 different sites at 100 μl/injection). The initial injection was followed by two booster injections of 100 μg of HtpB in 300 μl of incomplete Freund's adjuvant (3 different sites in the rabbit's back at 100 μl/injection). The injections were spaced 3 weeks apart. The rabbit was euthanized 9 weeks after the initial injection. Hyperimmune serum was recovered and kept frozen at –80 °C for long-term storage, or at 4 °C for short-term storage. Animals were cared for following guidelines outlined by the Canadian Council for Animal Care, under an approved protocol by the Dalhousie University Committee on Laboratory Animals.

3.4. Sodium Dodecyl Sulfate-Polyacrylamide Gel Electrophroresis (SDS-PAGE) and Immunoblotting

SDS-PAGE analysis of proteins was performed as described in Sambrook and Russell (2001). Laemlli sample buffer (Laemmli, 1970) without 2-mercaptoethanol (2ME) was used for electrophoresis of proteins under non-reducing conditions. Otherwise, 10 % 2ME (Sigma) was added to Laemlli sample buffer prior to addition to samples. Samples were boiled for 10 min. After a brief centrifugation, samples were loaded into the wells of a 5 % (w/v) polyacrylamide stacking gel cast above a 12 % polyacrylamide, vertical slab minigel (Bio-Rad). Electrophoresis was performed at 10

mA/stacking gel and 20 mA/separating gel in 1X running buffer (25 mM Tris base, 250 mM glycine, 0.1 % [w/v]) SDS) for 1 h. After electrophoresis, the gels were either Coomassie blue or silver stained, or the proteins within the gels were electro-transferred onto nitrocellulose for immunoblotting.

Coomassie staining was performed as follows: 1) gels were submerged in Coomassie stain (0.25 % Coomassie Brilliant Blue R-250 in 50 % [v/v] methanol and 10 % [v/v] acetic acid) for 2 h to overnight, 2) gels were destained in destain solution I (50% [v/v] methanol, 10 % [v/v] acetic acid) for 1-2 h, 3) gels were destained in destain solution II (5 % [v/v] methanol, 7 % [v/v] acetic acid) for 1 h, 4) gels washed in ddH_2O for 20 min, 5) gels were soaked in preservation solution (20 % [v/v] methanol, 3 % [v/v] glycerol) for at least 1 h prior to drying, and 6) gels were air-dried by sealing in cellophane and stretched in a drying plastic frame. All incubations were done with gentle agitation.

Silver staining was performed as previously described by Blum et al. (1987). All incubations were done with gentle agitation. Gels were fixed overnight in a 40 % (v/v) ethanol, 12 % (v/v) acetic acid, 0.05 % (v/v) formaldehyde solution, and then washed 3 x 20 min in 50 % (v/v) ethanol. Gels were sensitized with 0.02 % (w/v) sodium thiosulfate for 1 min, followed by 2 x 10 s washes in ddH_2O, and then treated with 0.2 % (w/v) silver nitrate solution for 20 min. Gels were developed with a solution of 3 % sodium carbonate, 0.025 % formalin until the desired staining intensity was achieved. Stain development was stopped with 2 x 2 min washes in ddH_2O, followed by 10 min in 40 % (v/v) ethanol, 12 % (v/v) acetic acid solution. Gels were soaked in 50 % (v/v) methanol

for at least 20 min, followed by soaking in preservation solution for at least 1 h prior to drying in cellophane.

Immunoblot procedures were performed as described by Towbin et al. (1979). All incubations were done with gentle agitation. Antibodies used in this study are listed in Table 3.2. Proteins were electroeluted onto nitrocellulose at 100 V for 2.5 h with a Bio-Rad electrotransfer apparatus. Blotted proteins were stained for 5 min with Ponceau S (2 % w/v Ponceau S in 30 % trichloroacetic acid and 30 % sulfosalicylic acid) to ensure proper transfer and equal loading among samples, followed by de-staining in PBS (137 mM NaCl, 2.7 mM KCl, 2 mM KH_2PO_4, 10 mM NaH_2PO_4, pH 7.4) for 10 min. Membranes were incubated in a blocking solution (1 % [w/v] skim milk, 1 % [w/v] BSA in TTBS [20mM Tris-HCl {ph 7.6}, 500 mM NaCl, 0.05 % {v/v} Tween 20]) for 1 h, and then washed with TTBS for 10 min. Blotted proteins were labeled with the appropriate primary and secondary antibodies diluted in TTBS containing 0.1 % (w/v) BSA. Membranes were incubated in primary antibody solution for 1 h followed by 3 x 10 min washes in TTBS, and then incubated in secondary antibody solution for 1 h. Following additional washes (2 x 10 min with TTBS, 2 x 10 min with TBS [20 mM Tris-HCl {pH 7.6}, 500 mM NaCl], and 2 x 5 min with developing buffer [0.1 M Tris-HCl {pH 9.5}, 0.1 M NaCl, 0.05 M $MgCl_2$]), the labeled proteins were developed in a solution of 10 mL developing buffer with 1.6 mg 5-bromo-4-chloro-3-indolylphosphate (BCIP, Sigma) and 44 μL of nitrobluetetrazolium (NBT) solution (75 mg/mL NBT in 70 % dimethylformamide and 30 % ddH_2O) as previously described (Garduno et al., 1998). The reaction was stopped by washing in ddH_2O once the color developed an appropriate intensity.

Table 3.2. Antibodies Used in This Study.

Antibodies	Description	Source or Reference
L. pneumophila HtpB Mab (GW2X4B2H6)	anti-HtpB mouse monoclonal	Helsel et al., 1988
L. pneumophila HtpB Pab1	anti-HtpB rabbit polyclonal; cross-reacts with GroEL	Dr. Rafael Garduno (Dalhousie University)
L. pneumophila HtpB Pab2	anti-HtpB rabbit polyclonal; cross-reacts with GroEL	Dr. Paul Hoffman (University of Virginia)
L. pneumophila MOMP Pab	anti-MOMP rabbit polyclonal	Butler and Hoffman, 1990
L. pneumophila LepA Pab	Anti-LepA rabbit polyclonal	Dr. Howard Shuman (Columbia University)
BiP-specific antibody	Anti-BiP rabbit antibody, recognizes mouse and rat BiP	Affinity Bioreagents
HA PAb	anti-hemagglutinin rabbit polyclonal	Dr. Roy Duncan (Dalhousie University)
DM1A	anti-α-tubulin rabbit polyclonal	Dr. Tom MacRae (Dalhousie University)
UH1 (CHO)	anti-LAMP1 mouse monoclonal	Developmental Studies Hybridoma bank, Iowa; Uthayakumar and Granger, 1995
Anti-rabbit IgG gold conjugate 10 nm	secondary antibody used for detection in immunoelectron microscopy	Sigma
Alexa Fluor 488 goat anti-rabbit IgG (H+L)	secondary antibody used for detection in fluorescence microscopy	Molecular Probes, Invitrogen
Alexa Fluor 546 goat anti-rabbit IgG (H+L)	secondary antibody used for detection in fluorescence microscopy	Molecular Probes, Invitrogen
Alexa Fluor 488 goat anti-mouse IgG (H+L)	secondary antibody used for detection in fluorescence microscopy	Molecular Probes, Invitrogen
Alexa Fluor 546 goat anti-mouse IgG (H+L)	secondary antibody used for detection in fluorescence microscopy	Molecular Probes, Invitrogen
Oregon Green 488 goat anti-rabbit IgG	secondary antibody used for detection in fluorescence microscopy	Molecular Probes, Invitrogen

Antibodies	Description	Source or Reference
alkaline phosphatase conjugated anti-rabbit IgG	secondary antibody used for detection in immunoblots	Cedarlane Laboratories Ltd
alkaline phosphatase conjugated anti-mouse IgG	secondary antibody used for detection in immunoblots	Cedarlane Laboratories Ltd

3.5. Purification of HtpB from *L. pneumophila*

Lp02 harboring the *htpAB* operon in RSF1010 (Allan, 2002) was grown at 30 °C for 48 h in 2 L of BYE broth containing kanamycin (30 μg/mL), followed by heat-shock at 42 °C for 2 h to induce maximum expression of HtpB. The culture was centrifuged at 6000 x *g* for 20 min, and the pelleted bacterial cells were resuspended in 40 mL of column buffer (50 mM Tris [pH7.6], 35 mM KCl, 25 mM NH_4Cl, 5 mM EDTA, 1 mM PMSF, 5 mM DTT). A crude bacterial lysate was made by passing this bacterial suspension four times through a French press cell at 20,000 psi. A few drops of 2 % Sarkosyl (Sigma) were added to the lysate prior to sonication in three cycles of 1 min followed by 4 min cooling on ice. The lysate was clarified by pelleting the cell debris at 8,800 x *g* for 10 min. HtpB was precipitated from the clarified lysate with ammonium sulfate (41 % saturation), re-solubilized in column buffer, and subjected to ion-exchange chromatography in a DE-52 (Whatman) column. Bound proteins were eluted in a 0 to 0.4 M KCl gradient, with HtpB eluting early within the first peak. Presence of HtpB in the different fractions was confirmed by dot blot and immunostaining with the HtpB-specific monoclonal antibody GW2X4B8B2H6 (subsequently referred to as HtpB MAb) (Helsel et al., 1988). Fractions containing HtpB were pooled and concentrated by ultrafiltration in a chamber (Amicon) pressurized with N_2 gas and equipped with a 10 000 molecular weight (MW) cutoff ultrafiltration membrane (Spectrapor). The concentrated sample was then sequentially run through a G200 Sephadex (Pharmacia) column, and a G75 Sephadex (Pharmacia) column. Again, fractions containing HtpB were pooled, dialyzed, and concentrated by ultrafiltration. Two final fractions were obtained: Fraction 1 contained the 80-kDa HtpB species, and Fraction 2 contained the 60-kDa and 80-kDa

HtpB species. Concentrations of the purified HtpB fractions were determined by the Bradford-based protein assay reagent according to the instructions by the manufacturer (Bio-Rad Laboratories). To determine the purity of the proteins from each fraction, approximately 10 μg of each purified HtpB fraction (1 μg/ μL) was subjected to SDS-PAGE, followed by Coomassie blue R-250 staining and immunoblotting (see above section 3.4). Immunoblots were specifically labeled with the HtpB PAb1 at a 1:1000 dilution or the HtpB MAb at a 1:200 dilution. Fraction 2 (containing the 60-kDa and 80-kDa HtpB species) was used for subsequent experiments after treatment with 50 mM dithiothreitol (DTT, Sigma) for 30 min at 4°C to reduce any higher molecular weight HtpB forms, followed by dialysis (membrane MW cutoff=6 000-8 000) against PBS overnight at 4 °C. Prior to use, the concentration of the dialyzed HtpB preparation was determined by a Bradford-based protein assay reagent (BioRad).

3.6. 80-kDa HtpB Characterization

To determine if MOMP is part of the purified 80-kDa HtpB species, 3.4 μg of Fraction 1 was subjected to SDS-PAGE under non-reducing conditions (no 2ME added to Laemlli sample buffer). Following electrophoresis, the gel was stained with Gel Code Blue (Pierce) for 10 min. Stain development was stopped with a 10 min wash in ddH_2O. The 80-kDa band was excised from the gel with a clean scalpel blade, and then passed through an 18 g needle several times followed by a 23 g needle to break up the polyacrylamide. The homogenized sample was resuspended in Laemlli sample buffer containing 10 % 2ME, boiled, and subjected to another round of SDS-PAGE. One gel was silver stained; the proteins within the second gel were electro-transferred onto

nitrocellulose for immunoblotting (see above section 3.4). One blot was developed with the anti-HtpB PAb1 (1:1000 dilution); the other blot was developed with the anti-MOMP polyclonal antibody (1:2000 dilution).

To ascertain whether LPS is part of the 80-kDa HtpB species, periodate-modified silver staining was performed as previously described by Tsai and Frasch (1982). Fifty micrograms of each purified HtpB fraction were digested by incubation with 10 μg of Proteinase K for 1 h at 60 °C. Samples were solubilized in sample buffer, boiled for 5 min, and subjected to SDS-PAGE. After electrophoresis, the gel was fixed overnight in 40 % (v/v) ethanol and 5 % (v/v) acetic acid solution in water, oxidized with 0.7 % (w/v) periodic acid for 5 min, washed 3 x 15 min with ddH_2O, stained for 10 min in a solution containing 1.3 % (v/v) concentrated NH_4OH, 0.1 M NaOH, 0.7 % (w/v) silver nitrate, washed 3 x 10 min with ddH_2O, and developed in a solution with 50 mg/L citric acid and 0.5 mL/L formalin. Stain development was stopped by soaking in ddH_2O.

To determine if the 80-kDa HtpB species could form spontaneously, 350 μg of Fraction 2 was subjected to SDS-PAGE under non-reducing (no 2ME added to Laemmli sample buffer) and reducing conditions. The 60-kDa HtpB species from gels run under each condition were excised and homogenized separately as described above. Each sample was subjected to another round of SDS-PAGE under non-reducing conditions. The gel was silver stained and the presence of the 80-kDa band was assessed.

3.7. Mitochondrial Malate Dehydrogenase Refolding Assay

A malate dehydrogenase refolding assay (Hayer-Hartl, 2000) was performed to determine whether the purified 60-kDa HtpB (Fraction 2) had any chaperonin activity.

Porcine heart mitochondrial malate dehydrogenase (mMDH), guanidinium hydrochloride, pyruvate kinase, phosphoenolpyruvate (PEP), reduced nicotinamide adenine dinucleotide (β-NADH), oxaloacetate, adenosine 5'-triphosphate (ATP), and 1,2-cyclodiaminohexanetetraacetic acid (CDTA) were obtained from Sigma; GroEL and GroES were obtained from Stressgen. The *Bordetella pertussis* GroES homolog, p10, was purified by Angela Riveroll (2005). Fifty micromolar mMDH was denatured (D-mMDH) in buffer A (20 mM 3-[N-morpholino]propane-sulfonic acid (MOPS)/KOH, pH 7.4, 100 mM KCl, 2 mM $Mg[OAc]_2$) containing 3 M guanidinium hydrochloride/5 mM dithiothriotol (DTT) at 37 °C for at least 30 min prior to use. mMDH refolding was performed at 37 °C in reaction mixtures containing buffer A, 20 mg/mL pyruvate kinase, 10 mM PEP, 1 mM ATP, 1 μM GroEL or HtpB, 2 μM GroES or p10, 1 μM D-mMDH and ddH_2O to 100 μL. Refolding mixtures without chaperonins or with 14 μM bovine serum albumin (BSA) in place of the chaperonins served as negative controls. Six times the recommended 2 μM concentration of *B. pertussis* p10 was used where indicated. At various time points, 5 μL aliquots from the refolding reactions were removed to immediately assay for mMDH activity. The activity of the refolded D-mMDH was measured relative to the activity of the native mMDH (N-mMDH). The assay for mMDH activity was performed at RT with an OLIS-14 spectrophotometer at 340 nm over 2min. A decrease in absorbance at 340 nm reflects the rate of β-NADH oxidation which is indicative of mMDH activity.

3.8. Protein-Coated Beads

Carboxylate-modified 1 μm polystyrene blue (365/415) and yellow-green (505/515) fluorescent beads (Molecular Probes, Invitrogen) were coated with BSA (Sigma), GroEL (Stressgen), or purified HtpB. A total of 200 μg of protein was used per reaction to coat ~9 x 10^9 beads using a carbodiimide kit (Polysciences) according to instructions provided by the manufacturer. Uncoated carboxylate-modified beads were processed similarly but were not incubated with protein so that they could be used as a blank control. The presence of bound GroEL and HtpB on the coated beads was confirmed by spotting 3 μl of beads (~6 x 10^6 beads) onto nitrocellulose, followed by immunostaining using HtpB PAb1 at 1:1000 dilution, followed by goat-anti-rabbit immunoglobulin G (IgG) conjugated to alkaline phosphatase (Cedarlane Laboratories) secondary antibody at 1:5000 dilution (Garduno et al., 1998). Protein-coated and uncoated beads were stored in PBS containing 0.05 % sodium azide (J. T. Baker Chemical Co.). Before use, all beads were washed three times with PBS, resuspended in PBS and counted by direct microscopy in a Petroff-Hausser chamber.

3.9. Bead Association with Cells

CHO-*htpB* cells were seeded onto 22 x 22 mm (Size 0) glass coverslips (Fisher Scientific) placed inside 6-well plates at 5 x 10^5 cells per coverslip. After 48 h incubation, the cells were washed three times with PBS, and the differently coated blue fluorescent beads were added to the monolayers at a bead:cell ratio of 20. The plates were centrifuged at 1000 x *g* for 5 min at 25 °C, and incubated for different times at 37 °C with 5 % CO_2. Unattached beads were removed by six washes with PBS. Cells were

then stained with 5 μM 5-chloromethylfluorescein diacetate (CMFDA, Molecular Probes) diluted in pre-warmed αMEM with antibiotics for 30 min at 37 °C with 5 % CO_2, washed three times with PBS to rinse off the labeling medium, and chased for 20 min with fresh αMEM with antibiotics. Cells were then fixed in 4 % paraformaldehyde for 10 min, and mounted with Vectashield mounting medium (Vector Laboratories) on glass slides. The number of associated beads per cell was determined by direct microscopy counts in a BX61 Olympus microscope.

3.10. Bead Trafficking Studies

3.10.1. Bead and *L. pneumophila* Association with Mitochondria

CHO-*htpB* cells were seeded onto coverslips and incubated with blue fluorescent beads as described above. Agar-grown *L. pneumophila* were harvested in ddH_2O, and the bacterial suspension was standardized to 1 optical density (O. D.) unit at 620 nm (~10^9 bacterial cells/mL). A final bacterial inoculum of ~4X10^8 bacteria (to provide an approximate MOI of 200) were prepared in αMEM without antibiotics, vortexed thoroughly, and added to wells. Plates were centrifuged at 1000 x *g* for 5 min at 25 °C to promote beads/bacteria contact with cells, and then incubated for 1 h to allow internalization. Unattached beads/bacteria were removed by six washes of PBS. The cells were either stained with Mitotracker Orange CMTMRos (Molecular Probes), or incubated for an additional 2 h with fresh medium at 37 °C with 5 % CO_2 prior to staining. The mitochondria of the host cells were stained with 300 nM Mitotracker Orange CMTMRos (Molecular Probes, Invitrogen) diluted in prewarmed αMEM-5 %

FBS with antibiotics for 45min at 37 °C with 5 % CO_2, washed three times with PBS to rinse off the labeling medium, and chased for 10 min in fresh αMEM-5 % FBS with antibiotics. Cells were fixed and mounted as described above. Bead association with mitochondria was quantitated by fluorescence microscopy using a BX61 Olympus microscope. Captured images were magnified 400 % for quantitation of mitochondria recruitment. Mitochondria in contact with or within one bead radius distance of a bead were scored as a recruitment event. Images were captured with an Evolution QET Monochrome camera (Media Cybernetics) and processed using Image Pro Plus (Media Cybernetics), version 5.0.1.

3.10.2. Bead and *L. pneumophila* Effect on Actin Organization

CHO-*htpB* cells were seeded onto coverslips, and either incubated with blue fluorescent beads or infected with *L. pneumophila* as described above. The cells were then fixed in 4 % paraformaldehyde for 10 min, permeabilized in 0.1 % Triton X-100 (Bio-Rad Laboratories) for 5 min, blocked in 2 % BSA in PBS for 30 min. To stain for filamentous actin (F-actin), the cells were then incubated for 20 min with 5 U/mL Alexa fluor 546 conjugated-phalloidin (Molecular Probes, Invitrogen). Tubulin was stained using monoclonal antibody DM1A (a gift from Dr. Tom MacRae, Dalhousie University) at 1:500 dilution, followed by Alexa fluor 546 conjugated goat anti-rabbit antibody (Molecular Probes) diluted at 1:200. Actin and tubulin organization were assessed by confocal microscopy using a Zeiss LSM 510 Laser Scanning Confocal Microscope with Argon 458/488 nm and Helium/Neon 548 nm lasers. Images were captured using 3D for LSM software, and processed using LSM 5 image browser (Zeiss).

3.10.3. Bead and *L. pneumophila* Association with Lysosomes in CHO-*htpB* Cells

The lysosomal compartment of CHO-*htpB* cells was stained using 100 μg/mL Texas Red Ovalbumin (TrOv, Molecular Probes) diluted in prewarmed αMEM-5 % FBS with antibiotics for 1 h at 37 °C with 5 % CO_2. The monolayers were washed three times with PBS to rinse off the labeling medium, and chased for 1 h in fresh αMEM-5 % FBS with antibiotics. Differently coated blue fluorescent beads and bacteria were added to the monolayers as described in the mitochondria staining section. Unattached beads/bacteria were removed by six washes of PBS then fixed with periodate-lysine-paraformaldehyde containing 5 % sucrose (McLean and Nakane, 1974) and mounted with ProLong Gold Antifade (Molecular Probes), or incubated for an additional 2 h with fresh medium at 37 °C with 5 % CO_2 prior to fixation and mounting.

The interaction between the beads or *L. pneumophila* with lysosomes was also assessed by examining the co-localization of beads/bacteria with LAMP-1. Differently coated blue fluorescent beads or bacteria were added to CHO-*htpB* cell monolayers as described above. Unattached beads/bacteria were removed by six washes of PBS and the cells were either stained immediately, or incubated for an additional 2 h with fresh medium at 37 °C with 5 % CO_2 prior to staining. Residual extracellular beads were labeled with 0.5 mg/mL Texas Red-dextran (TrDx, Molecular Probes) added to the washed monolayer for 1 min at room temperature. Intracellular beads were identified as blue fluorescent particles not stained with a rim of TrDx. The cells were fixed with periodate-lysine-paraformaldehyde containing 5 % sucrose, permeabilized by methanol extraction for 10 s, and blocked in 2 % BSA in PBS for 30 min. LAMP-1 was stained by monoclonal antibody UH1 (obtained as hybridoma cell culture supernatant from the

Developmental Studies Hybridoma bank, Iowa) at 1:2 dilution, followed by Alexa fluor 488 conjugated goat anti-mouse antibody (Molecular Probes) diluted at 1:200. The UH1 LAMP-1-specific antibody, developed by S. Uthayakumar and B. L. Granger, was obtained from the Developmental Studies Hybridoma Bank, developed under the auspices of the NICHD and maintained by the University of Iowa, Department of Biological Sciences, Iowa City, IA 52242. *L. pneumophila* was stained with rabbit anti-MOMP serum (Butler and Hoffman, 1990) at 1:2000 dilution, followed by Alexa fluor 546 conjugated goat anti-rabbit antibody (Molecular Probes) diluted at 1:1000. The co-localization of coated beads with TrOv or LAMP-1 labeled lysosomes was quantitated by fluorescence microscopy.

3.10.4. Bead Association with ER

CHO-*htpB* cells were incubated with yellow-green fluorescent beads as above. ER was then stained for 15 min with 1 μM ER-Tracker™ Blue-White DPX (Molecular Probes) diluted in prewarmed αMEM-5 % FBS with antibiotics, washed three times with PBS to rinse off the labeling medium, and chased for 10 min in fresh αMEM-5 % FBS with antibiotics. Cells were fixed and mounted as described above for observation in the fluorescence microscope.

CHO-*htpB* cells were incubated with blue fluorescent beads and fixed as described above for TrOv staining. CHO-*htpB* cells were permeabilized in cold methanol for 10 s, and then blocked with PBS containing 2 % goat serum (PBSG) for 30 min. The ER compartment was stained with a BiP-specific rabbit primary antibody (Affinity Bioreagents) diluted 1:250 in PBSG followed by Oregon Green 488 goat anti-rabbit IgG

secondary antibody (Molecular Probes, Invitrogen) diluted 1:1000 in PBSG. Coverslips were mounted with ProLong Gold Antifade (Molecular Probes, Invitrogen) on glass slides and observed by fluorescence microscopy.

3.11. Transmission Electron Microscopy

CHO-*htpB* and U937 cells were seeded into 6-well plates, and either incubated with blue fluorescent beads or infected with *L. pneumophila* as described above. Blue fluorescent beads were added to the CHO-*htpB* monolayer at a bead:cell ratio of 20, and to U937 cells at a ratio of 10. CHO-*htpB* cells were infected with Lp02 or *dotB* at an approximate MOI of 200. U937 cells were infected with Lp02 at an approximate MOI of 20, or with *dotB* at an approximate MOI of 200. Cells were lifted from the wells by gentle manual scraping and centrifuged at 500 X *g* for 5 min at 25 °C. With minimal disturbance of the pelleted cells, the media was removed and replaced with cacodylate buffer (0.1 M sodium cacodylate, pH 7) containing 2.5 % glutaraldehyde. The cells were fixed and allowed to settle by gravity overnight at 4 °C. The next day, the cell pellet was washed three times in cacodylate buffer before postfixation in 1 % osmium tetroxide for 1 h at 4 °C. Then, cells were *in-bloc* stained with aqueous uranyl acetate, dehydrated in acetone, embedded in epoxy resin, ultrathin sectioned, and post-stained with uranyl acetate and lead salts as described elsewhere (Garduno et al., 1998b). Sectioned specimens were observed on a JEOL JEM 1230 transmission electron microscope, and high-resolution images were captured with a Hamamatsu ORCA-HR digital camera.

3.12. Molecular Techniques

Plasmids used in this study are listed in Table 3.3. DNA preparations, restriction enzyme digestions, transformations, PCR, T/A cloning and DNA ligation have been described (Sambrook and Russell, 2001). Oligonucleotides were synthesized by Integrated DNA Technologies, Inc. (Coralville, IA).

3.12.1. Agarose Gel Electrophoresis

Electrophoresis of DNA was carried out at 96 V for desired periods of time in 1X Tris acetate ethylenediaminetetraacetic acid (EDTA) (TAE) buffer diluted from a 50X stock (242 g/L Tris base, 57 mL/L glacial acetic acid, 100 mL/L 0.5 M EDTA [pH 8.0]). Loading dye (MBI Fermentas) was added to DNA samples prior to loading into the wells of 0.8 % (w/v) agarose gels containing ethidium bromide (1 µl of a 1 mg/mL stock solution added to approximately 50 mL of molten agarose). DNA was visualized using a UV transilluminator (Forodyne, WI, USA). One kilobase (kb) or 100 basepair (bp) DNA ladders (MBI Fermentas) were used as reference.

3.12.2. Isolation of DNA Fragments from Agarose Gels

Purification of DNA from agarose was done in two ways depending on the size of the DNA fragment. For DNA fragments less than 10 kb in length, QIAquick gel purification spin column kits (QIAGEN) were used following the manufacturer's instructions for the centrifugation protocol. Agarose was melted using the provided

Table 3.3. Plasmids Used in This Study.

Plasmids	Description	Source or Reference
RSF1010::*htpAB*	Low copy broad host range vector with *htpAB*, Km^R	Allan, 2002
pSH16	pUC19 with *htpAB*, Amp^R	Hoffman et al., 1989
pBlueScript II KS (+)	High copy cloning vector, Amp^R	Stratagene
pBlueScript::*htpB*	pBlueScript II KS (+) with *htpB*	This study
pBlueScript::*groEL*	pBlueScript II KS (+) with *groEL*	This study
pDsRed2	prokaryotic expression vector that encodes red fluorescent protein (drFP583) from *Discosoma sp.*, pUC ori, P*lac,* Amp^R	BD Biosciences Clontech
pTRE2hyg	Mammalian expression vector for use with Tet-On and Tet-Off cell lines, $P_{hCMV*-1}$ Tet responsive promoter, ColE1, Amp^R, Hyg^R	Dr. Neal Ridgeway (Dalhousie University), BD Biosciences Clontech
pTRE2-*htpB*hyg	pTRE2hyg with *htpB*	This study
pTRE2-*groEL*hyg	pTRE2hyg with *groEL*	This study
pTRE2-*dsRed2*hyg	pTRE2hyg with *dsRed2*	This study
pCAGGS	eukaryotic expression vector with the hemagglutinin gene (from strain A/WSN/33) controlled by chicken β-actin promoter	Dr. Roy Duncan (Dalhousie University), Neumann et al., 1999
pBH6119::*htpAB*	pBH6119 with the *htpAB* promoter upstream of green fluorescence protein (*gfpmut3*); (pBH6119: RSF1010 ori, promoterless *gfpmut3*, thymidylate synthase, Amp^R)	Dr. Karen Brassinga (University of Virginia), Hammer and Swanson, 1999
pMMB207C	pMMB207 with Δ*mobA* (pMMB207: RSF1010 derivative, IncQ, *lac*Iq, Cm^R, P*tac, oriT*)	Chen et al., 2004; (Morales et al., 1991)
pJC158	pMMB207C with *lepA:cyaA*	Chen et al., 2004
pJC203	pMMB207C with *cyaA*	Chen et al., 2004
pAC17	pMMB207C with *htpB:cyaA*	This study
pAC2	pMMB207C with *cyaA:htpB*	This study
p2cyaA	pMMB207C with *cyaA:cyaA*	This study

Amp^R, Km^R, Hyg^R, and Cm^R indicate resistance markers to ampicillin, kanamycin, hygromycin B and chloramphenicol, respectively.

chaotropic salts at 55-65 °C until completely dissolved. To ensure proper pH prior to column application, 0.1 volume of 3 M sodium acetate (pH 5.0) was added to the melted agarose solution. DNA was eluted in 30 µL of elution buffer. For DNA fragments greater then 10 kb, UltraClean DNA purification kit (Mo Bio) was used following the manufacturer's instructions. DNA was eluted with the appropriate volume of sterile ddH_2O.

3.12.3. Plasmid Isolation

Plasmids for cloning procedures were isolated using QIAprep Spin Miniprep or Midiprep kit (QIAGEN). For minipreps, 5 mL of *E. coli* cultures were grown overnight and harvested by centrifugation (4500 x *g*, 6 min, room temperature [RT]); for midipreps, 50 mL cultures were grown overnight and harvested (4500 x *g*, 10 min, 4 °C). Protocol for column purification by centrifugation was followed exactly according manufacturer's instructions.

Plasmids for screening transformants were isolated by a standard alkaline lysis method (Sambrook and Russell, 2001). Briefly, 3 mL transformant cultures were grown overnight in selective broth, and harvested by centrifugation (18 000 x *g*, 1 min, RT). Bacterial pellets were completely resuspended in 200 µL Solution 1 (50 mM glucose, 25 mM Tris-HCl [pH 8.0], 10 mM EDTA), then lysed with the addition of 200 µL Solution 2 (0.2 N NaOH, 1 % SDS), and mixed by gentle inversion until the solution clarified. After 5 min incubation on ice, 200 µL Solution 3 (3 M sodium acetate [pH 5.0]) was added and the solution mixed by gentle inversion until precipitation occurred. The samples were centrifuged at 15 000 x *g* at 4 °C for 10 min. Two volumes of cold 95 %

ethanol were added to the resulting supernatants and vortexed. The solution was incubated on ice for 15 min, followed by centrifugation (15 000 x *g*, 15 min, 4 °C). The DNA pellet was washed twice with 70% ethanol (15 000 x *g*, 10 min, 4 °C) to remove residual salts, and then air dried. The final DNA pellet was resuspended in the desired volume of sterile ddH_2O (usually 10-20 μL).

3.12.4. Restriction Endonuclease Digestions

Restriction endonuclease digestions were performed with the appropriate restriction enzymes (New England Biolabs) using the supplied buffers under conditions described by the supplier.

3.12.5. Polymerase Chain Reaction (PCR)

Typical conditions used for PCR amplification were: Step 1 - 95 °C for 2 min, Step 2 – 94 °C for 30 s, Step 3 - the appropriate annealing temperature for 30 s, Step 4 – 72 °C for 1 min per kb of amplicon, Step 5 – repeat Steps 2 to 4 for a total of 30 cycles, Step 6 – 72 °C for 6 min. Annealing temperature used was 5 °C below the lower approximate melting temperature of each primer pair. The approximate melting temperature of each primer was calculated as the sum of 4 °C for each dGTP and dCTP residue, plus 2 °C for each dATP and dTTP residue.

Gene amplification by PCR using Platinum *Pfx* DNA polymerase (Invitrogen) was carried out with the buffer and conditions provided by the supplier. Each reaction contained 1X PCR buffer with $(NH_4)_2SO_4$ and $MgCl_2$, 0.2 mM dNTPs (Invitrogen), 4 μL

of each primer (100 ng/μL), 1.25 U of Platinum *Pfx* DNA polymerase, 50-100 ng of template DNA and the appropriate volume for ddH_2O required to bring the reaction volume to 50 μL.

PCR screening of transformants was performed using *Taq* DNA polymerase (MBI Fermentas) with the buffer and conditions provided by the supplier. Bacterial cells were harvested using a sterile toothpick into 100 μL of ddH2O, boiled for 10 min, and centrifuged (15 000 x *g*, 1 min, RT). Two microlitres of the supernatant was used as template for PCR reactions. Each reaction contained 1X PCR buffer with $(NH_4)_2SO_4$, 1.5 mM $MgCl_2$, 0.2 mM dNTPs (Invitrogen), 2 μL of each primer (100 ng/μL), 1.5 U of *Taq* DNA polymerase, 2 μL of template and the appropriate volume for ddH_2O required to bring the reaction volume to 25 μL.

3.12.6. T/A Cloning and DNA Ligation

T/A cloning (Sambrook and Russell, 2001) was used to clone PCR amplicons into pBlueScript (pBS) (Stratagene). Amplicons generated using Platinum *Pfx* DNA polymerase (Invitrogen) were incubated with Taq polymerase (2.5 U enzyme/100 μL volume) (MBI Fermentas) in 1X buffer (MBI Fermentas) containing 2 mM dATP (Invitrogen) for 2 h at 72 °C, followed by gel extraction purification. pBS was digested with *Eco*RV (New England Biolabs), then dTTPs (Invitrogen) were added to the plasmid as described above.

DNA ligations were performed using T4 DNA ligase (New England Biolabs) at 14 °C overnight. An insert/vector ratio of 5:1 was used. Ligation reactions consisted of

the appropriate volume of insert and vector DNA, 1 μL of T4 DNA ligase, 2 μL of 10X T4 DNA ligase buffer (New England Biolabs) with the final volume adjusted to 10 μL with sterile ddH_2O.

3.12.7. Preparation of Rubidium Chloride Competent *E. coli* Cells

A 10 mL *E. coli* culture grown overnight at 37 °C was subcultured 1:20 into 500 mL of LB broth and grown at 37 °C to an OD_{620} of 0.6-0.8. All centrifugations were done at 3000 x *g* for 15 min at 4 °C. Bacterial cells were harvested by centrifugation, resuspended in 200 mL cold Transformation Buffer 1 (30 mM potassium acetate, 100 mM rubidium chloride, 10 mM $CaCl_2 \cdot H_2O$, 50 mM $MnCl_2 \cdot 4H_2O$, 15 % glycerol), incubated on ice for 5 min and centrifuged again. The bacterial pellet was resuspended in 20 mL Transformation Buffer 2 (10 mM 3-(N-morpholino)propanesulfonic acid [MOPS], 75 mM $CaCl_2 \cdot H_2O$, 10 mM rubidium chloride, 15 % glycerol, adjusted to pH 6.3 with 1 M KOH). Bacterial cells were dispensed in 200 μL aliquots and stored at -80^0C.

3.12.8. Transformations

Ten microlitres of a standard ligation mixture (see section 3.12.6) or plasmid DNA were added to 200 μL of rubidium chloride competent *E. coli* thawed on ice. The mixture was incubated sequentially on ice for 20 min, at 37 °C for 90s, and on ice for 1 min. The transformed cells were then added to 2 mL of pre-warmed LB broth and incubated with slow agitation (100 rpm) for 1 hour at 37 °C. Cells were harvested (4800 x *g*, 6 minutes, 4 °C) and resuspended in 200 μl of LB broth. A range of volumes (5-100

μl) were then plated and spread on LB agar plates with the appropriate selection. Plates were then incubated at 30 °C overnight. Colonies were replica plated to fresh LB agar plates with the appropriate antibiotic selection, incubated overnight at 30 °C, and then stored at 4 °C.

3.12.9. Preparation of Electrocompetent *L. pneumophila* Cells

Electrocompetent *L. pneumophila* strains Lp02 and JR32 were prepared by Elizabeth Garduño. Overnight lawns of *L. pneumophila* inoculated from a 3 day old BCYE plate with appropriate selection was harvested into 20 mL sterile ddH_2O and centrifuged at 3000 x *g* for 10 min at 4 °C. The cells were resuspended in 20 mL of cold 15 % glycerol, washed twice in 10 mL 15 % glycerol, and finally resuspended in 200 μL cold 15 % glycerol. The cells were stored at -80 °C in 40 μL aliquots.

3.12.10. Electroporation

Electrocompetent *L. pneumophila* were thawed on ice. Five microlitres of plasmid DNA (at ~ 1 μg/μL) was added to the thawed cells and incubated on ice for 20 min. The DNA/cell mixture was transferred to a pre-chilled 1 mm gap electroporation cuvette, and electroporated at 2.1 kV. The cells were then transferred to 2 mL of pre-warmed BYE and incubated at 37 °C for 3 h with gentle agitation. The cells were centrifuged at 4500 x *g* for 5 min. The supernatant was removed, the cells gently resuspended with 125 μL of fresh pre-warmed BYE and plated onto BCYE agar at 5 μL, 10 μL, and 100 μL with the

appropriate selection. The plates were incubated at 30 °C for 5-7 days. Colonies were replica plated and screened either by PCR or immunoblot analysis.

3.13. *L. pneumophila* Phagosome Isolation

Four 25 cm^2 flasks containing activated U937 or CHO-*htpB* cells were each infected with 0.3 mL from a suspension of Lp02 cells harvested from a lawn grown overnight on BCYE and suspended at ~5 X 10^9 bacteria/mL. This infection ratio provided an approximate multiplicity of infection (MOI) of ~300. Flasks were centrifuged at 500 x *g*, 10 min, 25 °C in a swing-out tray rotor (Rotor No. 1622, Universal 32 R Centrifuge, Hettich), and then incubated for 3 h, with centrifugations (as above) every hour, to maximize contact between bacteria and cells and allow bacterial internalization and intracellular establishment. Then, cells were washed 3 times with PBS and scraped into 1 mL of cold homogenization buffer (250 mM sucrose, 20 mM HEPES-KOH [pH 7.0], 0.5 mM EGTA, 0.1 % gelatin). The suspended cells were lysed by 12 passages through a 27 g needle and the lysate was centrifuged at 400 x *g* for 10 min at 4 °C to remove large fragments and unbroken cells. The supernatant containing the released phagosomes was removed and centrifuged at 2000 x *g* for 20 min at 4 °C. The pellet was incubated overnight at 4 °C or for 1 h at 37 °C with rabbit hyperimmune serum raised against *L. pneumophila* HtpB (PAb2; Hoffman et al., 1989). Labeling controls included omission of primary antibodies (replaced by incubation with 1 % BSA in PBS), and incubation with rabbit anti-*L. pneumophila* major outer membrane protein serum (MOMP PAb; Butler and Hoffman, 1990) as the primary antibody. All primary antibodies were diluted 1:400 in PBS containing 1 % BSA. After washing once with PBS, the samples were fixed

in 2 % paraformaldehyde in PBS for 10 min at 4 °C. The fixed samples were then washed once with 30 mM glycine in PBS to quench any reactive aldehydes, and labeled with goat anti-rabbit IgG conjugated with 10 nm gold spheres (Sigma) diluted 1:100 in PBS containing 1 % BSA. After a final wash in PBS, samples were fixed in cacodylate buffer (0.1 M sodium cacodylate, pH 7) containing 2.5 % glutaraldehyde at 4 °C for 3 h, and centrifuged at 2000 x *g* for 20 min at 4 °C to collect the labeled phagosomes. Phagosomes were washed 3 times in cacodylate buffer before postfixation with 1 % OsO_4, *in bloc* stained with uranyl acetate, prepared for embedding, sectioned and poststained as previously described (Faulkner and Garduno, 2002; Garduno et al., 1998b). Stained ultrathin sections were observed on a JEOL JEM 1230 transmission electron microscope, and images were captured with a Hamamatsu ORCA-HR digital camera.

3.14. cAMP Assay

N- and C-terminal *htpB* fusions to *cyaA* were constructed in pJC158 (pMMB207C containing *lepA-cyaA* fusion) (Chen et al., 2004). To create the *htpB-cyaA* fusion, primers 5'-GGTACCATGATAATGGCTAAAGAATTACGTTTTGGT-3' and 5'-TCTAGACATCATTCCGCCCATGCCACCCAT-3' were used to amplify *htpB* from pSH16 (Hoffman et al., 1989). The PCR product was T/A cloned into the *Eco*RV site of pBluescript to create pBS::*htpB*. A *Kpn*I-*Xba*I fragment containing *lepA* in pJC158 was replaced with a *Kpn*I-*Xba*I fragment containing *htpB* from pBS::*htpB*, to generate pAC17 encoding the *htpB-cyaA* fusion. To construct the *cyaA-htpB* fusion, primers 5'-CCGGGGTACCATGCAGCAATCGCATCAGGCT-3' and 5'-

GCCTCTAGACGATCCCACCCCATCAAGGCT-3' were used to amplify *cyaA* from pJC203 (Chen et al., 2004). The PCR amplification product was directly cloned into pJC158 replacing the *Kpn*I-*Xba*I fragment containing *lepA*, to generate p2CyaA. Primers 5'-TCTAGAATGATAATGGCTAAAGAATTACGTTTTGGT-3' and 5'-GCATGCTTATTACATCATTCCGCCCATGCCACCCAT-3' were used to amplify *htpB* from pSH16 (Hoffman et al., 1989), which was T/A cloned into the EcoRV site of pBluescript to create pBS::*htpB*-2. The *Xba*I-*Sph*I fragment containing *cyaA* in p2CyaA was replaced with the *Xba*I-*Sph*I fragment containing *htpB* from pBS::*htpB*-2 to generate pAC2. Plasmids pAC17, pAC2, pJC203, pJC158, and pMMB207C were transformed into *L. pneumophila* strains Lp02 and JR32 by electroporation. *L. pneumophila* strains carrying plasmids pJC203 (Cya alone), pJC158 (LepA positive translocation control) and pMMB207C (empty vector control) served as controls for the protein translocation assay.

L. pneumophila strains Lp02 and JR32 carrying the plasmids pAC17, pAC2, pJC203, pJC158, or pMMB207C, were grown to mid-exponential phase at 37 °C in BYE containing 5 μg/mL chloramphenicol, and induced to express the plasmid-encoded proteins with 1 mM IPTG for 2 h. Bacterial cells were then resuspended in αMEM with 5 % FBS, chloramphenicol, and IPTG before infecting CHO-*htpB* cells at a MOI of ~600 in the presence of 1 mM IPTG and 5 μg/mL chloramphenicol. The infected cells were centrifuged at 500 x *g* for 10 min to promote bacterial contact with host cells, followed by incubation for 90 min at 37 °C in 5 % CO_2. To extract cAMP from the infected cells, these were washed 3 times with warm (37 °C) PBS, and then lysed with 250 μL of 50 mM HCl/0.1 % Triton X-100. The lysates were boiled for 5 min, and then neutralized with 30 μL of 0.5 M NaOH. Two volumes of cold ethanol were added to the lysates and

centrifuged for 5 min at 15 000 x *g*, and the supernatants containing cAMP were vacuum dried. The levels of cAMP were assayed using the cAMP enzyme immunoassay system (Amersham Pharmacia). A gentamicin protection assay was performed in parallel for quantitation of internalized bacteria as follows: After the 90 min infection period and the 3 washes with warm PBS, sister infected monolayers were treated for 90 min with αMEM containing 5 % FBS and 100 μg/mL gentamicin. The monolayers were then washed 3 times with PBS and lysed with ddH_2O to determine by dilution-plating, the number of bacteria that survived the gentamicin treatment (assumed to be intracellular). Bacterial viable cell counts by dilution-plating were performed using ddH_2O as diluent, and plating onto BCYE agar (with appropriate supplements when needed) to quantify CFU/well. Femtomoles of cAMP per internalized bacterium were then calculated for each strain.

Functionality and expression of the CyaA fusions was determined by incubating JR32 and CHO-*htpB* lysates, and quantifying cAMP as follows: After IPTG induction for 2 h, JR32 strains in late exponential phase were harvested and resuspended to ~10^9/mL in αMEM with 5 % FBS, 1 mM IPTG, and 86 μg/mL protease inhibitor cocktail (Sigma). CHO-*htpB* cells grown to confluency were trypsinized from a 25 cm^2 flask (~4 $X10^5$ cells) and resuspended in 7 mL of αMEM with 5 % FBS, 1 mM IPTG and 74 μg/mL protease inhibitor cocktail. Bacterial cells were sonicated in 10 cycles of 1 min pulses followed by 3 min incubation on ice; CHO-*htpB* cells were sonicated with the same cycle but only 3 times. One mL of bacterial lysate was then incubated with 0.8 mL of CHO-*htpB* lysate for 20 min at 37 °C. Proteins were precipitated from the lysate mixture with addition of 1 M HCl to a final concentration of 50 mM, and neutralized with 0.5 M

NaOH, followed by cAMP extraction and quantitation with the cAMP enzyme immunoassay system (Amersham Pharmacia) as described above.

3.15. Immunoblot Detection of Protein:CyaA Fusions

Five milliliter cultures of JR32 or Lp02 strains harboring either pAC2 (*cyaA:htpB*), pAC17 (*htpB:cyaA*), pJC158 (*lepA:cyaA*) or pJC203 (*cyaA*) were grown to mid-exponential phase (O.D. ~1.5-1.8). The cultures were induced with the addition of 1 mM IPTG at exponential phase, incubated for another 2 h, and harvested. For non-induced samples, bacterial cells were harvested prior to the addition of IPTG. Approximately equivalent numbers of cells (estimated by equivalent cell densities) were harvested using the formula ($0.8/A_{620}$) x 1000 μL x 2. The bacterial cells were centrifuged for 1 min at 15 000 x *g*, and resuspended in 100 μL of 2X Laemlli sample buffer containing 10 % 2ME. Samples were boiled for 10 min, 40 μL of sample was loaded into each well, and then subjected to SDS-PAGE. Proteins were electrotransferred onto nitrocellulose at 0.5 mA for 2 h with a Bio-Rad electrotransfer apparatus at 4°C in transfer buffer lacking SDS (0.025 M Tris base, 0.192 M glycine, 10 % methanol).. Blotted proteins were either labeled with the anti-LepA PAb diluted at 1:5000 or the anti-HtpB MAb diluted at 1:100, followed by the appropriate alkaline phosphatase conjugated secondary antibody diluted at 1:5000. The blot was developed as described in Section 3.4.

3.16. Construction of pTRE2-*htpB*hyg, pTRE2-*groEL*hyg, pTRE2-*DsRed2*hyg

Three tetracycline regulated mammalian expression vectors were constructed in pTRE2hyg. Forward primer 5'–AGTCTAGACAGCCGCCATGGCTAAAGAA**CTG**CGTTTTGGTGATGA-3' and reverse primer 5'-ACCTCTAGAAACTTACATCATTCCGCC-3' were used for PCR amplification of *htpB* from pSH16 (Hoffman et al., 1989). A Kozak sequence (Kozak, 1987), underlined in the forward primer above, was added, and the leucine codon (in bold) was optimized for expression in Chinese hamster ovary (CHO) cells. The PCR product was first T/A cloned into the *Eco*RV site of pBluescript, and the *Bam*HI-*Cla*I fragment containing *htpB* was subcloned into pTRE2hyg to generate pTRE2-*htpB*hyg.

Primers 5'-AGCGGCCGCCGCCATGGCAGCTAAAGACGTA-3' and 5'-GTGTCGACCACTTACATCATGCCGCCCAT-3' were used to amplify *groEL* from DH5α chromosomal DNA (a gift from Gary Sisson, Dalhousie University). The PCR product was T/A cloned into the EcoRV site of pBluescript to create pBS::*groEL*, and then *groEL* was moved into pTRE2hyg by subcloning the *Not*I-*Sal*I fragment from pBS::*groEL* to generate pTRE2-*groEL*hyg.

The *Bam*HI-*Not*I fragment containing *DsRed2* from pDsRed2 (BD Biosciences Clontech) was subcloned into pTRE2hyg to generate pTRE2-*Dsred2*hyg.

All constructs were checked by DNA sequencing (DalGen, Dalhousie University) to confirm the integrity of the entire inserts.

3.17. CHO-AA8 Transfections

CHO-AA8 Tet-Off cells were transiently transfected with pTRE2-*htpB*hyg, pTRE2-*groEL*hyg, pTRE2-*dsRed2*hyg, or pCAGGs using Lipofectamine 2000 (Invitrogen) according to the manufacturer's instructions. pCAGGS (a gift from Dr. Roy Duncan, Dalhousie University) contains an insert coding for haemagglutinin (HA) from influenza 1, serotype HIN1 (Neumann et al., 1999). A ratio of 1:2.5 (DNA [in μg]:Lipofectamine 2000 [in μL]) was used to transfect CHO-AA8 Tet-Off cells seeded in 12 well-plates at ~80 % confluence. DNA and Lipofectamine 2000 were diluted in OPTI-MEM®I Reduced Serum Medium (OPTI-MEM) (Gibco, Invitrogen). Prior to transfection, the monolayer was washed once with OPTI-MEM, and replaced with fresh OPTI-MEM. Cells were incubated with DNA:Lipofectamine 2000 complexes at 37 °C with 5 % CO_2 for 5 h. OPTI-MEM containing 10 % FBS was added to each well and incubated for 24 h. The media was replace with αMEM containing 5 % FBS, and after another 24 h incubation, the cells were either harvested for immunoblotting or fixed for indirect immunofluorescence. Expression of the various proteins encoded in the pTRE2-hyg constructs was induced in the absence of doxycycline, and repressed in the presence of 10 ng/mL doxycycline.

Stably transfected CHO-AA8 Tet-Off cells containing pTRE2-*htpB*hyg were established by addition of hygromycin B to the media and isolating single colonies by dilution cloning. Stable clones expressing *htpB* were screened by immunoblot and confirmed by indirect immunofluorescence microscopy. CHO-*htpB* cells were maintained in αMEM supplemented with 5 % FBS, 100 U/mL penicillin, 100 μg/mL

streptomycin, 250 ng/mL amphotericin B, 300 μg/mL geneticin, 200 μg/mL Hygromycin B, and 10 ng/mL doxycycline to prevent expression of HtpB.

3.18. CHO-*htpB* Characterization

3.18.1. Doxycycline Regulation of HtpB Expression in CHO-*htpB* Cells

CHO-*htpB* cells were plated at a density of ~5 x 10^5 cells/well into 6-well plates (Falcon). Doxycycline was removed or exchanged with different concentrations 48 h prior to the cells being harvested to allow for adequate expression of *htpB*. Cells were harvested from wells with 2 mg/mL trypsin (Sigma), washed once with PBS, and resuspended in fresh PBS for quantitation by direct microscopy using an improved neubauer counting chamber. Five microliters of 5X Laemlli sample buffer containing 10 % 2ME was added to ~6 X 10^5 cells resuspended in 10 μl PBS. Samples were boiled for 10 min, and then subjected to SDS-PAGE and immunoblotting. Blotted proteins were labeled with the anti-HtpB MAb diluted at 1:200, followed by the secondary antibody (alkaline phophatase conjugate of anti-mouse IgG; Cedarlane Laboratories Ltd) diluted at 1:5000. Densitometric analysis was performed using Image Pro Plus (Media Cybernetics).

3.18.2. Indirect Immunofluorescence Staining for Surface Localization of HtpB in CHO-*htpB* Cells

CHO-*htpB* cells were seeded onto 35 mm plates (Falcon) for 48 h prior to staining. Doxycycline was removed when CHO-*htpB* cells were seeded to allow for

expression of *htpB*. All fluorescence staining reagents were diluted in PBS. CHO-*htpB* cells were fixed in freshly made 2 % paraformaldehyde for 10 min at 37 °C. Fixed cells were washed 3 times with PBS, permeabilized with 0.1 % Triton X-100 for 5 min when required, and blocked in 2 % BSA for 0.5 -2 h. For indirect immunofluorescence labeling of HtpB in CHO-*htpB* cells, the cells were labeled with HtpB PAb1 diluted 1:1000, and Alexa Fluor 546-conjugated goat anti-rabbit IgG (Molecular Probes, Invitrogen) diluted 1:200. Tubulin was stained using monoclonal antibody DM1A at 1:500 dilution, followed by Alexa fluor 546 conjugated goat anti-rabbit antibody (Molecular Probes, Invitrogen) diluted at 1:200. HA staining was performed 48 h after transfection. HA was stained in transiently transfected CHO-AA8 cells with a rabbit polyclonal antibody against the H1 protein (a gift from Dr. Roy Duncan, Dalhousie University) at a dilution of 1:200, followed by Alexa fluor 546 conjugated goat anti-rabbit antibody (Molecular Probes) diluted at 1:200. Stained cells were mounted with ProLong® Gold Antifade reagent (Molecular Probes, Invitrogen) onto glass slides. Stained cells were observed by fluorescence microscopy using an IX61 Olympus microscope using a 40X objective. Images were captured with an Evolution QET Monochrome camera (Media Cybernetics), and processed using Image Pro Plus (Media Cybernetics, version 5.0.1) and Adobe Photoshop (version 7.0).

3.18.3. CHO Cell Growth Rate and Morphology

CHO-AA8 Tet-Off, CHO-*htpB*hyg (+Dox), or CHO-*htpB*hyg (-Dox) were seeded onto 24-well plates at ~1 X 10^5 cells/well. Doxycyline was removed at the time of plating. Cells were detached from wells with 2 mg/mL trypsin, and counted by direct

microscopy using an improved neubauer counting chamber at 24 h intervals up to 72 h. Each time point was quantitated in triplicate.

CHO cells were plated onto 12-well plates with 4 X 10^5 cells/well for 48 h prior to observation and quantitation by light microscopy on an IX61 Olympus microscope using a 40X objective. Doxycycline was removed at the time of plating.

3.18.4. Fluorescence Organellar Staining

CHO-*htpB* cells were seeded onto 12 mm, No. 1 glass coverslips (Fisher Scientific) in 24 well plates for 48 h prior to staining. Doxycycline was removed when CHO-*htpB* cells were seeded to allow for expression of *htpB*. Media was removed and the cells washed once with PBS. Mitochondria were stained with 300 nM Mitotracker Orange CMTMRos (Molecular Probes, Invitrogen) for 45 min; ER were stained with 1 μM ER-Tracker™ Blue-White DPX (Molecular Probes, Invitrogen) for 30 min. Both dyes were diluted in pre-warmed αMEM-5 % FBS with antibiotics. After incubation at 37 °C with 5 % CO_2, the cells were washed three times with PBS to rinse off the labeling medium, and chased for 10 min in fresh αMEM-5 % FBS with antibiotics. Following three PBS washes, cells were fixed in 4 % paraformaldehyde for 10 min and mounted with Vectashield mounting medium (Vector Laboratories) on glass slides. Lysosomes were visualized by indirect immunofluorescence staining of LAMP-1, a lysosomal marker protein. Cells were fixed with periodate-lysine-paraformaldehyde containing 5 % sucrose (MacLean and Nakane, 1974), permeabilized by methanol extraction for 10 s, and blocked in 2 % BSA in PBS for 30 min. LAMP-1 was stained by monoclonal antibody UH1 at 1:2 dilution, followed by Alexa fluor 488 conjugated goat anti-mouse

antibody (Molecular Probes, Invitrogen) diluted at 1:200. After three PBS washes, the coverslips were mounted with ProLong Gold Antifade onto glass slides.

3.19. Quantitation of the Intensity of Phalloidin Staining

CHO-*htpB* cells were seeded onto 22 X 22 cm, size 0 glass coverslips (Fisher Scientific) placed inside 6-well plates. Doxycycline was removed 48 h prior to infection to allow for expression of *htpB*. All fluorescence staining reagents were diluted in PBS. Sub-confluent monolayers of CHO-*htpB* cells were then fixed in 2 % paraformaldehyde for 10 min at 37 °C. Fixed cells were washed 3 times with PBS, permeabilized with 0.1 % Triton X-100 for 5 min, and blocked in 2 % BSA for 0.5 -2 h. For indirect immunofluorescence labeling of HtpB or GroEL expressed in CHO-*htpB* cells, the cells were labeled with the rabbit hyperimmune serum against *L. pneumophila* HtpB (PAb1) diluted 1:1000, and Alexa Fluor 546-conjugated goat anti-rabbit IgG (Molecular Probes, Invitrogen) diluted 1:200. Filamentous actin (F-actin) was labeled for 20 min at room temperature with 5 U/mL phalloidin conjugated with Alexa Fluor 488 (Molecular Probes, Invitrogen). Cells were mounted with ProLong Gold Antifade reagent (Molecular Probes, Invitrogen) onto glass slides for observation, and F-actin organization was assessed by confocal microscopy using a Zeiss LSM 510 Laser Scanning Confocal Microscope with Argon 458/488 nm and Helium/Neon 548 nm lasers. Images were captured using 3D for LSM software, and processed using LSM 5 image browser (Zeiss).

Images to evaluate the intensity of the actin staining were captured with an Evolution QET Monochrome camera (Media Cybernetics), and analyzed with Image Pro Plus (Media Cybernetics), version 5.0.1, by averaging the integrated optical density

(IOD) of 100 cells per sample. These values were then expressed as a ratio relative to the average IOD of 100 control CHO-*htpB* cells (CHO-*htpB* cells not expressing HtpB). Relative values from three independent experiments were averaged before graphing.

3.20. Actin Filament Co-Sedimentation Assay

Co-sedimentation of purified HtpB (see above) and purified human non-muscle actin (Cytoskeleton Inc.) was performed as described by the manufacturer. Briefly, polymerization of 1 mg/mL of purified G-actin into F-actin spontaneously occurred within 1 h after solubilizing the G-actin in polymerization buffer (10 mM Tris, 50 mM KCl, 2 mM $MgCl_2$, 1 mM ATP, pH 7.5) at room temperature. For the binding reaction, the following proteins were added to 18 μM F-actin in 11 X 34 mm polycarbonate tubes (No. 343778, Beckman): 17 μM HtpB, 22 μM GroEL (Stressgen Biotechnologies Corp), 1 μM α-actinin (Cytoskeleton Inc), and 1 μM BSA (Cytoskeleton Inc). The protein mixtures were incubated at room temperature for 30 min, and then centrifuged for 1.5 h at 25 °C, 100,000 x *g* in a MLA130 rotor (Beckman). The pellets were washed once by resuspending them in actin polymerization buffer, and centrifuging at 100 000 x *g* for 1.5 h at 25 °C. Equal amounts of protein from the pellet and supernatant fractions were analyzed by SDS-PAGE and Coomassie Blue staining.

3.21. Overlay Assay

Spots of BSA (2 μg), F-actin (2 μg), and a range of HtpB concentrations (0 μg-5 μg) were immobilized in duplicate onto a nitrocellulose membrane using the Bio-dot SF

microfiltration apparatus (Bio-Rad Laboratories). The membrane was cut to separate the BSA, F-actin and HtpB blots, and the blots were then blocked in PBS containing 1 % BSA and 1 % skim milk for 1 h at room temperature. After three washes in PBS, the BSA and F-actin blots (but not the blots with different concentrations of HtpB) were floated in PBS containing different concentrations of HtpB (0 μg/mL, 5 μg/mL, 10 μg/mL, 20 μg/mL, and 30 μg/mL) for 1 h at room temperature with gentle agitation. Excess HtpB was then removed by three 10 min washes with PBS. HtpB was detected in all blots by immunostaining with the *L. pneumophila* HtpB-specific MAb diluted at 1:200, followed by a secondary antibody (alkaline phosphatase conjugate of anti-mouse IgG; Cedarlane Laboratories Ltd) diluted at 1:5000. Following three 10 min washes with PBS, labeled spots were developed with BCIP and NBT as previously described (Garduno et al., 1998), before image capture with an Epson ES1200C scanner. Densitometric analysis of the crude digital images was performed using the Dot-Blot function of GelPro software (Media Cybernetics) to obtain the IOD values for each spot. The average IOD values of the spots containing known amounts of blotted HtpB were used to construct a standard curve, to interpolate the amounts of HtpB bound to the BSA and F-actin blots.

3.22. Invasion and Intracellular Growth Assays

CHO-*htpB* cells were seeded at a density of 2 x 10^5 cells/well into 24-well plates 48 h before infection. When required, doxycycline was removed 48 h prior to infection to allow for adequate expression of *htpB*. Immediately before the assays, monolayers were washed three times with PBS to remove antibiotics, and replenished with fresh αMEM-5 % FBS without antibiotics. Agar-grown *L. pneumophila* was harvested in ddH_2O, and

the bacterial suspension was standardized to 1 O.D. unit at 620 nm (~10^9 bacterial cells/mL). A final bacterial inoculum of ~10^8 bacteria (to provide an approximate MOI of 200) and 5 x 10^6 beads (to provide an approximate bead:cell ratio of 10) were prepared in αMEM without antibiotics (except for doxycycline when required), vortexed thoroughly, and added to wells in triplicate. Plates were centrifuged at 1000 x *g* for 5 min at 25 °C to promote bead/bacteria contact with cells, and then incubated for 1 h to allow internalization. Monolayers were washed six times with PBS, treated for 1.5 h with αMEM-5 % FBS containing 100 μg/mL gentamicin, and washed three times with PBS. The monolayers were either: (i) lysed immediately to determine both bacterial invasiveness, and time 0 h counts for intracellular growth assays, or (ii) replenished with αMEM-5 %FBS to be incubated for an additional 24 h, 48 h, or 72 h. All bacterial viable cell counts for intracellular growth assays were performed using ddH_2O as diluent, and plating onto BCYE agar to quantify CFU/well.

3.23. Statistics

Statistical significance was assessed using the Student *t*-test, or a one-way ANOVA test (http://www.physics.csbsju.edu/stats/anova.html). The Bonferroni test was used for comparisons of multiple samples (http://graphpad.com/quickcalcs/posttest1.cfm).

Chapter 4: Characterization of HtpB Purified from *Legionella pneumophila* Strain Lp02

4.1. Introduction

Although chaperonins contain no known secretion signal sequences, they have been detected on the cell surface of an increasing number of bacterial pathogens (Ensgraber and Loos, 1992; Frisk et al., 1998; Garduno et al., 1998; Hennequin et al., 2001). These extracytoplasmic chaperonins have been found to be involved in bacterial pathogenesis, mainly by mediating attachment to host cells.

The *L. pneumophila* 60-kDa chaperonin, HtpB, is surface exposed and is involved in the entry into host cells (Garduno et al., 1998a; Garduno et al., 1998). In cross-linking studies performed to assess the oligomeric state of surface exposed HtpB or its closest protein partners, a different form of HtpB migrating at ~80-kDa was observed (Allan, 2002). This 80-kDa complex was confirmed to contain HtpB by immunoblot, and was also detected in whole cell lysates of *L. pneumophila* resolved by SDS-PAGE under non-reducing conditions and in the absence of cross-linkers (Allan, 2002). Disulfide bond formation was, thus, implicated in the generation of the 80-kDa complex under non-reducing conditions (Allan, 2002). Since disulfide bonds are characteristic of extracytoplasmic proteins, it was speculated that the 80-kDa species of HtpB may be the surface exposed form involved in virulence-associated functions. Therefore, it was important to characterize this species to determine which form of HtpB would be relevant for use in bead trafficking studies (Chapter 5).

Garduno et al. (1998a) reported that while latex beads coated with BSA were found in spacious endosomes, beads coated with HtpB resided within tight fitting

endosomes and associated with host vesicles in HeLa cells. This observation suggested that HtpB may be capable of modulating the trafficking of endocytosed particles, and as such warranted further investigation. Whereas the previous bead trafficking study was done using recombinant HtpB isolated from *E. coli*, the HtpB used in this study was purified from the *L. pneumophila* strain, Lp02. Thus, the specific objectives in this chapter were to purify both forms of HtpB, and to characterize the 80-kDa form as the potential form in which HtpB exists on the cell surface of *L. pneumophila*.

4.2. Results

4.2.1. HtpB Purification

HtpB was successfully purified from the lysate of Lp02 over-expressing HtpB through a series of anion exchange and gel filtration columns (Fig 4.1). Two final fractions containing HtpB were obtained after the purification process (Fig 4.1). The purity of the two fractions was assessed by SDS-PAGE under non-reducing conditions and Coomassie Blue staining (Fig 4.2A). The identity of the purified proteins was confirmed by immunoblots with the HtpB MAb (Fig 4.2B), which recognizes the 60kDa form but not the 80-kDa form of HtpB, and PAb1 (Fig 4.2C). Fraction 1 contained mostly the 80-kDa species (Fig 4.2Aand Fig 4.2C). The 60-kDa species, along with several lower molecular weight bands, were also recognized by the HtpB PAb indicating protein degradation in Fraction 1 (Fig 4.2C). Fraction 2 was enriched for the 60-kDa species, but it also contained the 80-kDa species when subjected to non-reducing SDS-PAGE (Fig 4.2A). The identity of the 60-kDa band from Fraction 2 was confirmed by immunoblot

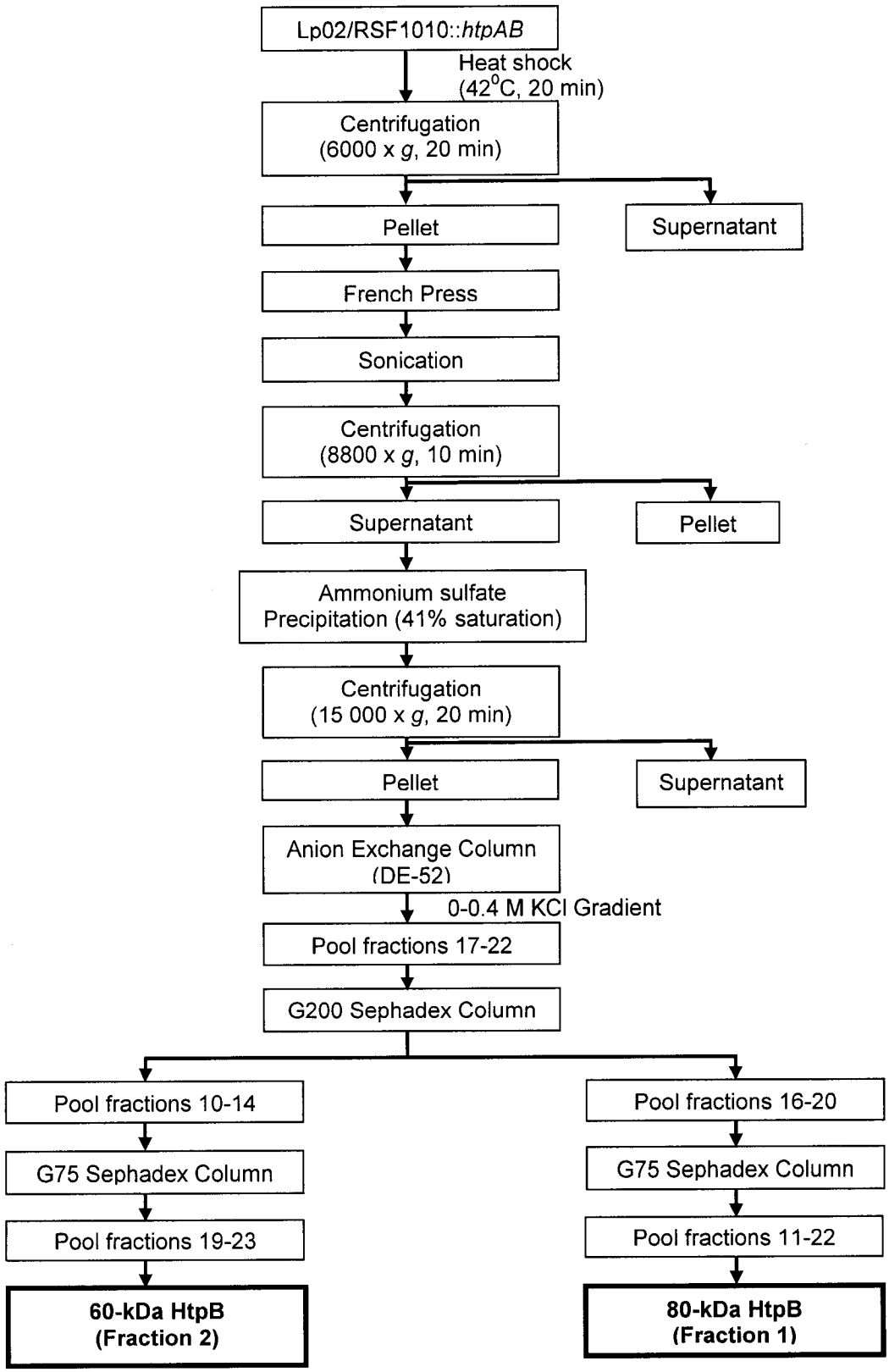

Figure 4.1. Flowchart of HtpB Purification.
See materials and methods (Section 3.5) for details.

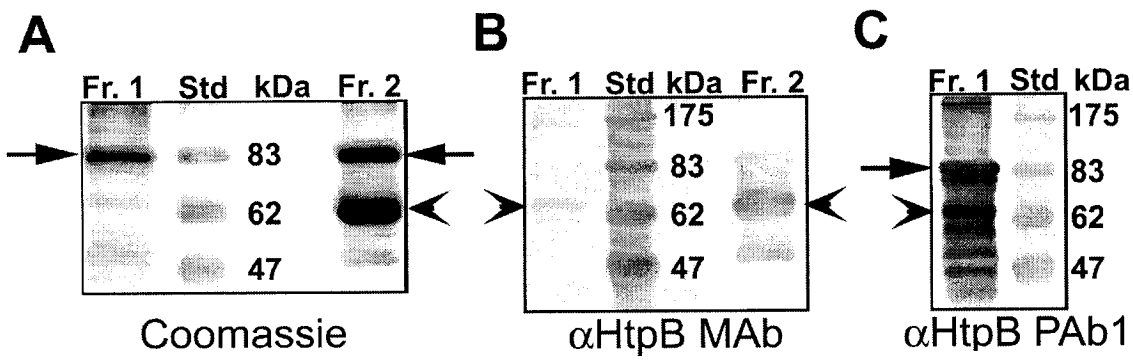

Figure 4.2. HtpB Fractions Purified from Heat Shocked *L. pneumophila* Strain Lp02 Overexpressing *htpAB*.

Protein fractions containing purified HtpB were separated by SDS-PAGE under non-reducing conditions. Protein concentrations were determined by the Bradford colorimetric assay using BSA as a standard; approximately 10 μg of protein was loaded into each lane. (A) Coomassie stained polyacrylamide gel. (B) Immunoblot developed with the HtpB Mab. (C) Immublot developed with the HtpB PAb1. Fr. 1, Purified fraction 1 containing mainly the 80-kDa form of HtpB; Std, Broad range molecular weight markers; Fr. 2, Purified fraction 2 containing mainly the 60-kDa form of HtpB. Arrows indicate the 80-kDa form of HtpB; arrowheads indicate the 60-kDa form of HtpB.

with the HtpB MAb (Fig 4.2B). The presence of a lower molecular weight band recognized by the HtpB MAb suggests some protein degradation (Fig 4.2B). As previously reported by Alan (2002), the 80-kDa HtpB from either fraction was not recognized by the HtpB MAb (Fig 4.2B). In summary, the 80-kDa HtpB complex could not be resolved by conventional chromatography from the 60-kDa fraction. In addition, the 60-kDa monomeric HtpB is always accompanied by the 80-kDa complex, suggesting that the 80-kDa complex may be spontaneously formed by purified HtpB kept under non-reducing conditions.

4.2.2. Characterization of the 80-kDa HtpB Complex

The 80-kDa species may result from formation of a complex between the 60-kDa species with smaller fragments of HtpB, or with other *L. pneumophila* components or proteins. MOMP was suspected to complex with HtpB to form the higher molecular weight species because immunoblot analysis of the reduced 80-kDa HtpB from Lp02 lysates showed that the MOMP PAb recognized an 80-kDa band, a 62-kDa band, and a double of 31 and 28-kDa bands characteristic of MOMP (Allan, 2002). The 80-kDa species from Fraction 1, excised from a gel run under non-reducing conditions, was reduced to the 60-kDa species and several lower molecular weight bands when subjected to SDS-PAGE under reducing conditions (Fig 4.3A and 4.3B). The MOMP PAb did not recognize any bands from the blot of the reduced 80-kDa species indicating that MOMP is not part of the higher molecular weight HtpB (Fig 4.3C).

The possibility that the 80-kDa HtpB form is composed of HtpB and LPS was explored because LPS has been reported to be complexed or co-purified with Hsp60s

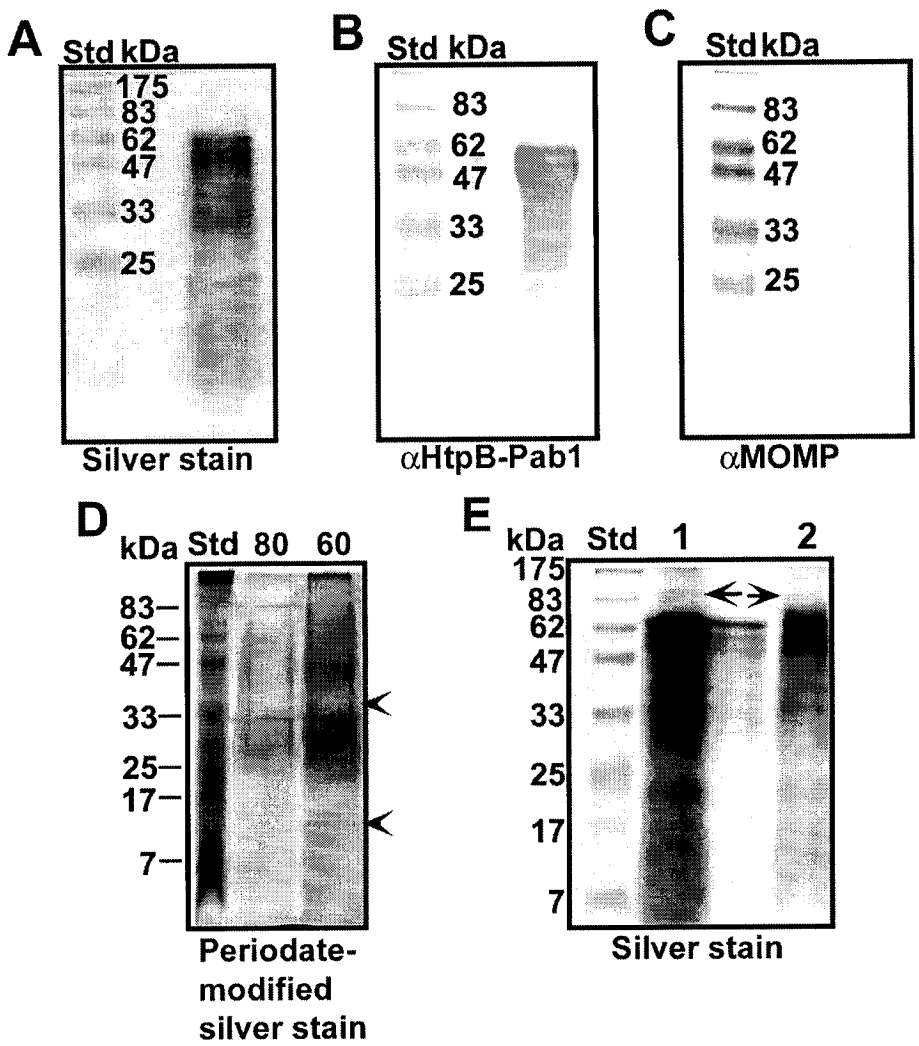

Figure 4.3. Characterization of the 80-kDa HtpB. The 80-kDa Species of HtpB Forms Spontaneously, and Is Not Associated with MOMP or LPS.
(A) Silver-stained polyacrylamide gel, (B) immunoblot developed with HtpB PAb1, and (C) immunoblot developed with MOMP PAb. All three panels (A-C) contain the 80-kDa band from purified HtpB fraction 1 excised from a polyacrylamide gel run under non-reducing conditions, and subjected to another round of SDS-PAGE under reducing conditions. (D) Periodate-modified silver stained polyacrylamide gel to compare the LPS patterns associated with the 80-kDa species (80) and 60-kDa species (60) of purified HtpB. Proteinase K digested proteins were electrophoresed out of the gel, leaving residual intact LPS. Arrowheads indicate LPS bands unique to the 60-kDa species of HtpB. (E) Silver-stained polyacrylamide gel of HtpB samples resolved by SDS-PAGE under non-reducing conditions from excised gel bands. Lane 1 contains excised material from the 60-kDa band run under reducing conditions. Lane 2 contains excised material from the 60-kDa band run under non-reducing conditions. Arrows point at a small amount of the 80-kDa species formed spontaneously under non-reducing conditions. Std, Broad range molecular weight markers.

(Hartley et al., 2004; Jensen et al., 1993; Osterloh et al., 2004). The presence of LPS bands associated with the purified HtpB indicated LPS contamination (Fig 4.3D). Comparison of the LPS patterns associated with the 80-kDa and the 60-kDa forms revealed two bands that were uniquely associated with the 60-kDa form (Fig 4.3D). There were no LPS bands that were unique to the 80-kDa form. The 80-kDa band was observed when the 60-kDa form of HtpB from Fraction 2, excised from gels run under reducing and non-reducing conditions, separately, was subjected to SDS-PAGE under non-reducing conditions. This suggests that the 80-kDa species could form spontaneously from the 60-kDa species when kept under non-reducing conditions (Fig 4.3E). The bands observed in the lane between lanes 1 and 2 in Fig 4.3E is due to overloading of the well from lane 1.

4.2.3. Chaperonin-Assisted mMDH Refolding Assay

Denatured pig heart mitochondrial malate dehydrogenase (D-mMDH) was used as the substrate in a refolding assay to determine whether the protein folding ability of purified HtpB (Fraction 2) was retained. mMDH catalyzes the conversion of L-malate to oxaloacetate. This conversion is coupled with the oxidation of the co-factor β-NADH which is easily measured spectrophotometrically at 340 nm (Hayer-Hartl, 2000). Thus, chaperonin folding function was determined indirectly by assessing mMDH activity after incubation in a refolding mixture. Activities of the refolded mMDH were expressed as a percentage of native mMDH (N-mMDH) activity.

Figure 4.4. Time Course of Chaperonin-Assisted and Spontaneous Refolding of mMDH.

mMDH was treated with 3 M guanidinium hydrochloride/5 mM DTT at 37 °C to generate denatured mMDH (D-mMDH). (A) Refolding was initiated by dilution of D-mMDH into a refolding mixture that either contained D-mMDH alone (i.e., no chaperonins), GroEL/GroES, BSA, HtpB, or HtpB/GroES. (B) Refolding was initiated by dilution of D-mMDH into a refolding mixture that either contained D-mMDH alone (i.e., no chaperonins), GroEL/GroES, HtpB/p10, or HtpB/p10 (at 6X the suggested concentration). HtpB/p10 (6X) was measured in a refolding mixture lacking D-mMDH [HtpB/p10 (6X), No mMDH]. β-NADH oxidation activity of the native mMDH (N-mMDH) activity and of D-mMDH activity was measured at indicated times after incubation in refolding mixtures at 37 °C. mMDH activity is expressed as a percentage of the native mMDH (N-mMDH). Dial. = dialyzed sample against PBS.

A

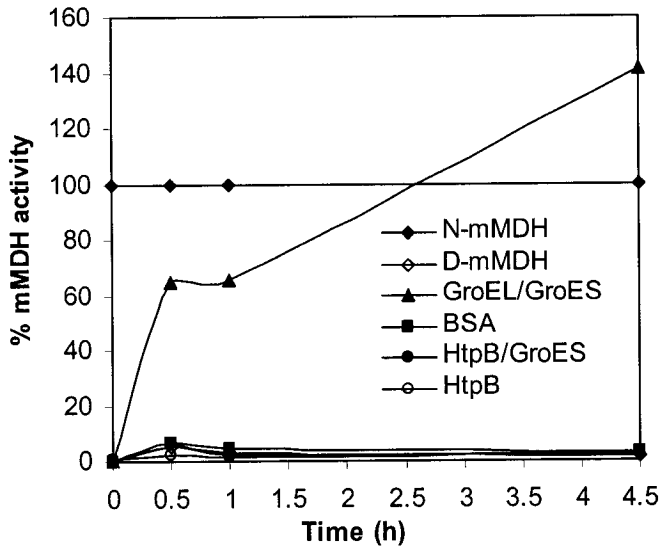
160
140
120
100
80
60
40
20
0
% mMDH activity
0 0.5 1 1.5 2 2.5 3 3.5 4 4.5
Time (h)
N-mMDH
D-mMDH
GroEL/GroES
BSA
HtpB/GroES
HtpB

B

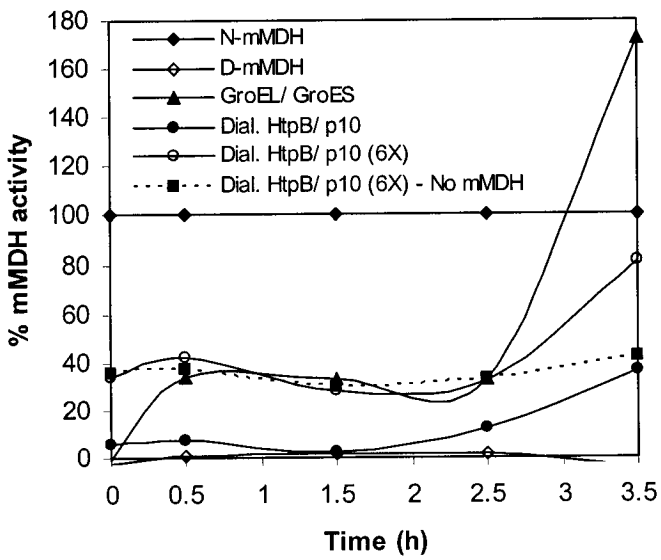
180
160
140
120
100
80
60
40
20
0
% mMDH activity
0 0.5 1 1.5 2 2.5 3 3.5
Time (h)
N-mMDH
D-mMDH
GroEL/ GroES
Dial. HtpB/ p10
Dial. HtpB/ p10 (6X)
Dial. HtpB/ p10 (6X) - No mMDH

Chaperonins require co-chaperonins for protein folding (Bukau and Horwich, 1998; Lin and Rye, 2006). The co-chaperonins from *E. coli* (GroES) and *B. pertussis* (p10) were used in substitution of the *L. pneumophila* co-chaperonin (HtpA) because we did not have a readily available stock of purified HtpA. Approximately 65 % and 35 % of mMDH activity was recovered after 0.5 h of incubation in refolding mixtures containing GroEL/GroES (Fig 4.4A and B, respectively). mMDH activity continued to increase after extended incubations in refolding mixtures containing GroEL/GroES. Incubation of D-mMDH in refolding mixtures containing HtpB (Fig 4.4A), HtpB/GroES (Fig 4.4A), or HtpB/p10 (Fig 4.4B) resulted in less than 10% recovery of mMDH activity. No increase in mMDH activities were obtained with extended D-mMDH incubations (3.5 h and 4.5 h) in refolding mixtures containing HtpB with the various co-chaperonins (Fig 4.4A and B). This level of mMDH activity was similar to that recovered in the absence of chaperonin-assisted folding (negative controls: D-mMDH and BSA). Higher mMDH activity was recovered when incubated in refolding mixtures containing HtpB and 6X the suggested molar concentrations of p10 (12 μM) in comparison to D-mMDH; however, a similar level of β-NADH oxidation activity was observed from refolding mixtures containing HtpB/p10 (6X) in the absence of mMDH (37 %) indicating that the observed activity from these samples resulted from a contaminant in the p10 preparation (Fig 4.4B).

4.3. Discussion

HtpB was purified as two fractions from a bacterial lysate of Lp02 over-expressing *htpAB*. Using a gel filtration column packed with G200 Sephadex matrix, fractions enriched for the 60-kDa species of HtpB eluted before those enriched for the 80-

kDa species (Fig 4.1). This elution profile indicated that the latter eluted true to its 80-kDa molecular weight form, whereas the 60-kDa HtpB eluted in either an oligomeric form or bound to a contaminant. The conserved C-terminus of chaperonins, also present in HtpB, is responsible for oligomerization (Burnett et al., 1994; McLennan et al., 1994). Because the HtpB MAb recognizes an epitope at the C-terminus of the protein (Hoffman et al., 1990), the inability of the HtpB MAb to recognize the 80-kDa form indicates that this region is structurally altered or inaccessible to the antibody. Thus, it would be reasonable to speculate that the 80-kDa HtpB cannot oligomerize as readily as the 60-kDa form because the C-terminus region in the 80-kDa form is either hindered from mediating such interactions, or already committed in a protein-protein interaction that leads to the 80-kDa complex formation.

In contrast to previous results (Allan 2002), I was unable to detect MOMP as part of the purified 80-kDa HtpB. In the study by Allan (2002), the 80-kDa band was excised from a SDS-PAGE gel containing Lp02 whole cell lysate rather than the extensively purified HtpB that I worked with. Therefore, it is likely that the excised band that Allan (2002) worked with was contaminated with MOMP oligomers co-migrating with the 80-kDa HtpB. This hypothesis is supported by the observation that the MOMP PAb reacted with multiple high molecular weight bands (including the 80-kDa band) from Lp02 lysates run under non reducing conditions in Allan's work (Allan, 2002).

It remains inconclusive whether LPS is complexed with HtpB or whether LPS was co-purified as a contaminant since carbohydrate moieties (presumed to be associated with LPS core components) were detected in both purified fractions. None were unique to the fraction enriched for the higher molecular weight form, indicating that the 80-kDa

HtpB does not result from the 60-kDa HtpB complexed with additional LPS fragments. The two bands unique to the 60-kDa HtpB fraction may result from a contaminant co-eluted with the fractions enriched for the 60-kDa species. Therefore, an appropriate control was included in the bead trafficking studies presented in Chapter 5 to rule out the possibility of the observed effects being caused by LPS or another contaminant.

Purification of the 60-kDa species away from the 80-kDa complex was not achieved in this study as the 80-kDa complex always formed when the reduced monomeric HtpB was exposed to air. However, a preparation with minimal amounts of the higher molecular weight HtpB could be maintained in the presence of a reducing agent (Fig 4.3A and B). This observation suggests that the formation of disulfide bonds occurs either within HtpB itself or with fragments of degraded HtpB. Due to the reductive nature of the cytoplasm and the oxidative nature of extracytoplasmic environments, proteins containing stable disulfide bonds are usually located in extracytoplasmic compartments or secreted into the extracellular milieu (Rietsch and Beckwith, 1998). Disulfide bond formation can occur spontaneously in extracellular compartments, but the process tends to be catalyzed in vivo by the periplasmically localized Dsb proteins (Rietsch and Beckwith, 1998). Since it is likely that any extracytoplasmic HtpB would be prone to oxidation, some of the surface exposed HtpB on *L. pneumophila* would likely exist as the 80-kDa complex. Similarly, beads coated with purified HtpB (for trafficking studies in Chapter 5) would also have a portion of the 80-kDa complex resulting from spontaneous oxidation. Although it remains unclear whether the 80-kDa complex represents the surface exposed HtpB, the results here indicate that the 80-kDa form is composed only of HtpB and possibly HtpB degradation

products. Thus, Fraction 2 was used as the source of HtpB for subsequent experiments, after reduction with dithiothreitol to minimize the formation of the 80-kDa complex.

Assessment of the folding activity of HtpB was inconclusive as it was unclear whether the inability of HtpB to mediate refolding was due to the loss of chaperonin function during the purification process, or due to the inability of co-chaperonins from other bacterial species to functionally replace HtpA. The *E. coli* co-chaperonin, GroES, can be functionally interchanged with various co-chaperonins in the GroEL-assisted folding of polypeptides in vitro. Human mitochondrial Hsp10, spinach chloroplast co-chaperonin (Cpn21), and bacteriophage encoded co-chaperonins (Gp31 and CocO) form productive protein folding complexes with GroEL (Ang et al., 2001; Baneyx et al., 1995; Richardson et al., 2001; van der Vies et al., 1994). Not all chaperonins, though, are as functionally flexible as GroEL with co-chaperonin swapping. The human mitochondrial Hsp60 is unable to assist in citrate synthase folding with GroES or Gp31 in place of hmHsp10 (Richardson et al., 2001). This may also be the case with HtpB. Pursuing the assay with HtpB paired with its cognate co-chaperonin HtpA would not only reveal whether the purified HtpB displays any biological activity, but it could also reveal whether HtpB is more functionally selective with its co-chaperonin partners than GroEL.

Chapter 5: The *Legionella pneumophila* Chaperonin, HtpB, Affects the Trafficking of Mitochondria

5.1. Abstract

A fraction of the *Legionella pneumophila* chaperonin, HtpB, is found on the bacterial cell surface where it can mediate invasion of HeLa cells. HtpB continues to be produced and released by HeLa cell-internalized *L. pneumophila*, suggesting that this chaperonin may also play post-internalization roles. We investigated here the functional competence of HtpB in mimicking the early intracellular trafficking of *L. pneumophila* that is characterized by recruitment of host cell vesicles and mitochondria, inhibition of phagosome-lysosome fusion, and association with the endoplasmic reticulum (ER). Fluorescence and electron microscopy studies in CHO and U937 cells indicated that HtpB-coated beads readily recruited mitochondria. In addition, virulent *L. pneumophila* and HtpB-coated beads induced transient changes in the actin organization of CHO cells, an event conceivably linked to mitochondrial recruitment. Phagosomes containing HtpB-coated beads fused with lysosomes, though they did so somewhat more slowly than phagosomes containing control beads, as determined by co-localization studies with the soluble endocytic probe Texas red ovalbumin, and the lysosomal protein marker LAMP-1. Association of HtpB-coated beads with the ER was not detectable, either by co-localization with fluorescent markers or by ultrastructural studies. These results indicate that HtpB mimics two of the early post-internalization events that typify the trafficking of virulent *L. pneumophila*: mitochondrial recruitment and actin rearrangement.

5.2. Introduction

The Gram-negative bacterium *Legionella pneumophila* is an opportunistic intracellular pathogen of humans that preferentially infects the lungs of immuno-compromised individuals, targeting alveolar macrophages (Horwitz and Silverstein, 1980). Lung infection by *L. pneumophila* manifests as an atypical pneumonia known as Legionnaires' disease (Winn, 1988). The early infection events of *L. pneumophila* have been well described. *L. pneumophila* can be internalized via conventional phagocytosis (Gibson et al., 1994; Payne and Horwitz, 1987; Steinert et al., 1994), coiling phagocytosis (Cirillo et al., 1999; Horwitz, 1984) or macropinocytosis (Watarai et al., 2001). It is not surprising for such a variety of internalization mechanisms to be linked to numerous genes, e.g. *rtxA* and *enhC* (Cirillo et al., 2000; Cirillo et al., 2001), *lpnE* (Newton et al., 2006), and *lvhB2* (Ridenour et al., 2003) (these genes are described in Section 2.1.4.1). Once internalized, *L. pneumophila* remains contained within a membrane-bound compartment which is transformed into a specialized vacuole (referred to as the *Legionella*-containing vacuole, or LCV) suitable for *L. pneumophila* replication (Lu and Clarke, 2005; Roy et al., 1998). Early events of LCV conditioning include recruitment of small vesicles and mitochondria, avoidance of both acidification and fusion with lysosomes (Horwitz and Maxfield, 1984; Horwitz, 1983b; Horwitz, 1983c; Sauer et al., 2005b; Sturgill-Koszycki and Swanson, 2000; Wieland et al., 2004), and association with the endoplasmic reticulum (ER) (Horwitz, 1983b; Swanson and Isberg, 1995; Tilney et al., 2001). Although in murine macrophages the LCV eventually acidifies and fuses with lysosomes (Sturgill-Koszycki and Swanson, 2000), LCVs do not acidify in human monocytes (Wieland et al., 2004), nor do they acquire the LAMP-1

lysosomal marker (Sauer et al., 2005b), suggesting that in some mammalian hosts the early post-internalization events that lead to inhibition of phagosome-lysosome fusion might be transient. Association of the LCV with the rough ER correlates with the onset of *L. pneumophila* replication. While contact with mitochondria and the ER may peak at different post-infection times in different host cell types, the LCV remains associated with mitochondria and the rough ER until bacterial replication ceases (Garduno et al., 1998b; Horwitz, 1983b; Oldham and Rodgers, 1985), suggesting that after its initial establishment, *L. pneumophila* actively maintains the LCV and continues to affect normal organelle and vesicular trafficking.

LCV-conditioning begins within minutes after *L. pneumophila* internalization (Kagan and Roy, 2002; Derre and Isberg, 2004; Kagan et al., 2004; Lu and Clarke, 2005; Robinson and Roy, 2006). In addition, antibiotic-treated legionellae (incapable of *de novo* protein synthesis) are not affected in attachment or invasion (Garduno et al., 1998b), and manage to both become established intracellularly and resume growth immediately after removal of the antibiotic (Horwitz and Silverstein, 1983). Collectively, these observations have led to the hypothesis that the factors involved in the internalization of *L. pneumophila* and the early events of LCV conditioning must be pre-formed, and either surface exposed or ready to be secreted (Joshi et al., 2001; Segal and Shuman, 1998a). Moreover, it is possible that the same factors that mediate internalization also participate in the early steps of LCV conditioning. Mutations that affect the Dot/Icm type IV secretion system of *L. pneumophila* abrogate LCV conditioning, suggesting the role of type IV secretion in translocating the required factors into host cells (Berger and Isberg, 1993; Berger et al., 1994; Coers et al., 2000; Marra et al., 1992).

HtpB is an essential protein of *L. pneumophila* and a member of the chaperonin family, a group of evolutionarily conserved and essential molecular chaperones with well-characterized roles in protein folding (Gupta, 1995). The function of chaperonins, however, is not limited to protein folding. Chaperonins can mediate invasion of mammalian cells (Frisk et al., 1998), stabilize lipid membranes (Török et al., 1997), paralyze insects (Yoshida et al., 2001), and interfere with eukaryotic signaling cascades (Zhang et al., 2001; Zhang et al., 2004a). Previous studies have shown that HtpB is an unusual chaperonin: (i) HtpB expression is up-regulated in response to host cells and high levels of expression are maintained during the course of intracellular infection (Fernandez et al., 1996), (ii) spontaneous salt-tolerant avirulent mutants of *L. pneumophila* are unable to up-regulate the expression of HtpB upon contact with host cells (Fernandez et al., 1996), (iii) HtpB is found free in the lumen of the LCV, and in association with the vacuolar membrane (Garduno et al., 1998), (iv) abundant HtpB is found in association with the *L. pneumophila* cytoplasmic membrane (Blander and Horwitz, 1993; Gabay and Horwitz, 1985), and (v) HtpB mediates invasion of HeLa cells (Garduno et al., 1998a). The continued production of HtpB after *L. pneumophila* internalization, and its apparent release into the lumen of the LCV, prompted us to investigate whether this unique chaperonin plays a role in the intracellular establishment of *L. pneumophila*. Since HtpB is an essential protein whose encoding gene cannot be deleted from the *L. pneumophila* genome (Dr. Paul Hoffman, personal communication), we have devised a number of biochemical, cell biological and surrogate gene expression approaches to learn about its apparently unique functions. In this study, we show that microbeads coated with purified HtpB (but not uncoated beads or beads coated with

control proteins) attract mitochondria and transiently modify microfilament organization in mammalian cells, thus mimicking early trafficking events of virulent *L. pneumophila*.

5.3. Results

5.3.1. Association of Differently Coated Polystyrene Microbeads with CHO Cells

Although our previous work with HtpB-coated beads was conducted in HeLa cells (Garduno et al., 1998a), we chose the Chinese hamster ovary (CHO) cell model here because CHO cells take up beads more readily than HeLa cells. For instance, while at a bead:cell ratio of 20, HeLa cells internalized <1 BSA-coated bead per cell (Garduno et al., 1998a), CHO cells could internalize on average >2 beads per cell (Figure 5.1B). In particular, we used CHO-*htpB* cells (refer to experimental procedures) to allow a future direct comparison of the effects of HtpB-coated beads with the effects resulting from the cytoplasmic expression of recombinant HtpB. However, in all the studies reported here, no expression of recombinant HtpB was induced in the CHO-*htpB* cells, as demonstrated by immuno-fluorescence microscopy and immuno-blotting (See Fig 6.3).

First, we evaluated the association of coated beads with CHO-*htpB* cells. After testing bead:cell ratios ranging from 5 to 100, a bead:cell ratio of 20 was chosen because lower ratios resulted in to few cells with internalized beads whereas higher ratios resulted in too many beads/cell interactions. One hour after adding the differently coated beads to CHO-*htpB* cells, HtpB-coated beads and the uncoated beads showed similar levels of cell association, and both bead types associated slightly better with CHO-*htpB* cells than BSA- and GroEL-coated beads (Fig 5.1A). After 3 h of incubation, the number of cells associated with HtpB-coated beads was significantly higher ($P<0.05$) than those

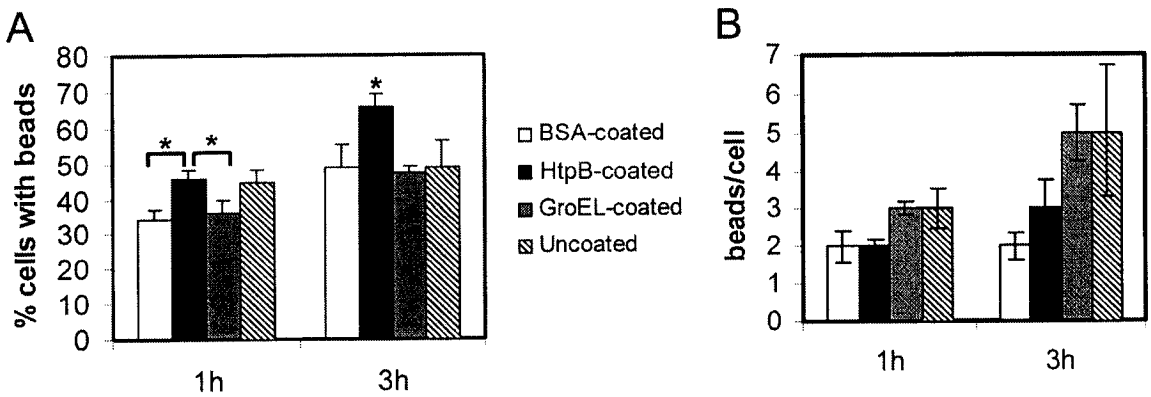

Figure 5.1. CHO-*htpB* Cells Associate with Similar Numbers of Differently Coated Beads per Cell.

(A) Percentage of CHO-*htpB* cells associated with beads. (B) Average number of beads per CHO-*htpB* cell associated with beads. CHO-*htpB* cells were incubated with differently coated beads at a bead:cell ratio of 20. Error bars correspond to one standard deviation from the mean of three independent experiments. P-values were calculated using a 1-way ANOVA followed by the Bonferroni test. P-values are only marked for significant differences (*$P<0.05$) in relation to HtpB-coated beads.

associated with all other beads (Fig 5.1A). The number or beads per cell after 1 or 3 h incubations fluctuated between 2 and 5, with GroEL-coated and uncoated beads reaching the highest numbers (Fig. 5.1B). However, differences in the number of beads per cell were not statistically significant for any particular type of bead (Fig 5.1B). Thus, HtpB-coated beads interacted with a higher percentage of cells in the monolayers, but the number of beads associated with each cell was comparable for all types of beads, a convenient situation for our experiments described below.

5.3.2. Mitochondria Recruitment by HtpB-Coated Beads

Nascent phagosomes containing *L. pneumophila* immediately avoid acidification and fusion with lysosomes. Instead, these nascent phagosomes rapidly become surrounded by small vesicles and mitochondria (Horwitz, 1983b; Horwitz, 1983c). Because previous results in HeLa cells suggested that HtpB-coated beads recruit vesicles (Garduno et al., 1998a), the intracellular trafficking of differently coated beads in CHO cells was examined by electron and fluorescence microscopy.

Transmission electron microscopy (TEM) revealed that in CHO-*htpB* cells mitochondrial recruitment to vacuoles containing *L. pneumophila* strain Lp02 occurs immediately upon internalization (Fig 5.2A). At 1 h after addition of beads to CHO-*htpB* cells, vacuoles containing HtpB-coated beads readily interacted with mitochondria (Fig 5.2B), as Lp02 did, whereas vacuoles containing the various control beads did not (Fig 5.2C and 5.2D). These observations were confirmed by fluorescence microscopy, which allowed quantitation. After 1 h incubation, significantly more HtpB-coated beads (53 ± 3%) were closely surrounded by mitochondria in relation to BSA-coated beads

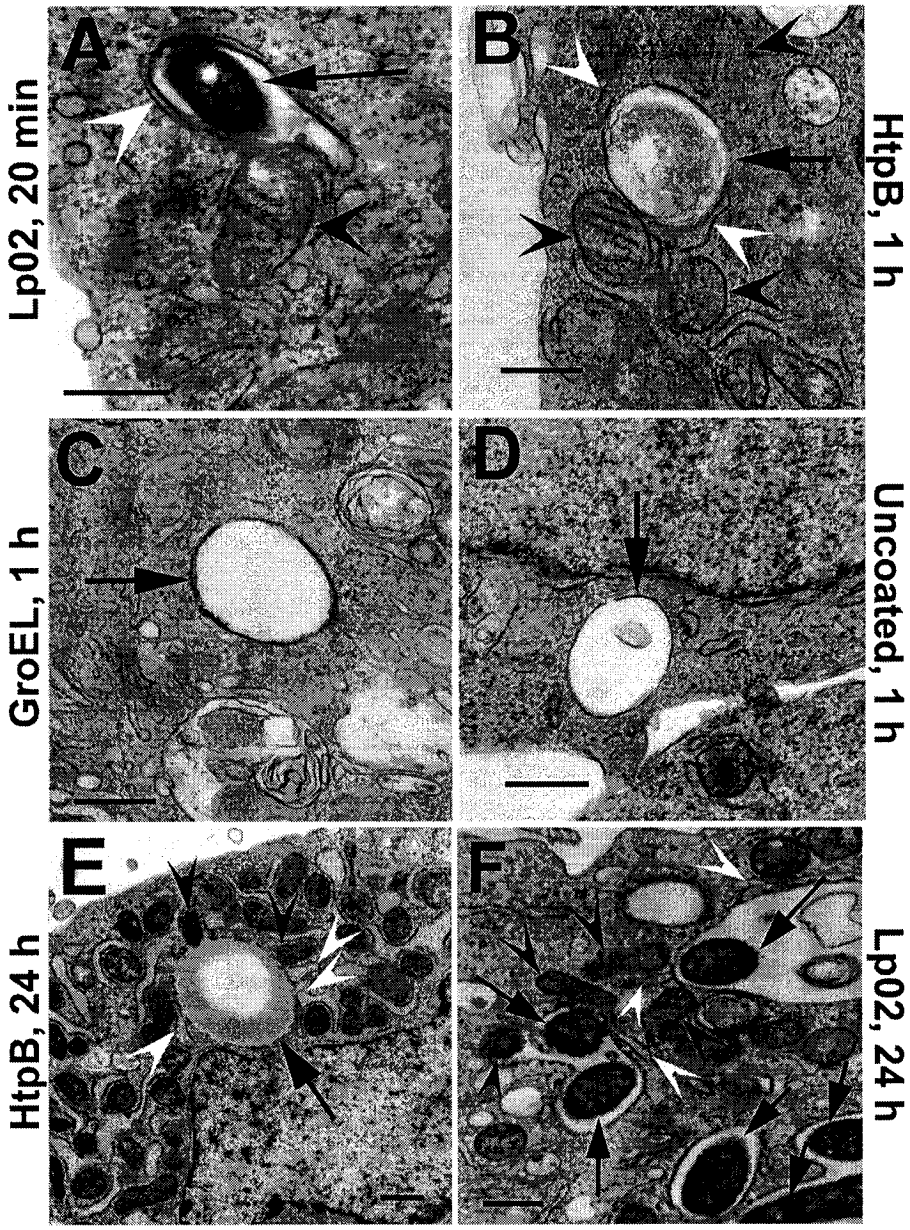

Figure 5.2. Intracellular Events Scored by TEM Show that Lp02 and HtpB-Coated Beads Attract Mitochondria and Portions of Smooth Endoplasmic Reticulum (ER) in CHO-*htpB* Cells.

CHO-*htpB* cells infected with *L. pneumophila* Lp02 for ~20 min (A) or 24 h (F) prior to processing. CHO-*htpB* cells were incubated with HtpB- (B), BSA- (C), or GroEL- (D) coated beads for 1 h. CHO-*htpB* cells were incubated with HtpB-coated beads for 24 h (E). Arrows indicate sectioned bacteria or beads, black arrowheads indicate mitochondria, and white arrowheads indicate smooth ER. Bars = 0.5 μm.

(30 ± 5%), GroEL-coated beads (38 ± 5%), uncoated beads (35 ± 2%) or an Lp02 dotB mutant (36 ± 5%). The small difference between the percent association of HtpB and Lp02 (53 ± 3% and 59 ± 4%, respectively) was not statistically significant, suggesting that the bead-attached HtpB is as competent as virulent Lp02 in attracting mitochondria (Fig 5.3A).

The levels of mitochondrial association with HtpB-coated beads dropped from 53 ± 3% to 40 ± 4% upon bead pre-treatment with antibody, and no longer showed statistically significant differences to the association levels of control beads and Lp02 dotB. This result strengthened the conclusion that HtpB is the primary effector of mitochondrial recruitment by the coated beads. HtpB-coated beads and Lp02 maintained their significantly higher levels of association with mitochondria for at least 3 h (Fig 5.3A), although TEM attested to longer periods of association (up to 24 h, Fig 5.2E and F). Representative fluorescence microscopy images are shown in Fig 5.3B-G, which also illustrate how fluorescent blue coated beads were scored by their contact or close vicinity with Mitotracker Orange-stained mitochondria. It should be noted that the absolute number of mitochondria associated with *L. pneumophila* or the differently-coated beads was not determined. Therefore, a bacterium or a bead closely surrounded by, or in contact, with mitochondria was scored as one positive event (Fig. 5.3), regardless of how many mitochondria were involved. Consequently, the effect of HtpB may have been underestimated.

Mitochondrial recruitment by HtpB-coated beads in U937 cells was also very apparent, as judged by ultrastructural studies. At 3 h post inoculation, phagosomes containing internalized Lp02 or HtpB coated beads were clearly associated with

Figure 5.3. Quantitative Fluorescence Microscopy Analysis Showing Mitochondria Recruitment by *L. pneumophila* Lp02 and HtpB-Coated Beads in CHO-*htpB* Cells. (A) Percentage of bacteria or beads associated with Mitotracker Orange CMTMRos stained mitochondria at 1 h and 3 h post inoculation. Bars correspond to the mean and error bars correspond to one standard deviation from three independent experiments. P-values were calculated in relation to HtpB-coated beads using a 1-way ANOVA followed by the Bonferroni test, and are shown as **($P<0.01$), * ($P<0.05$), and ns (no significance). Representative overlay images of CHO-*htpB* cells infected for 1 h with GFP-expressing Lp02 (B) or GFP-expressing Lp02dotB (D), or incubated for 1 h with blue fluorescent beads coated with either HtpB (C), BSA (E), GroEL (F), or uncoated (G). Mitochondria appear red-orange after staining with Mitotracker Orange CMTMRos. Mitochondria within one bead radius distance from a bead were considered as positive for recruitment. Arrows point to beads or bacteria surrounded by, or in contact with, mitochondria; whereas arrowheads point to beads or bacteria considered not to be associated with mitochondria. As a reference for size, beads are ~1 μm in diameter.

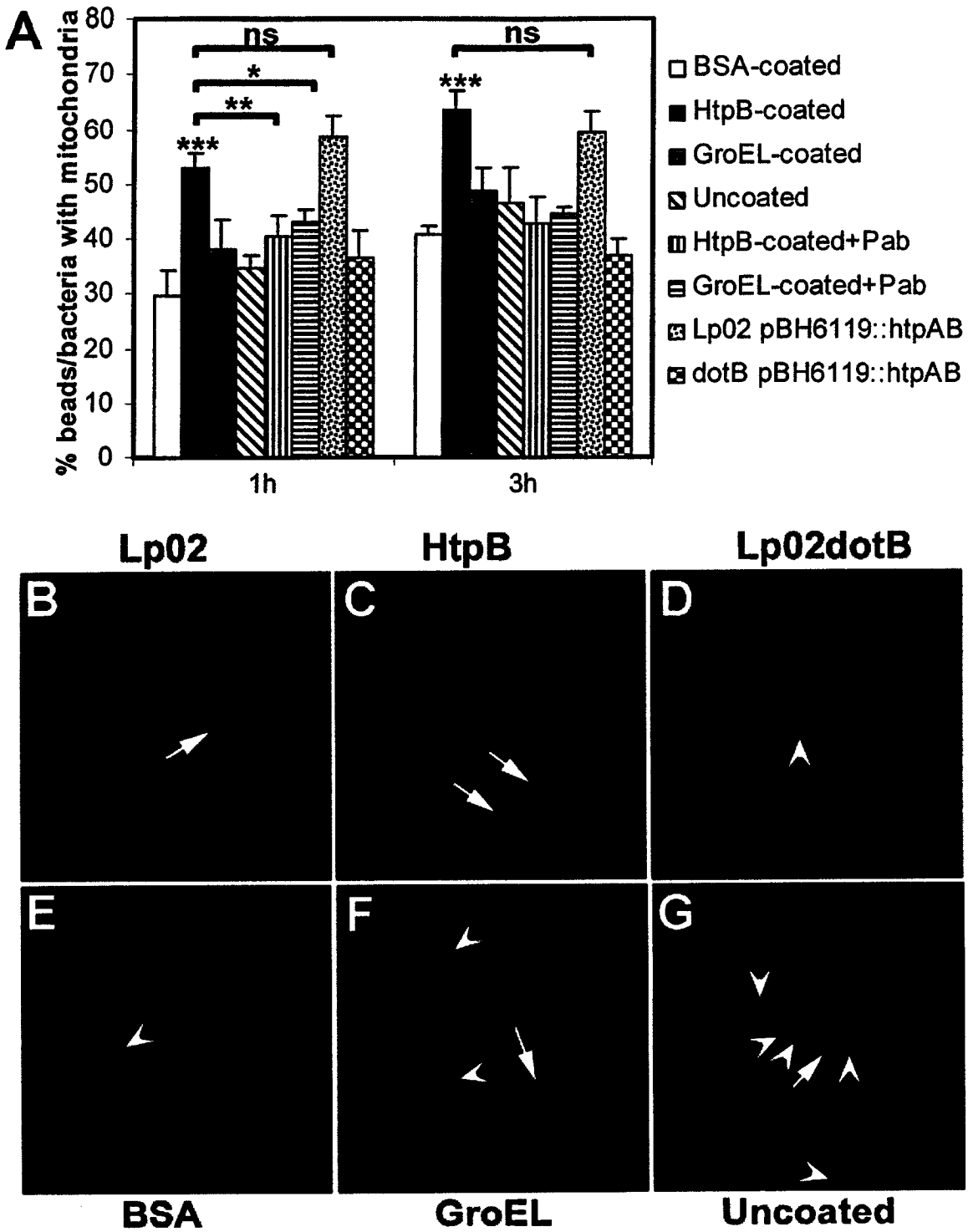
A
% beads/bacteria with mitochondria
80
70
60
50
40
30
20
10
0
ns
*
**
***
ns
***
1h
3h
BSA-coated
HtpB-coated
GroEL-coated
Uncoated
HtpB-coated+Pab
GroEL-coated+Pab
Lp02 pBH6119::htpAB
dotB pBH6119::htpAB
Lp02
HtpB
Lp02dotB
B
C
D
E
F
G
BSA
GroEL
Uncoated

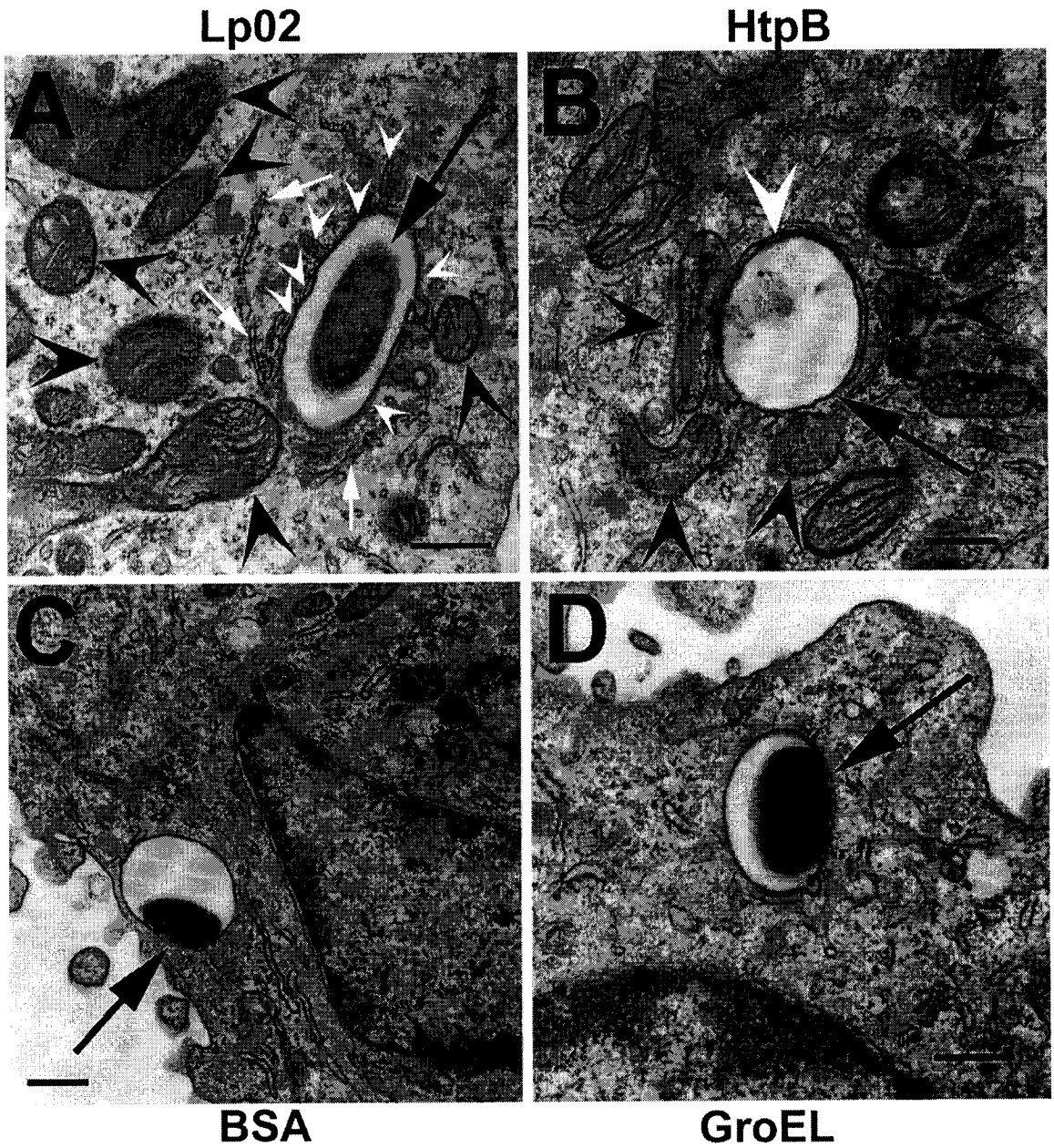

Figure 5.4. Electron Micrographs Show that *L. pneumophila* Lp02 and HtpB-Coated Beads Recruit Mitochondria in U937 Macrophages.
L. pneumophila strain Lp02 (A) and HtpB-coated beads (B) consistently attracted mitochondria and portions of smooth endoplasmic reticulum after internalization in U937 cells, whereas BSA- (C), or GroEL- (D) coated beads did not. All images were captured from specimens fixed 1 h after infection or bead addition. Black arrows indicate sectioned bacteria or beads, black arrowheads indicate mitochondria, white arrows indicate rough ER, and white arrowheads indicate smooth ER. Bars = 0.5 μm.

mitochondria in U937 macrophages (Fig 5.4A and 5.4B), whereas mitochondrial recruitment was not observed with internalized control beads (Fig. 5.4C and 5.4D) or the Lp02 dotB mutant. Since the resolution of Mitotracker staining in U937 macrophages was poor (mainly because U937 cells were not thinly stretched, and their mitochondria were quite slender and numerous in relation to those of CHO cells), the quantification of mitochondrial recruitment by fluorescence microscopy was not possible. These results indicate that HtpB specifically recruits mitochondria and that this ability is not shared by the HtpB homologue, GroEL.

5.3.3. Effect of HtpB-Coated Beads on Cytoskeletal Organization

Cytoskeletal rearrangements, in particular those involving F-actin, have been previously observed in host cells infected with *L. pneumophila* (Coxon et al., 1998; Khelef et al., 2001; Susa and Marre, 1999). These actin rearrangements appear to represent an additional activity distinct from the well-documented actin microfilament rearrangements required for the internalization of *L. pneumophila* in macrophages (Elliott and Winn, 1986), lung fibroblasts (Susa and Marre, 1999), monocytes (Coxon et al., 1998; King et al., 1991), HeLa cells (Garduno et al., 1998b) and *Dictyostelium discoideum* (Lu and Clarke, 2005). Intact microtubules also seem to directly or indirectly participate in the early steps of mammalian cell infection by *L. pneumophila*, including entry (Garduno et al., 1998b; Lu and Clarke, 2005). Since F-actin and microtubules are also involved in organelle trafficking (Boldogh and Pon, 2006; Morris and Hollenbeck, 1995; Simon and Pon, 1996; Summerhayes et al., 1983), we examined whether HtpB-

coated beads had an effect on the microfilament and microtubule networks of CHO-*htpB* cells, for insight into the mechanism of mitochondrial recruitment by *L. pneumophila*.

CHO-*htpB* cells stained for F-actin with Alexa Fluor 546-conjugated phalloidin showed fine filamentous structures in the form of stress fibers (Fig 5.5A). Infection of CHO-*htpB* cells with *L. pneumophila* strain Lp02 resulted in the disappearance of stress fibers (compare Fig 5.5A with 5.5B), which correlated with a strong staining of F-actin bundles along the periphery of the cells. Similarly, incubation of CHO-*htpB* cells with HtpB-coated beads resulted in the accumulation of peripheral actin bundles along with the loss of stress fibers (Fig 5.5C). Approximately half (51 ± 4%) of the CHO-*htpB* cells infected with Lp02 for 1 h exhibited this phenotype, and 66 ± 1% exhibited this phenotype when incubated with HtpB-coated beads for 1 h (Fig 5.5G). In contrast, significantly fewer CHO-*htpB* cells incubated with BSA-coated beads (38 ± 4%), GroEL-coated beads (38 ± 2%), uncoated beads (37 ± 5%), or infected with the Lp02dotB mutant (28 ± 6%), displayed this altered F-actin phenotype (Fig 5.5G). The baseline percent of cells without stress fibers was determined to be 36 ± 5% in the untreated control. Importantly, pretreatment of HtpB-coated beads with an HtpB-specific polyclonal antibody neutralized the induction of F-actin rearrangements (Fig 5.5G), pointing at HtpB as the primary effector of this altered phenotype. At the 3 h point, there was a significant decrease in the percentage of CHO cells without stress fibers in the Lp02 and HtpB-coated beads groups, suggesting that this effect is transient (Fig 5.5G).

Immunostaining with a tubulin-specific antibody showed no change in the microtubule pattern of CHO-*htpB* cells infected with Lp02, or incubated with HtpB-coated beads, in relation to untreated cells. All cells showed an apparently intact network

Figure 5.5. Confocal Microscopy Analysis Showing the F-Actin Rearrangements Induced by *L. pneumophila* Strain Lp02 and HtpB-Coated Beads in CHO-*htpB* Cells.

Representative single slice overlay images of F-actin rearrangement in CHO-*htpB* cells that were untreated (A), infected with GFP-expressing Lp02 (B), GFP-expressing Lp02dotB (D), or incubated with green fluorescent HtpB- (C), BSA- (E), or GroEL- (F) coated beads for 1 h. F-actin was labeled with phalloidin conjugated to Alexa Fluor 546 (in red). Note the absence of stress fibers (central thin red lines) in the cells shown in panels (B) and (C). Bars=10 μm. (G) Percentage of CHO-*htpB* cells associated with bacteria or beads, which show loss of cytoplasmic F-actin stress fibers and the accentuation of peripheral F-actin bundle framing at 1 h and 3 h after infection or bead addition. Bars correspond to the mean, and the error bars correspond to one standard deviation, from three independent experiments. P-values were calculated using a 1-way ANOVA followed by the Bonferroni test, and are shown as **($P<0.01$) and * ($P<0.05$) in relation to HtpB-coated beads.

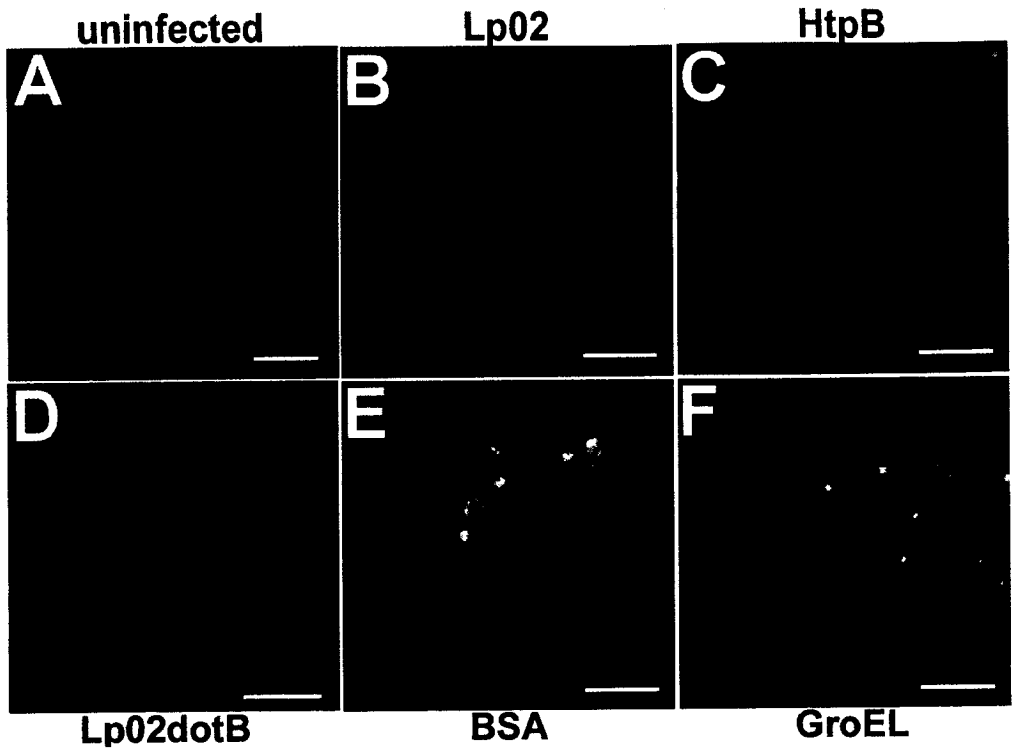
uninfected
Lp02
HtpB
A
B
C
D
E
F
Lp02dotB
BSA
GroEL

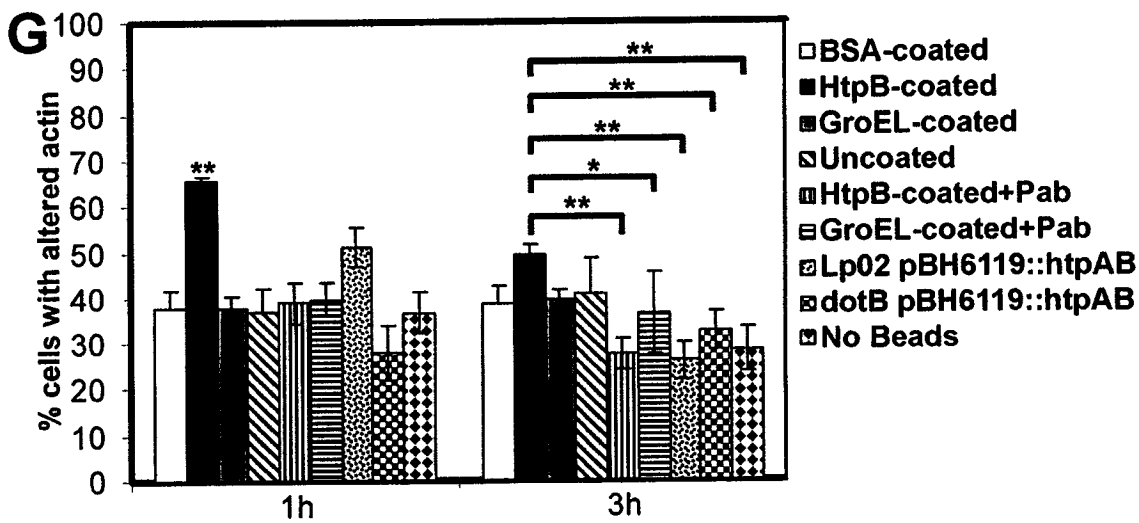
G
% cells with altered actin
100
90
80
70
60
50
40
30
20
10
0
1h
3h
**
**
**
**
*
**
BSA-coated
HtpB-coated
GroEL-coated
Uncoated
HtpB-coated+Pab
GroEL-coated+Pab
Lp02 pBH6119::htpAB
dotB pBH6119::htpAB
No Beads

of microtubules radiating from a central region as shown for CHO-*htpB* cells stained for tubulin in Fig. 6.6i and 6.6j. We thus concluded that HtpB specifically and strongly mediated a transient rearrangement of F-actin (as Lp02 does), and that this ability was not shared by the HtpB homologue, GroEL.

5.3.4. Interaction of HtpB-Coated Beads with the ER and Lysosomal Networks

Shortly after internalization, *L. pneumophila* associates with the ER and the LCV acquires ER markers. Therefore, we examined the interaction of the differently coated beads with the ER network. No association between beads and the ER was conclusively detected in CHO-*htpB* cells by fluorescence microscopy, either through indirect immunostaining of BiP (an ER-marker protein), or direct staining with ER-Tracker Blue-White DPX. Likewise, ribosome studding and rough ER association with endosomes containing HtpB-coated beads was not observed by TEM at 1 h (Fig 5.2B), or at 3 h, 6 h and 24 h incubations (Fig. 5.2E), indicating that HtpB does not mediate an association with the ER, as clearly seen for LCVs.

Maturation of LCVs or bead-containing phagosomes along the endocytic pathway was first evaluated by scoring the co-localization with LAMP-1, a protein of late endosomes and lysosomes. At 1 h and 3 h after infection, Lp02 LCVs seldom co-localized with LAMP-1, but phagosomes containing the dotB mutant clearly acquired LAMP-1 staining (Table 5.1). Regardless of the type of coating, phagosomes containing beads all showed positive LAMP-1 staining at significantly higher frequencies in relation to Lp02 LCVs, or even the dotB mutant-containing phagosomes ($P<0.05$, Table 5.1).

Table 5.1. Fluorescence Microscopy Quantitation of Bead and Bacterial Co-Localization with LAMP-1 in CHO-*htpB* Cells.

Bead coating	% beads colocalized with LAMP-1[a]					
	1 h			3 h		
	Mean	SD	p-value[b]	Mean	SD	p-value[b]
BSA-coated	71	2	ns	77	7	ns
HtpB-coated	67	4		75	10	
GroEL-coated	68	9	ns	76	4	ns
Uncoated	71	8	ns	74	5	ns
HtpB-coated + Ab	74	9	ns	76	10	ns
GroEL-coated + Ab	71	7	ns	76	12	ns
Lp02	8	0	<0.05	13	3	<0.05
dotB	25	2	<0.05	39	4	<0.05

[a]50 beads were scored for each type of coating. Results are shown as mean and standard deviation (SD) from three independent experiments (n=3).
[b]p-values are calculated in relation to HtpB-coated beads, ns = no significance.

Table 5.2. Fluorescence Microscopy Quantitation of Bead and Bacterial Co-Localization with the Lysosomal Compartment, Pre-Labeled with Texas Red Ovalbumin, in CHO-*htpB* Cells.

Bead coating	% beads colocalized with Texas Red ovalbumin[a]					
	1 h			3 h		
	Mean	SD	p-value[b]	Mean	SD	p-value[b]
BSA-coated	33	3	<0.05	40	4	<0.05
HtpB-coated	23	2		32	3	
GroEL-coated	29	1	<0.05	34	2	ns
Uncoated	32	1	<0.05	37	1	ns
HtpB-coated + Ab	31	4	<0.05	38	2	ns
GroEL-coated + Ab	41	1	<0.05	34	3	ns
Lp02	<1	0	<0.05	<1	0	<0.05
dotB	<1	0	<0.05	<1	0	<0.05

[a]100 beads were scored for each type of coating. Results shown are from one experiment representative of two independent ones and are presented as mean and standard deviation (SD) from triplicate wells (n=3).
[b]p-values are calculated in relation to HtpB-coated beads, ns = no significance.

We next assessed delivery of the beads to the lysosomal compartment, using TrOv stained lysosomes in CHO-*htpB* cells. In agreement with the findings of Joshi et al. (2001), phagosomes containing Lp02 or the dotB mutant rarely colocalized with TrOv at either 1 h or 3 h post-infection (Table 5.2). In contrast, phagosomes containing beads (regardless of the type of coating) all colocalized with TrOv at significantly higher frequencies in relation to live *L. pneumophila* ($P<0.05$, Table 5.2). However, among all bead types used, HtpB-coated beads consistently showed, at 1 h post inoculation, the lowest frequency of co-localization with TrOv (Table 5.2). Collectively, these results indicate that HtpB modestly slows but does not block fusion of phagosomes with lysosomes.

5.3.5. Intracellular Growth of *L. pneumophila* in the Presence of HtpB-Coated Beads

Intracellular growth of a dotA avirulent mutant in macrophages can be restored when the mutant is co-internalized into the same phagosome with wild-type *L. pneumophila* (Coers et al., 1999). Therefore, we set out to determine whether HtpB-coated beads could rescue the intracellular growth of a dotA mutant in CHO cells. TEM of CHO-*htpB* cells infected with Lp02 in the presence of BSA-coated or HtpB-coated beads showed that bacterial cells and beads did not co-localize in the same phagosome (Fig 5.6A and 5.6B). However, ~ 50 % of the internalized dotA mutants co-localized with BSA-coated or HtpB-coated beads in CHO-*htpB* cells (Fig 5.6C and 5.6D). We concluded that, despite having similar invasion rates (Lp02 = 0.28 ± 0.04 % inoculum, and Lp02dotA = 0.31 ± 0.07 % inoculum), Lp02 and the dotA mutant clearly followed different pathways of internalization in CHO-*htpB* cells.

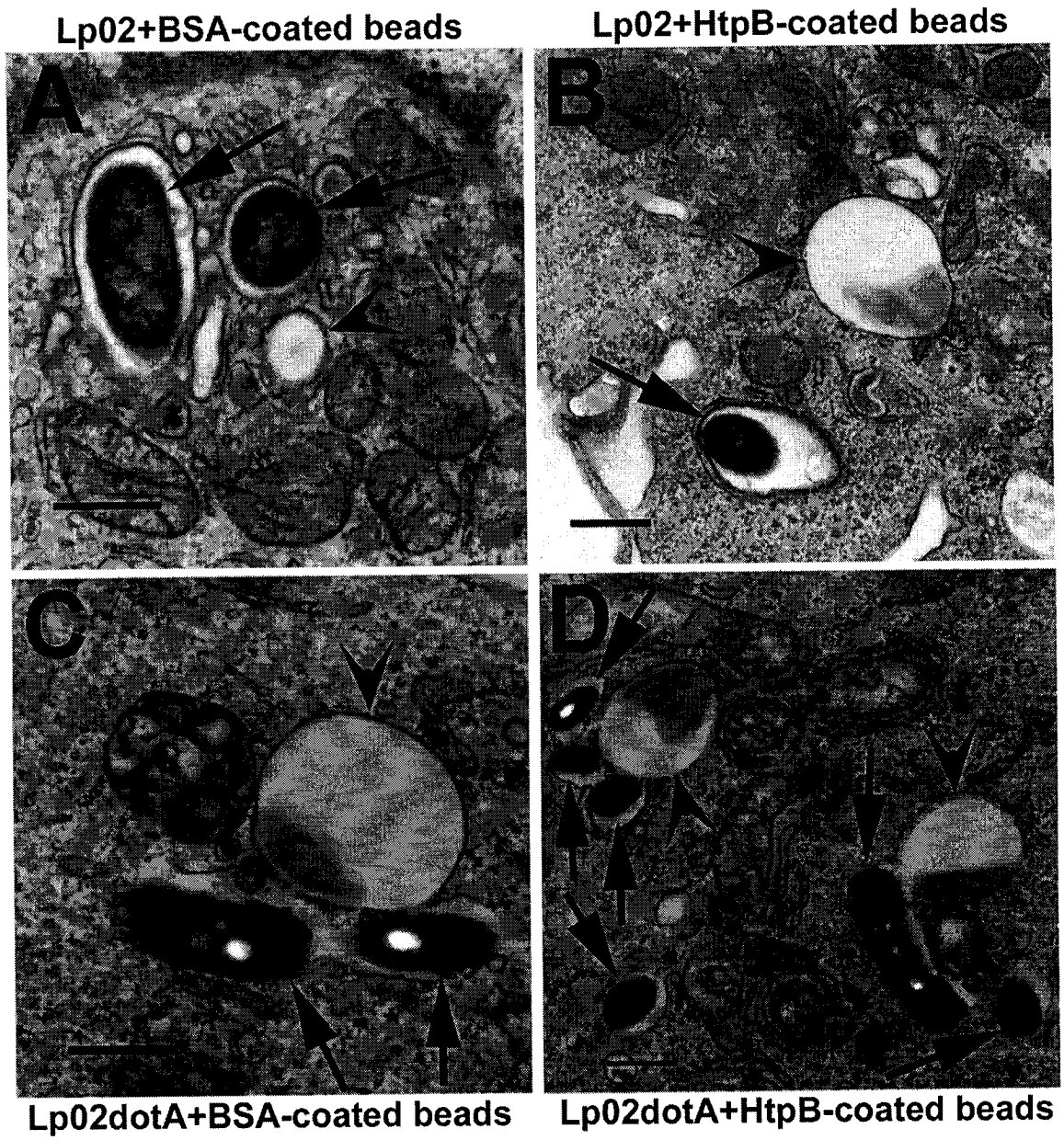

Figure 5.6. Electron Micrographs of *L. pneumophila* Internalized by CHO-*htpB* Cells in the Presence of Coated Beads Show that Only Lp02dotA Is Co-Internalized with Beads.

CHO-*htpB* cells were infected for 1 h with Lp02 and BSA-coated beads (A), Lp02 and HtpB-coated beads (B), Lp02 dotA and BSA-coated beads (C), or Lp02dotA and HtpB-coated beads (D). TEM sections were scored for the co-localization of bacteria and coated beads in the same phagosome. Arrows point at bacteria, whereas arrowheads point at beads. Bars = 0.5 μm.

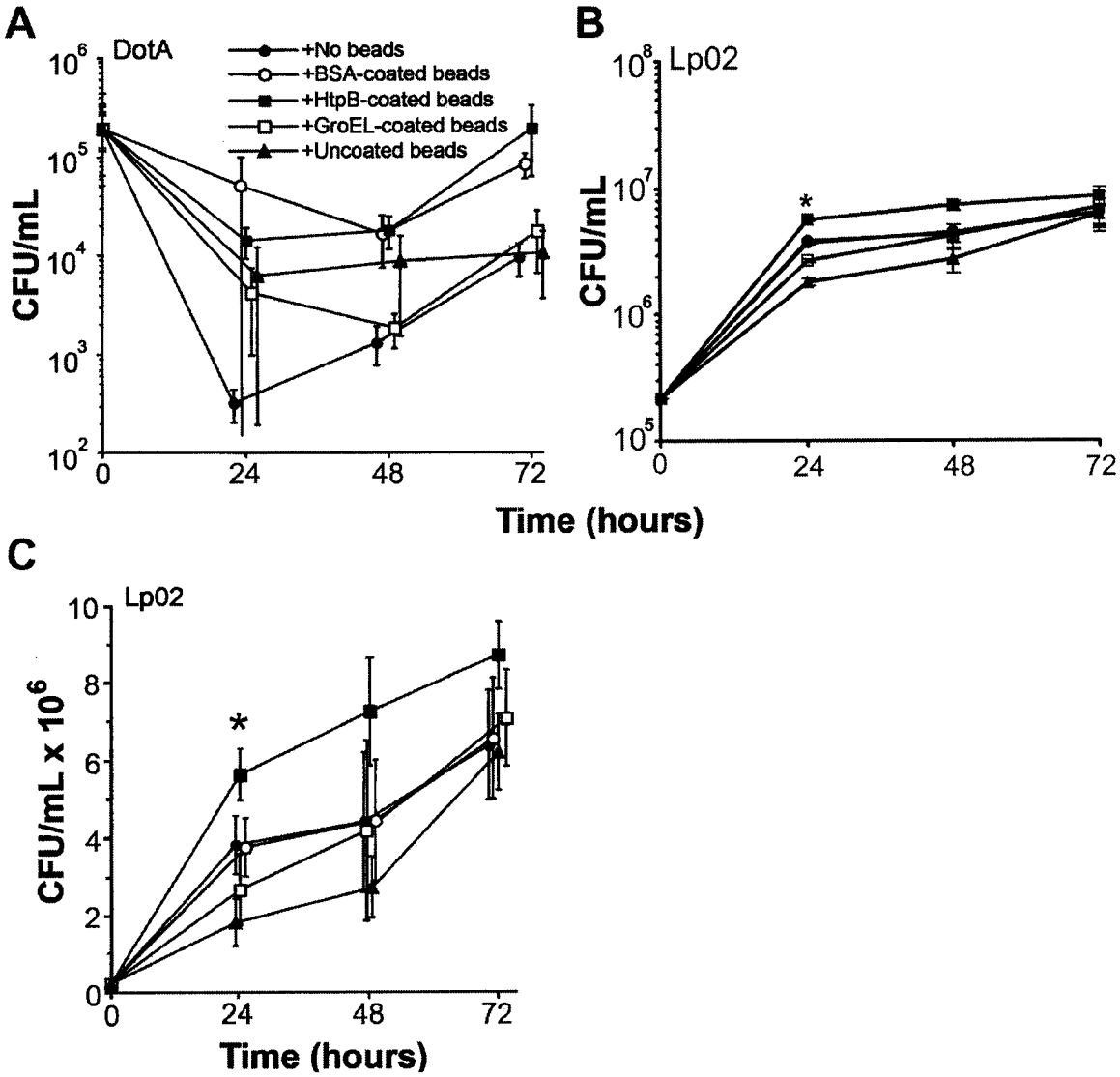

Figure 5.7. Intracellular Growth of *L. pneumophila* Lp02 and Lp02dotA in the Presence of Coated Beads Shows that HtpB Enhances the Growth of Lp02.
CHO-*htpB* cells were infected with Lp02dotA (A), or strain Lp02 (B and C) in the presence of BSA-coated, HtpB-coated, GroEL-coated, or uncoated beads. (C) The Lp02 intracellular growth curves in (B) were plotted using a linear y-axis for better visualization of the differences among each sample. Points represent the mean number of viable intracellular bacteria and error bars ± one standard deviation from two independent experiments done in triplicate. * P=<0.05.

Even though HtpB-coated beads attracted mitochondria to the phagosomes shared with Lp02dotA (e.g. Fig. 5.6D), they did not rescue the intracellular growth of the mutant (Fig. 5.7A). However, when we examined the effect of the differently coated beads on the intracellular growth of Lp02, there was a slight but consistent improvement of growth in the presence of HtpB-coated beads (Fig. 5.7B and C). The fact that Lp02 and HtpB-coated beads did not co-localize in the same phagosome, suggests that the beneficial effect of the beads was perhaps mediated through a signaling mechanism. These results indicated that while HtpB might promote the growth of virulent *L. pneumophila* in-trans, it cannot compensate for all the signals and factors missing from the dotA mutant, which would be necessary for LCV maturation and initiation of intracellular growth.

5.4. Discussion

As first described for *L. pneumophila*-infected human monocytes (Horwitz, 1983a), shortly after the internalization of virulent *L. pneumophila* by host cells, phagosomes associate with smooth vesicles and mitochondria. The recruited mitochondria then remain associated with the LCV for different lengths of time, as shown by ultrastructural studies of infected monocytes (Horwitz, 1983b), HeLa cells (Garduno et al., 1998b) and MRC-5 cells (Oldham & Rodgers, 1985). Here we have shown that phagosomes containing HtpB-coated beads consistently and persistently associate with mitochondria in CHO and U937 cells, thereby demonstrating that the purified *L. pneumophila* chaperonin emulates this *L. pneumophila* trait. The fact that GroEL-coated beads were unable to associate with mitochondria above the levels observed for control beads, indicates that mitochondrial recruitment is not a general effect of all bacterial

chaperonins, and further suggests that specific protein domains present in HtpB but not in GroEL may be responsible for such an effect.

The mechanism by which *L. pneumophila* recruits mitochondria is not known, but now we have identified a *L. pneumophila* HtpB preparation that produces this effect. Recruitment of host mitochondria to the LCV in human monocytes seems to depend on a functional Dot/Icm system, as retrospectively inferred from experiments with a spontaneous *L. pneumophila* mutant (Horwitz, 1987) that regains a wild-type phenotype by genetic complementation with the *icm* locus (Marra et al., 1992). We also observed here that *dotA* and *dotB* mutants were unable to attract mitochondria in CHO or U937 cells, corroborating the need of a functional Dot/Icm system for mitochondrial recruitment. This observation implies that a potential link exists between HtpB and the Dot/Icm system (also suggested by Allan [2002] who showed that surface localization of HtpB in *L. pneumophila* is Dot/Icm-dependent), or that other factors mobilized by the Dot/Icm system (which may have also been co-purified with HtpB) are required for mitochondrial recruitment. Although at this point we cannot rule out the latter, it seems that the *L. pneumophila* chaperonin is sufficient to attract mitochondria.

L. pneumophila infection of CHO cells induced a rearrangement of the actin cytoskeleton, but the interaction of CHO cells with HtpB-coated beads induced a more dramatic rearrangement. Since HtpB mediates invasion of HeLa cells (Garduno et al., 1998a), a valid question here is whether this actin rearrangement is linked to the actin polymerization changes required for internalization. Protein-coated beads and uncoated beads were all internalized by CHO cells, but only HtpB-coated beads induced the disappearance of stress fibers. In addition, as previously suggested by Khelef et al.

(2001), the Dot/Icm system is not necessarily required to effect the actin polymerization changes that mediate *L. pneumophila* internalization, because in our hands Lp02 and Lp02*dotA* showed similar invasion rates in CHO cells (data not shown). However, a functional Dot/Icm system is required in the transient induction of stress fiber disappearance because the *dotB* mutant failed to induce this effect in CHO cells. Therefore, we concluded that the observed transient disappearance of stress fibers represents a post-internalization HtpB-mediated event that is independent from the actin polymerization changes required for the entry of *L. pneumophila* and microbeads.

The microtubule network remained unaffected during *L. pneumophila* infection of CHO cells. It is possible that perturbation of the actin cytoskeleton by *L. pneumophila* (via HtpB) in the presence of an intact microtubule network may be required for the recruitment of mitochondria to the LCV. Mitochondrial movement mainly occurs along microtubule tracks in eukaryotic cells (Summerhayes et al., 1983), although short-distance movement can also involve actin microfilaments (Kuznetsov et al., 1994; Morris and Hollenbeck, 1995). Of relevance to our mechanistic hypothesis is the observation that disruption of actin microfilaments results in increased mitochondrial movement along microtubule tracks in sea urchin coelomocytes (Krendel et al., 1998). Also, the transient clustering of mitochondria around the nucleus in response to vaccinia virus-mediated changes in the actin organization of infected PtK2 cells is dependent on intact microtubules (Schepis et al., 2006). It remains to be determined whether mitochondria recruitment by *L. pneumophila* is susceptible to inhibitors of tubulin polymerization. These experiments, however, may be challenging since microtubule disrupting agents also tend to inhibit the internalization of *L. pneumophila* and microbeads. Both

disruption of the actin organization and recruitment of mitochondria were two robust effects induced by the same protein attached onto beads. This causal convergence (in addition to the common dependence on the Dot/Icm system) suggests a link between these two phenotypes. Therefore, we predict that the transient *L. pneumophila*-induced changes in actin organization result in mitochondrial recruitment to the LCV.

Mitochondrial recruitment is not a trafficking feature unique to the LCV. It is a feature shared with the parasitophorous vacuoles of *Chlamydia psittaci* (Matsumoto et al., 1991; Peterson and de la Maza, 1988), *Toxoplasma gondii* (Sinai and Joiner, 2001; Sinai et al., 1997), and *Enchephalitozoon* microsporidia (Scanlon et al., 2004). As far as we know, the molecular mechanism of recruitment has been described only in the case of *T. gondii*, where the N-terminus of ROP2, a *T. gondii* protein localized to the parasitophorous vacuole membrane, has characteristics of a mitochondrial targeting signal sequence and is exposed to the host cytosol (Sinai and Joiner, 2001). ROP2 inserts into the mitochondrial membrane tethering the organelle to the vacuole. HtpB is abundantly released into the lumen of the LCV (Garduno et al., 1998), and possesses the conserved glycine- and methionine-rich C-terminus thought to be responsible for the membrane-targeted lipochaperonin activity previously reported for GroEL (Török et al., 1997). Therefore, while HtpB could still associate with the LCV membrane and act through a mechanism similar to that reported for ROP2, the lack of both a predicted mitochondrial targeting signal and homology to ROP2 indicate that HtpB recruits mitochondria by a novel, yet to be described mechanism. If we were to speculate about such a mechanism, it seems reasonable to propose an HtpB-mediated signaling process across the phagosomal membrane. In this respect, it is known that chaperonins, in

general, are capable of intracellular and intercellular signaling (reviewed by Maguire et al., 2002), and that HtpB, in particular, triggers a Ras2-transduced signal in yeast that induces pseudohyphal growth (Riveroll, 2005). The combined results from Figs. 5.6 & 5.7 also suggest that HtpB promotes the early growth of Lp02 by a signaling event. Alternatively, HtpB might recruit host factors and have an indirect effect, as reported for other *L. pneumophila* proteins that recruit host effectors to regulate phagosome trafficking (Derre and Isberg, 2004; Kagan et al., 2004).

Based on previous and current data, the HtpB-mediated events in the early trafficking of *L. pneumophila* could be summarized as follows. In response to an unidentified signal from host cells, *L. pneumophila* upregulates the synthesis of HtpB, and releases this protein to be displayed on the bacterial cell surface (Fernandez et al., 1996; Garduno et al., 1998), where it is in a position to contribute to the association of *L. pneumophila* with host cells (Garduno et al., 1998a). Once *L. pneumophila* is internalized, surface-exposed and free HtpB released into the LCV (Fernandez et al., 1996; Garduno et al., 1998) trigger actin rearrangements (Fig. 5.5) and promote the association of the LCV with mitochondria (Figs. 5.2-5.4). These HtpB-mediated early events seem to favor the growth of virulent *L. pneumophila* (Fig. 5.7). Throughout its replication phase *L. pneumophila* continues to produce abundant amounts of HtpB, which accumulate within the LCV (Garduno et al., 1998; Hoffman et al., 1990). The function of HtpB at this advanced stage of the intracellular growth cycle remains a target of future investigation.

Remarkable progress has been made in understanding the intracellular trafficking of *L. pneumophila* (Derre and Isberg, 2004; Derre and Isberg, 2005; Kagan et al., 2004;

Robinson and Roy, 2006), but the molecular players involved remain to be fully elucidated. Our studies provide evidence for the specific involvement of HtpB in the recruitment of mitochondria, not only revealing another seemingly unique function of HtpB in the cell biology of host-pathogen interactions, but also a novel facet of chaperonin biology.

Chapter 6: The *Legionella pneumophila* Chaperonin Reaches the Cytoplasm of Infected Cells Where It Can Induce Actin Cytoskeletal Rearrangements

6.1. Abstract

The intracellular pathogen *Legionella pneumophila* replicates in host cells within a specialized vacuole. The *L. pneumophila* chaperonin, HtpB, is up-regulated during infection, and abundantly released into the lumen of this specialized vacuole. Although there is evidence for the association of HtpB with the vacuolar membrane, it is not known whether HtpB has access to the host cytosol. Using HtpB-adenylate cyclase fusions we determined that HtpB is translocated into the cytoplasm of host cells. Immunogold labeling of *Legionella*-containing vacuoles (LCV) isolated from U937 and CHO cells also revealed that HtpB localizes to the cytoplasmic face of the LCV. To define potential roles of the translocated HtpB, the *htpB* gene was transfected into, and expressed in the cytoplasm of Chinese hamster ovary (CHO) cells. CHO cells expressing HtpB displayed a rearrangement of the actin cytoskeleton, but not CHO cells expressing the HtpB homolog from *Escherichia coli*, GroEL. We demonstrated the ability of both HtpB and GroEL to co-sediment with, and induce de-polymerization of F-actin in vitro, suggesting a direct interaction between bacterial chaperonins and actin. Based on the inability of GroEL to alter actin fibers, we have excluded the direct interaction with actin as the mechanism underlying cytoskeletal remodeling, and propose a model where cytoplasmic or membrane-associated HtpB initiates an intracellular signal that affects actin organization.

6.2. Introduction

Chaperonins constitute a family of highly conserved proteins found in all prokaryotic and eukaryotic organisms (Gupta, 1995). Their primary role is to facilitate the folding of nascent and stress denatured proteins to their functional native state through the binding and hydrolysis of ATP (Lin and Rye, 2006). Group I chaperonins, referred to as Hsp60 or GroEL, are prokaryotic proteins found in bacteria and the eukaryotic organelles mitochondria and chloroplasts (Gupta, 1995). The protein folding form of the Group I chaperonins (Cpn60, GroEL, or Hsp60) is a homo-oligomeric double-ring assembly of fourteen subunits with a central cavity in each ring being the site for binding and folding of unfolded substrates (Bukau and Horwich, 1998; Lin and Rye, 2006). Association of the GroEL rings with a third heptameric ring comprised of a co-chaperonin (Cpn10, GroES, or Hsp10) is required for protein folding (Bukau and Horwich, 1998; Lin and Rye, 2006). Group II chaperonins (also known as CCT or TCP-1 proteins), found in the eukaryotic cytosol and in Archaebacteria, form hetero-oligomeric double-ring assemblies of eight- or nine-fold symmetry, and do not work in conjunction with a co-chaperonin (Valpuesta et al., 2002).

Most of the characteristics of the Group I chaperonins, determined from structural and functional studies of the *E. coli* GroEL, have firmly established their role as intracellular folding machineries (Bochkareva et al., 1988; Braig et al., 1994; Zeilstra-Ryalls et al., 1991). GroEL is an essential protein in *E. coli* (Fayet et al., 1989; Kusukawa and Yura, 1988), and its levels elevate dramatically as a protective response to different stressful stimuli (Lund, 2001; VanBogelen et al., 1987). However, the paradigm of Hsp60s as intracellular protein-folding machinery has changed with accumulating reports

of surface- and membrane-associated chaperonins. Extracytoplasmic Hsp60s from *Haemophilus ducreyi* (Frisk et al., 1998), *Helicobacter pylori* (Cao et al., 1998; Yamaguchi et al., 1997), *Borrelia burgdoferi* (Scopio et al., 1994), and *Clostridium difficile* (Hennequin et al., 2001) have all been implicated in non-chaperone functions such as adhesins or invasins. Other studies demonstrating the functional flexibility of the Group I chaperonins include the Hsp60 of *Mycobacterium leprae* as a protease (Portaro et al., 2002), and the GroEL of *Enterobacter aerogenes* as an insect toxin (Yoshida et al., 2001). In fact, the *E. coli* GroEL has also been reported to possess a lipid membrane association and stabilizing capability (Török et al., 1997).

Legionella pneumophila, a Gram-negative facultative intracellular bacterium, is an opportunistic human pathogen that causes Legionnaires' disease (Horwitz and Silverstein, 1980; Winn, 1988). The *L. pneumophila* 60-kDa chaperonin, HtpB, is expressed at high levels under steady state conditions with only a 2-fold increase in expression following heat shock. This is in sharp contrast to the normally low levels of expression of GroEL in *E. coli*, and the ~20-fold increase in expression upon heat shock (Hoffman et al., 1989; Lema et al., 1988). More than 50% of the cell-associated HtpB detectable by immunogold labelling is either membrane-associated, periplasmic or cell-surface localized in *L. pneumophila* (Garduno et al., 1998). We have previously established a role for the surface-localized HtpB as an adhesion and invasion molecule (Garduno et al., 1998a); functions relevant to the early steps of intracellular establishment. However, the continued expression of HtpB late in infection, its abundant release into the LCV, and its apparent association with the LCV membrane (Fernandez et al., 1996; Garduno et al., 1998a), suggest that HtpB may have additional functions. In this

study, we determined that the extracytoplasmic localization of HtpB during infection in not limited to the LCV lumen, but HtpB is also delivered into the host cell cytosol where it is associates on the cytoplasmic face of the LCV. In addition, ectopic expression of HtpB caused actin cytoskeletal rearrangements in CHO cells. Our results suggest that HtpB may be involved in LCV trafficking.

6.3. Results

6.3.1. HtpB Localization during Infection of Mammalian Cells

Although HtpB localizes to the surface of *L. pneumophila* (Garduno et al., 1998) and is found free in the LCV lumen (Fernandez et al., 1996; Garduno et al., 1998b), it is not known whether it remains restricted to the LCV or accesses the host cell cytoplasm. HtpB-specific immunogold labeling of pre-embedded LCVs isolated from infected CHO-*htpB* cells (Fig 6.1A and 6.1B) or U937 cells (Fig 6.1C) displayed sparse but highly specific labeling of the cytoplasmic side of the LCV membrane. Isolated LCVs were not only identified by the presence of a surrounding third membrane with a lighter staining density, but also by the presence of host vesicles and organelles, most notably mitochondria, tightly associated with the LCV surface (Fig 6.1A-D, F), as previously observed by Tilney et al. (2001). In contrast, free Lp02 cells not enclosed within a vacuole were not found in close association with host vesicles or mitochondria (Fig 6.1E). These free Lp02 cells displayed ample HtpB labeling along the periphery of the bacterial cell (Fig 6.1E) confirming the previously reported surface localization of HtpB (Garduno et al., 1998a) in intracellular legionellae. Because the LCV preparations were labeled with the HtpB-specific antibody prior to fixation and embedding, it is highly

unlikely that HtpB labeling of the LCV is due to permeabilization of the phagosome membrane. Immunogold labeling of isolated LCVs with an antibody against the major outer membrane protein (OmpS) of *L. pneumophila* did not reveal any surface labeling of LCVs, confirming both the integrity of the LCV membrane and the specificity of the HtpB labeling (Fig 6.1D). Bacteria not enclosed within LCVs were densely labeled by the OmpS-specific antibody (Fig 6.1F). Host vesicles and organelles from the same preparations were not labeled by either HtpB- or OmpS-specific antibody demonstrating the specificity of the antibodies, and indicating that labeling on the LCV was not due to HtpB contamination from lysed or free bacteria. Non-specific labeling of the isolated LCVs by the secondary antibody (primary antibody omitted) was not observed.

Translocation of multiple *L. pneumophila* effectors into the eukaryotic host cytosol has been demonstrated using the *Bordetella pertussis* adenylate cyclase (CyaA) reporter system (Campodonico et al., 2005; Chen et al., 2004; Nagai et al., 2005; Shohdy et al., 2005; de Felipe et al., 2005). CyaA requires calmodulin, present only in the eukaryotic cell cytosol, as a cofactor. Therefore, a CyaA-mediated cAMP increase in cells infected with bacteria producing CyaA hybrid proteins indicates translocation of the hybrid proteins into the eukaryotic cell. To confirm our immunogold labeling observations, we generated both C-terminal (HtpB:CyaA) and N-terminal (CyaA:HtpB) HtpB:cyclase protein fusions and tested the ability of *L. pneumophila* strains Lp02 and JR32 to deliver the hybrid proteins into host cells by measuring the cAMP levels in *L. pneumophila* infected CHO-*htpB* cells.

As determined by immunoblot analysis, the levels of LepA:CyaA, HtpB:CyaA, and CyaA:HtpB expressed by Lp02 after induction for 2 h with 1 mM IPTG were

Figure 6.1. HtpB Is Localized to the Cytoplasmic Side of LCVs Isolated from CHO-*htpB* and U937 Cells.
Ultrathin sections of LCVs isolated from host cells infected with Lp02 for 3 h. LCVs were labeled with primary antibodies prior to fixation. Primary antibody staining was visualized with a secondary anti-rabbit antibody conjugated to 10 nm gold particles. (A) A phagosome containing Lp02 isolated from CHO-*htpB* cells labelled with anti-HtpB PAb. (B) Higher magnification of the area outlined in (A). Phagosomes containing Lp02 isolated from U937 cells labelled with (C) anti-HtpB PAb or (D) anti-MOMP. Extracellular Lp02 from LCV isolation preparations labeled with (E) anti-HtpB PAb or (F) anti-MOMP. Black arrows indicate phagosome or bacterial membranes; white arrows indicate immunogold staining on the cytoplasmic side of the phagosome. V, host vesicle.

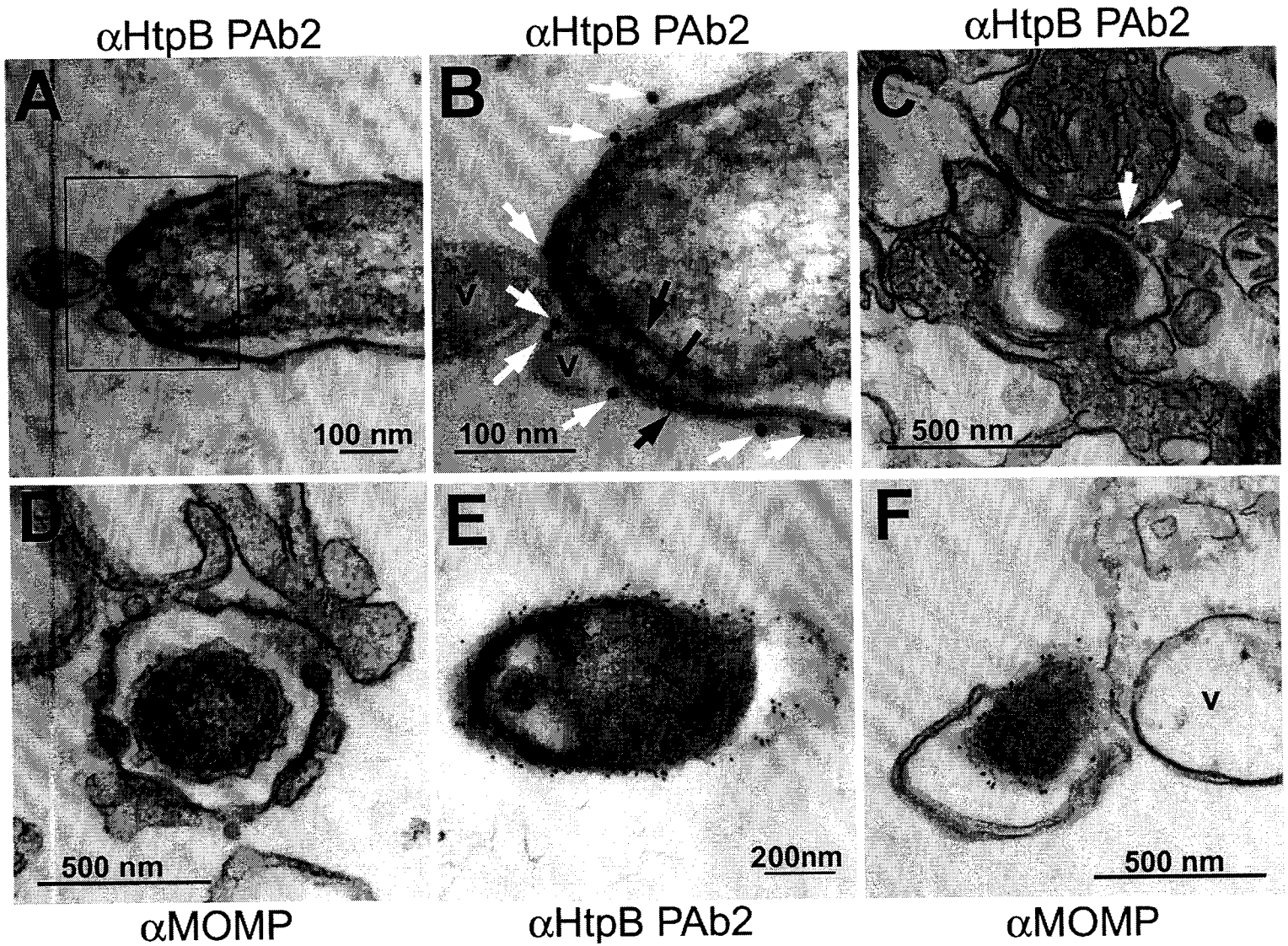
αHtpB PAb2
αHtpB PAb2
αHtpB PAb2
A
B
C
100 nm
100 nm
500 nm
V
V
D
E
F
V
500 nm
200nm
500 nm
αMOMP
αHtpB PAb2
αMOMP

Figure 6.2. HtpB Is Translocated into the Cytosol of CHO-*htpB* Cells.
(A) Immunoblot analysis of the expression of LepA:CyaA, HtpB:CyaA, and CyaA:HtpB fusions from lysates of *L. pneumophila* strains Lp02 (upper panels) and JR32 (bottom panels) not expressing (uninduced, IPTG -) or expressing (2 h induction, IPTG +) CyaA constructs developed with either the LepA PAb (left panels) or the HtpB MAb (right panels). Lysates from *L. pneumophila* expressing CyaA only were used as negative controls. Protein:CyaA fusions are indicated by the arrowheads; HtpB is indicated by the arrows. Std, Broad range molecular weight markers. (B) cAMP levels of CHO-*htpB* cells infected for 90 min with Lp02 or JR32 expressing cyaA fusion proteins were measured using the cAMP Biotrak Enzyme immunoassay System (Amersham Pharmacia). HtpB is considered to be translocated since there is an increase in host cAMP levels following infection with *L. pneumophila* strains expressing HtpB:CyaA in comparison to cells infected with *L. pneumophila* strains with the empty vector pMMB207C and strains expressing CyaA only. LepA:CyaA, an effector protein previously shown to be translocated, served as a positive control (Chen et al., 2004). (C) cAMP levels measured from incubation of CHO-*htpB* cell lysate with JR32 lysates (expressing CyaA fusions). The adenylate cyclase domain of CyaA:HtpB is functional since there is an increase in cAMP levels following incubation of CHO-*htpB* lysate with the lysate from JR32 expressing CyaA:HtpB in comparison to the cAMP levels of the CHO-*htpB* lysate only. cAMP levels measured from incubation of CHO-*htpB* cell lysate with the lysate from JR32 expressing LepA:CyaA served as a positive control. Means and standard deviations were obtained from triplicate wells. Results shown are from a representative experiment of two independent experiments.

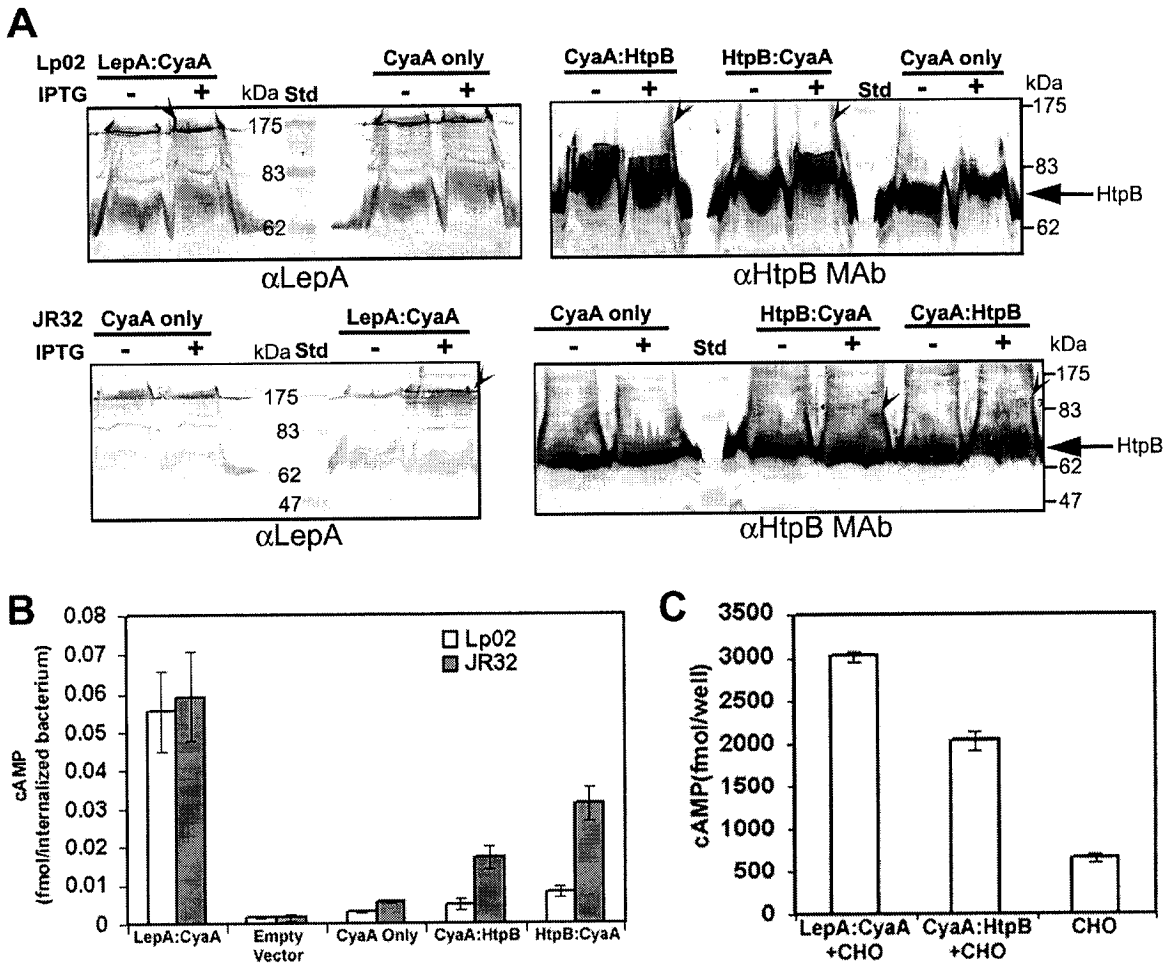
A
Lp02
LepA:CyaA
CyaA only
IPTG
kDa Std
175
83
62
αLepA
CyaA:HtpB
HtpB:CyaA
CyaA only
Std
kDa
HtpB
αHtpB MAb
JR32
47
B
cAMP (fmol/internalized bacterium)
Lp02
JR32
LepA:CyaA
Empty Vector
CyaA Only
CyaA:HtpB
HtpB:CyaA
C
cAMP(fmol/well)
LepA:CyaA +CHO
CyaA:HtpB +CHO
CHO

minimal (Fig 6.2A). No increases in the expression levels of any of the protein fusions were observed when the cultures were induced for a longer period of time (up to 4 h). Because the expression of hybrid proteins in Lp02 was poor, we decided to use strain JR32 in addition to strain Lp02. Furthermore, the vector system that we used to construct the hybrid protein was originally developed for JR32 (Chen et al. 2004). Compared to Lp02, the expression of LepA:CyaA by JR32 was more robust (Fig 6.2A). Expression of HtpB:CyaA by JR32 was slightly higher than expression in Lp02; however, the expression level of CyaA:HtpB by JR32 was similar to that observed for Lp02. Overall, the expression of the protein:CyaA fusions were slightly better when using strain JR32 (Fig 6.2A).

CHO-*htpB* cells infected with Lp02 expressing HtpB:CyaA showed a 5-, 3-, and 1.5-fold increase in cAMP levels compared to host cells infected with Lp02 harbouring the empty vector pMMB207C, Lp02 expressing CyaA only, and Lp02 expressing CyaA:HtpB, respectively ($P<0.05$, Fig 6.2B). However, the cAMP levels generated by cells infected with Lp02 expressing LepA:CyaA, a known translocated effector (Chen et al., 2004), was 7-fold higher than cAMP levels from cells infected with Lp02 expressing HtpB:CyaA. A similar, though more obvious, trend of cAMP levels was observed from cells infected with JR32 expressing HtpB:CyaA in comparison to host cells infected with JR32 harboring the empty vector pMMB207C, expressing CyaA only and expressing CyaA:HtpB ($P<0.01$, Fig 6.2B). cAMP levels generated by cells infected with JR32 expressing LepA:CyaA was 2-fold higher than cAMP levels from cells infected with JR32 expressing HtpB:CyaA (Fig 6.2B). Lower cAMP levels from cells infected with *L. pneumophila* expressing HtpB:CyaA in comparison to LepA:CyaA suggests low levels of

HtpB translocation into the host cell cytoplasm, as indicated by the sparse labeling of HtpB on the LCV surface in Figure 1A and 1C. Discrepancy between cAMP levels generated by CHO-*htpB* cells infected with JR32 versus Lp02 may be due to more consistent growth in broth culture prior to infection and more efficient induction of the fusion proteins by the former strain (data not shown).

The large increase in cAMP detected from incubating CHO-*htpB* cell lysate with lysate from JR32 expressing CyaA:HtpB compared to the cAMP level from CHO-*htpB* cell lysate only suggested that the lower level of cAMP production from CHO-*htpB* infected with *L. pneumophila* expressing CyaA:HtpB was not due to a defect in the hybrid construct, but to reduced translocation. This result thus implies that the N-terminus of HtpB may be more involved than the C-terminus in translocation (Fig 6.2C). The CyaA only and the empty vector controls showed that the presence of the HtpB or LepA sequence was required for increased cAMP production (Fig 6.2B). Together with the immunoelectron microscopy observations, these results reveal that HtpB is associated on the cytoplasmic face of the LCV where it can potentially interact with host cytosolic components.

6.3.2. Characterization of CHO-*htpB* Cells

To study the biological effects of HtpB in mammalian cells, a CHO cell line was chosen as a surrogate expression model due to the ease of transfection and the availability of a tetracycline-regulated expression system in these cells. Conditional expression of HtpB in CHO cells would allow for direct comparison of the effects of the recombinant protein (HtpB) in the same cell line. CHO-AA8 Tet-Off cells, in which the gene of

interest is expressed in the absence of doxycycline (a tetracycline derivative) but not in the presence of doxycycline, were stably transfected with pTRE2-*htpB*hyg, an expression vector containing *htpB* downstream of a tetracycline responsive promoter.

6.3.2.1. Doxycycline Regulation of *htpB* Expression in CHO-*htpB* Cells

A stably transfected clone (CHO-*htpB*) was selected and screened for doxycycline-regulated HtpB expression by immunoblot and indirect immunofluorescence analysis (Fig 6.3). Recombinant HtpB expression by CHO-*htpB* was barely detectable at 1 ng/mL and 0.1 ng/mL of doxcycline, observed in the presence of 0.01 ng/mL or less doxycline, but not at concentrations of 1 ng/mL or higher by immunoblot analysis (Fig 6.3A). By densitometric analysis, a 9-fold increase in expression was observed from cells cultured without doxycycline compared to cell cultured with 1 ng/mL doxycycline (Fig 6.3A). HtpB PAb1 did not cross react with the mitochondrial chaperonin (mCpn60) in CHO-*htpB* cells since no bands at ~60-kDa were detected in the absence of HtpB induction (Fig 6.3A, Lanes 5 and 6). Furthermore, a mitochondrial labeling pattern was not observed by indirect immunofluorescence confirming the specificity of the antibody labeling (Fig 6.3B). Recombinant HtpB was diffusely labeled throughout the cytoplasm and the nucleus of CHO-*htpB* cells when visualized by indirect immunofluorescence microscopy (Fig 6.3B). Although immunoblot and densitometric analysis shows that induction of HtpB expression could be regulated in a dose dependent manner, indirect immunofluorescence microscopy showed that HtpB expression was highly variable among cells at 0.01 ng/mL doxycycline, whereas HtpB expression levels were more comparable among cells cultured in the absence of doxycycline (Fig 6.3B). To

characterize the effects of HtpB expression in CHO-*htpB* cells, expression of the protein was induced in the absence of doxycycine because of the variability in expression levels among cells cultured with low doxycycline levels.

6.3.2.2. Localization of Recombinant HtpB in CHO-*htpB* Cells

Indirect immunofluorescence of Triton X-100 permeabilized CHO-*htpB* cells expressing HtpB revealed diffuse labeling of HtpB throughout the cytoplasm and nucleus (Figs 6.3B and 6.4d). No HtpB labeling was observed in fixed, non-permeabilized CHO-*htpB* cells indicating that recombinant HtpB was not localized to the surface of these cells (Fig 6.4b). As expected, no labeling of α-tubulin was observed on the surface of CHO-*htpB* cells in the absence of permeabilization (Fig 6.4f), although a typical microtubule labeling pattern was observed in permeabilized CHO-*htpB* cells (Fig 6.4h). Indirect immunofluorescence labeling of hemagglutinin (HA) in non-permeabilized CHO-*htpB* cells, included as a positive control, indicated surface localization of HA (Fig 6.4j).

6.3.2.3. HtpB Expression Does Not Affect CHO-*htpB* Growth Rate, Cell Shape, or Organelle Distribution

The growth rate of CHO-*htpB* cells not expressing HtpB was similar to the growth rate of its parental CHO-AA8 Tet-Off cell line indicating that the stable maintenance of pTRE2-*htpB*hyg did not affect the ability of CHO-AA8 Tet-Off cells to multiply. Expression of recombinant HtpB had little effect on the growth of CHO-*htpB* cells since the growth rate of CHO-*htpB* cells expressing HtpB was only slightly lower than CHO-*htpB* cells not expressing HtpB and the parental CHO-AA8 Tet-Off cells

Figure 6.3. Doxycycline Regulation of *htpB* Expression in CHO-*htpB* Cells.
(A) Immunoblot analysis of *htpB* expression by CHO-*htpB* cells incubated for 48 h in various concentrations of doxycycline. On the top panel, electrotransferred proteins were Ponceau S stained to ensure proper transfer and equal loading among samples. The lysate of ~ 6 X 10^5 cells was loaded into each well. On the bottom panel, HtpB was detected using HtpB PAb1 in lanes 2-6; the immunoblot was developed in the absence of primary antibody for lane 7. Densitometric analysis was quantitated relative to HtpB detected in Lane 5. Lane 1, Broad range molecular weight markers; Lanes 2 and 7, No doxycycline; Lane 3, 0.01 ng/mL doxycycline; Lane 4, 0.1 ng/mL doxycycline; Lane 5, 1 ng/mL doxycycline; Lane 6, 10 ng/mL doxycycline. Densitometric analysis of the fold increase of HtpB expression relative to CHO-*htpB* cells cultured in the presence of 1 ng/mL (Lane 5) are shown at the bottom of panel A. Arrow indicates position of HtpB within the boxed region. (B) Representative images of HtpB expression in CHO-*htpB* cells detected by indirect immunofluorescence using HtpB PAb1. The expression level of HtpB was consistent among CHO-*htpB* cells incubated without doxycycline, but differ among CHO-*htpB* cells incubated with 0.01 ng/mL doxycycline. No HtpB expression was detected in CHO-*htpB* cells incubated with 1 ng/mL or 10 ng/mL doxycycline.

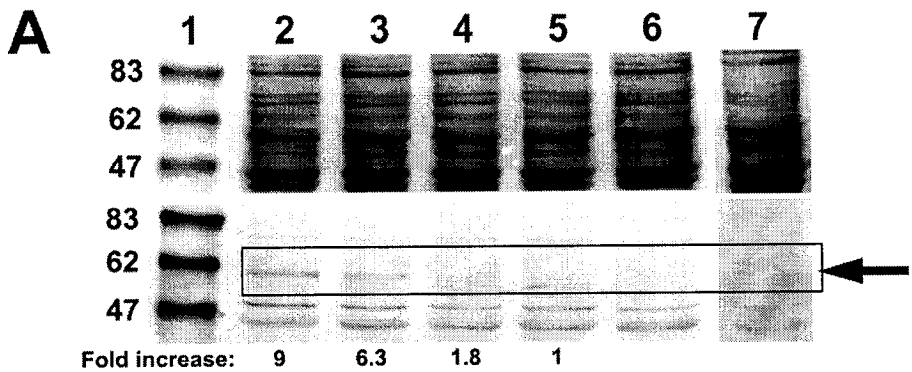
A
1
2
3
4
5
6
7
83
62
47
83
62
47
Fold increase:
9
6.3
1.8
1

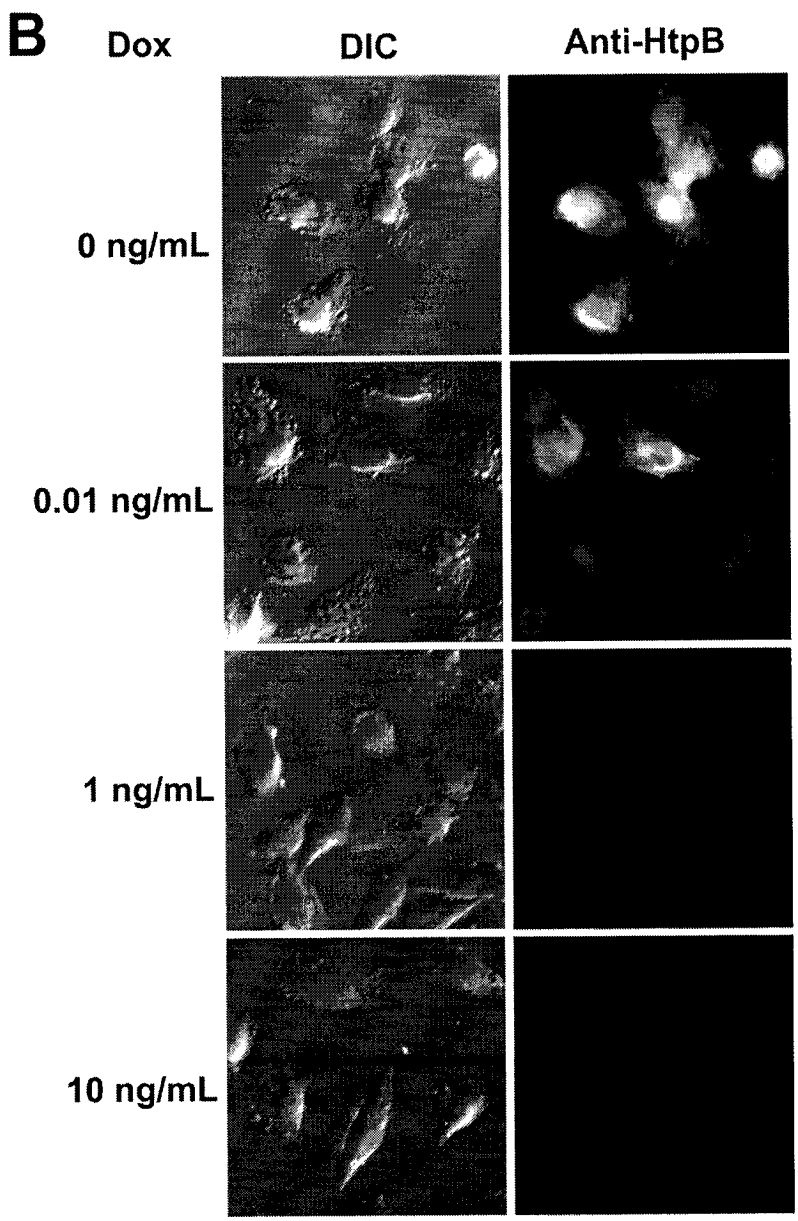
B
Dox
DIC
Anti-HtpB
0 ng/mL
0.01 ng/mL
1 ng/mL
10 ng/mL

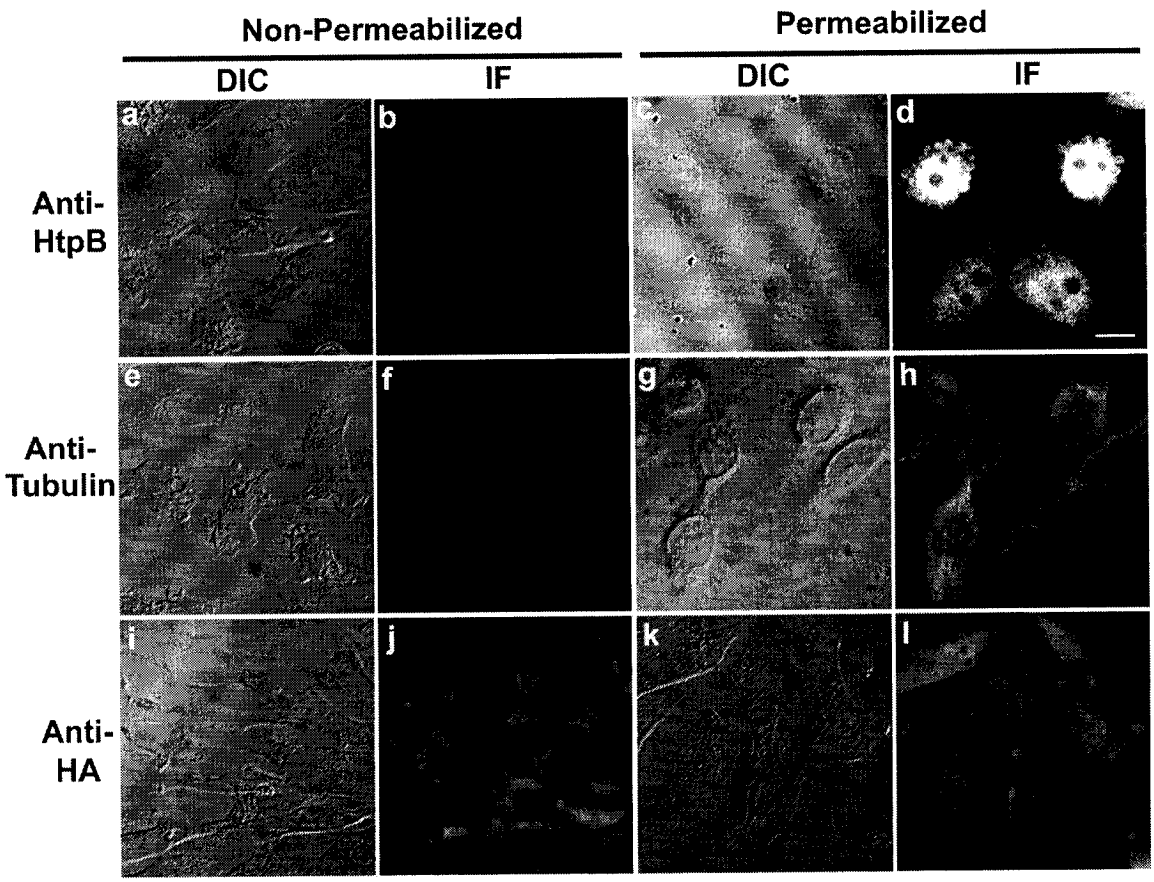

Figure 6.4. Recombinant HtpB Does Not Localize to the Surface of CHO-*htpB* Cells. CHO cells were fixed, permeabilized (c, d, g, h, k, l), and stained 48 h after removal of doxycycline (a-h) or 48 h after transfection (i-l). Representative images of non-permeabilized and permeabilized CHO-*htpB* cells expressing HtpB (a-h) and CHO-AA8 Tet-Off cells expressing HA (i-l). HtpB was detected using HtpB PAb1 (b and d); tubulin was detected using DM1A antibody (f and h); HA was detected using HA PAb (j and l). Primary antibody labeling was detected using a secondary Alexa Fluor 546-conjugated goat anti-rabbit antibody. For non-premeabilized cells, only indirect immunofluorescence labling for HA was detected indicating surface localization. Bar = 10 μm.

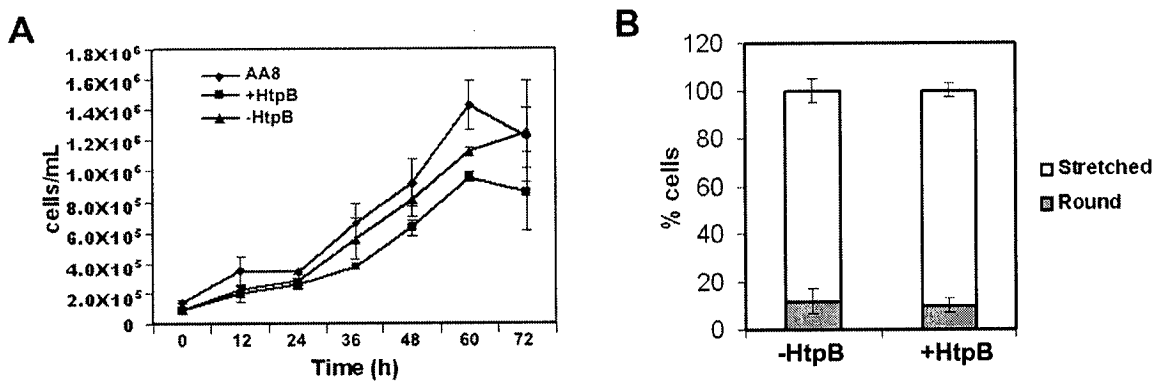

Figure 6.5. Recombinant HtpB Does Not Affect CHO-*htpB* Cell Growth Rate or Morphology.
(A) Growth rates of CHO-AA8 Tet off cells (AA8), CHO-*htpB* cells expressing HtpB (+HtpB) in the absence of doxycycline, and CHO-*htpB* cells not expressing HtpB (-HtpB) in the presence of doxycycline. Results shown are from one experiment representative of two independent ones. Points represent mean and standard deviation from triplicate wells. (B) Percentage of stretched or round CHO-*htpB* cells not expressing HtpB (-HtpB) and expressing HtpB (+HtpB). Bars correspond to the mean, and error bars correspond to one standard deviation from three independent experiments.

Figure 6.6. Recombinant HtpB Does Not Affect CHO-*htpB* Organelle Distribution. CHO-*htpB* cells were fixed and processed 48 h after removal of doxycycline. Ultrathin sections of CHO-*htpB* cells (a) not expressing HtpB in the presence of doxycycline and (b) expressing HtpB in the absence of doxycycline. Mitotracker Orange CMTMRos staining of the mitochondria in CHO-*htpB* cells (c) not expressing HtpB and (d) expressing HtpB. ER-Tracker™ Blue-White DPX staining of the ER network in CHO-*htpB* cells (e) not expressing HtpB and (f) expressing HtpB. Visualization of the lysosomal compartment by indirect immunofluorescence staining of LAMP-1 with the UH1 antibody in CHO-*htpB* cells (g) not expressing HtpB and (h) expressing HtpB; UH1 labeling was detected with Alexa Fluor 546 goat anti-mouse IgG. Visualization of the microtubule organization by indirect immunofluorescence staining of α-tubulin with the DM1A antibody in CHO-*htpB* cells (i) not expressing HtpB and (j) expressing HtpB; DM1A labeling was detected with Alexa Fluor 488 goat anti-rabbit IgG.

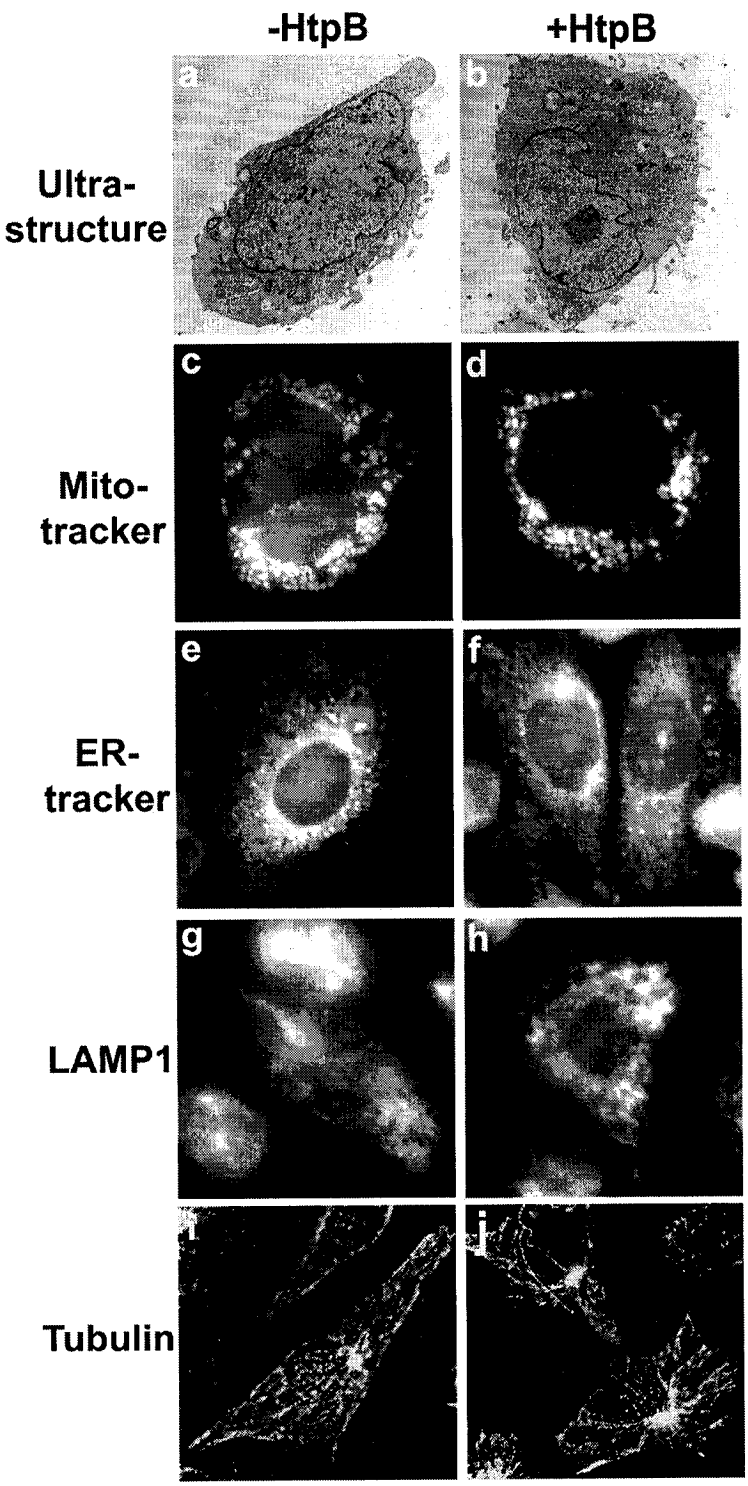
-HtpB
+HtpB
Ultra-structure
Mito-tracker
ER-tracker
LAMP1
Tubulin
a
b
c
d
e
f
g
h
i
j

over 72 h (Fig 6.5A). Most of the attached CHO-*htpB* cells not expressing HtpB displayed a stretched oblong morphology (88 ± 5%) whereas a small proportion displayed a rounded morphology (12 ± 5%) (Fig 6.5B). A similar distribution of stretched (90 ± 3%) and rounded (10 ± 3%) cells was observed for cells expressing HtpB indicating that CHO-*htpB* cell morphology was unaffected by the expression of HtpB (Fig 6.5B).

Ultrastructural comparison between CHO-*htpB* cells expressing and not expressing HtpB did not reveal any obvious differences (Fig 6.6a and 6.6b). Organelle and tubulin staining in CHO-*htpB* cells not expressing HtpB revealed typical distributions of mitochondria, ER, lysosomes, and microtubule network. Mitochondria were abundantly dispersed throughout the cell cytoplasm (Fig 6.6c), the ER network was abundantly localized to the perinuclear region as well as throughout the cell (Fig 6.6e), late endosome/lysosomes appeared as punctuate spots distributed throughout the cell (Fig 6.6g), and microtubule cytoskeleton appeared as an intact network emanating from a central perinuclear region (Fig 6.6i). The distribution of these organelles and of the microtubule network were not obviously perturbed by the expression of HtpB (Fig 6.6d, f, h, and j).

6.3.2.4. Effect of Recombinant HtpB on Actin Organization

Uptake and intracellular replication of *L. pneumophila* induce cytoskeletal rearrangements in various cell types (Coxon et al., 1998; Khelef et al., 2001; Susa and Marre, 1999). We have found that infection of CHO-*htpB* cells with *L. pneumophila* induces actin rearrangements in a dot/icm dependent manner (See Chapter 5).

Furthermore, incubation of CHO-*htpB* cells with HtpB-coated beads mimics this *L. pneumophila*-mediated change in F-actin arrangement (See Chapter 5). Thus, we examined the effect of HtpB expression on actin organization in CHO cells. CHO-AA8 Tet-Off cells and CHO-*htpB* cells not expressing HtpB fluorescently that were stained for F-actin with Alexa Fluor 488-conjugated phalloidin showed fine filamentous structures in the form of stress fibers (Fig 6.7A). Expression of the *L. pneumophila* chaperonin, HtpB, by CHO-*htpB* cells resulted in both the disappearance of stress fibers and a strong staining of F-actin in the form of bundles along the periphery of the cells (Fig 6.7A). Transiently transfected CHO-AA8 Tet-Off cells expressing HtpB revealed the same altered actin morphology indicating that the observed effect was not due to integration of the expression vector into a chromosomal locus that affects the actin cytoskeleton (Fig 6.7A), but to HtpB expression. The F-actin staining pattern of CHO-AA8 Tet-Off cells expressing DsRed2 (Fig 6.7A) or GroEL (Fig 6.7A) were similar to the pattern observed in untransfected CHO-AA8 Tet-Off cells. The microtubule network of CHO-AA8 Tet-Off cells was not affected by expression of HtpB, GroEL, or DsRed2 (Fig 6.6 and data not shown).

The disappearance of actin stress fibers and the appearance of peripheral F-actin bundles (what we called the 'framing' effect) was observed in 25 ± 5% of control untransfected CHO-AA8 Tet-Off cells, establishing a background level of cells displaying this actin morphology (Fig 6.7B). The percentage of CHO-AA8 Tet-Off cells expressing DsRed2 (27 ± 4%) and GroEL (34 ± 2%) exhibiting these altered actin arrangements did not show statistically significant differences in comparison to background levels. This actin morphology was observed in 30 ± 4% of CHO-*htpB* cells

Figure 6.7. F-Actin Rearrangements Induced by Ectopic Expression of HtpB in CHO-*htpB* Cells.

(A) Representative confocal microscopy images of the actin cytoskeleton in untransfected CHO-AA8 Tet-Off cells (a); in stable CHO-AA8 Tet-Off transfectants expressing (+HtpB, b-d) or not expressing HtpB (-HtpB, e-g); and transient CHO-AA8 Tet-Off transfectants expressing HtpB (h-j), DsRed2 (k-m), or GroEL (n-p). Cells were fixed and stained 48 h after induction of expression (b-g) or after transfection (h-p). HtpB and GroEL were visualized by labeling with rabbit serum against *L. pneumophila* HtpB (PAb1) followed by secondary Alexa Fluor 546-conjugated goat anti-rabbit antibody (b, e, h, and n). Microfilaments were visualized by staining with Alexa Fluor 488-conjugated phalloidin (a, c, f, i, l, and o). Bar=10μm. (B) Percentage of differently transfected CHO-AA8 Tet-Off cells showing loss of cytoplasmic F-actin stress fibers and peripheral F-actin bundle framing (e.g., Panel d and j). One hundred cells were scored for each sample. Bars correspond to the average and the error bars correspond to the standard deviation of three independent experiments. For the transient samples (left side of panel B), P-values were calculated in relation to CHO-AA8 Tet-Off cells expressing HtpB by 1-way ANOVA and Bonferroni test; for the stable samples (right side of panel B), the P-value was calculated by the Student *t*-test comparing CHO-*htpB* cells expressing and not expressing HtpB (*$P<0.01$).

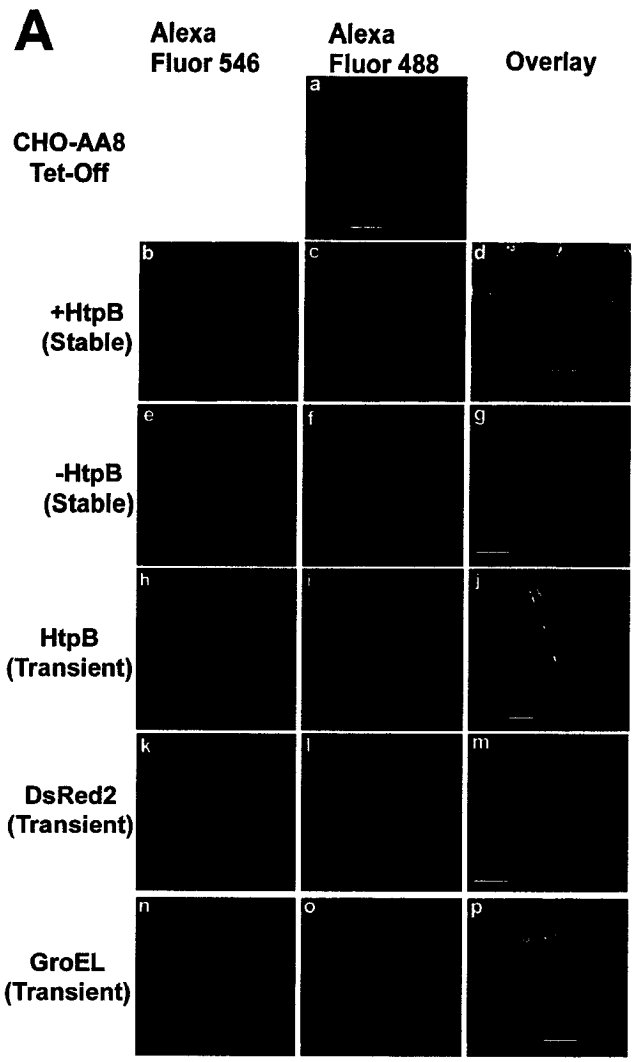
A
Alexa Fluor 546
Alexa Fluor 488
Overlay
CHO-AA8 Tet-Off
+HtpB (Stable)
-HtpB (Stable)
HtpB (Transient)
DsRed2 (Transient)
GroEL (Transient)
a
b
c
d
e
f
g
h
i
j
k
l
m
n
o
p

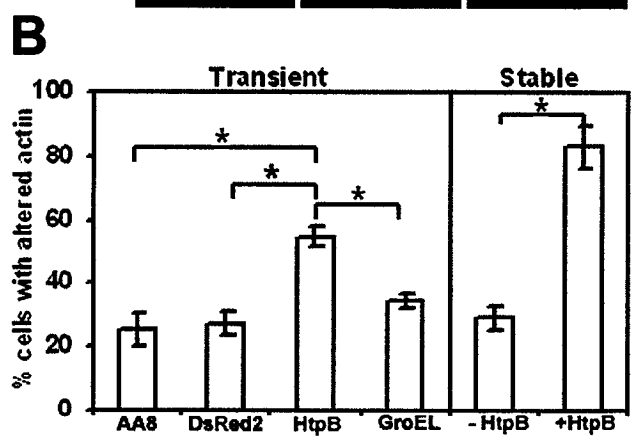
B
Transient
Stable
% cells with altered actin
100
80
60
40
20
0
*
*
*
*
AA8
DsRed2
HtpB
GroEL
- HtpB
+HtpB

not expressing HtpB, which served as a control for comparison with CHO-*htpB* cells expressing HtpB. In contrast, a significantly higher percentage of cells expressing HtpB, both transiently (55 ± 3%) and stably transfected (83 ± 6%) variants, showed altered actin arrangements when compared to their respective controls ($P<0.01$). These results indicate that HtpB specifically mediates F-actin rearrangement in CHO cells.

6.3.3. F-Actin Rearrangements Are Not Due to Overall Actin Depolymerization

The loss of F-actin stress fibers observed in CHO cells expressing HtpB suggested that there is depolymerization of F-actin. To assess whether HtpB induced a net decrease in polymerized actin, the average total amount of F-actin per cell was estimated and compared amongst different cell types. The fluorescence intensity of CHO-*htpB* cells expressing HtpB and stained with AlexaFluor 488-conjugated phalloidin was slightly lower (0.84 ± 0.06) in relation to the fluorescence of the CHO-*htpB* cells not expressing HtpB, which was arbitrarily set at 1(Bar in Fig 6.8). The relative fluorescence intensity of CHO-*htpB* cells not expressing HtpB, but infected with Lp02 (1.02 ± 0.03), or incubated with HtpB-coated beads (0.96 ± 0.03) for 1 h (Fig 6.8), suggested a rearrangement of F-actin, rather than its gross depolymerization. In other words, the amount of F-actin present as stress fibers is equivalent to the amount of F-actin present as thick peripheral bundles.

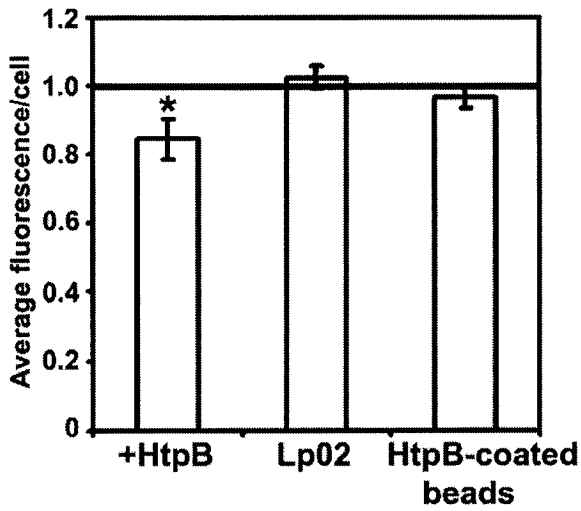

Figure 6.8. Loss of Stress Fibers in CHO-*htpB* Cells Is Not Due to Overall Depolymerization of F-Actin.

The average fluorescence of F-actin staining of CHO-*htpB* cells expressing HtpB internally (+HtpB), infected with Lp02 pBH6119::*htpAB* for 1 h, or incubated with HtpB-coated beads for 1 h, relative to control CHO-*htpB* cells (not expressing HtpB) (line) is comparable. Average cell fluorescence was quantitated by fluorescence microscopy using Image Pro Plus software. Bars correspond to the average and the error bars correspond to the standard deviation of three independent experiments. P-values were calculated in comparison to the control by the Student *t*-test (*$P<0.05$).

6.3.4. HtpB Interacts with F-Actin In Vitro

A co-sedimentation assay was performed to assess the ability of HtpB to interact with F-actin in vitro. More HtpB was observed in the pellet fraction when F-actin was present, as compared to HtpB alone (P lanes for HtpB and HtpB+actin in Fig 6.9A). The same was observed for GroEL (P lanes for GroEL and GroEL+actin in Fig 6.9A) consistent with a previous report that GroEL binds to β-actin (Tian et al., 1995). In addition, more actin was found in the supernatant lanes in the presence of HtpB or GroEL in relation to the presence of α-actinin or BSA (Fig 6.9A), which suggests a weak depolymerization effect. This depolymerization of F-actin in the presence of HtpB and GroEL further strengthens the notion of a direct interaction between F-actin and chaperonins.

An overlay assay was used to confirm the HtpB-F-actin interaction and to attempt the calculation of the dissociation constant for this interaction. Dose-dependent binding of HtpB to immobilized actin, but not to immobilized BSA, was detected by immunobloting (Fig 6.9B). The estimated dissociation constant (K_d) of 2.3 μM for the HtpB-F-actin interaction was extrapolated from the Lineweaver-Burke plot (inset Fig 6.9C) of the densitometric analysis data. These results collectively indicate that both HtpB and GroEL not only interact with F-actin, but also induce slight depolymerization.

6.3.5. Invasion and Intracellular Growth of *L. pneumophila* in CHO-*htpB* Cells

Expression of HtpB did not have a significant effect on the internalization of Lp02, or the Lp02*dotA* mutant by CHO-*htpB* cells (Fig 6.10A). In addition, the

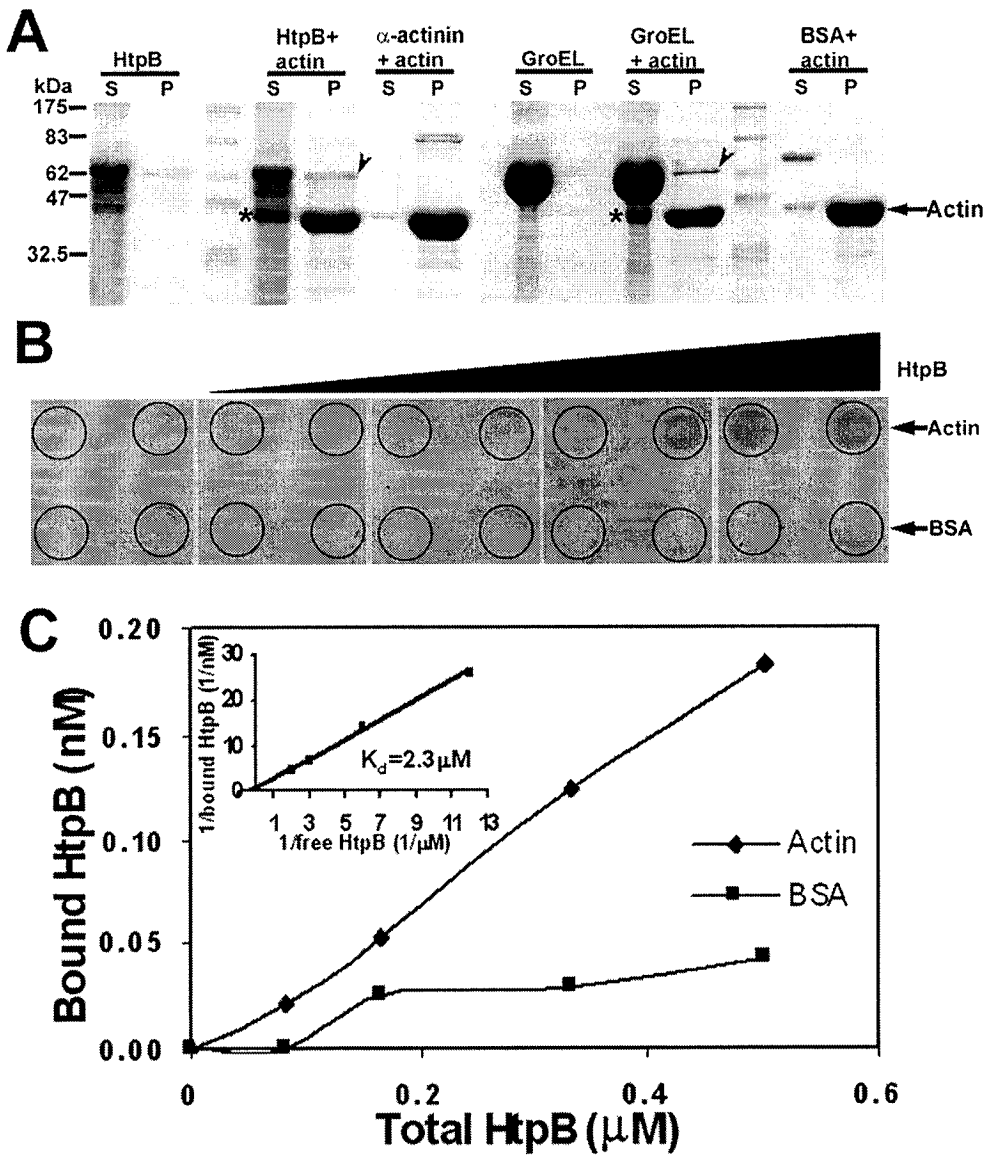

Figure 6.9. HtpB Interaction with F-Actin In Vitro.
(A) HtpB and GroEL interact with F-actin in a co-sedimentation assay. F-actin (18 μM) was incubated with HtpB (17 μM), α-actinin (1 μM), GroEL (22 μM), or BSA (1 μM). Supernatants (S) and pellets (P) resulting from a 100,000 x *g* ultracentrifugation of the samples were analyzed by SDS-PAGE and stained by Coomassie Blue. Molecular weight markers are indicated. Arrowhead indicates the presence of HtpB or GroEL in pellet fractions; asterisk indicates actin present in supernatant fractions; arrow indicates actin. (B) HtpB binds to F-actin in an overlay assay. F-actin (2 μg/dot) and BSA (2 μg/dot) were immobilized onto nitrocellose filter (circular outlines). Filters were floated in PBS containing different concentrations of HtpB. HtpB binding was detected by immunoblotting with the *L. pneumophila* HtpB MAb. (C) Densitometric quantitation of HtpB binding to immobilized F-actin and BSA in (B). The dissociation constant (K_d) of the HtpB:F-actin interaction was extrapolated from the Lineweaver-Burke plot (inset).

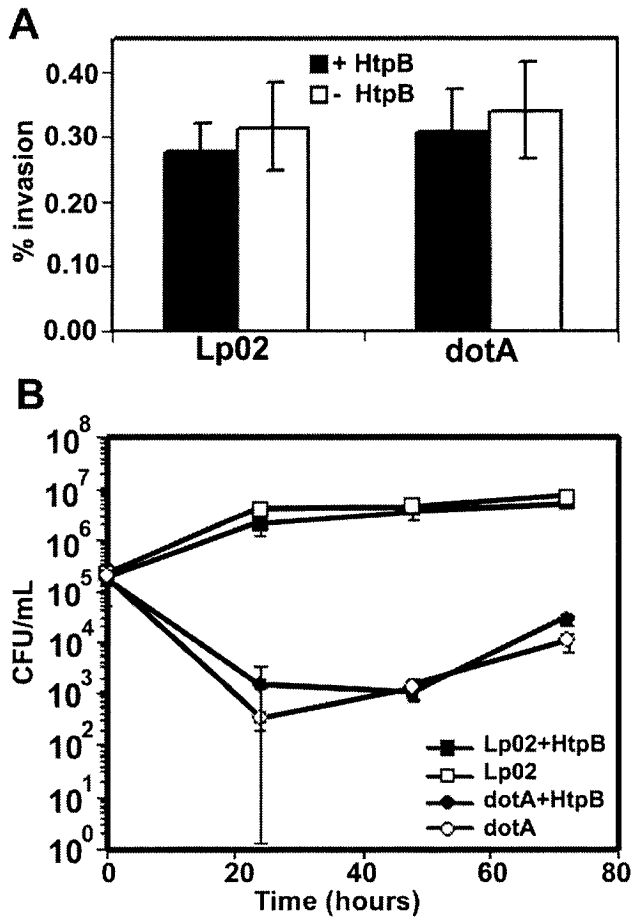

Figure 6.10. Invasion and Intracellular Growth of *L. pneumophila* in CHO-*htpB* Cells.

(A) Ectopic expression of HtpB by CHO-*htpB* cells (+HtpB) had no effect on the invasiveness of Lp02 and *dotA* in comparison to CHO-*htpB* cells not expressing HtpB. Invasiveness is recorded as percentage of the bacterial inoculum added to the CHO-*htpB* cells that survived a gentamicin treatment (presumed to represent intracellular bacteria). (B) Ectopic expression of HtpB by CHO-*htpB* cells (+HtpB) had no effect on the intracellular growth of Lp02 and *dotA* in comparison to CHO-*htpB* cells not expressing HtpB. Shown are means and standard deviations of the means determined from two independent experiments each run in triplicate.

intracellular growth of Lp02 in CHO-*htpB* cells was very similar in the presence or absence of recombinant HtpB (Fig 6.10B). Furthermore, production of recombinant HtpB did not restore the intracellular growth of the *dotA* mutant (Fig 6.10B). Thus, regardless of whether HtpB is presented to host cells on microbeads (Chapter 5) or by ectopicexpression (this chapter), it is not sufficient for restoring the intracellular growth of the non-virulent *dotA* mutant.

6.4. Discussion

L. pneumophila internalized by L929 or HeLa cells releases its HtpB chaperonin into the LCV lumen (Fernandez et al., 1996; Garduno et al., 1998). Furthermore, immunogold labeling of ultrathin sections of infected L929 cells shows that HtpB may associate with the LCV membrane (Fernandez et al., 1996). We deemed important to define whether the HtpB that is released by intracellular *L. pneumophila* remains confined to the LCV lumen, or reaches the cytoplasm of the host cell, either by translocation or membrane association. Here, we have determined by immunoelectron microscopy that HtpB is exposed on the external face of LCVs isolated from infected CHO and U937 cells. In addition, using the cAMP reporter assay, we established that an HtpB:CyaA fusion protein reaches the cytoplasm of *L. pneumophila*-infected CHO cells. This new data suggests that in addition to its role as an invasion factor in non-phagocytic cells (Garduno et al., 1998a), HtpB may play a post-internalization role.

It could be speculated that a post-internalization role for HtpB is related to LCV biogenesis, simply because to date, all *L. pneumophila* effectors known to localize on the cytoplasmic face of the LCV are somehow involved in modulating the trafficking of the

LCV. In addition, these effectors show a Dot/Icm-dependent translocation across the LCV membrane. RalF (Nagai et al., 2002), LidA (Derre and Isberg, 2005), and DrrA/SidM (Machner and Isberg, 2006; Murata et al., 2006) are LCV membrane-associated Dot/Icm substrates that modulate LCV maturation by recruitment of host molecules (e.g., Arf1, Rab1), which in turn regulate vesicular traffic. SidC (Luo and Isberg, 2004), and its paralog SdcA, bind to phosphatidylinositol(4) phosphate (PI4P) on the LCV and likely mediate protein-protein interactions involved in LCV biogenesis (Weber et al., 2006). The fact that mutants lacking any of the aforementioned effectors do not display important intracellular growth defects in macrophages, have suggested the multifactorial and redundant nature of the mechanism used by *L. pneumophila* to subvert organelle and vesicular trafficking. Therefore, given its localization, HtpB could be a contributor to this multifactorial process.

The low levels of cAMP detected in cells infected with *L. pneumophila* carrying the HtpB:CyaA fusion (in relation to the much higher cAMP levels attained after translocation of the LepA:CyaA fusion), suggests that either *L. pneumophila* intentionally releases small amounts of HtpB into the host cell cytoplasm, or that fusion to CyaA artificially reduces the efficiency of HtpB translocation. The accidental delivery of HtpB into the host cell cytoplasm (e.g. after bacterial cell lysis) is unlikely as it was controlled for by the very low levels of cAMP observed after infection with *L. pneumophila* carrying either the CyaA only construct, or the CyaA:HtpB fusion. Given the essential role that chaperonins play in the bacterial cytoplasm as protein folders, we propose that the translocation of HtpB into the host cell is intentionally low and differs from the Dot/Icm-dependent translocation of LepA, RalF, LidA and the Sid effectors.

Since HtpB is clearly released into the lumen of the LCV by intracellular *L. pneumophila* (Fernandez et al., 1996; Garduno et al., 1998), we hypothesize that the fraction of HtpB that is exposed to the host cell cytoplasm originates from this lumenal pool, rather than directly from the bacterial cytoplasmic pool. In this model, there are two possible mechanisms for HtpB translocation across the LCV membrane. One is by delivery through perforations in the LCV membrane formed by the Dot/Icm system, a mechanism previously proposed by Molofsky et al. (2006) for the delivery of flagellin to the host cytosol. The second mechanism involves insertion of lumenal HtpB into the LCV membrane and its subsequent emergence on the cytoplasmic face of the membrane, effected by conformational changes. In support of the ability of HtpB to cross membranes, we observed by immunofluorescence microscopy that HtpB was diffusely localized in the nucleus of CHO-*htpB* cells (Fig 6.3B, 6.4d, 6.7A-b). Nuclear localization of HtpB is not simply an artifact of over-expression because the over-expression of GroEL did not result in nuclear localization (Fig 6.7A-n). Of interest here is the lipochaperonin activity previously described for GroEL, because this activity depends on the interaction of GroEL with lipid bilayers via a conserved glycine- and methionine-rich C-terminal tail (Török et al., 1997), also found in HtpB. The fact that GroEL is unable to translocate to the nucleus suggests that the hydrophobic C-terminus tail is not involved. Therefore, the mechanism by which HtpB translocates into the nucleus (or across the LCV) remains unclear since HtpB neither contains a nuclear targeting signal, nor has the basic amino acid motif found in self-translocated proteins such as antennapedia from *Drosophila* (Thorén et al., 2000) and Tat from HIV-1 (Vivés et al., 1997).

By proposing that the translocation of HtpB differs from the Dot/Icm-dependent translocation of LepA, RalF, LidA and the Sid effectors, we do not necessarily rule out any involvement of the Dot/Icm system. We have previously observed that *dotA* and *dotB* mutants of *L. pneumophila* have reduced amounts of surface-exposed HtpB, and appear to accumulate HtpB in the periplasm (Allan, 2002). Perhaps then, the release of HtpB into the LCV lumen still is a Dot/Icm-dependent process. We are in the process of determining whether infection of CHO cells with a Lp02 or JR32 *dotA* mutant carrying the HtpB:CyaA fusion leads to increases in cAMP levels.

Another relevant aspect of the work presented here is the HtpB-mediated actin rearrangement, as it mimics what *L. pneumophila* does during the early steps of host CHO cell infection (Fig 6.7, and Chapter 5). The same actin rearrangements were also observed when microbeads coated with HtpB, but not beads coated with GroEL or BSA, were added to CHO cells (See Chapter 5), suggesting that HtpB is capable of inducing actin rearrangements "from without" and "from within" the host cell. Furthermore, internalized HtpB-coated beads also mimicked the ability of intracellular *L. pneumophila* to attract mitochondria (Chapter 5). A possible explanation to account for the effect on F-actin from either side of the phagosome membrane could involve the insertion of HtpB into the phagosome membrane from where HtpB could directly or indirectly initiate a signaling process, perhaps by interacting with integral membrane signaling proteins. Evidence to support the signaling hypothesis are: 1) the morphological resemblance between the altered F-actin pattern in CHO cells expressing HtpB and in porcine aortic endothelial cells over-expressing constitutively activated Rnd1 GTPase (Aspenstrom et al., 2004), 2) bacterial chaperonins have been shown to modulate host ERK1/2 signaling

pathways when added to the cell culture medium (Zhang et al., 2001; Zhang et al., 2004a), 3) HtpB modulates cytokine mRNA levels and IL-1 secretion in macrophages via a protein kinase C-dependent signaling pathway (Retzlaff et al., 1996), and 4) HtpB has the ability to deliver an intracellular signal transduced by Ras2p that results in pseudohyphae formation in *Saccharomyces cerevisiae* (Riveroll, 2005). We also considered that the observed HtpB-mediated actin rearrangements could be a result of the direct interaction between HtpB and F-actin, and experimentally found that HtpB is indeed capable of interacting with F-actin in vitro (Fig 6.9). An example of an effector that binds to actin and induces actin filament rearrangements in host cells is SipA, a *Salmonella typhimurium* effector protein involved in bacterial internalization (Zhou et al., 1999). However, this hypothesis is unlikely simply because GroEL, which was also found to directly interact with F-actin in vitro, was unable to induce rearrangements of the actin cytoskeleton (Figs 6.7). Thus, a possible function of the HtpB fraction localized to the cytoplasmic face of the LCV membrane is to activate a signaling cascade that results in alteration of F-actin organization. Actin rearrangements, in turn, could lead to alterations in organelle trafficking, as I have proposed in Chapter 5 to explain the HtpB-mediated recruitment of mitochondria to phagosomes.

Despite its presence in the host cell cytoplasm and its ability to induce actin rearrangements, recombinant HtpB had no effect on the intracellular growth of *L. pneumophila* in CHO-*htpB* cells. Establishment of the LCV is a complex process that involves the avoidance of the endocytic pathway (Horwitz and Maxfield, 1984; Horwitz, 1983c; Joshi et al., 2001; Sauer et al., 2005b), and association with various host organelles such as the mitochondria, ER-derived vesicles, rER, and ribosomes (Garduno

et al., 1998b; Horwitz, 1983b; Kagan and Roy, 2002; Robinson and Roy, 2006; Swanson and Isberg, 1995; Tilney et al., 2001). The Dot/Icm secretion system, shown to translocate numerous effectors into the host cell, is crucial in LCV establishment (Andrews et al., 1998; Berger et al., 1994; Marra et al., 1992; Segal and Shuman, 1998a; Vogel et al., 1998; Zuckman et al., 1999). Therefore, it was not surprising to find that HtpB could not restore the intracellular growth of a *dotA* mutant, regardless of whether HtpB is provided on a bead (as shown in Chapter 5), or by intracellular expression as shown in this chapter (Fig 6.10B). HtpB is therefore unable to compensate for all the factors necessary to establish a replicative niche, which would be absent in the *dotA* mutant. Our findings that HtpB is associated with the cytoplasmic surface of the LCV, and the effect of HtpB on the host actin cytoskeleton have implicated a role for HtpB in LCV trafficking. Future studies to identify the eukaryotic interacting partners of HtpB (e.g., yeast two-hybrid screens or co-immunoprecipitation) should provide insights into the mechanism of actin cytoskeleton rearrangements, as well as the versatility of chaperonin functions in bacterial pathogenesis.

Chapter 7: Discussion

L. pneumophila uses its surface-exposed chaperonin, HtpB, to mediate attachment and entry into host cells (Garduno et al., 1998a). Less invasive avirulent mutants display virtually no HtpB on their surface implying a link between HtpB and virulence (Allan, 2002; Hoffman et al., 1990). Interestingly, HtpB continues to be abundantly expressed and released into the LCV during the course of intracellular infection (Fernandez et al., 1996; Garduno et al., 1998). These observations suggest that HtpB may have other role(s) associated with virulence in addition to functioning as an invasin. Therefore, my investigation into the potential post-internalization function(s) of HtpB was motivated by the continued high-expression of HtpB after entry and the opportune localization of HtpB at various stages in the infection cycle of *L. pneumophila*.

7.1 Coated Bead Model versus Surrogate Expression Model

Genetic studies of essential genes are difficult since knockout mutants, by definition of essentiality, are not viable. The function of GroEL from *E. coli* was investigated through the characterization of temperature sensitive mutants. Although viable, these mutants displayed a plethora of phenotypes that include reduced cell division (Georgopoulos and Eisen, 1974), reduced DNA and RNA synthesis (Wada and Itikawa, 1984), and altered protease activity (Donnelly and Walker, 1989; Straus et al., 1988). I did not attempt to use conditional mutants in my investigations because the pleiotropic effects resulting from the disruption of the essential protein folding function of HtpB would overshadow the effects directly associated with accessory functions of the

protein itself, such as those related to infection and intracellular establishment. Alternatively, antisense RNA knockdown strategies have been employed successfully to investigate the functions of essential genes. This approach has been used to identify and characterize essential genes in *S. aureus* (Ji et al., 2001), *S. mutans* (Sato et al., 1998; Wang and Kuramitsu, 2003), *E. coli* (Wang and Kuramitsu, 2003) and *Thermus thermophilus* (Moreno et al., 2004). Unfortunately, preliminary attempts to knockdown HtpB expression in *L. pneumophila* by antisense RNA were not promising. Introduction of an HtpB antisense construct resulted in higher HtpB expression levels, so this method was not further pursued in this study (data not shown). Instead, two functional models were used to investigate the virulence-related functions of HtpB: 1) a bead trafficking model (Chapter 5), and 2) a surrogate expression model (Chapter 6).

The coated bead model imitates the context in which HtpB is presented to host cells during infection by *L. pneumophila* and provides a method to observe the effects of HtpB at different stages of intracellular trafficking. Each *L. pneumophila* cell was estimated from SDS-polyacrylamide gels and immunoblots to contain ~10 fg of HtpB (Garduno et al., 1998a). In typical *L. pneumophila* sections, ~40 % of the immunogold labeled HtpB epitopes were found on the outer membrane or surface of the bacterium (Garduno et al., 1998a). Based on these estimations, the density of HtpB on the bacterial surface (using average dimensions of 0.5 μm in width and 2 μm in length) was calculated to be ~1 fg/μm^2. The density of BSA (both bead types: ~1 fg/μm^2), GroEL (both bead types: ~2 fg/$\mu m^{2)}$ and HtpB (blue beads: ~1 fg/μm^2, green beads: ~5 fg/μm^2) coated onto the beads (1 μm in diameter) were calculated to be in a similar range as the estimated HtpB density on the surface of *L. pneumophila*. On the other hand, the bead model is

limited in its ability to fully mimic the delivery of HtpB to host cells since the beads are unable to secrete or release HtpB into its endosome the way that *L. pneumophila* does.

A concern regarding this model is the purity of the HtpB preparation used to coat the beads. Given that chaperonins have an affinity for hydrophobic molecules, appropriate measures and/or controls should be used to exclude the possibility of contaminants contributing to the effects observed in experimental systems. In particular, LPS contamination is a common concern because many of the signaling features induced by purified chaperonins are similar to those induced by LPS (See Section 2.2.4.2). For example, Gao and Tsan (2003) found that the observed TNF-α inducing activity in a recombinant human Cpn60 preparation was due to LPS contamination. The immunoprotective pattern afforded by the *Francisella tularensis* chaperonin was found to be due to co-purified LPS (Hartley et al., 2004). HtpB-coated beads pretreated with an HtpB-specific antibody were included in the assays in this study to determine whether or not the effects on mitochondria trafficking and actin organization were due to contaminants. Mitochondrial recruitment to HtpB-coated beads and actin remodeling in CHO-*htpB* cells were neutralized by pretreatment of coated beads with HtpB-specific antibodies, strongly indicating that these effects are caused by HtpB (Figs 5.3 and 5.5). To rule out the involvement of contaminating LPS, it would be beneficial to determine whether beads coated with LPS from *L. pneumophila* are able to recruit mitochondria or alter actin organization in CHO-*htpB* cells. Similarly, examining whether or not recombinant HtpB purified from *E. coli* coated on to beads mediates the same effects as HtpB purified from *L. pneumophila* would exclude the possibility of other *L.*

pneumophila contaminants (proteins that may have been co-purified with HtpB) contributing to these effects.

Future HtpB purifications should employ the use of a removable affinity tag (e. g., His-tag, GST [glutathione-S-transferase]-tag) to minimize the need to control for contaminating proteins, but the affinity purified protein would not be free of LPS contamination. LPS can be removed from protein solutions by selective adsorption onto affinity chromatographic sorbents such as histamine, histidine, polymyxin B, poly-L-lysine, and DEAE ligands (Anspach and Hilbeck, 1995; Issekutz, 1983; Matsumae et al., 1990). Based on results using BSA (pI 4.8) as the test protein, Anspach and Hilbeck (1995) concluded that negatively charged proteins (such as HtpB [pI 5]) are best decontaminated (at pH 7 with low ionic strength solutions [$\leq$ 20 mM phosphate]) using poly-L-lysine-Sepharose because of the higher protein recovery and equivalent LPS clearance in comparison to immobilized histamine, histidine, and polymyxin B ligands. DEAE demonstrated the highest rate of LPS clearance, but less than 20 % recovery of BSA (Anspach and Hilbeck, 1995).

By expressing HtpB in the mammalian cell cytoplasm, the second experimental approach provides another context in which the host cell may encounter HtpB during infection by *L. pneumophila*, and rules out protein purity concerns. Our finding that HtpB is delivered to the host cytoplasm (Figs 6.1 and 6.2) validates this approach for investigating the virulence related functions of HtpB. Furthermore, this strategy has proven fruitful since a biological function for HtpB in the eukaryotic cell was discovered by recombinant expression of HtpB in a yeast model (Riveroll, 2005). HtpB expression in *S. cerevisiae* activated a signaling cascade regulated by Ras2p resulting in the induction

of pseudohyphal growth. Additionally, overexpression of HtpB by *E. coli* and *L. pneumophila* has been found to induce filamentous bacterial growth (Allan, 2002). Used in combination, these models help define the effect of HtpB in mammalian cells when presented from 'without' (bead model) and from 'within' (surrogate expression model), and offer insight into its potential involvement in the pathogenesis of *L. pneumophila*.

7.2. The Functional Relevance of Mitochondrial Recruitment by *L. pneumophila*

Much progress has been made in understanding how *L. pneumophila* interacts with the host ER network and secretory pathways to generate a suitable replicative environment. It is now known that the vesicles recruited to the LCV are ER-derived (Robinson and Roy, 2006; Tilney et al., 2001). *L. pneumophila* translocates effectors (RalF, LidA, SidM) into the host cytoplasm that target host factors (Arf1, Rab1, Sec22b) involved in regulating early secretory traffic to transform the LCV into an ER-like compartment (Derre and Isberg, 2005; Machner and Isberg, 2006; Murata et al., 2006; Nagai et al., 2002). Although the exact mechanisms behind the avoidance of lysosomal fusion remain to be fully elucidated, progress has been made on this front as well. Inhibition of phagosome-lysosome fusion is a process involving Dot/Icm dependent (Berger et al., 1994; Horwitz, 1987; Marra et al., 1992; Roy et al., 1998; Swanson and Isberg, 1996; Wiater et al., 1998) and independent factors (Fernandez-Moreira et al., 2006; Joshi et al., 2001; Molofsky et al., 2005). In contrast, little else is known about mitochondrial recruitment to the LCV beyond the ultrastructural observations that revealed this phenomenon (Garduno et al., 1998b; Horwitz, 1983b; Oldham and Rodgers, 1985) and that it is a Dot/Icm dependent process (Horwitz, 1987; Marra et al., 1992).

The work presented here demonstrated that recruitment of mitochondria is mediated by HtpB coated onto latex beads (Figs 5.3 and 5.4). In support of earlier findings, we have also found that a functional Dot/Icm system is required for attracting mitochondria to the LCV (Fig 5.3). The nature of the mitochondrion-LCV interaction remains to be determined; however, it is worth speculating that mitochondria, in addition to the ER, might serve as an energy and lipid source for the vacuole-enclosed *L. pneumophila*. It has long been established that mitochondria provide energy in the form of ATP for cellular processes (Hatefi, 1985; Pedersen and Amzel, 1993). Sinai et al. (1997) postulated that the mitochondrion might serve as a 'go-between' for trafficking lipids from the ER to the *T. gondii* parsitophorous vacuole, as there is a direct link between the ER and mitochondria in the bulk transport of eukaryotic cell lipids (Rusinol et al., 1994; Vance and Shiao, 1996; Voelker, 1991). Intravacuolar *L. pneumophila* could be acquiring lipids through this route.

Insight into the importance of mitochondrial association with the LCV could be gained by investigating the relevance of mitochondria to the intracellular development of *L. pneumophila*. *C. trachomatis* elementary bodies failed to develop and replicate in host cells treated with ethidium bromide before and within the first 24 h of infection (Becker and Asher, 1972). The synthesis of mitochondrial nucleic acids is selectively inhibited by exposure to low levels (50 ng/mL – 2 μg/mL) of ethidium bromide resulting in mammalian cell lines lacking active mitochondria (Knight, 1969; Zylber et al., 1969). The importance of mitochondria to the intracellular trafficking and growth of *L. pneumophila* could be assessed by infection of ethidium bromide-treated cell lines as long as *L. pneumophila* is not affected by the concentrations of ethidium bromide used.

7.3. Future Directions

7.3.1. Identifying Potential HtpB Interacting Partners

Identification of potential host proteins that interact with HtpB could shed light on the mechanism(s) by which HtpB affects actin organization and mitochondrial trafficking, and whether or not the two phenotypes are related. Using a yeast two-hybrid system, four HeLa cell proteins were previously identified by Riveroll (2005) as putative proteins that interact with HtpB. These proteins were: ribosomal protein L4 (RPL4), phosphoribosylaminoimidazole succinocarboxiaminde synthetase (PAICS), cdc2/cdc28 kinase subunit *Homo sapiens* 1 (Ckshs1), and Merlin associated protein (MAP) (Riveroll, 2005). Of these four proteins, MAP is the most interesting as it may have bearing on the mechanism by which HtpB affects actin organization and mitochondrial trafficking. MAP is a Rab-GAP-like protein since it possesses two domains similar to those found in Rab-GAP proteins (Ichioka et al., 2005; Lee et al., 2004). Furthermore, MAP has been found to interact with Merlin (Lee et al., 2004), a neurofibromatosis type 2 tumor suppressor protein that directly interacts with actin and is involved in actin reorganization (Bashour et al., 2002; Manchanda et al., 2005; Xu and Gutmann, 1998). MAP also interacts with Alix/AIP1 (Ichioka et al., 2005), a protein that participates in actin organization, endosome distribution and cell adhesion (Cabezas et al., 2005; Schmidt et al., 2003). Thus, HtpB could interfere with pathways influenced by Merlin and Alix/AIP1 through interaction with MAP to affect actin organization and mitochondrial trafficking.

These putative interactions need to be confirmed since two-hybrid screens have a reputation for producing false positives. Another consideration that needs to be addressed is the possibility of endogenous yeast proteins acting as bridging factors implying a direct

interaction between HtpB and the identified proteins. It could be beneficial to use a mammalian two-hybrid system to identify interactions between mammalian proteins that may not fold properly in yeast or require post-translational modification not present in yeast. Co-immunoprecipitation studies using HeLa or CHO-*htpB* cells expressing HtpB could validate the results from the two-hybrid assays, and may identify other HtpB interacting partners. Co-localization studies either by immunofluorescence or immunogold labeling would also be an alternative method to validate the interactions identified by the two-hybrid assay. Once a true interaction has been confirmed, *L. pneumophila* infection of a mutant cell line either with a dominant negative allele of or lacking the HtpB interacting partner could be used to assess the importance of such an interaction to the virulence of *L. pneumophila*.

7.3.2. Identifying Domains Responsible for HtpB-Induced Effects

High sequence conservation among Group I chaperonins supports the idea that these proteins fulfill a universally important function (Gupta, 1995; Karlin and Brocchieri, 2000). Multiple sequence alignments across 43 diverse chaperonin sequences revealed that the most highly conserved regions were related to chaperonin structure and function: the ATP/ADP binding site, GroES contact positions, and the interface regions between monomer and domains (Brocchieri and Karlin, 2000). Highly conserved sequences signify regions essential for protein function and/or structure, whereas sequence variations are accommodated in regions either lacking functional significance or with highly specialized function adapted within a species for its specific environment. For example, the toxin function of the *E. aerogenes* chaperonin is conferred by four

critical amino acids that differ from GroEL (Yoshida et al., 2001). All four residues are located far from the polypeptide-, ATP- and GroES-binding domains (Val 100, Thr 101, and Gly 471 are located in the equatorial domain, and Glu 338 is located in the apical domain). A converse situation was described for the the *Buchnera* GroEL. Fares *et al.* (2002) found a higher rate of non-synonymous substitutions among codons that affect polypeptide and GroES binding efficiency, and proposed that these substitutions allow the endosymbiotic bacterium to tolerate the accumulation of deleterious mutations by binding to a larger repertoire of substrates. Both examples illustrate the role in which chaperonins play in the adaptive evolution of bacteria.

Similarly, HtpB residues not necessary for protein function would be allowed to evolve under less selective constraints. These amino acid substitutions could confer new function(s) to HtpB that may have allowed *L. pneumophila* to adapt to an intracellular environment. Despite the 86 % amino acid sequence similarity with the *L. pneumophila* HtpB, the *E. coli* GroEL does not induce pseudohyphae formation in yeast, or actin reorganization and mitochondrial recruitment in mammalian cells, suggesting that variation in the remaining 14 % of the amino acid sequence is responsible for these differences. Additionally, the cloned *htpAB* operon (pSH16) was unable to complement a *groEL* temperature-sensitive mutation in *E. coli* indicating that these chaperonins may have highly specific functions within their respective species (Hoffman et al., 1989). Thus, a sequence comparison approach can be used to determine the variable regions in HtpB that should be targeted for domain swapping with GroEL. The hybrid proteins could be screened to determine which regions are required to induce actin reorganization, mitochondrial recruitment, translocation or pseudohyphal growth. Once identified, the

process can be repeated with smaller and smaller domain swaps within the corresponding region(s) to pinpoint the residues responsible for inducing these phenotypes. Key amino acids identified by sequence comparison or by domain swaps could be altered by site-directed mutagenesis and tested for the ability to induce these phenotypes. Alternatively, deletions or truncations of the targeted regions could be generated in HtpB and screened similarly. To test for relevance in the virulence of *L. pneumophila*, the wildtype copy of *htpB* in *L. pneumophila* could be replaced with a mutant copy of *htpB* (mutated within the target region) and assessed for ability to replicate in amoebae and macrophages.

7.4. Conclusions

The work in this thesis has revealed additional functions of HtpB that may be involved in the adaptation of *L. pneumophila* to the mammalian intracellular environment. Using a bead trafficking model, I determined that HtpB is responsible for the recruitment of mitochondria and reorganization of the actin cytoskeleton, which are phenotypes also induced by *L. pneumophila* during the infection of mammalian cells. The same actin rearrangements were also induced in CHO-*htpB* cells upon the expression of recombinant HtpB. The connection between mitochondrial recruitment and actin cytoskeleton alterations remains to be explored. Interestingly, the ectopic expression of HtpB had no obvious effect on the spatial distribution of mitochondria in CHO-*htpB* cells. That ectopically expressed HtpB did not affect organellar distribution, microtubule organization, cell morphology or cell growth indicates that the effects mediated by HtpB in mammalian cells are specifically targeted. An especially significant finding presented in this thesis is the delivery of HtpB into the host cytoplasm and its association with the

cytoplasmic face of the LCV, demonstrating that HtpB has the potential to interact with host components that may impact LCV trafficking. Such a localization for HtpB during infection suggests that the actin rearrangements induced by HtpB expressed in the cytoplasm of CHO-*htpB* cells is relevant to the pathogenesis of *L. pneumophila*, although a direct role for HtpB with respect to the biogenesis of the replicative vacuole still remains to be determined. The ability of HtpB to alter mammalian cytoskeletal organization and mitochondrial trafficking, in combination with its ability to alter eukaryotic signaling pathways, provide addition support for the hypothesis that HtpB is a *L. pneumophila* virulence factor, and endorse the emerging view of chaperonins as functionally flexible proteins involved in various aspects of bacterial infection and adaptation.

References

Abu Kwaik,Y. (1996) The phagosome containing *Legionella pneumophila* within the protozoan *Hartmannella vermiformis* is surrounded by the rough endoplasmic reticulum. *Appl.Environ.Microbiol.*, **62,** 2022-2028.

Abu Kwaik,Y., Gao,L.Y., Stone,B.J., Venkataraman,C. and Harb,O.S. (1998) Invasion of protozoa by *Legionella pneumophila* and its role in bacterial ecology and pathogenesis. *Appl.Environ.Microbiol.*, **64,** 3127-3333.

Abu Kwaik,Y., Eisenstein,B.I. and Engleberg,N.C. (1993) Phenotypic modulation by *Legionella pneumophila* upon infection of macrophages. *Infect.Immun.*, **61,** 1320-1329.

Abu-Zant,A., Asare,R., Graham,J.E. and Abu Kwaik,Y. (2006) Role for RpoS but not RelA of *Legionella pneumophila* in modulation of phagosome biogenesis and adaptation to the phagosomal microenvironment. *Infect.Immun.*, **74,** 3021-3026.

Abu-Zant,A., Jones,S., Asare,R., Suttles,J., Price,C., Graham,J. and Kwaik,Y.A. (2007) Anti-apoptotic signalling by the Dot/Icm secretion system of *L. pneumophila*. *Cell.Microbiol.*, **9,** 246-264.

Abu-Zant,A., Santic,M., Molmeret,M., Jones,S., Helbig,J. and Abu Kwaik,Y. (2005) Incomplete activation of macrophage apoptosis during intracellular replication of *Legionella pneumophila*. *Infect.Immun.*, **73,** 5339-5349.

Allan,D.S. (2002) MSc. Thesis. Secretion of Hsp60 chaperonin (GroEL) homologs by *L. pneumophila*. Dalhousie University, Nova Scotia, Canada.

Alli,O.A., Gao,L.Y., Pedersen,L.L., Zink,S., Radulic,M., Doric,M. and Abu Kwaik,Y. (2000) Temporal pore formation-mediated egress from macrophages and alveolar epithelial cells by *Legionella pneumophila*. *Infect.Immun.*, **68,** 6431-6440.

Amer,A.O. and Swanson,M.S. (2005) Autophagy is an immediate macrophage response to *Legionella pneumophila*. *Cell.Microbiol.*, **7,** 765-778.

Andrews,H.L., Vogel,J.P. and Isberg,R.R. (1998) Identification of linked *Legionella pneumophila* genes essential for intracellular growth and evasion of the endocytic pathway. *Infect.Immun.*, **66,** 950-958.

Ang,D., Richardson,A., Mayer,M.P., Keppel,F., Krisch,H. and Georgopoulos,C. (2001) Pseudo-T-even bacteriophage RB49 encodes CocO, a cochaperonin for GroEL, which can substitute for *Escherichia coli*'s GroES and Bacteriophage T4's Gp31. *J.Biol.Chem.*, **276,** 8720-8726.

Anspach,F.B. and Hilbeck,O. (1995) Removal of endotoxins by affinity sorbents. *J.Chromatogr.A,* **711,** 81-92.

Arata,S., Newton,C., Klein,T.W., Yamamoto,Y. and Friedman,H. (1993) *Legionella pneumophila* induced tumor necrosis factor production in permissive versus nonpermissive macrophages. *Proc.Soc.Exp.Biol.Med.*, **203,** 26-29.

Archer,K.A. and Roy,C.R. (2006) MyD88-dependent responses involving toll-like receptor 2 are important for protection and clearance of *Legionella pneumophila* in a mouse model of Legionnaires' disease. *Infect.Immun.*, **74,** 3325-3333.

Archibald,J.M., Logsdon,J.M.,Jr and Doolittle,W.F. (2000) Origin and evolution of eukaryotic chaperonins: phylogenetic evidence for ancient duplications in CCT genes. *Mol.Biol.Evol.*, **17,** 1456-1466.

Aspenstrom,P., Fransson,A. and Saras,J. (2004) Rho GTPases have diverse effects on the organization of the actin filament system. *Biochem.J.*, **377,** 327-337.

Babst,M., Hennecke,H. and Fischer,H.M. (1996) Two different mechanisms are involved in the heat-shock regulation of chaperonin gene expression in *Bradyrhizobium japonicum*. *Mol.Microbiol.*, **19,** 827-839.

Bachman,M.A. and Swanson,M.S. (2004) The LetE protein enhances expression of multiple LetA/LetS-dependent transmission traits by *Legionella pneumophila*. *Infect.Immun.*, **72,** 3284-3293.

Bachman,M.A. and Swanson,M.S. (2001) RpoS co-operates with other factors to induce *Legionella pneumophila* virulence in the stationary phase. *Mol.Microbiol.*, **40,** 1201-1214.

Banerjee,S., Hess,D., Majumder,P., Roy,D. and Das,S. (2004) The Interactions of *Allium sativum* leaf agglutinin with a chaperonin group of unique receptor protein isolated from a bacterial endosymbiont of the mustard aphid. *J.Biol.Chem.*, **279,** 23782-23789.

Baneyx,F., Bertsch,U., Kalbach,C.E., van der Vies,S.M., Soll,J. and Gatenby,A.A. (1995) Spinach chloroplast cpn21 co-chaperonin possesses two functional domains fused together in a toroidal structure and exhibits nucleotide-dependent binding to plastid chaperonin 60. *J.Biol.Chem.*, **270,** 10695-10702.

Barbaree,J.M., Fields,B.S., Feeley,J.C., Gorman,G.W. and Martin,W.T. (1986) Isolation of protozoa from water associated with a legionellosis outbreak and demonstration of intracellular multiplication of *Legionella pneumophila*. *Appl.Environ.Microbiol.*, **51,** 422-424.

Bardill,J.P., Miller,J.L. and Vogel,J.P. (2005) IcmS-dependent translocation of SdeA into macrophages by the *Legionella pneumophila* type IV secretion system. *Mol.Microbiol.*, **56,** 90-103.

Barker,J., Brown,M.R., Collier,P.J., Farrell,I. and Gilbert,P. (1992) Relationship between *Legionella pneumophila* and *Acanthamoeba polyphaga*: physiological status and susceptibility to chemical inactivation. *Appl.Environ.Microbiol.*, **58,** 2420-2425.

Barker,J., Lambert,P.A. and Brown,M.R. (1993) Influence of intra-amoebic and other growth conditions on the surface properties of *Legionella pneumophila*. *Infect.Immun.*, **61,** 3503-3510.

Barker,J., Scaife,H. and Brown,M.R. (1995) Intraphagocytic growth induces an antibiotic-resistant phenotype of *Legionella pneumophila*. *Antimicrob.Agents Chemother.*, **39,** 2684-2688.

Barlowe,C. (2002) COPII-dependent transport from the endoplasmic reticulum. *Curr.Opin.Cell Biol.*, **14,** 417-422.

Bashour,A.M., Meng,J.J., Ip,W., MacCollin,M. and Ratner,N. (2002) The neurofibromatosis type 2 gene product, Merlin, reverses the F-actin cytoskeletal defects in primary human Schwannoma cells. *Mol.Cell.Biol.*, **22,** 1150-1157.

Becker,Y. and Asher,Y. (1972) Obligate parasitism of trachoma agent: lack of trachoma development in ethidium bromide-treated cells. *Antimicrob.Agents Chemother.*, **1,** 171-173.

Bellinger-Kawahara,C. and Horwitz,M.A. (1990) Complement component C3 fixes selectively to the major outer membrane protein (MOMP) of *Legionella pneumophila* and mediates phagocytosis of liposome-MOMP complexes by human monocytes. *J.Exp.Med.*, **172,** 1201-1210.

Berger,K.H. and Isberg,R.R. (1993) Two distinct defects in intracellular growth complemented by a single genetic locus in *Legionella pneumophila*. *Mol.Microbiol.*, **7,** 7-19.

Berger,K.H., Merriam,J.J. and Isberg,R.R. (1994) Altered intracellular targeting properties associated with mutations in the *Legionella pneumophila dotA* gene. *Mol.Microbiol.*, **14,** 809-822.

Bergonzelli,G.E., Granato,D., Pridmore,R.D., Marvin-Guy,L.F., Donnicola,D. and Corthesy-Theulaz,I.E. (2006) GroEL of *Lactobacillus johnsonii* La1 (NCC 533) is cell surface associated: potential role in interactions with the host and the gastric pathogen *Helicobacter pylori*. *Infect.Immun.*, **74,** 425-434.

Berk,S.G., Ting,R.S., Turner,G.W. and Ashburn,R.J. (1998) Production of respirable vesicles containing live *Legionella pneumophila* cells by two *Acanthamoeba* spp. *Appl.Environ.Microbiol.*, **64,** 279-286.

Blander,S.J. and Horwitz,M.A. (1993) Major cytoplasmic membrane protein of *Legionella pneumophila*, a genus common antigen and member of the hsp60 family of heat shock proteins, induces protective immunity in a guinea pig model of Legionnaires' disease. *J.Clin.Invest.*, **91,** 717-723.

Blander,S.J. and Horwitz,M.A. (1991) Vaccination with the major secretory protein of *Legionella* induces humoral and cell-mediated immune responses and protective immunity across different serogroups of *Legionella pneumophila* and different species of *Legionella*. *J.Immunol.*, **147,** 285-291.

Blum,H., Beier,H. and Gross,H.J. (1987) Improved silver staining of plant proteins, RNA and DNA in polyacrylamide gels. *Electrophoresis,* **8,** 93-99.

Bochkareva,E.S., Lissin,N.M. and Girshovich,A.S. (1988) Transient association of newly synthesized unfolded proteins with the heat-shock GroEL protein. *Nature,* **336,** 254-257.

Bozue,J.A. and Johnson,W. (1996) Interaction of *Legionella pneumophila* with *Acanthamoeba castellanii*: uptake by coiling phagocytosis and inhibition of phagosome-lysosome fusion. *Infect.Immun.*, **64,** 668-673.

Braig,K., Adams,P.D. and Brunger,A.T. (1995) Conformational variability in the refined structure of the chaperonin GroEL at 2.8 A resolution. *Nat.Struct.Biol.*, **2,** 1083-1094.

Braig,K., Otwinowski,Z., Hegde,R., Boisvert,D.C., Joachimiak,A., Horwich,A.L. and Sigler,P.B. (1994) The crystal structure of the bacterial chaperonin GroEL at 2.8 A. *Nature,* **371,** 578-586.

Braig,K., Simon,M., Furuya,F., Hainfeld,J.F. and Horwich,A.L. (1993) A polypeptide bound by the chaperonin GroEL is localized within a central cavity. *Proc.Natl.Acad.Sci.U.S.A.*, **90,** 3978-3982.

Brassinga,A.K., Hiltz,M.F., Sisson,G.R., Morash,M.G., Hill,N., Garduno,E., Edelstein,P.H., Garduno,R.A. and Hoffman,P.S. (2003) A 65-kilobase pathogenicity island is unique to Philadelphia-1 strains of *Legionella pneumophila*. *J.Bacteriol.*, **185,** 4630-4637.

Brieland,J., McClain,M., Heath,L., Chrisp,C., Huffnagle,G., LeGendre,M., Hurley,M., Fantone,J. and Engleberg,C. (1996) Coinoculation with *Hartmannella vermiformis* enhances replicative *Legionella pneumophila* lung infection in a murine model of Legionnaires' disease. *Infect.Immun.*, **64,** 2449-2456.

Brieland,J.K., Fantone,J.C., Remick,D.G., LeGendre,M., McClain,M. and Engleberg,N.C. (1997) The role of *Legionella pneumophila*-infected *Hartmannella vermiformis* as an infectious particle in a murine model of Legionnaire's disease. *Infect.Immun.*, **65,** 5330-5333.

Brinker,A., Pfeifer,G., Kerner,M.J., Naylor,D.J., Hartl,F.U. and Hayer-Hartl,M. (2001) Dual function of protein confinement in chaperonin-assisted protein folding. *Cell,* **107,** 223-233.

Brocchieri,L. and Karlin,S. (2000) Conservation among HSP60 sequences in relation to structure, function, and evolution. *Protein Sci.*, **9,** 476-486.

Bruggemann,H., Hagman,A., Jules,M., Sismeiro,O., Dillies,M.A., Gouyette,C., Kunst,F., Steinert,M., Heuner,K., Coppee,J.Y. and Buchrieser,C. (2006) Virulence strategies for infecting phagocytes deduced from the in vivo transcriptional program of *Legionella pneumophila*. *Cell.Microbiol.*, **8,** 1228-1240.

Bukau,B. and Horwich,A.L. (1998) The Hsp70 and Hsp60 chaperone machines. *Cell,* **92,** 351-366.

Bulut,Y., Faure,E., Thomas,L., Karahashi,H., Michelsen,K.S., Equils,O., Morrison,S.G., Morrison,R.P. and Arditi,M. (2002) Chlamydial heat shock protein 60 activates macrophages and endothelial cells through Toll-like receptor 4 and MD2 in a MyD88-dependent pathway. *J.Immunol.*, **168,** 1435-1440.

Bulut,Y., Michelsen,K.S., Hayrapetian,L., Naiki,Y., Spallek,R., Singh,M. and Arditi,M. (2005) *Mycobacterium tuberculosis* heat shock proteins use diverse Toll-like receptor pathways to activate pro-inflammatory signals. *J.Biol.Chem.*, **280,** 20961-20967.

Burnett,B.P., Horwich,A.L. and Low,K.B. (1994) A carboxy-terminal deletion impairs the assembly of GroEL and confers a pleiotropic phenotype in *Escherichia coli* K-12. *J.Bacteriol.*, **176,** 6980-6985.

Buscher,B.A., Conover,G.M., Miller,J.L., Vogel,S.A., Meyers,S.N., Isberg,R.R. and Vogel,J.P. (2005) The DotL protein, a member of the TraG-coupling protein family, is essential for viability of *Legionella pneumophila* strain Lp02. *J.Bacteriol.*, **187,** 2927-2938.

Byrd,T.F. and Horwitz,M.A. (1989) Interferon gamma-activated human monocytes downregulate transferrin receptors and inhibit the intracellular multiplication of *Legionella pneumophila* by limiting the availability of iron. *J.Clin.Invest.*, **83,** 1457-1465.

Byrne,B. and Swanson,M.S. (1998) Expression of *Legionella pneumophila* virulence traits in response to growth conditions. *Infect.Immun.*, **66,** 3029-3034.

Cabezas,A., Bache,K.G., Brech,A. and Stenmark,H. (2005) Alix regulates cortical actin and the spatial distribution of endosomes. *J.Cell.Sci.*, **118,** 2625-2635.

Campodonico,E.M., Chesnel,L. and Roy,C.R. (2005) A yeast genetic system for the identification and characterization of substrate proteins transferred into host cells by the *Legionella pneumophila* Dot/Icm system. *Mol.Microbiol.*, **56,** 918-933.

Cao,P., McClain,M.S., Forsyth,M.H. and Cover,T.L. (1998) Extracellular release of antigenic proteins by *Helicobacter pylori*. *Infect.Immun.*, **66,** 2984-2986.

Capela,D., Barloy-Hubler,F., Gouzy,J., Bothe,G., Ampe,F., Batut,J., Boistard,P., Becker,A., Boutry,M., Cadieu,E., Dreano,S., Gloux,S., Godrie,T., Goffeau,A., Kahn,D., Kiss,E., Lelaure,V., Masuy,D., Pohl,T., Portetelle,D., Puhler,A., Purnelle,B., Ramsperger,U., Renard,C., Thebault,P., Vandenbol,M., Weidner,S. and Galibert,F. (2001) Analysis of the chromosome sequence of the legume symbiont *Sinorhizobium meliloti* strain 1021. *Proc.Natl.Acad.Sci.U.S.A.*, **98,** 9877-9882.

Celli,J. (2006) Surviving inside a macrophage: the many ways of *Brucella*. *Res.Microbiol.*, **157,** 93-98.

Chang,B., Kura,F., Amemura-Maekawa,J., Koizumi,N. and Watanabe,H. (2005) Identification of a novel adhesion molecule involved in the virulence of *Legionella pneumophila*. *Infect.Immun.*, **73,** 4272-4280.

Chatterji,D. and Ojha,A.K. (2001) Revisiting the stringent response, ppGpp and starvation signaling. *Curr.Opin.Microbiol.*, **4,** 160-165.

Chaudhuri,T.K., Farr,G.W., Fenton,W.A., Rospert,S. and Horwich,A.L. (2001) GroEL/GroES-mediated folding of a protein too large to be encapsulated. *Cell,* **107,** 235-246.

Checroun,C., Wehrly,T.D., Fischer,E.R., Hayes,S.F. and Celli,J. (2006) Autophagy-mediated reentry of *Francisella tularensis* into the endocytic compartment after cytoplasmic replication. *Proc.Natl.Acad.Sci.U.S.A.*, **103,** 14578-14583.

Chen,J., de Felipe,K.S., Clarke,M., Lu,H., Anderson,O.R., Segal,G. and Shuman,H.A. (2004) *Legionella* effectors that promote nonlytic release from protozoa. *Science,* **303,** 1358-1361.

Chen,Y.A. and Scheller,R.H. (2001) SNARE-mediated membrane fusion. *Nat.Rev.Mol.Cell Biol.*, **2,** 98-106.

Chien,M., Morozova,I., Shi,S., Sheng,H., Chen,J., Gomez,S.M., Asamani,G., Hill,K., Nuara,J., Feder,M., Rineer,J., Greenberg,J.J., Steshenko,V., Park,S.H., Zhao,B., Teplitskaya,E., Edwards,J.R., Pampou,S., Georghiou,A., Chou,I.C., Iannuccilli,W., Ulz,M.E., Kim,D.H., Geringer-Sameth,A., Goldsberry,C., Morozov,P., Fischer,S.G., Segal,G., Qu,X., Rzhetsky,A., Zhang,P., Cayanis,E., De Jong,P.J., Ju,J., Kalachikov,S., Shuman,H.A. and Russo,J.J. (2004) The genomic sequence of the accidental pathogen *Legionella pneumophila*. *Science,* **305,** 1966-1968.

Christie,P.J. and Vogel,J.P. (2000) Bacterial type IV secretion: conjugation systems adapted to deliver effector molecules to host cells. *Trends Microbiol.*, **8,** 354-360.

Cianciotto,N.P., Eisenstein,B.I., Mody,C.H. and Engleberg,N.C. (1990) A mutation in the *mip* gene results in an attenuation of *Legionella pneumophila* virulence. *J.Infect.Dis.*, **162,** 121-126.

Cianciotto,N.P., Eisenstein,B.I., Mody,C.H., Toews,G.B. and Engleberg,N.C. (1989) A *Legionella pneumophila* gene encoding a species-specific surface protein potentiates initiation of intracellular infection. *Infect.Immun.*, **57,** 1255-1262.

Cianciotto,N.P. and Fields,B.S. (1992) *Legionella pneumophila mip* gene potentiates intracellular infection of protozoa and human macrophages. *Proc.Natl.Acad.Sci.U.S.A.*, **89,** 5188-5191.

Ciervo,A., Visca,P., Petrucca,A., Biasucci,L.M., Maseri,A. and Cassone,A. (2002) Antibodies to 60-kilodalton heat shock protein and outer membrane protein 2 of *Chlamydia pneumoniae* in patients with coronary heart disease. *Clin.Diagn.Lab.Immunol.*, **9,** 66-74.

Cirillo,J.D., Cirillo,S.L., Yan,L., Bermudez,L.E., Falkow,S. and Tompkins,L.S. (1999) Intracellular growth in *Acanthamoeba castellanii* affects monocyte entry mechanisms and enhances virulence of *Legionella pneumophila*. *Infect.Immun.*, **67,** 4427-4434.

Cirillo,J.D., Falkow,S. and Tompkins,L.S. (1994) Growth of *Legionella pneumophila* in *Acanthamoeba castellanii* enhances invasion. *Infect.Immun.*, **62,** 3254-3261.

Cirillo,S.L., Bermudez,L.E., El-Etr,S.H., Duhamel,G.E. and Cirillo,J.D. (2001) *Legionella pneumophila* entry gene *rtxA* is involved in virulence. *Infect.Immun.*, **69,** 508-517.

Cirillo,S.L., Lum,J. and Cirillo,J.D. (2000) Identification of novel loci involved in entry by *Legionella pneumophila*. *Microbiology,* **146 (Pt 6),** 1345-1359.

Cirillo,S.L., Yan,L., Littman,M., Samrakandi,M.M. and Cirillo,J.D. (2002) Role of the *Legionella pneumophila rtxA* gene in amoebae. *Microbiology,* **148,** 1667-1677.

Clemens,D.L. (1996) Characterization of the *Mycobacterium tuberculosis* phagosome. *Trends Microbiol.*, **4,** 113-118.

Clemens,D.L. and Horwitz,M.A. (1995) Characterization of the *Mycobacterium tuberculosis* phagosome and evidence that phagosomal maturation is inhibited. *J.Exp.Med.*, **181,** 257-270.

Clemens,D.L., Lee,B.Y. and Horwitz,M.A. (2000) Deviant expression of Rab5 on phagosomes containing the intracellular pathogens *Mycobacterium tuberculosis* and *Legionella pneumophila* is associated with altered phagosomal fate. *Infect.Immun.*, **68,** 2671-2684.

Coers,J., Kagan,J.C., Matthews,M., Nagai,H., Zuckman,D.M. and Roy,C.R. (2000) Identification of Icm protein complexes that play distinct roles in the biogenesis of an organelle permissive for *Legionella pneumophila* intracellular growth. *Mol.Microbiol.*, **38,** 719-736.

Conover,G.M., Derre,I., Vogel,J.P. and Isberg,R.R. (2003) The *Legionella pneumophila* LidA protein: a translocated substrate of the Dot/Icm system associated with maintenance of bacterial integrity. *Mol.Microbiol.*, **48,** 305-321.

Cossart,P. and Lecuit,M. (1998) Interactions of *Listeria monocytogenes* with mammalian cells during entry and actin-based movement: bacterial factors, cellular ligands and signaling. *EMBO J.*, **17,** 3797-3806.

Coxon,P.Y., Summersgill,J.T., Ramirez,J.A. and Miller,R.D. (1998) Signal transduction during *Legionella pneumophila* entry into human monocytes. *Infect.Immun.*, **66,** 2905-2913.

Danieli,M.G., Markovits,D., Gabrielli,A., Corvetta,A., Giorgi,P.L., van der Zee,R., van Embden,J.D., Danieli,G. and Cohen,I.R. (1992) Juvenile rheumatoid arthritis patients manifest immune reactivity to the mycobacterial 65-kDa heat shock protein, to its 180-188 peptide, and to a partially homologous peptide of the proteoglycan link protein. *Clin.Immunol.Immunopathol.*, **64,** 121-128.

de Felipe,K.S., Pampou,S., Jovanovic,O.S., Pericone,C.D., Ye,S.F., Kalachikov,S. and Shuman,H.A. (2005) Evidence for acquisition of *Legionella* type IV secretion substrates via interdomain horizontal gene transfer. *J.Bacteriol.*, **187,** 7716-7726.

de Graeff-Meeder,E.R., van Eden,W., Rijkers,G.T., Prakken,B.J., Zegers,B.J. and Kuis,W. (1993) Heat-shock proteins and juvenile chronic arthritis. *Clin.Exp.Rheumatol.*, **11,** S25-8.

Derre,I. and Isberg,R.R. (2005) LidA, a translocated substrate of the *Legionella pneumophila* type IV secretion system, interferes with the early secretory pathway. *Infect.Immun.*, **73,** 4370-4380.

Derre,I. and Isberg,R.R. (2004) *Legionella pneumophila* replication vacuole formation involves rapid recruitment of proteins of the early secretory system. *Infect.Immun.*, **72,** 3048-3053.

Donnelly,C.E. and Walker,G.C. (1989) *groE* mutants of *Escherichia coli* are defective in umuDC-dependent UV mutagenesis. *J.Bacteriol.*, **171,** 6117-6125.

Dorer,M.S., Kirton,D., Bader,J.S. and Isberg,R.R. (2006) RNA interference analysis of *Legionella* in *Drosophila* cells: exploitation of early secretory apparatus dynamics. *PLoS Pathog.*, **2,** e34.

Duclos,S., Corsini,R. and Desjardins,M. (2003) Remodeling of endosomes during lysosome biogenesis involves 'kiss and run' fusion events regulated by Rab5. *J.Cell.Sci.*, **116,** 907-918.

Dumenil,G. and Isberg,R.R. (2001) The *Legionella pneumophila* IcmR protein exhibits chaperone activity for IcmQ by preventing its participation in high-molecular-weight complexes. *Mol.Microbiol.*, **40,** 1113-1127.

Dumenil,G., Montminy,T.P., Tang,M. and Isberg,R.R. (2004) IcmR-regulated membrane insertion and efflux by the *Legionella pneumophila* IcmQ protein. *J.Biol.Chem.*, **279,** 4686-4695.

Dunn,W.A.,Jr. (1990) Studies on the mechanisms of autophagy: formation of the autophagic vacuole. *J.Cell Biol.*, **110,** 1923-1933.

Elliott,J.A. and Winn,W.C.,Jr. (1986) Treatment of alveolar macrophages with cytochalasin D inhibits uptake and subsequent growth of *Legionella pneumophila*. *Infect.Immun.*, **51,** 31-36.

Ellis,R.J. (1993) The general concept of molecular chaperones. *Philos.Trans.R.Soc.Lond.B.Biol.Sci.*, **339,** 257-261.

Ensgraber,M. and Loos,M. (1992) A 66-kilodalton heat shock protein of *Salmonella typhimurium* is responsible for binding of the bacterium to intestinal mucus. *Infect.Immun.*, **60,** 3072-3078.

Ewann,F. and Hoffman,P.S. (2006) Cysteine metabolism in *Legionella pneumophila*: characterization of an L-cystine-utilizing mutant. *Appl.Environ.Microbiol.*, **72,** 3993-4000.

Fares,M.A., Barrio,E., Sabater-Munoz,B. and Moya,A. (2002) The evolution of the heat-shock protein GroEL from *Buchnera*, the primary endosymbiont of aphids, is governed by positive selection. *Mol.Biol.Evol.*, **19,** 1162-1170.

Fares,M.A., Moya,A. and Barrio,E. (2005) Adaptive evolution in GroEL from distantly related endosymbiotic bacteria of insects. *J.Evol.Biol.*, **18,** 651-660.

Faulkner,G. and Garduno,R.A. (2002) Ultrastructural analysis of differentiation in *Legionella pneumophila*. *J.Bacteriol.*, **184,** 7025-7041.

Fayet,O., Ziegelhoffer,T. and Georgopoulos,C. (1989) The *groES* and *groEL* heat shock gene products of *Escherichia coli* are essential for bacterial growth at all temperatures. *J.Bacteriol.*, **171,** 1379-1385.

Feng,Y., Press,B. and Wandinger-Ness,A. (1995) Rab7: an important regulator of late endocytic membrane traffic. *J.Cell Biol.*, **131,** 1435-1452.

Fenton,W.A., Kashi,Y., Furtak,K. and Horwich,A.L. (1994) Residues in chaperonin GroEL required for polypeptide binding and release. *Nature*, **371,** 614-619.

Fernandez,R.C., Logan,S.M., Lee,S.H. and Hoffman,P.S. (1996) Elevated levels of *Legionella pneumophila* stress protein Hsp60 early in infection of human monocytes and L929 cells correlate with virulence. *Infect.Immun.*, **64,** 1968-1976.

Fernandez-Moreira,E., Helbig,J.H. and Swanson,M.S. (2006) Membrane vesicles shed by *Legionella pneumophila* inhibit fusion of phagosomes with lysosomes. *Infect.Immun.*, **74,** 3285-3295.

Fernandez-Prada,C.M., Hoover,D.L., Tall,B.D., Hartman,A.B., Kopelowitz,J. and Venkatesan,M.M. (2000) *Shigella flexneri* IpaH(7.8) facilitates escape of virulent bacteria from the endocytic vacuoles of mouse and human macrophages. *Infect.Immun.*, **68,** 3608-3619.

Fettes,P.S., Forsbach-Birk,V., Lynch,D. and Marre,R. (2001) Overexpresssion of a *Legionella pneumophila* homologue of the *E. coli* regulator *csrA* affects cell size, flagellation, and pigmentation. *Int.J.Med.Microbiol.*, **291,** 353-360.

Fields,B.S., Sanden,G.N., Barbaree,J.M., Morrill,W.E., Wadowsky,R.M., White,E.H. and Feeley,J.C. (1989) Intracellular multiplication of *Legionella pneumophila* in amoebae isolated from hospital hot water tanks. *Curr. Microbiol.*, **18,** 131-137.

Fields,B.S. (1996) The molecular ecology of *Legionellae*. *Trends Microbiol.*, **4,** 286-290.

Fields,B.S., Benson,R.F. and Besser,R.E. (2002) *Legionella* and Legionnaires' disease: 25 years of investigation. *Clin.Microbiol.Rev.*, **15,** 506-526.

Fields,K.A. and Hackstadt,T. (2002) The chlamydial inclusion: escape from the endocytic pathway. *Annu.Rev.Cell Dev.Biol.*, **18,** 221-245.

Fiers,W., Beyaert,R., Declercq,W. and Vandenabeele,P. (1999) More than one way to die: apoptosis, necrosis and reactive oxygen damage. *Oncogene,* **18,** 7719-7730.

Filichkin,S.A., Brumfield,S., Filichkin,T.P. and Young,M.J. (1997) In vitro interactions of the aphid endosymbiotic SymL chaperonin with barley yellow dwarf virus. *J.Virol.*, **71,** 569-577.

Finlay,B.B. and Cossart,P. (1997) Exploitation of mammalian host cell functions by bacterial pathogens. *Science,* **276,** 718-725.

Fischer,G., Bang,H., Ludwig,B., Mann,K. and Hacker,J. (1992) Mip protein of *Legionella pneumophila* exhibits peptidyl-prolyl-cis/trans isomerase (PPIase) activity. *Mol.Microbiol.*, **6,** 1375-1383.

Fischer,S.F., Vier,J., Muller-Thomas,C. and Hacker,G. (2006) Induction of apoptosis by *Legionella pneumophila* in mammalian cells requires the mitochondrial pathway for caspase activation. *Microbes Infect.*, **8,** 662-669.

Fliermans,C.B., Cherry,W.B., Orrison,L.H., Smith,S.J., Tison,D.L. and Pope,D.H. (1981) Ecological distribution of *Legionella pneumophila*. *Appl.Environ.Microbiol.*, **41,** 9-16.

Fontes,P., Alvarez-Martinez,M.T., Gross,A., Carnaud,C., Kohler,S. and Liautard,J.P. (2005) Absence of evidence for the participation of the macrophage cellular prion protein in infection with *Brucella suis*. *Infect.Immun.*, **73,** 6229-6236.

Fraser,D.W., Tsai,T.R., Orenstein,W., Parkin,W.E., Beecham,H.J., Sharrar,R.G., Harris,J., Mallison,G.F., Martin,S.M., McDade,J.E., Shepard,C.C. and Brachman,P.S. (1977) Legionnaires' disease: description of an epidemic of pneumonia. *N.Engl.J.Med.*, **297,** 1189-1197.

Friedland,J.S., Shattock,R., Remick,D.G. and Griffin,G.E. (1993) Mycobacterial 65-kD heat shock protein induces release of proinflammatory cytokines from human monocytic cells. *Clin.Exp.Immunol.*, **91,** 58-62.

Frisk,A., Ison,C.A. and Lagergard,T. (1998) GroEL heat shock protein of *Haemophilus ducreyi*: association with cell surface and capacity to bind to eukaryotic cells. *Infect.Immun.*, **66,** 1252-1257.

Frydman,J., Nimmesgern,E., Erdjument-Bromage,H., Wall,J.S., Tempst,P. and Hartl,F.U. (1992) Function in protein folding of TRiC, a cytosolic ring complex containing TCP-1 and structurally related subunits. *EMBO J.*, **11,** 4767-4778.

Gabay,J.E. and Horwitz,M.A. (1985) Isolation and characterization of the cytoplasmic and outer membranes of the Legionnaires' disease bacterium (*Legionella pneumophila*). *J.Exp.Med.*, **161,** 409-422.

Galdiero,M., de l'Ero,G.C. and Marcatili,A. (1997) Cytokine and adhesion molecule expression in human monocytes and endothelial cells stimulated with bacterial heat shock proteins. *Infect.Immun.*, **65,** 699-707.

Gal-Mor,O. and Segal,G. (2003) The *Legionella pneumophila* GacA homolog (LetA) is involved in the regulation of *icm* virulence genes and is required for intracellular multiplication in *Acanthamoeba castellanii*. *Microb.Pathog.*, **34,** 187-194.

Gao,B. and Tsan,M.F. (2003) Recombinant human heat shock protein 60 does not induce the release of tumor necrosis factor alpha from murine macrophages. *J.Biol.Chem.*, **278,** 22523-22529.

Gao,L.Y. and Abu Kwaik,Y. (1999a) Activation of caspase 3 during *Legionella pneumophila*-induced apoptosis. *Infect.Immun.*, **67,** 4886-4894.

Gao,L.Y. and Abu Kwaik,Y. (1999b) Apoptosis in macrophages and alveolar epithelial cells during early stages of infection by *Legionella pneumophila* and its role in cytopathogenicity. *Infect.Immun.*, **67,** 862-870.

Gao,L.Y., Harb,O.S. and Abu Kwaik,Y. (1997) Utilization of similar mechanisms by *Legionella pneumophila* to parasitize two evolutionarily distant host cells, mammalian macrophages and protozoa. *Infect.Immun.*, **65,** 4738-4746.

Gao,L.Y. and Kwaik,Y.A. (2000) The mechanism of killing and exiting the protozoan host *Acanthamoeba polyphaga* by *Legionella pneumophila*. *Environ.Microbiol.*, **2,** 79-90.

Gao,L.Y., Stone,B.J., Brieland,J.K. and Abu Kwaik,Y. (1998) Different fates of *Legionella pneumophila pmi* and *mil* mutants within macrophages and alveolar epithelial cells. *Microb.Pathog.*, **25,** 291-306.

Gao,Y., Thomas,J.O., Chow,R.L., Lee,G.H. and Cowan,N.J. (1992) A cytoplasmic chaperonin that catalyzes beta-actin folding. *Cell,* **69,** 1043-1050.

Garduno,R.A., Faulkner,G., Trevors,M.A., Vats,N. and Hoffman,P.S. (1998) Immunolocalization of Hsp60 in *Legionella pneumophila*. *J.Bacteriol.*, **180,** 505-513.

Garduno,R.A., Garduno,E., Hiltz,M. and Hoffman,P.S. (2002) Intracellular growth of *Legionella pneumophila* gives rise to a differentiated form dissimilar to stationary-phase forms. *Infect.Immun.*, **70,** 6273-6283.

Garduno,R.A., Garduno,E. and Hoffman,P.S. (1998a) Surface-associated Hsp60 chaperonin of *Legionella pneumophila* mediates invasion in a HeLa cell model. *Infect.Immun.*, **66,** 4602-4610.

Garduno,R.A., Quinn,F.D. and Hoffman,P.S. (1998b) HeLa cells as a model to study the invasiveness and biology of *Legionella pneumophila*. *Can.J.Microbiol.*, **44,** 430-440.

Georgopoulos,C.P. and Eisen,H. (1974) Bacterial mutants which block phage assembly. *J.Supramol.Struct.*, **2,** 349-359.

Gibson,F.C.,3rd, Tzianabos,A.O. and Rodgers,F.G. (1994) Adherence of *Legionella pneumophila* to U-937 cells, guinea-pig alveolar macrophages, and MRC-5 cells by a novel, complement-independent binding mechanism. *Can.J.Microbiol.*, **40,** 865-872.

Girard,R., Pedron,T., Uematsu,S., Balloy,V., Chignard,M., Akira,S. and Chaby,R. (2003) Lipopolysaccharides from *Legionella* and *Rhizobium* stimulate mouse bone marrow granulocytes via Toll-like receptor 2. *J.Cell.Sci.*, **116,** 293-302.

Glick,T.H., Gregg,M.B., Berman,B., Mallison,G., Rhodes,W.W.,Jr and Kassanoff,I. (1978) Pontiac fever. An epidemic of unknown etiology in a health department: I. Clinical and epidemiologic aspects. *Am.J.Epidemiol.*, **107,** 149-160.

Greub,G. and Raoult,D. (2003) Morphology of *Legionella pneumophila* according to their location within *Hartmannella vermiformis*. *Res.Microbiol.*, **154,** 619-621.

Gupta,R.S. (1995) Evolution of the chaperonin families (Hsp60, Hsp10 and Tcp-1) of proteins and the origin of eukaryotic cells. *Mol.Microbiol.*, **15,** 1-11.

Gutsche,I., Essen,L.O. and Baumeister,W. (1999) Group II chaperonins: new TRiC(k)s and turns of a protein folding machine. *J.Mol.Biol.*, **293,** 295-312.

Hagele,S., Hacker,J. and Brand,B.C. (1998) *Legionella pneumophila* kills human phagocytes but not protozoan host cells by inducing apoptotic cell death. *FEMS Microbiol.Lett.*, **169,** 51-58.

Hales,L.M. and Shuman,H.A. (1999) The *Legionella pneumophila rpoS* gene is required for growth within *Acanthamoeba castellanii. J.Bacteriol.*, **181,** 4879-4889.

Hammer,B.K., Tateda,E.S. and Swanson,M.S. (2002) A two-component regulator induces the transmission phenotype of stationary-phase *Legionella pneumophila. Mol.Microbiol.*, **44,** 107-118.

Harb,O.S., Gao L.Y., and Abu Kwaik,Y. (2000) From protozoa to mammalian cells: a new paradigm in the life cycle of intracellular bacterial pathogens. *Environ Microbiol.*, **2,** 251-265.

Harb,O.S., Venkataraman,C., Haack,B.J., Gao,L.Y. and Kwaik,Y.A. (1998) Heterogeneity in the attachment and uptake mechanisms of the Legionnaires' disease bacterium, *Legionella pneumophila*, by protozoan hosts. *Appl.Environ.Microbiol.*, **64,** 126-132.

Hartley,M.G., Green,M., Choules,G., Rogers,D., Rees,D.G., Newstead,S., Sjostedt,A. and Titball,R.W. (2004) Protection afforded by heat shock protein 60 from *Francisella tularensis* is due to copurified lipopolysaccharide. *Infect.Immun.*, **72,** 4109-4113.

Hatefi,Y. (1985) The mitochondrial electron transport and oxidative phosphorylation system. *Annu.Rev.Biochem.*, **54,** 1015-1069.

Hawn,T.R., Verbon,A., Lettinga,K.D., Zhao,L.P., Li,S.S., Laws,R.J., Skerrett,S.J., Beutler,B., Schroeder,L., Nachman,A., Ozinsky,A., Smith,K.D. and Aderem,A. (2003) A common dominant TLR5 stop codon polymorphism abolishes flagellin signaling and is associated with susceptibility to Legionnaires' disease. *J.Exp.Med.*, **198,** 1563-1572.

Hayer-Hartl,M. (2000) Assay of Malate Dehydrogenase. *A substrate for the E. coli Chaperonins GroEL and GroES.* In Schneider,C. (ed.), *Methods in Molecular Biology, vol. 140: Chaperonin Protocols.* Humana Press Inc., Totowa, NJ, pp. 127-132.

Heinzen,R.A., Hackstadt,T. and Samuel,J.E. (1999) Developmental biology of *Coxiella burnettii. Trends Microbiol.*, **7,** 149-154.

Helbig,J.H., Konig,B., Knospe,H., Bubert,B., Yu,C., Luck,C.P., Riboldi-Tunnicliffe,A., Hilgenfeld,R., Jacobs,E., Hacker,J. and Fischer,G. (2003) The PPIase active site of *Legionella pneumophila* Mip protein is involved in the infection of eukaryotic host cells. *Biol.Chem.*, **384,** 125-137.

Helsel,L.O., Bibb,W.F., Butler,C.A., Hoffman,P.S. and McKinney,R.M. (1988) Recognition of a genus-wide antigen of *Legionella* by a monoclonal antibody. *Curr. Microbiol.*, **16,** 201-208.

Hemmingsen,S.M., Woolford,C., van der Vies,S.M., Tilly,K., Dennis,D.T., Georgopoulos,C.P., Hendrix,R.W. and Ellis,R.J. (1988) Homologous plant and bacterial proteins chaperone oligomeric protein assembly. *Nature,* **333,** 330-334.

Hennequin,C., Porcheray,F., Waligora-Dupriet,A., Collignon,A., Barc,M., Bourlioux,P. and Karjalainen,T. (2001) GroEL (Hsp60) of *Clostridium difficile* is involved in cell adherence. *Microbiology,* **147,** 87-96.

Heuner,K., Dietrich,C., Skriwan,C., Steinert,M. and Hacker,J. (2002) Influence of the alternative sigma(28) factor on virulence and flagellum expression of *Legionella pneumophila. Infect.Immun.,* **70,** 1604-1608.

Hilbi,H., Segal,G. and Shuman,H.A. (2001) Icm/dot-dependent upregulation of phagocytosis by *Legionella pneumophila. Mol.Microbiol.,* **42,** 603-617.

Hoffman,P.S. (1997) Invasion of eukaryotic cells by *Legionella pneumophila*: A common strategy for all hosts? *Can.J.Infect.Dis,* **8,** 139-146.

Hoffman,P.S., Butler,C.A. and Quinn,F.D. (1989) Cloning and temperature-dependent expression in *Escherichia coli* of a *Legionella pneumophila* gene coding for a genus-common 60-kilodalton antigen. *Infect.Immun.,* **57,** 1731-1739.

Hoffman,P.S., Houston,L. and Butler,C.A. (1990) *Legionella pneumophila htpAB* heat shock operon: nucleotide sequence and expression of the 60-kilodalton antigen in *L. pneumophila*-infected HeLa cells. *Infect.Immun.,* **58,** 3380-3387.

Hogenhout,S.A., van der Wilk,F., Verbeek,M., Goldbach,R.W. and van den Heuvel,J.F. (1998) Potato leafroll virus binds to the equatorial domain of the aphid endosymbiotic GroEL homolog. *J.Virol.,* **72,** 358-365.

Horwitz,M.A. (1987) Characterization of avirulent mutant *Legionella pneumophila* that survive but do not multiply within human monocytes. *J.Exp.Med.,* **166,** 1310-1328.

Horwitz,M.A. (1984) Phagocytosis of the Legionnaires' disease bacterium (*Legionella pneumophila*) occurs by a novel mechanism: engulfment within a pseudopod coil. *Cell,* **36,** 27-33.

Horwitz,M.A. (1983a) Cell-mediated immunity in Legionnaires' disease. *J.Clin.Invest.,* **71,** 1686-1697.

Horwitz,M.A. (1983b) Formation of a novel phagosome by the Legionnaires' disease bacterium (*Legionella pneumophila*) in human monocytes. *J.Exp.Med.,* **158,** 1319-1331.

Horwitz,M.A. (1983c) The Legionnaires' disease bacterium (*Legionella pneumophila*) inhibits phagosome-lysosome fusion in human monocytes. *J.Exp.Med.,* **158,** 2108-2126.

Horwitz,M.A. and Maxfield,F.R. (1984) *Legionella pneumophila* inhibits acidification of its phagosome in human monocytes. *J.Cell Biol.,* **99,** 1936-1943.

Horwitz,M.A. and Silverstein,S.C. (1983) Intracellular multiplication of Legionnaires' disease bacteria (*Legionella pneumophila*) in human monocytes is reversibly inhibited by erythromycin and rifampin. *J.Clin.Invest.*, **71,** 15-26.

Horwitz,M.A. and Silverstein,S.C. (1981a) Activated human monocytes inhibit the intracellular multiplication of Legionnaires' disease bacteria. *J.Exp.Med.*, **154,** 1618-1635.

Horwitz,M.A. and Silverstein,S.C. (1981b) Interaction of the legionnaires' disease bacterium (*Legionella pneumophila*) with human phagocytes. II. Antibody promotes binding of *L. pneumophila* to monocytes but does not inhibit intracellular multiplication. *J.Exp.Med.*, **153,** 398-406.

Horwitz,M.A. and Silverstein,S.C. (1980) Legionnaires' disease bacterium (*Legionella pneumophila*) multiples intracellularly in human monocytes. *J.Clin.Invest.*, **66,** 441-450.

Houry,W.A. (2001) Mechanism of substrate recognition by the chaperonin GroEL. *Biochem.Cell Biol.*, **79,** 569-577.

Houry,W.A., Frishman,D., Eckerskorn,C., Lottspeich,F. and Hartl,F.U. (1999) Identification of in vivo substrates of the chaperonin GroEL. *Nature,* **402,** 147-154.

Husmann,L.K. and Johnson,W. (1992) Adherence of *Legionella pneumophila* to guinea pig peritoneal macrophages, J774 mouse macrophages, and undifferentiated U937 human monocytes: role of Fc and complement receptors. *Infect.Immun.*, **60,** 5212-5218.

Ichioka,F., Horii,M., Katoh,K., Terasawa,Y., Shibata,H. and Maki,M. (2005) Identification of Rab GTPase-activating protein-like protein (RabGAPLP) as a novel Alix/AIP1-interacting protein. *Biosci.Biotechnol.Biochem.*, **69,** 861-865.

Issekutz,A.C. (1983) Removal of gram-negative endotoxin from solutions by affinity chromatography. *J.Immunol.Methods,* **61,** 275-281.

Jensen,P., Fomsgaard,A., Shand,G., Hindersson,P. and Hoiby,N. (1993) Antigenic analysis of *Pseudomonas aeruginosa* and *Pseudomonas cepacia* GroEL proteins and demonstration of a lipopolysaccharide-associated GroEL fraction in *P. aeruginosa*. *APMIS,* **101,** 621-630.

Ji,Y., Zhang,B., Van,S.F., Horn, Warren,P., Woodnutt,G., Burnham,M.K. and Rosenberg,M. (2001) Identification of critical staphylococcal genes using conditional phenotypes generated by antisense RNA. *Science,* **293,** 2266-2269.

Joshi,A.D., Sturgill-Koszycki,S. and Swanson,M.S. (2001) Evidence that Dot-dependent and -independent factors isolate the *Legionella pneumophila* phagosome from the endocytic network in mouse macrophages. *Cell.Microbiol.*, **3,** 99-114.

Kagan,J.C. and Roy,C.R. (2002) *Legionella* phagosomes intercept vesicular traffic from endoplasmic reticulum exit sites. *Nat.Cell Biol.*, **4,** 945-954.

Kagan,J.C., Stein,M.P., Pypaert,M. and Roy,C.R. (2004) *Legionella* subvert the functions of Rab1 and Sec22b to create a replicative organelle. *J.Exp.Med.*, **199,** 1201-1211.

Kaneda,K., Masuzawa,T., Yasugami,K., Suzuki,T., Suzuki,Y. and Yanagihara,Y. (1997) Glycosphingolipid-binding protein of *Borrelia burgdorferi sensu lato*. *Infect.Immun.*, **65,** 3180-3185.

Karlin,S. and Brocchieri,L. (2000) Heat shock protein 60 sequence comparisons: duplications, lateral transfer, and mitochondrial evolution. *Proc.Natl.Acad.Sci.U.S.A.*, **97,** 11348-11353.

Karunakaran,K.P., Noguchi,Y., Read,T.D., Cherkasov,A., Kwee,J., Shen,C., Nelson,C.C. and Brunham,R.C. (2003) Molecular analysis of the multiple GroEL proteins of *Chlamydiae*. *J.Bacteriol.*, **185,** 1958-1966.

Katz,S.M. and Nash,P. (1978) Legionnaires' disease: structural characteristics of the organism. *Science,* **199,** 896-897.

Kaufmann,A.F., McDade,J.E., Patton,C.M., Bennett,J.V., Skaliy,P., Feeley,J.C., Anderson,D.C., Potter,M.E., Newhouse,V.F., Gregg,M.B. and Brachman,P.S. (1981) Pontiac fever: isolation of the etiologic agent (*Legionella* pneumophilia) and demonstration of its mode of transmission. *Am.J.Epidemiol.*, **114,** 337-347.

Kerner,M.J., Naylor,D.J., Ishihama,Y., Maier,T., Chang,H.C., Stines,A.P., Georgopoulos,C., Frishman,D., Hayer-Hartl,M., Mann,M. and Hartl,F.U. (2005) Proteome-wide analysis of chaperonin-dependent protein folding in *Escherichia coli*. *Cell,* **122,** 209-220.

Khelef,N., Shuman,H.A. and Maxfield,F.R. (2001) Phagocytosis of wild-type *Legionella pneumophila* occurs through a wortmannin-insensitive pathway. *Infect.Immun.*, **69,** 5157-5161.

Kilvington,S. and Price,J. (1990) Survival of *Legionella pneumophila* within cysts of *Acanthamoeba polyphaga* following chlorine exposure. *J.Appl.Bacteriol.*, **68,** 519-525.

Kim,J. and Klionsky,D.J. (2000) Autophagy, cytoplasm-to-vacuole targeting pathway, and pexophagy in yeast and mammalian cells. *Annu.Rev.Biochem.*, **69,** 303-342.

King,C.H., Fields,B.S., Shotts,E.B.,Jr and White,E.H. (1991) Effects of cytochalasin D and methylamine on intracellular growth of *Legionella pneumophila* in amoebae and human monocyte-like cells. *Infect.Immun.*, **59,** 758-763.

Kirby,A.C., Meghji,S., Nair,S.P., White,P., Reddi,K., Nishihara,T., Nakashima,K., Willis,A.C., Sim,R. and Wilson,M. (1995) The potent bone-resorbing mediator of *Actinobacillus actinomycetemcomitans* is homologous to the molecular chaperone GroEL. *J.Clin.Invest.*, **96,** 1185-1194.

Kirby,J.E., Vogel,J.P., Andrews,H.L. and Isberg,R.R. (1998) Evidence for pore-forming ability by *Legionella pneumophila*. *Mol.Microbiol.*, **27,** 323-336.

Knight,E.,Jr. (1969) Mitochondria-associated ribonucleic acid of the HeLa cell. Effect of ethidium bromide on the synthesis of ribosomal and 4S ribonucleic acid. *Biochemistry,* **8,** 5089-5093.

Köhler,R., Fanghanel,J., Konig,B., Luneberg,E., Frosch,M., Rahfeld,J.U., Hilgenfeld,R., Fischer,G., Hacker,J. and Steinert,M. (2003) Biochemical and functional analyses of the Mip protein: influence of the N-terminal half and of peptidylprolyl isomerase activity on the virulence of *Legionella pneumophila*. *Infect.Immun.*, **71,** 4389-4397.

Kol,A., Bourcier,T., Lichtman,A.H. and Libby,P. (1999) Chlamydial and human heat shock protein 60s activate human vascular endothelium, smooth muscle cells, and macrophages. *J.Clin.Invest.*, **103,** 571-577.

Kol,A., Lichtman,A.H., Finberg,R.W., Libby,P. and Kurt-Jones,E.A. (2000) Cutting edge: heat shock protein (HSP) 60 activates the innate immune response: CD14 is an essential receptor for HSP60 activation of mononuclear cells. *J.Immunol.*, **164,** 13-17.

Kol,A., Sukhova,G.K., Lichtman,A.H. and Libby,P. (1998) Chlamydial heat shock protein 60 localizes in human atheroma and regulates macrophage tumor necrosis factor-alpha and matrix metalloproteinase expression. *Circulation,* **98,** 300-307.

Kong,T.H., Coates,A.R., Butcher,P.D., Hickman,C.J. and Shinnick,T.M. (1993) *Mycobacterium tuberculosis* expresses two chaperonin-60 homologs. *Proc.Natl.Acad.Sci.U.S.A.*, **90,** 2608-2612.

Kozak,M. (1987) At least six nucleotides preceding the AUG initiator codon enhance translation in mammalian cells. *J.Mol.Biol.*, **196,** 947-950.

Krendel,M., Sgourdas,G. and Bonder,E.M. (1998) Disassembly of actin filaments leads to increased rate and frequency of mitochondrial movement along microtubules. *Cell Motil.Cytoskeleton,* **40,** 368-378.

Kubota,H., Hynes,G., Carne,A., Ashworth,A. and Willison,K. (1994) Identification of six Tcp-1-related genes encoding divergent subunits of the TCP-1-containing chaperonin. *Curr.Biol.*, **4,** 89-99.

Kusukawa,N. and Yura,T. (1988) Heat shock protein GroE of *Escherichia coli*: key protective roles against thermal stress. *Genes Dev.*, **2,** 874-882.

Kuznetsov,S.A., Rivera,D.T., Severin,F.F., Weiss,D.G. and Langford,G.M. (1994) Movement of axoplasmic organelles on actin filaments from skeletal muscle. *Cell Motil.Cytoskeleton,* **28,** 231-242.

Kwiatkowska,K. and Sobota,A. (1999) Signaling pathways in phagocytosis. *Bioessays,* **21,** 422-431.

Laemmli,U.K. (1970) Cleavage of structural proteins during the assembly of the head of bacteriophage T4. *Nature,* **227,** 680-685.

Laguna,R.K., Creasey,E.A., Li,Z., Valtz,N. and Isberg,R.R. (2006) A *Legionella pneumophila*-translocated substrate that is required for growth within macrophages and protection from host cell death. *Proc.Natl.Acad.Sci.U.S.A.,* **103,** 18745-18750.

Lee,I.K., Kim,K.S., Kim,H., Lee,J.Y., Ryu,C.H., Chun,H.J., Lee,K.U., Lim,Y., Kim,Y.H., Huh,P.W., Lee,K.H., Han,S.I., Jun,T.Y. and Rha,H.K. (2004) MAP, a protein interacting with a tumor suppressor, merlin, through the run domain. *Biochem.Biophys.Res.Commun.,* **325,** 774-783.

Lema,M.W., Brown,A., Butler,C.A. and Hoffman,P.S. (1988) Heat-shock response in *Legionella pneumophila. Can.J.Microbiol.,* **34,** 1148-1153.

Lewis,V.A., Hynes,G.M., Zheng,D., Saibil,H. and Willison,K. (1992) T-complex polypeptide-1 is a subunit of a heteromeric particle in the eukaryotic cytosol. *Nature,* **358,** 249-252.

Lin,Z. and Rye,H.S. (2006) GroEL-mediated protein folding: making the impossible, possible. *Crit.Rev.Biochem.Mol.Biol.,* **41,** 211-239.

Llorca,O., Marco,S., Carrascosa,J.L. and Valpuesta,J.M. (1994) The formation of symmetrical GroEL-GroES complexes in the presence of ATP. *FEBS Lett.,* **345,** 181-186.

Llorca,O., Martin-Benito,J., Gomez-Puertas,P., Ritco-Vonsovici,M., Willison,K.R., Carrascosa,J.L. and Valpuesta,J.M. (2001) Analysis of the interaction between the eukaryotic chaperonin CCT and its substrates actin and tubulin. *J.Struct.Biol.,* **135,** 205-218.

Lu,H. and Clarke,M. (2005) Dynamic properties of *Legionella*-containing phagosomes in *Dicyostelium* amoebae. *Cell.Microbiol.,* **7,** 995-1007.

Lund,P.A. (2001) Microbial molecular chaperones. *Adv.Microb.Physiol.,* **44,** 93-140.

Luo,Z.Q. and Isberg,R.R. (2004) Multiple substrates of the *Legionella pneumophila* Dot/Icm system identified by interbacterial protein transfer. *Proc.Natl.Acad.Sci.U.S.A.,* **101,** 841-846.

Machner,M.P. and Isberg,R.R. (2006) Targeting of host Rab GTPase function by the intravacuolar pathogen *Legionella pneumophila. Dev.Cell.,* **11,** 47-56.

Maguire,M., Coates,A.R. and Henderson,B. (2002) Chaperonin 60 unfolds its secrets of cellular communication. *Cell Stress Chaperones,* **7,** 317-329.

Manchanda,N., Lyubimova,A., Ho,H.Y., James,M.F., Gusella,J.F., Ramesh,N., Snapper,S.B. and Ramesh,V. (2005) The NF2 tumor suppressor Merlin and the ERM proteins interact with N-WASP and regulate its actin polymerization function. *J.Biol.Chem.*, **280,** 12517-12522.

Marra,A., Blander,S.J., Horwitz,M.A. and Shuman,H.A. (1992) Identification of a *Legionella pneumophila* locus required for intracellular multiplication in human macrophages. *Proc.Natl.Acad.Sci.U.S.A.*, **89,** 9607-9611.

Marrie,T.J., Raoult,D., La Scola,B., Birtles,R.J., de Carolis,E. and Canadian Community-Acquired Pneumonia Study Group. (2001) *Legionella*-like and other amoebal pathogens as agents of community-acquired pneumonia. *Emerg.Infect.Dis.*, **7,** 1026-1029.

Marston,B.J., Lipman,H.B. and Breiman,R.F. (1994) Surveillance for Legionnaires' disease. Risk factors for morbidity and mortality. *Arch.Intern.Med.*, **154,** 2417-2422.

Matlack,K.E., Mothes,W. and Rapoport,T.A. (1998) Protein translocation: tunnel vision. *Cell,* **92,** 381-390.

Matsumae,H., Minobe,S., Kindan,K., Watanabe,T., Sato,T. and Tosa,T. (1990) Specific removal of endotoxin from protein solutions by immobilized histidine. *Biotechnol.Appl.Biochem.*, **12,** 129-140.

Matsumoto,A., Bessho,H., Uehira,K. and Suda,T. (1991) Morphological studies of the association of mitochondria with chlamydial inclusions and the fusion of chlamydial inclusions. *J.Electron.Microsc.(Tokyo),* **40,** 356-363.

Matthews,M. and Roy,C.R. (2000) Identification and subcellular localization of the *Legionella pneumophila* IcmX protein: a factor essential for establishment of a replicative organelle in eukaryotic host cells. *Infect.Immun.*, **68,** 3971-3982.

McDade,J.E., Shepard,C.C., Fraser,D.W., Tsai,T.R., Redus,M.A. and Dowdle,W.R. (1977) Legionnaires' disease: isolation of a bacterium and demonstration of its role in other respiratory disease. *N.Engl.J.Med.*, **297,** 1197-1203.

McLean,I.W. and Nakane,P.K. (1974) Periodate-lysine-paraformaldehyde fixative. A new fixation for immunoelectron microscopy. *J.Histochem.Cytochem.*, **22,** 1077-1083.

McLennan,N.F., McAteer,S. and Masters,M. (1994) The tail of a chaperonin: the C-terminal region of *Escherichia coli* GroEL protein. *Mol.Microbiol.*, **14,** 309-321.

Medzhitov,R. (2001) Toll-like receptors and innate immunity. *Nat.Rev.Immunol.*, **1,** 135-145.

Meghji,S., White,P.A., Nair,S.P., Reddi,K., Heron,K., Henderson,B., Zaliani,A., Fossati,G., Mascagni,P., Hunt,J.F., Roberts,M.M. and Coates,A.R. (1997) *Mycobacterium tuberculosis* chaperonin 10 stimulates bone resorption: a potential contributory factor in Pott's disease. *J.Exp.Med.*, **186,** 1241-1246.

Minnick,M.F., Smitherman,L.S. and Samuels,D.S. (2003) Mitogenic effect of *Bartonella bacilliformis* on human vascular endothelial cells and involvement of GroEL. *Infect.Immun.*, **71,** 6933-6942.

Mody,C.H., Paine,R.,3rd, Shahrabadi,M.S., Simon,R.H., Pearlman,E., Eisenstein,B.I. and Toews,G.B. (1993) *Legionella pneumophila* replicates within rat alveolar epithelial cells. *J.Infect.Dis.*, **167,** 1138-1145.

Moffat,J.F. and Tompkins,L.S. (1992) A quantitative model of intracellular growth of *Legionella pneumophila* in *Acanthamoeba castellanii*. *Infect.Immun.*, **60,** 296-301.

Mogk,A., Homuth,G., Scholz,C., Kim,L., Schmid,F.X. and Schumann,W. (1997) The GroE chaperonin machine is a major modulator of the CIRCE heat shock regulon of Bacillus subtilis. *EMBO J.*, **16,** 4579-4590.

Molmeret,M., Alli,O.A., Zink,S., Flieger,A., Cianciotto,N.P. and Kwaik,Y.A. (2002) *icmT* is essential for pore formation-mediated egress of *Legionella pneumophila* from mammalian and protozoan cells. *Infect.Immun.*, **70,** 69-78.

Molmeret,M., Zink,S.D., Han,L., Abu-Zant,A., Asari,R., Bitar,D.M. and Abu Kwaik,Y. (2004) Activation of caspase-3 by the Dot/Icm virulence system is essential for arrested biogenesis of the *Legionella*-containing phagosome. *Cell.Microbiol.*, **6,** 33-48.

Molofsky,A.B., Byrne,B.G., Whitfield,N.N., Madigan,C.A., Fuse,E.T., Tateda,K. and Swanson,M.S. (2006) Cytosolic recognition of flagellin by mouse macrophages restricts *Legionella pneumophila* infection. *J.Exp.Med.*, **203,** 1093-1104.

Molofsky,A.B., Shetron-Rama,L.M. and Swanson,M.S. (2005) Components of the *Legionella pneumophila* flagellar regulon contribute to multiple virulence traits, including lysosome avoidance and macrophage death. *Infect.Immun.*, **73,** 5720-5734.

Molofsky,A.B. and Swanson,M.S. (2004) Differentiate to thrive: lessons from the *Legionella pneumophila* life cycle. *Mol.Microbiol.*, **53,** 29-40.

Molofsky,A.B. and Swanson,M.S. (2003) *Legionella pneumophila* CsrA is a pivotal repressor of transmission traits and activator of replication. *Mol.Microbiol.*, **50,** 445-461.

Morales,V.M., Backman,A. and Bagdasarian,M. (1991) A series of wide-host-range low-copy-number vectors that allow direct screening for recombinants. *Gene,* **97,** 39-47.

Moreno,R., Hidalgo,A., Cava,F., Fernandez-Lafuente,R., Guisan,J.M. and Berenguer,J. (2004) Use of an antisense RNA strategy to investigate the functional significance of Mn-catalase in the extreme thermophile *Thermus thermophilus*. *J.Bacteriol.*, **186,** 7804-7806.

Morita,M., Kanemori,M., Yanagi,H. and Yura,T. (1999) Heat-induced synthesis of sigma32 in *Escherichia coli*: structural and functional dissection of *rpoH* mRNA secondary structure. *J.Bacteriol.*, **181,** 401-410.

Morris,R.L. and Hollenbeck,P.J. (1995) Axonal transport of mitochondria along microtubules and F-actin in living vertebrate neurons. *J.Cell Biol.*, **131,** 1315-1326.

Muller,A., Hacker,J. and Brand,B.C. (1996) Evidence for apoptosis of human macrophage-like HL-60 cells by *Legionella pneumophila* infection. *Infect.Immun.*, **64,** 4900-4906.

Murata,T., Delprato,A., Ingmundson,A., Toomre,D.K., Lambright,D.G. and Roy,C.R. (2006) The *Legionella pneumophila* effector protein DrrA is a Rab1 guanine nucleotide-exchange factor. *Nat.Cell Biol.*, **8,** 971-977.

Murga,R., Forster,T.S., Brown,E., Pruckler,J.M., Fields,B.S. and Donlan,R.M. (2001) Role of biofilms in the survival of *Legionella pneumophila* in a model potable-water system. *Microbiology,* **147,** 3121-3126.

Nagai,H., Cambronne,E.D., Kagan,J.C., Amor,J.C., Kahn,R.A. and Roy,C.R. (2005) A C-terminal translocation signal required for Dot/Icm-dependent delivery of the *Legionella* RalF protein to host cells. *Proc.Natl.Acad.Sci.U.S.A.*, **102,** 826-831.

Nagai,H., Kagan,J.C., Zhu,X., Kahn,R.A. and Roy,C.R. (2002) A bacterial guanine nucleotide exchange factor activates ARF on *Legionella* phagosomes. *Science,* **295,** 679-682.

Nagai,H. and Roy,C.R. (2001) The DotA protein from *Legionella pneumophila* is secreted by a novel process that requires the Dot/Icm transporter. *EMBO J.*, **20,** 5962-5970.

Nash,T.W., Libby,D.M. and Horwitz,M.A. (1988) IFN-gamma-activated human alveolar macrophages inhibit the intracellular multiplication of *Legionella pneumophila*. *J.Immunol.*, **140,** 3978-3981.

Neild,A.L. and Roy,C.R. (2004) Immunity to vacuolar pathogens: what can we learn from *Legionella*? *Cell.Microbiol.*, **6,** 1011-1018.

Neild,A.L. and Roy,C.R. (2003) *Legionella* reveal dendritic cell functions that facilitate selection of antigens for MHC class II presentation. *Immunity,* **18,** 813-823.

Neumann,G., Watanabe,T., Ito,H., Watanabe,S., Goto,H., Gao,P., Hughes,M., Perez,D.R., Donis,R., Hoffmann,E., Hobom,G. and Kawaoka,Y. (1999) Generation of influenza A viruses entirely from cloned cDNAs. *Proc.Natl.Acad.Sci.U.S.A.*, **96,** 9345-9350.

Newton,C.A., Perkins,I., Widen,R.H., Friedman,H. and Klein,T.W. (2007) Role of Toll-Like Receptor 9 in *Legionella pneumophila*-Induced Interleukin-12 p40 Production in Bone Marrow-Derived Dendritic Cells and Macrophages from Permissive and Nonpermissive Mice. *Infect.Immun.*, **75,** 146-151.

Newton,H.J., Sansom,F.M., Bennett-Wood,V. and Hartland,E.L. (2006) Identification of *Legionella pneumophila*-specific genes by genomic subtractive hybridization with *Legionella micdadei* and identification of *lpnE*, a gene required for efficient host cell entry. *Infect.Immun.*, **74,** 1683-1691.

Ninio,S., Zuckman-Cholon,D.M., Cambronne,E.D. and Roy,C.R. (2005) The *Legionella* IcmS-IcmW protein complex is important for Dot/Icm-mediated protein translocation. *Mol.Microbiol.*, **55,** 912-926.

Ogawa,M. and Sasakawa,C. (2006) Intracellular survival of *Shigella*. *Cell.Microbiol.*, **8,** 177-184.

Oldham,L.J. and Rodgers,F.G. (1985) Adhesion, penetration and intracellular replication of *Legionella pneumophila*: an *in vitro* model of pathogenesis. *J Gen Microbiol,* **131,** 697-706.

Orrison,L.H., Cherry,W.B., Fliermans,C.B., Dees,S.B., McDougal,L.K. and Dodd,D.J. (1981) Characteristics of environmental isolates of *Legionella pneumophila*. *Appl.Environ.Microbiol.*, **42,** 109-115.

Osterloh,A., Meier-Stiegen,F., Veit,A., Fleischer,B., von Bonin,A. and Breloer,M. (2004) Lipopolysaccharide-free heat shock protein 60 activates T cells. *J.Biol.Chem.*, **279,** 47906-47911.

Otto,G.P., Wu,M.Y., Clarke,M., Lu,H., Anderson,O.R., Hilbi,H., Shuman,H.A. and Kessin,R.H. (2004) Macroautophagy is dispensable for intracellular replication of *Legionella pneumophila* in *Dicyostelium discoideum*. *Mol.Microbiol.*, **51,** 63-72.

Pantzar,M., Teneberg,S. and Lagergard,T. (2006) Binding of *Haemophilus ducreyi* to carbohydrate receptors is mediated by the 58.5-kDa GroEL heat shock protein. *Microbes Infect.*, **8,** 2452-2458.

Parsons,L.M., Limberger,R.J. and Shayegani,M. (1997) Alterations in levels of DnaK and GroEL result in diminished survival and adherence of stressed *Haemophilus ducreyi*. *Infect.Immun.*, **65,** 2413-2419.

Payne,N.R. and Horwitz,M.A. (1987) Phagocytosis of *Legionella pneumophila* is mediated by human monocyte complement receptors. *J.Exp.Med.*, **166,** 1377-1389.

Pedersen,P.L. and Amzel,L.M. (1993) ATP synthases. Structure, reaction center, mechanism, and regulation of one of nature's most unique machines. *J.Biol.Chem.*, **268,** 9937-9940.

Peterson,E.M. and de la Maza,L.M. (1988) *Chlamydia* parasitism: ultrastructural characterization of the interaction between the chlamydial cell envelope and the host cell. *J.Bacteriol.*, **170,** 1389-1392.

Portaro,F.C., Hayashi,M.A., De Arauz,L.J., Palma,M.S., Assakura,M.T., Silva,C.L. and de Camargo,A.C. (2002) The *Mycobacterium leprae* Hsp65 displays proteolytic activity. Mutagenesis studies indicate that the *M. leprae* Hsp65 proteolytic activity is catalytically related to the HslVU protease. *Biochemistry,* **41,** 7400-7406.

Prakken,B., Wauben,M., van Kooten,P., Anderton,S., van der Zee,R., Kuis,W. and van Eden,W. (1998) Nasal administration of arthritis-related T cell epitopes of heat shock protein 60 as a promising way for immunotherapy in chronic arthritis. *Biotherapy,* **10,** 205-211.

Rambukkana,A., Das,P.K., Witkamp,L., Yong,S., Meinardi,M.M. and Bos,J.D. (1993) Antibodies to mycobacterial 65-kDa heat shock protein and other immunodominant antigens in patients with psoriasis. *J.Invest.Dermatol.,* **100,** 87-92.

Rao,S.P., Ogata,K., Morris,S.L. and Catanzaro,A. (1994) Identification of a 68-kDa surface antigen of *Mycobacterium avium* that binds to human macrophages. *J.Lab.Clin.Med.,* **123,** 526-535.

Reddi,K., Meghji,S., Nair,S.P., Arnett,T.R., Miller,A.D., Preuss,M., Wilson,M., Henderson,B. and Hill,P. (1998) The *Escherichia coli* chaperonin 60 (GroEL) is a potent stimulator of osteoclast formation. *J.Bone Miner.Res.,* **13,** 1260-1266.

Retzlaff,C., Yamamoto,Y., Hoffman,P.S., Friedman,H. and Klein,T.W. (1994) Bacterial heat shock proteins directly induce cytokine mRNA and interleukin-1 secretion in macrophage cultures. *Infect.Immun.,* **62,** 5689-5693.

Retzlaff,C., Yamamoto,Y., Okubo,S., Hoffman,P.S., Friedman,H. and Klein,T.W. (1996) *Legionella pneumophila* heat-shock protein-induced increase of interleukin-1 beta mRNA involves protein kinase C signalling in macrophages. *Immunology,* **89,** 281-288.

Reynolds,H.Y. and Newball,H.H. (1974) Analysis of proteins and respiratory cells obtained from human lungs by bronchial lavage. *J.Lab.Clin.Med.,* **84,** 559-573.

Rha,Y.H., Taube,C., Haczku,A., Joetham,A., Takeda,K., Duez,C., Siegel,M., Aydintug,M.K., Born,W.K., Dakhama,A. and Gelfand,E.W. (2002) Effect of microbial heat shock proteins on airway inflammation and hyperresponsiveness. *J.Immunol.,* **169,** 5300-5307.

Richardson,A., Schwager,F., Landry,S.J. and Georgopoulos,C. (2001) The importance of a mobile loop in regulating chaperonin/ co-chaperonin interaction: humans versus *Escherichia coli. J.Biol.Chem.,* **276,** 4981-4987.

Ridenour,D.A., Cirillo,S.L., Feng,S., Samrakandi,M.M. and Cirillo,J.D. (2003) Identification of a gene that affects the efficiency of host cell infection by *Legionella pneumophila* in a temperature-dependent fashion. *Infect.Immun.,* **71,** 6256-6263.

Rietsch,A. and Beckwith,J. (1998) The genetics of disulfide bond metabolism. *Annu.Rev.Genet.,* **32,** 163-184.

Riffo-Vasquez,Y., Spina,D., Page,C., Tormay,P., Singh,M., Henderson,B. and Coates,A. (2004) Effect of *Mycobacterium tuberculosis* chaperonins on bronchial eosinophilia and hyper-responsiveness in a murine model of allergic inflammation. *Clin.Exp.Allergy,* **34,** 712-719.

Rinke de Wit,T.F., Bekelie,S., Osland,A., Miko,T.L., Hermans,P.W., van Soolingen,D., Drijfhout,J.W., Schoningh,R., Janson,A.A. and Thole,J.E. (1992) *Mycobacteria* contain two *groEL* genes: the second *Mycobacterium leprae groEL* gene is arranged in an operon with *groES. Mol.Microbiol.,* **6,** 1995-2007.

Riveroll,A.L. (2005) PhD. Thesis. The *Legionella pneumophila* chaperonin - An investigation of virulence-related roles in a yeast model. Dalhousie University, Nova Scotia, Canada.

Robinson,C.G. and Roy,C.R. (2006) Attachment and fusion of endoplasmic reticulum with vacuoles containing *Legionella pneumophila. Cell.Microbiol.,* **8,** 793-805.

Rodgers,F.G. (1979) Ultrastructure of *Legionella pneumophila. J.Clin.Pathol.,* **32,** 1195-1202.

Rogers,J. and Keevil,C.W. (1992) Immunogold and fluorescein immunolabelling of *Legionella pneumophila* within an aquatic biofilm visualized by using episcopic differential interference contrast microscopy. *Appl.Environ.Microbiol.,* **58,** 2326-2330.

Rohr,U., Weber,S., Michel,R., Selenka,F. and Wilhelm,M. (1998) Comparison of free-living amoebae in hot water systems of hospitals with isolates from moist sanitary areas by identifying genera and determining temperature tolerance. *Appl.Environ.Microbiol.,* **64,** 1822-1824.

Rowbotham,T.J. (1986) Current views on the relationships between amoebae, *Legionella*e and man. *Isr.J.Med.Sci.,* **22,** 678-689.

Rowbotham,T.J. (1980) Preliminary report on the pathogenicity of *Legionella pneumophila* for freshwater and soil amoebae. *J.Clin.Pathol.,* **33,** 1179-1183.

Roy,C.R., Berger,K.H. and Isberg,R.R. (1998) *Legionella pneumophila* DotA protein is required for early phagosome trafficking decisions that occur within minutes of bacterial uptake. *Mol.Microbiol.,* **28,** 663-674.

Roy,C.R. and Isberg,R.R. (1997) Topology of *Legionella pneumophila* DotA: an inner membrane protein required for replication in macrophages. *Infect.Immun.,* **65,** 571-578.

Rusanganwa,E. and Gupta,R.S. (1993) Cloning and characterization of multiple *groEL* chaperonin-encoding genes in *Rhizobium meliloti. Gene,* **126,** 67-75.

Rusinol,A.E., Cui,Z., Chen,M.H. and Vance,J.E. (1994) A unique mitochondria-associated membrane fraction from rat liver has a high capacity for lipid synthesis and contains pre-Golgi secretory proteins including nascent lipoproteins. *J.Biol.Chem.*, **269,** 27494-27502.

Rye,H.S., Burston,S.G., Fenton,W.A., Beechem,J.M., Xu,Z., Sigler,P.B. and Horwich,A.L. (1997) Distinct actions of cis and trans ATP within the double ring of the chaperonin GroEL. *Nature,* **388,** 792-798.

Rye,H.S., Roseman,A.M., Chen,S., Furtak,K., Fenton,W.A., Saibil,H.R. and Horwich,A.L. (1999) GroEL-GroES cycling: ATP and nonnative polypeptide direct alternation of folding-active rings. *Cell,* **97,** 325-338.

Sambrook,J. and Russell,D.W. (2001) *Molecular cloning: a laboratory manual.* Cold Spring Harbor Laboratory Press, Cold Spring Harbor, N.Y.

Sampson,J.S., Plikaytis,B.B. and Wilkinson,H.W. (1986) Immunologic response of patients with legionellosis against major protein-containing antigens of *Legionella pneumophila* serogroup 1 as shown by immunoblot analysis. *J.Clin.Microbiol.*, **23,** 92-99.

Sasu,S., LaVerda,D., Qureshi,N., Golenbock,D.T. and Beasley,D. (2001) *Chlamydia pneumoniae* and chlamydial heat shock protein 60 stimulate proliferation of human vascular smooth muscle cells via toll-like receptor 4 and p44/p42 mitogen-activated protein kinase activation. *Circ.Res.*, **89,** 244-250.

Sato,T., Wu,J. and Kuramitsu,H. (1998) The *sgp* gene modulates stress responses of *Streptococcus mutans*: utilization of an antisense RNA strategy to investigate essential gene functions. *FEMS Microbiol.Lett.*, **159,** 241-245.

Sauer,J.D., Bachman,M.A. and Swanson,M.S. (2005a) The phagosomal transporter A couples threonine acquisition to differentiation and replication of *Legionella pneumophila* in macrophages. *Proc.Natl.Acad.Sci.U.S.A.*, **102,** 9924-9929.

Sauer,J.D., Shannon,J.G., Howe,D., Hayes,S.F., Swanson,M.S. and Heinzen,R.A. (2005b) Specificity of *Legionella pneumophila* and *Coxiella burnetii* vacuoles and versatility of *Legionella pneumophila* revealed by coinfection. *Infect.Immun.*, **73,** 4494-4504.

Scanlon,M., Leitch,G.J., Visvesvara,G.S. and Shaw,A.P. (2004) Relationship between the host cell mitochondria and the parasitophorous vacuole in cells infected with *Encephalitozoon* microsporidia. *J.Eukaryot.Microbiol.*, **51,** 81-87.

Schepis,A., Schramm,B., de Haan,C.A. and Locker,J.K. (2006) Vaccinia virus-induced microtubule-dependent cellular rearrangements. *Traffic,* **7,** 308-323.

Schmidt,M.H., Chen,B., Randazzo,L.M. and Bogler,O. (2003) SETA/CIN85/Ruk and its binding partner AIP1 associate with diverse cytoskeletal elements, including FAKs, and modulate cell adhesion. *J.Cell.Sci.*, **116,** 2845-2855.

Schulz,A. and Schumann,W. (1996) *hrcA*, the first gene of the *Bacillus subtilis dnaK* operon encodes a negative regulator of class I heat shock genes. *J.Bacteriol.*, **178,** 1088-1093.

Scopio,A., Johnson,P., Laquerre,A. and Nelson,D.R. (1994) Subcellular localization and chaperone activities of *Borrelia burgdorferi* Hsp60 and Hsp70. *J.Bacteriol.*, **176,** 6449-6456.

Segal,G., Feldman,M. and Zusman,T. (2005) The Icm/Dot type-IV secretion systems of *Legionella pneumophila* and *Coxiella burnetii*. *FEMS Microbiol.Rev.*, **29,** 65-81.

Segal,G., Purcell,M. and Shuman,H.A. (1998) Host cell killing and bacterial conjugation require overlapping sets of genes within a 22-kb region of the *Legionella pneumophila* genome. *Proc.Natl.Acad.Sci.U.S.A.*, **95,** 1669-1674.

Segal,G. and Ron,E.Z. (1996) Heat shock activation of the *groESL* operon of *Agrobacterium tumefaciens* and the regulatory roles of the inverted repeat. *J.Bacteriol.*, **178,** 3634-3640.

Segal,G., Russo,J.J. and Shuman,H.A. (1999) Relationships between a new type IV secretion system and the *icm/dot* virulence system of *Legionella pneumophila*. *Mol.Microbiol.*, **34,** 799-809.

Segal,G. and Shuman,H.A. (1999) *Legionella pneumophila* utilizes the same genes to multiply within *Acanthamoeba castellanii* and human macrophages. *Infect.Immun.*, **67,** 2117-2124.

Segal,G. and Shuman,H.A. (1998a) How is the intracellular fate of the *Legionella pneumophila* phagosome determined? *Trends Microbiol.*, **6,** 253-255.

Segal,G. and Shuman,H.A. (1998b) Intracellular multiplication and human macrophage killing by *Legionella pneumophila* are inhibited by conjugal components of IncQ plasmid RSF1010. *Mol.Microbiol.*, **30,** 197-208.

Segal,R. and Ron,E.Z. (1996) Regulation and organization of the *groE* and *dnaK* operons in Eubacteria. *FEMS Microbiol.Lett.*, **138,** 1-10.

Sexton,J.A., Miller,J.L., Yoneda,A., Kehl-Fie,T.E. and Vogel,J.P. (2004a) *Legionella pneumophila* DotU and IcmF are required for stability of the Dot/Icm complex. *Infect.Immun.*, **72,** 5983-5992.

Sexton,J.A., Pinkner,J.S., Roth,R., Heuser,J.E., Hultgren,S.J. and Vogel,J.P. (2004b) The *Legionella pneumophila* PilT homologue DotB exhibits ATPase activity that is critical for intracellular growth. *J.Bacteriol.*, **186,** 1658-1666.

Sexton,J.A. and Vogel,J.P. (2002) Type IVB secretion by intracellular pathogens. *Traffic,* **3,** 178-185.

Shi,C., Forsbach-Birk,V., Marre,R. and McNealy,T.L. (2006) The *Legionella pneumophila* global regulatory protein LetA affects DotA and Mip. *Int.J.Med.Microbiol.,* **296,** 15-24.

Shohdy,N., Efe,J.A., Emr,S.D. and Shuman,H.A. (2005) Pathogen effector protein screening in yeast identifies *Legionella* factors that interfere with membrane trafficking. *Proc.Natl.Acad.Sci.U.S.A.,* **102,** 4866-4871.

Sinai,A.P. and Joiner,K.A. (2001) The *Toxoplasma gondii* protein ROP2 mediates host organelle association with the parasitophorous vacuole membrane. *J.Cell Biol.,* **154,** 95-108.

Sinai,A.P., Webster,P. and Joiner,K.A. (1997) Association of host cell endoplasmic reticulum and mitochondria with the *Toxoplasma gondii* parasitophorous vacuole membrane: a high affinity interaction. *J.Cell.Sci.,* **110 (Pt 17),** 2117-2128.

Smitherman,L.S. and Minnick,M.F. (2005) *Bartonella bacilliformis* GroEL: effect on growth of human vascular endothelial cells in infected cocultures. *Ann.N.Y.Acad.Sci.,* **1063,** 286-298.

Spandorfer,S.D., Neuer,A., LaVerda,D., Byrne,G., Liu,H.C., Rosenwaks,Z. and Witkin,S.S. (1999) Previously undetected *Chlamydia trachomatis* infection, immunity to heat shock proteins and tubal occlusion in women undergoing in-vitro fertilization. *Hum.Reprod.,* **14,** 60-64.

Spang,A. (2002) ARF1 regulatory factors and COPI vesicle formation. *Curr.Opin.Cell Biol.,* **14,** 423-427.

Spiess,C., Meyer,A.S., Reissmann,S. and Frydman,J. (2004) Mechanism of the eukaryotic chaperonin: protein folding in the chamber of secrets. *Trends Cell Biol.,* **14,** 598-604.

Steinert,M., Ott,M., Luck,P.C., Tannich,E. and Hacker,J. (1994) Studies on the uptake and intracellular replication of *Legionella pneumophila* in protozoa and in macrophage-like cells. *FEMS Microbiol. Ecol.,* **15,** 299-308.

Sternlicht,H., Farr,G.W., Sternlicht,M.L., Driscoll,J.K., Willison,K. and Yaffe,M.B. (1993) The T-complex polypeptide 1 complex is a chaperonin for tubulin and actin in vivo. *Proc.Natl.Acad.Sci.U.S.A.,* **90,** 9422-9426.

Stone,B.J. and Abu Kwaik,Y. (1998) Expression of multiple pili by *Legionella pneumophila*: identification and characterization of a type IV pilin gene and its role in adherence to mammalian and protozoan cells. *Infect.Immun.,* **66,** 1768-1775.

Straus,D.B., Walter,W.A. and Gross,C.A. (1988) *Escherichia coli* heat shock gene mutants are defective in proteolysis. *Genes Dev.*, **2,** 1851-1858.

Sturgill-Koszycki,S. and Swanson,M.S. (2000) *Legionella pneumophila* replication vacuoles mature into acidic, endocytic organelles. *J.Exp.Med.*, **192,** 1261-1272.

Summerhayes,I.C., Wong,D. and Chen,L.B. (1983) Effect of microtubules and intermediate filaments on mitochondrial distribution. *J.Cell.Sci.*, **61,** 87-105.

Susa,M. and Marre,R. (1999) *Legionella pneumophila* invasion of MRC-5 cells induces tyrosine protein phosphorylation. *Infect.Immun.*, **67,** 4490-4498.

Susa,M., Ticac,B., Rukavina,T., Doric,M. and Marre,R. (1998) *Legionella pneumophila* infection in intratracheally inoculated T cell-depleted or -nondepleted A/J mice. *J.Immunol.*, **160,** 316-321.

Swanson,M.S. and Hammer,B.K. (2000) *Legionella pneumophila* pathogenesis: a fateful journey from amoebae to macrophages. *Annu.Rev.Microbiol.*, **54,** 567-613.

Swanson,M.S. and Isberg,R.R. (1996) Identification of *Legionella pneumophila* mutants that have aberrant intracellular fates. *Infect.Immun.*, **64,** 2585-2594.

Swanson,M.S. and Isberg,R.R. (1995) Association of *Legionella pneumophila* with the macrophage endoplasmic reticulum. *Infect.Immun.*, **63,** 3609-3620.

Tan,M., Wong,B. and Engel,J.N. (1996) Transcriptional organization and regulation of the *dnaK* and *groE* operons of *Chlamydia trachomatis*. *J.Bacteriol.*, **178,** 6983-6990.

Temmerman,R., Vervaeren,H., Noseda,B., Boon,N. and Verstraete,W. (2006) Necrotrophic growth of *Legionella pneumophila*. *Appl.Environ.Microbiol.*, **72,** 4323-4328.

Theofilopoulos,A.N. (1995) The basis of autoimmunity: Part I. Mechanisms of aberrant self-recognition. *Immunol.Today,* **16,** 90-98.

Thorén,P.E., Persson,D., Karlsson,M. and Norden,B. (2000) The antennapedia peptide penetratin translocates across lipid bilayers - the first direct observation. *FEBS Lett.*, **482,** 265-268.

Tian,G., Vainberg,I.E., Tap,W.D., Lewis,S.A. and Cowan,N.J. (1995) Specificity in chaperonin-mediated protein folding. *Nature,* **375,** 250-253.

Tilney,L.G., Harb,O.S., Connelly,P.S., Robinson,C.G. and Roy,C.R. (2001) How the parasitic bacterium *Legionella pneumophila* modifies its phagosome and transforms it into rough ER: implications for conversion of plasma membrane to the ER membrane. *J.Cell.Sci.*, **114,** 4637-4650.

Todd,M.J., Viitanen,P.V. and Lorimer,G.H. (1994) Dynamics of the chaperonin ATPase cycle: implications for facilitated protein folding. *Science,* **265,** 659-666.

Török,Z., Horvath,I., Goloubinoff,P., Kovacs,E., Glatz,A., Balogh,G. and Vigh,L. (1997) Evidence for a lipochaperonin: association of active protein-folding GroESL oligomers with lipids can stabilize membranes under heat shock conditions. *Proc.Natl.Acad.Sci.U.S.A.,* **94,** 2192-2197.

Towbin,H., Staehelin,T. and Gordon,J. (1979) Electrophoretic transfer of proteins from polyacrylamide gels to nitrocellulose sheets: procedure and some applications. *Proc.Natl.Acad.Sci.U.S.A.,* **76,** 4350-4354.

Tsai,C.M. and Frasch,C.E. (1982) A sensitive silver stain for detecting lipopolysaccharides in polyacrylamide gels. *Anal. Biochem,* **119,** 115-119.

Uthayakumar,S. and Granger,B.L. (1995) Cell surface accumulation of overexpressed hamster lysosomal membrane glycoproteins. *Cell.Mol.Biol.Res.,* **41,**

Vabulas,R.M., Ahmad-Nejad,P., da Costa,C., Miethke,T., Kirschning,C.J., Hacker,H. and Wagner,H. (2001) Endocytosed HSP60s use toll-like receptor 2 (TLR2) and TLR4 to activate the toll/interleukin-1 receptor signaling pathway in innate immune cells. *J.Biol.Chem.,* **276,** 31332-31339.

Valpuesta,J.M., Martin-Benito,J., Gomez-Puertas,P., Carrascosa,J.L. and Willison,K.R. (2002) Structure and function of a protein folding machine: the eukaryotic cytosolic chaperonin CCT. *FEBS Lett.,* **529,** 11-16.

van der Vies,S.M., Gatenby,A.A. and Georgopoulos,C. (1994) Bacteriophage T4 encodes a co-chaperonin that can substitute for *Escherichia coli* GroES in protein folding. *Nature,* **368,** 654-656.

van Eden,W., Thole,J.E., van der Zee,R., Noordzij,A., van Embden,J.D., Hensen,E.J. and Cohen,I.R. (1988) Cloning of the mycobacterial epitope recognized by T lymphocytes in adjuvant arthritis. *Nature,* **331,** 171-173.

VanBogelen,R.A., Acton,M.A. and Neidhardt,F.C. (1987) Induction of the heat shock regulon does not produce thermotolerance in *Escherichia coli. Genes Dev.,* **1,** 525-531.

Vance,J.E. and Shiao,Y.J. (1996) Intracellular trafficking of phospholipids: import of phosphatidylserine into mitochondria. *Anticancer Res.,* **16,** 1333-1339.

VanRheenen,S.M., Dumenil,G. and Isberg,R.R. (2004) IcmF and DotU are required for optimal effector translocation and trafficking of the *Legionella pneumophila* vacuole. *Infect.Immun.,* **72,** 5972-5982.

Venkataraman,C., Haack,B.J., Bondada,S. and Abu Kwaik,Y. (1997) Identification of a Gal/GalNAc lectin in the protozoan *Hartmannella vermiformis* as a potential receptor for attachment and invasion by the Legionnaires' disease bacterium. *J.Exp.Med.*, **186,** 537-547.

Venkataraman,C. and Kwaik,Y.A. (2000) Signal transduction in the protozoan host *Hartmannella vermiformis* upon attachment to *Legionella pneumophila. Microbes Infect.*, **2,** 867-875.

Vincent,C.D., Friedman,J.R., Jeong,K.C., Buford,E.C., Miller,J.L. and Vogel,J.P. (2006) Identification of the core transmembrane complex of the *Legionella* Dot/Icm type IV secretion system. *Mol.Microbiol.*, **62,** 1278-1291.

Vincent,C.D. and Vogel,J.P. (2006) The *Legionella pneumophila* IcmS-LvgA protein complex is important for Dot/Icm-dependent intracellular growth. *Mol.Microbiol.*, **61,** 596-613.

Vivés,E., Brodin,P. and Lebleu,B. (1997) A truncated HIV-1 Tat protein basic domain rapidly translocates through the plasma membrane and accumulates in the cell nucleus. *J.Biol.Chem.*, **272,** 16010-16017.

Voelker,D.R. (1991) Organelle biogenesis and intracellular lipid transport in eukaryotes. *Microbiol.Rev.*, **55,** 543-560.

Vogel,J.P., Andrews,H.L., Wong,S.K. and Isberg,R.R. (1998) Conjugative transfer by the virulence system of *Legionella pneumophila. Science,* **279,** 873-876.

Wada,M. and Itikawa,H. (1984) Participation of *Escherichia coli* K-12 *groE* gene products in the synthesis of cellular DNA and RNA. *J.Bacteriol.*, **157,** 694-696.

Wang,B. and Kuramitsu,H.K. (2003) Assessment of the utilization of the antisense RNA strategy to identify essential genes in heterologous bacteria. *FEMS Microbiol.Lett.*, **220,** 171-176.

Watarai,M., Derre,I., Kirby,J., Growney,J.D., Dietrich,W.F. and Isberg,R.R. (2001) *Legionella pneumophila* is internalized by a macropinocytotic uptake pathway controlled by the Dot/Icm system and the mouse Lgn1 locus. *J.Exp.Med.*, **194,** 1081-1096.

Watarai,M., Kim,S., Erdenebaatar,J., Makino,S., Horiuchi,M., Shirahata,T., Sakaguchi,S. and Katamine,S. (2003) Cellular prion protein promotes *Brucella* infection into macrophages. *J.Exp.Med.*, **198,** 5-17.

Weber,S.S., Ragaz,C., Reus,K., Nyfeler,Y. and Hilbi,H. (2006) *Legionella pneumophila* exploits PI(4)P to anchor secreted effector proteins to the replicative vacuole. *PLoS Pathog.*, **2,** e46.

Weeratna,R., Stamler,D.A., Edelstein,P.H., Ripley,M., Marrie,T., Hoskin,D. and Hoffman,P.S. (1994) Human and guinea pig immune responses to *Legionella pneumophila* protein antigens OmpS and Hsp60. *Infect.Immun.*, **62,** 3454-3462.

Weissgerber,P., Faigle,M., Northoff,H. and Neumeister,B. (2003) Investigation of mechanisms involved in phagocytosis of *Legionella pneumophila* by human cells. *FEMS Microbiol.Lett.*, **219,** 173-179.

Weissman,J.S., Hohl,C.M., Kovalenko,O., Kashi,Y., Chen,S., Braig,K., Saibil,H.R., Fenton,W.A. and Horwich,A.L. (1995) Mechanism of GroEL action: productive release of polypeptide from a sequestered position under GroES. *Cell,* **83,** 577-587.

Weissman,J.S., Kashi,Y., Fenton,W.A. and Horwich,A.L. (1994) GroEL-mediated protein folding proceeds by multiple rounds of binding and release of nonnative forms. *Cell,* **78,** 693-702.

Wiater,L.A., Dunn,K., Maxfield,F.R. and Shuman,H.A. (1998) Early events in phagosome establishment are required for intracellular survival of *Legionella pneumophila*. *Infect.Immun.*, **66,** 4450-4460.

Wieland,H., Goetz,F. and Neumeister,B. (2004) Phagosomal acidification is not a prerequisite for intracellular multiplication of *Legionella pneumophila* in human monocytes. *J.Infect.Dis.*, **189,** 1610-1614.

Wilson,A.C., Wu,C.C., Yates,J.R.,3rd and Tan,M. (2005) Chlamydial GroEL autoregulates its own expression through direct interactions with the HrcA repressor protein. *J.Bacteriol.*, **187,** 7535-7542.

Winn,W.C.,Jr. (1988) Legionnaires disease: historical perspective. *Clin.Microbiol.Rev.*, **1,** 60-81.

Wintermeyer,E., Ludwig,B., Steinert,M., Schmidt,B., Fischer,G. and Hacker,J. (1995) Influence of site specifically altered Mip proteins on intracellular survival of *Legionella pneumophila* in eukaryotic cells. *Infect.Immun.*, **63,** 4576-4583.

Witkin,S.S., Jeremias,J., Toth,M. and Ledger,W.J. (1993) Cell-mediated immune response to the recombinant 57-kDa heat-shock protein of *Chlamydia trachomatis* in women with salpingitis. *J.Infect.Dis.*, **167,** 1379-1383.

Xu,H.M. and Gutmann,D.H. (1998) Merlin differentially associates with the microtubule and actin cytoskeleton. *J.Neurosci.Res.*, **51,** 403-415.

Xu,Z., Horwich,A.L. and Sigler,P.B. (1997) The crystal structure of the asymmetric GroEL-GroES-$(ADP)_7$ chaperonin complex. *Nature,* **388,** 741-750.

Yamaguchi,H., Osaki,T., Kurihara,N., Taguchi,H., Hanawa,T., Yamamoto,T. and Kamiya,S. (1997) Heat-shock protein 60 homologue of *Helicobacter pylori* is associated with adhesion of *H. pylori* to human gastric epithelial cells. *J.Med.Microbiol.*, **46,** 825-831.

Yokota,S., Tsubaki,K., Kuriyama,T., Shimizu,H., Ibe,M., Mitsuda,T., Aihara,Y., Kosuge,K. and Nomaguchi,H. (1993) Presence in Kawasaki disease of antibodies to mycobacterial heat-shock protein HSP65 and autoantibodies to epitopes of human HSP65 cognate antigen. *Clin.Immunol.Immunopathol.*, **67,** 163-170.

Yoshida,N., Oeda,K., Watanabe,E., Mikami,T., Fukita,Y., Nishimura,K., Komai,K. and Matsuda,K. (2001) Protein function. Chaperonin turned insect toxin. *Nature,* **411,** 44.

Yu,V.L., Plouffe,J.F., Pastoris,M.C., Stout,J.E., Schousboe,M., Widmer,A., Summersgill,J., File,T., Heath,C.M., Paterson,D.L. and Chereshsky,A. (2002) Distribution of *Legionella* species and serogroups isolated by culture in patients with sporadic community-acquired legionellosis: an international collaborative survey. *J.Infect.Dis.*, **186,** 127-128.

Yuan,G. and Wong,S.L. (1995) Regulation of *groE* expression in *Bacillus subtilis*: the involvement of the sigma A-like promoter and the roles of the inverted repeat sequence (CIRCE). *J.Bacteriol.*, **177,** 5427-5433.

Yura,T., Nagai,H. and Mori,H. (1993) Regulation of the heat-shock response in bacteria. *Annu.Rev.Microbiol.*, **47,** 321-350.

Zeilstra-Ryalls,J., Fayet,O. and Georgopoulos,C. (1991) The universally conserved GroE (Hsp60) chaperonins. *Annu.Rev.Microbiol.*, **45,** 301-325.

Zerial,M. and McBride,H. (2001) Rab proteins as membrane organizers. *Nat.Rev.Mol.Cell Biol.*, **2,** 107-117.

Zhang,L., Pelech,S. and Uitto,V.J. (2004a) Bacterial GroEL-like heat shock protein 60 protects epithelial cells from stress-induced death through activation of ERK and inhibition of caspase 3. *Exp.Cell Res.*, **292,** 231-240.

Zhang,L., Pelech,S. and Uitto,V.J. (2004b) Long-term effect of heat shock protein 60 from *Actinobacillus actinomycetemcomitans* on epithelial cell viability and mitogen-activated protein kinases. *Infect.Immun.*, **72,** 38-45.

Zhang,L., Pelech,S.L., Mayrand,D., Grenier,D., Heino,J. and Uitto,V.J. (2001) Bacterial heat shock protein-60 increases epithelial cell proliferation through the ERK1/2 MAP kinases. *Exp.Cell Res.*, **266,** 11-20.

Zhou,D., Mooseker,M.S. and Galan,J.E. (1999) Role of the *S. typhimurium* actin-binding protein SipA in bacterial internalization. *Science,* **283,** 2092-2095.

Zhou,Y.N., Kusukawa,N., Erickson,J.W., Gross,C.A. and Yura,T. (1988) Isolation and characterization of *Escherichia coli* mutants that lack the heat shock sigma factor sigma 32. *J.Bacteriol.*, **170,** 3640-3649.

Zink,S.D., Pedersen,L., Cianciotto,N.P. and Abu Kwaik,Y. (2002) The Dot/Icm type IV secretion system of *Legionella pneumophila* is essential for the induction of apoptosis in human macrophages. *Infect.Immun.*, **70,** 1657-1663.

Zuckman,D.M., Hung,J.B. and Roy,C.R. (1999) Pore-forming activity is not sufficient for *Legionella pneumophila* phagosome trafficking and intracellular growth. *Mol.Microbiol.*, **32,** 990-1001.

Zusman,T., Gal-Mor,O. and Segal,G. (2002) Characterization of a *Legionella pneumophila relA* insertion mutant and roles of RelA and RpoS in virulence gene expression. *J.Bacteriol.*, **184,** 67-75.

Zylber,E., Vesco,C. and Penman,S. (1969) Selective inhibition of the synthesis of mitochondria-associated RNA by ethidium bromide. *J.Mol.Biol.*, **44,** 195-204.